JAN 1972
RECEIVED
NASA STI FACILITY
INPUT BRANCH

B.B.
Vol III

(NASA-CR-145598) APOLLO NOTES, VOLUME 3 (Bissett-Berman Corp.) 308 p

N75-77158

Unclas
00/98 39882

Vol III
Notes 101-150 complete
Vbm 4-29-65

APOLLO NOTES
TABLE OF CONTENTS

No.	Title	Author
101.	An Approximate Evaluation of Range-Rate Orbit Parameter Determination	L. Horowitz
102.	Orbit Parameter Determination - A Comparison of Range With Range-Rate	L. Horowitz/ W. Iwata
103.	Statistics of Minimum Rendezvous Range	H. Dale
104.	The Calculation of the Covariance of Estimator Errors For Two Cross Correlated Data Sources	J. R. Holdsworth
105.	Normal Displacements From Rectilinear Trajectories	C. Siska
106.	Bissett-Berman (NASA) Presentation	G. F. Floyd
107.	An Approximate Method for Dealing with Auto-Correlated Noise in the Error Analysis of Orbit Parameter Estimators	J. R. Holdsworth
108.	Station Location Errors	H. Engel
109.	Effect of the Longitude of the LEM Landing Site on the Errors in Determining Rendezvous Position by the MSFN	H. Dale
110.	Error Sources for Range and Range-Rate Measurements	H. Epstein
111.	Suggested MSFN Operation For LEM Rendezvous	G. F. Floyd

112	Differential Range Accuracy	H. Epstein
113	MSFN Directed LEM Ascent	H. Engel
114	Calculation of Covariance Matrices for Hyperbolic Orbits (A Revision of Apollo Note No. 82)	H. Dale
115	The Calculation of the Covariance Matrix of the Errors in the Estimators of the Orbit Parameters When the Estimates are Based Upon Data Which Is Contaminated by Auto-Correlated Noise	J. R. Holdsworth
116	MSFN Lunar Coverage	G. F. Floyd
117	Earth-Moon and Moon-Earth Trajectories	H. Engel
118	Effect of the Solar Plasma on the Doppler Measurements for Mariner II	C. Black
119	Lunar Ascent and Rendezvous Using a Realistic Estimate of the Sub-Lunar Point and Available Tracking Stations	H. Dale
120	Bias Effects on Orbit Parameter Determination	L. Horowitz/ W. Iwata
121	Simplified Evaluation of MSFN Errors	G. F. Floyd
122	Estimate of Earth-Moon Injection Errors Using Two MSFN Stations	H. Dale
123	Orbit Determination with Range Change As the Measurable	L. Lustick
124	Errors in Predicted Position and Velocity	H. Engel
125	Range Observations of LEM from Madrid and CSM	H. Engel

126.	Canonical Diagonalization of Covariance Matrices	L. Horowitz
127.	Comparison of $\dot{R}$ and ΔR Data	H. Engel
128.	Preliminary Results of the Effect of Range Bias Errors	H. Dale/ H. Engel
129.	Experimental Precision Doppler Accuracy	G. F. Floyd
130.	The Effect of Noise Auto-Correlation on the Accuracy of the Estimators of the Orbit Parameters	J. R. Holdswort
131.	A Method of Manufacturing a Proper Rotation Matrix Which Converts the Covariance Matrix to Diagonal Form	W. Iwata
132.	Convergence of Successive Iteration on the Orbit Parameter Estimators	L. Horowitz
133.	Clock Accuracy	G. F. Floyd
134.	Doppler Propagation Errors in Lunar Navigation from the Earth	C. F. Black
135.	Computer Results for Lunar Ascent Using Range and Range Rate Data From 1, 2, and 3 Stations	C. H. Dale
136.	MSFN Radar Angle Data in LEM Ascent	H. Engel
137.	Analytical Treatment of Ring Around System	L. Lustick
138.	Combination of MSFN and CSM Observation	H. Engel
139.	MSFN Station Locations and Lunar Rendezvous Determination	H. Engel
140.	Some Comments on Frequency and Time Standards	H. Epstein
141.	Range Versus Doppler Measurements	G. F. Floyd
142.	Further Estimates of Earth-Moon Injection Errors	C. H. Dale
143.	Communication and Computation Load	H. Engel
144.	Earth Orbit Injection and Tracking Errors	C. H. Dale

145.	Optimum One-Boost Correction to LEM Ascent	H. Engel
146.	Bissett-Berman Presentation at Goddard Space Flight Center	G. F. Floyd
147.	MSFN Station Locations and Lunar Rendezvous Determination, II	H. Engel
148.	Range-Rate Prediction of Rendezvous	H. Engel
149.	Modifications of Orbit Determination Program for Velocity of Light and Gravitational Attraction Uncertainty	H. Engel/ L. Lustick
150.	Comparison of Kalman-Schmitt and Linear Least Squares	H. Engel

APOLLO NOTE NO. 101

L. Horowitz
6 September 1963

AN APPROXIMATE EVALUATION OF RANGE-RATE ORBIT PARAMETER DETERMINATION

Introduction

This study obtains the covariance matrix of the maximum likelihood estimators corresponding to a slightly perturbed circular lunar orbit. Using the results of Apollo Note No. 7, small perturbations from the known circular reference orbit are considered by introducing a local system of rotating co-ordinates. The equations of motion for the slightly perturbed body are then solved in the accelerated reference system and higher order terms neglected as in Apollo Note No. 7. Range-rate is written in terms of co-ordinates in the rotating system, and the desired information matrix obtained by replacing discrete summation with continuous time integration. Finally, the covariance matrix of the maximum likelihood estimators is obtained by inverting the information matrix as in Apollo Note No. 43.

Values for all parameters are taken to correspond to nominal LEM orbit determination by ground support stations on Earth. Results are summarized in the concluding section.

Geometrical Formulation

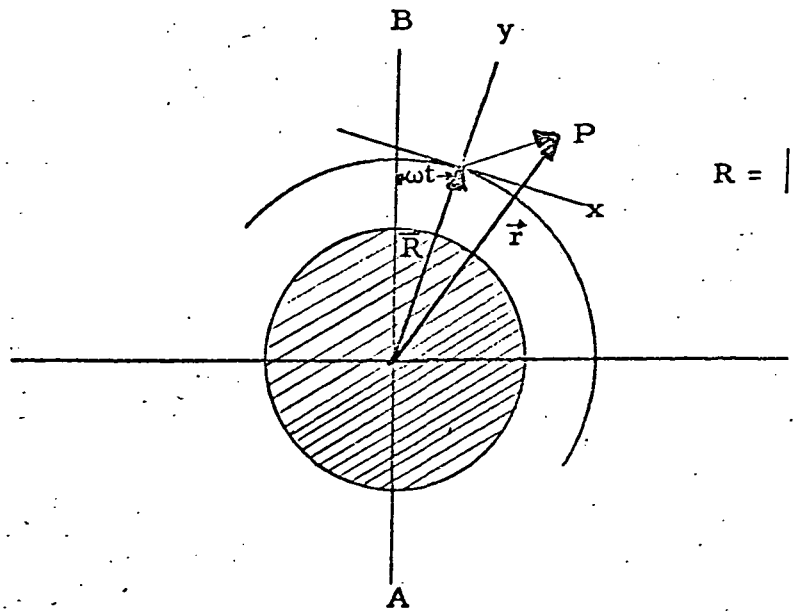

Figure 1.

The indicated x-y co-ordinate system rotates with origin on the known circular orbit in such a way that y increases radially outward. The measured quantity is V_D ("Doppler Velocity"); the "range-rate" of P as measured from an infinitely distant Earth along line AB. Then from Figure 1,

$$V_D = (\dot{x} + R\omega) \sin \omega t - \dot{y} \cos \omega t \quad . \tag{1}$$

For this simplified two-dimensional case, the unknown orbit parameters are $x_o, y_o, \dot{x}_o, \dot{y}_o$. We wish to determine how well we can estimate these orbit parameters by observation of V_D for $\frac{\pi}{2\omega}$ seconds.

Equations of Motion

In the rotating system, motion is given by:

$$\ddot{\bar{r}} + 2(\bar{\omega} \times \dot{\bar{r}}) + \bar{\omega} \times (\bar{\omega} \times \bar{r}) = \frac{-\mu}{r^3} \bar{r} \, , \tag{2}$$

where μ is the lunar gravitational constant. Since x and y are small with respect to R, we make the approximations given on page 129 of Apollo Note No. 7 to obtain:

$$x = \left[\frac{4\dot{x}_o}{\omega} + 6y_o\right] \sin \omega t + \frac{2\dot{y}_o}{\omega} \cos \omega t - \left[6y_o + \frac{3\dot{x}_o}{\omega}\right] \omega t + x_o - \frac{2\dot{y}_o}{\omega}$$

$$y = \frac{\dot{y}_o}{\omega} \sin \omega t - \left[\frac{2\dot{x}_o}{\omega} + 3y_o\right] \cos \omega t + 4y_o + \frac{2\dot{x}_o}{\omega}$$

$$\dot{x} = \left[4\dot{x}_o + 6\omega y_o\right] \cos \omega t - 2\dot{y}_o \sin \omega t - 6\omega y_o - 3\dot{x}_o \tag{3}$$

$$\dot{y} = \dot{y}_o \cos \omega t + \left[2\dot{x}_o + 3\omega y_o\right] \sin \omega t$$

Equation (3) is the solution of (2) in terms of the orbit parameters x_o, y_o, $\dot{x}_o$, $\dot{y}_o$.

Calculation of the Covariance Matrix

In order to compute the covariance matrix of the maximum likelihood estimators of the orbit parameters, we need to evaluate the four terms:

$$\frac{\partial V_D}{\partial x_o}, \quad \frac{\partial V_D}{\partial y_o}, \quad \frac{\partial V_D}{\partial \dot{x}_o}, \quad \frac{\partial V_D}{\partial \dot{y}_o}$$

as explained on page 5 of Apollo Note No. 43.

From Equation (3), we see that:

$$\begin{aligned}
\frac{\partial \dot{x}}{\partial x_o} &= 0 & \frac{\partial \dot{y}}{\partial x_o} &= 0 \\
\frac{\partial \dot{x}}{\partial y_o} &= 6\omega \left[\cos \omega t - 1 \right] & \frac{\partial \dot{y}}{\partial y_o} &= 3\omega \sin \omega t \\
\frac{\partial \dot{x}}{\partial \dot{x}_o} &= 4 \cos \omega t - 3 & \frac{\partial \dot{y}}{\partial \dot{x}_o} &= 2 \sin \omega t \\
\frac{\partial \dot{x}}{\partial \dot{y}_o} &= -2 \sin \omega t & \frac{\partial \dot{y}}{\partial \dot{y}_o} &= \cos \omega t
\end{aligned} \tag{4}$$

Then from Equation (1),

$$\frac{\partial V_D}{\partial x_o} = \frac{\partial \dot{x}}{\partial x_o} \sin \omega t - \frac{\partial \dot{y}}{\partial x_o} \cos \omega t$$

$$\frac{\partial V_D}{\partial y_o} = \frac{\partial \dot{x}}{\partial y_o} \sin \omega t - \frac{\partial \dot{y}}{\partial y_o} \cos \omega t$$

$$\frac{\partial V_D}{\partial \dot{x}_o} = \frac{\partial \dot{x}}{\partial \dot{x}_o} \sin \omega t - \frac{\partial \dot{y}}{\partial \dot{x}_o} \cos \omega t$$

$$\frac{\partial V_D}{\partial \dot{y}_o} = \frac{\partial \dot{x}}{\partial \dot{y}_o} \sin \omega t - \frac{\partial \dot{y}}{\partial \dot{y}_o} \cos \omega t$$

(5)

Combining Equation (4) with (5), we obtain the required ingredients for forming the information matrix:

$$\frac{\partial V_D}{\partial x_o} = 0$$

$$\frac{\partial V_D}{\partial y_o} = 3 \omega \sin \omega t (\cos \omega t - 2)$$

$$\frac{\partial V_D}{\partial \dot{x}_o} = \sin \omega t (2 \cos \omega t - 3)$$

$$\frac{\partial V_D}{\partial \dot{y}_o} = -(1 + \sin^2 \omega t)$$

(6)

We note that since $\frac{\partial V_D}{\partial x_o} = 0$, we cannot estimate the orbit parameter x_o at all by employing this perturbation technique to V_D measurements.

For notational convenience, let

$$a_1 = y_o$$

$$a_2 = \dot{x}_o$$

$$a_3 = \dot{y}_o .$$

Then the terms of the information matrix are obtained from N observations of V_D by

$$C_{i,j} = \frac{1}{N} \sum_{k=1}^{N} \frac{\partial V_D(k)}{\partial a_i} \frac{\partial V_D(k)}{\partial a_j} \tag{7}$$

as in Apollo Note No. 43. For the nominal lunar orbit (80 n. mi.), we assume 1 observation per minute, so that $N = \frac{\pi}{120\omega} = 31$ observations over 1/4 period. Letting Δt be the time interval between observations and $t_m = N\Delta t$, we have from Equation (7):

$$C_{i,j} = \frac{1}{N} \sum_{k=1}^{N} \frac{\partial V_D(k)}{\partial a_i} \frac{\partial V_D(k)}{\partial a_j}$$

$$= \frac{1}{N\Delta t} \sum_{k=1}^{N} \frac{\partial V_D(k)}{\partial a_i} \frac{\partial V_D(k)}{\partial a_j} \Delta t$$

$$\approx \frac{1}{N\Delta t} \int_{o}^{t_m} \frac{\partial V_D(t)}{\partial a_i} \frac{\partial V_D(t)}{\partial a_j} dt$$

$$C_{i,j} \approx \frac{2\omega}{\pi} \int_{o}^{\pi/2\omega} \frac{\partial V_D(t)}{\partial a_i} \frac{\partial V_D(t)}{\partial a_j} \, dt \, . \qquad (8)$$

The elements of the information matrix C are then obtained by using Equation (6) in (8) for i, j = 1, 2, 3.

Conclusions

Carrying out these computations and using N = 31 and σ = .03 meters/sec, the resulting covariance matrix is:

$$\text{Cov}\,(\hat{a}_i, \hat{a}_j) = \frac{\sigma^2}{N} C^{-1} ;$$

$$\text{Cov}\,(\hat{a}_i, \hat{a}_j) = \begin{array}{c} \\ (y_o) \\ (\dot{x}_o) \\ (\dot{y}_o) \end{array} \begin{pmatrix} (y_o) & (\dot{x}_o) & (\dot{y}_o) \\ 2226.0 \ m^2 & -3.4836 \ \frac{m^2}{sec} & -0.6841 \ \frac{m^2}{sec} \\ -3.4836 \ \frac{m^2}{sec} & 55.340 \times 10^{-4} \ \frac{m^2}{sec^2} & 9.9362 \times 10^{-4} \ \frac{m^2}{sec^2} \\ -0.6841 \ \frac{m^2}{sec} & 9.9362 \times 10^{-4} \ \frac{m^2}{sec^2} & 2.9501 \times 10^{-4} \ \frac{m^2}{sec^2} \end{pmatrix}$$

where again,

$$a_1 = y_o$$
$$a_2 = \dot{x}_o$$
$$a_3 = \dot{y}_o$$

This covariance matrix corresponds to 31 observations taken over 1/4 period.

APOLLO NOTE NO. 102

L. Horowitz/
W. Iwata
12 September 1963

ORBIT PARAMETER DETERMINATION - A COMPARISON OF RANGE WITH RANGE-RATE

Introduction

In Apollo Note No. 101, the covariance matrix of the orbit parameter maximum likelihood estimators was obtained for nominal ground support range-rate tracking. Following Apollo Note No. 7, small perturbations from a known circular orbit were considered and the equations of motion solved in a convenient rotating reference system. The required covariance matrix was then calculated by inverting the "information matrix" thus obtained.

This study provides an analogous development of the covariance matrix of the maximum likelihood estimators corresponding to ground support range tracking, and compares the results thus obtained with those derived from range-rate tracking.

Values for all parameters are taken to correspond to nominal LEM orbit determination by ground support stations on Earth. Results are summarized in the concluding section.

Geometrical Formulation

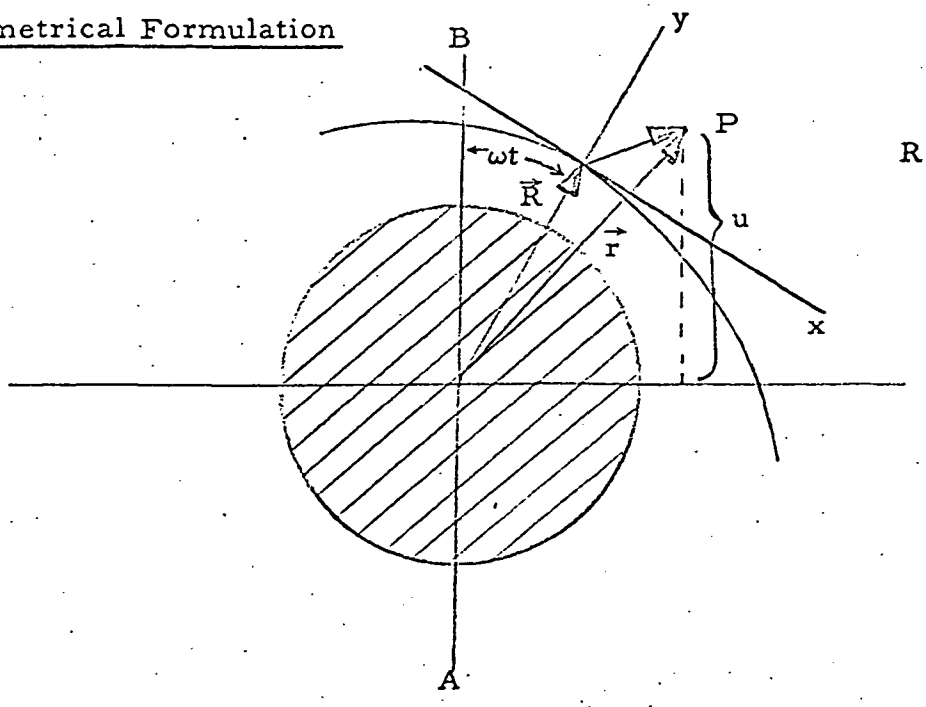

$R = |\vec{R}|$

Figure 1.

The indicated co-ordinate system rotates with origin on the known circular orbit and with y increasing radially outward. Assuming an infinitely distant Earth, the measured quantity is the range u as shown in Figure 1:

$$u = (R + y) \cos \omega t - x \sin \omega t \tag{1}$$

Precisely as in Apollo Note No. 101, the unknown orbit parameters are x_o, y_o, $\dot{x}_o$, $\dot{y}_o$ in this simplified two-dimensional representation. We wish to determine how well we can estimate these orbit parameters by observation of u for $\pi/2\omega$ seconds.

Equations of Motion

We use the approximations of Apollo Note No. 7 (which assume x and y small with respect to R) to obtain Equation (3) of Apollo Note No. 101:

$$\begin{aligned}
x &= \left[\frac{4\dot{x}_o}{\omega} + 6y_o\right] \sin \omega t + \frac{2\dot{y}_o}{\omega} \cos \omega t - \left[6y_o + \frac{3\dot{x}_o}{\omega}\right] \omega t + x_o - \frac{2\dot{y}_o}{\omega} \\
y &= \frac{\dot{y}_o}{\omega} \sin \omega t - \left[\frac{2\dot{x}_o}{\omega} + 3y_o\right] \cos \omega t + 4y_o + \frac{2\dot{x}_o}{\omega} \\
\dot{x} &= \left[4\dot{x}_o + 6\omega y_o\right] \cos \omega t - 2\dot{y}_o \sin \omega t - 6\omega y_o - 3\dot{x}_o \\
\dot{y} &= \dot{y}_o \cos \omega t + \left[2\dot{x}_o + 3\omega y_o\right] \sin \omega t
\end{aligned} \tag{2}$$

As previously explained, Equation (2) is the approximate solution of:

$$\ddot{\bar{r}} + 2(\bar{\omega} \times \dot{\bar{r}}) + \bar{\omega} \times (\bar{\omega} \times \bar{r}) = -\frac{\mu}{r^3} \bar{r};$$

the equation of motion in the rotating co-ordinate system.

Calculation of the Covariance Matrix

To obtain the covariance matrix of the maximum likelihood estimators of the orbit parameters, we need the four terms:

$$\frac{\partial u}{\partial x_o}, \quad \frac{\partial u}{\partial y_o}, \quad \frac{\partial u}{\partial \dot{x}_o}, \quad \frac{\partial u}{\partial \dot{y}_o} \quad ;$$

again as explained on page 5 of Apollo Note No. 43.

From Equation (2),

$$\frac{\partial x}{\partial x_o} = 1 \qquad \frac{\partial y}{\partial x_o} = 0$$

$$\frac{\partial x}{\partial y_o} = 6 (\sin \omega t - \omega t) \qquad \frac{\partial y}{\partial y_o} = 4 - 3 \cos \omega t$$

$$\frac{\partial x}{\partial \dot{x}_o} = \frac{4}{\omega} \sin \omega t - 3 t \qquad \frac{\partial y}{\partial \dot{x}_o} = \frac{2}{\omega} (1 - \cos \omega t) \qquad (3)$$

$$\frac{\partial x}{\partial \dot{y}_o} = \frac{2}{\omega} (\cos \omega t - 1) \qquad \frac{\partial y}{\partial \dot{y}_o} = \frac{1}{\omega} \sin \omega t$$

Then from Equation (1),

$$\frac{\partial u}{\partial x_o} = \cos \omega t \frac{\partial y}{\partial x_o} - \sin \omega t \frac{\partial x}{\partial x_o}$$

$$\frac{\partial u}{\partial y_o} = \cos \omega t \frac{\partial y}{\partial y_o} - \sin \omega t \frac{\partial x}{\partial y_o}$$

$$\frac{\partial u}{\partial \dot{x}_o} = \cos \omega t \frac{\partial y}{\partial \dot{x}_o} - \sin \omega t \frac{\partial x}{\partial \dot{x}_o}$$

$$\frac{\partial u}{\partial \dot{y}_o} = \cos \omega t \frac{\partial y}{\partial \dot{y}_o} - \sin \omega t \frac{\partial x}{\partial \dot{y}_o} \quad (4)$$

So from Equation (3) and (4), we have:

$$\frac{\partial u}{\partial x_o} = -\sin \omega t$$

$$\frac{\partial u}{\partial y_o} = \cos \omega t (4 - 3 \cos \omega t) - 6 \sin \omega t (\sin \omega t - \omega t)$$

$$\frac{\partial u}{\partial \dot{x}_o} = \frac{2}{\omega} \cos \omega t (1 - \cos \omega t) - \sin \omega t \left(\frac{4}{\omega} \sin \omega t - 3t \right)$$

$$\frac{\partial u}{\partial \dot{y}_o} = \frac{1}{\omega} \sin \omega t (2 - \cos \omega t) \quad (5)$$

Let

$$a_1 = x_o$$

$$a_2 = y_o$$

$$a_3 = \dot{x}_o$$

$$a_4 = \dot{y}_o$$

Then the terms of the information matrix C are given by Equation (7) of Apollo Note No. 101:

$$C_{i,j} = \frac{1}{N} \sum_{k=1}^{N} \frac{\partial u(k)}{\partial a_i} \frac{\partial u(k)}{\partial a_j} \tag{6}$$

For N observations over $t_m = \frac{\pi}{2\omega}$ seconds, we approximate the discrete sum (Equation 6) by the continuous time integral (Equation 7) from zero to t_m:

$$C_{i,j} \approx \frac{1}{t_m} \int_o^{t_m} \frac{\partial u(t)}{\partial a_i} \frac{\partial u(t)}{\partial a_j} \, dt, \tag{7}$$

again as in Apollo Note No. 101. The required information matrix C is then obtained by using Equation (5) in Equation (7) for i, j = 1, 2, 3, 4 to obtain:

C:

$$a_{11} = \frac{1}{2}$$

$$a_{12} = \frac{2}{\pi}\left(\frac{3}{2} - \frac{3\pi^2}{8}\right)$$

$$a_{13} = \frac{1}{8\pi\omega}\left(\frac{76}{3} - 3\pi^2\right)$$

$$a_{14} = \frac{2}{\pi\omega}\left(\frac{1}{3} - \frac{\pi}{2}\right)$$

$$a_{21} = \frac{2}{\pi}\left(\frac{3}{2} - \frac{3\pi^2}{8}\right)$$

$$a_{22} = \frac{1}{\pi}\left(\frac{3\pi^3}{2} + \frac{403\pi}{8} - 192\right)$$

$$a_{23} = \frac{2}{\pi\omega}\left(\frac{3\pi^3}{8} + \frac{115\pi}{8} - 56\right)$$

$$a_{24} = \frac{2}{\pi\omega}\left(\frac{3\pi^2}{4} - \pi - \frac{3}{4}\right)$$

$$a_{31} = \frac{1}{8\pi\omega}\left(\frac{76}{3} - 3\pi^2\right)$$

$$a_{32} = \frac{2}{\pi\omega}\left(\frac{3\pi^3}{8} + \frac{115\pi}{8} - 56\right)$$

$$a_{33} = \frac{2}{\pi\omega^2}\left(\frac{3\pi^3}{16} + \frac{67\pi}{8} - 32\right)$$

$$a_{34} = \frac{1}{\pi\omega^2}\left(\frac{3\pi^2}{4} - \pi - \frac{10}{3}\right)$$

$$a_{41} = \frac{2}{\pi\omega}\left(\frac{1}{3} - \frac{\pi}{2}\right)$$

$$a_{42} = \frac{2}{\pi\omega}\left(\frac{3\pi^2}{4} - \pi - \frac{3}{4}\right)$$

$$a_{43} = \frac{1}{\pi\omega^2}\left(\frac{3\pi^2}{4} - \pi - \frac{10}{3}\right)$$

$$a_{44} = \frac{2}{\pi\omega^2}\left(\frac{17\pi}{16} - \frac{4}{3}\right)$$

Conclusions:

For the nominal lunar orbit (80 n.mi.), we assume 1 observation per minute, with range measurements over 1/4 period = $\frac{\pi}{2\omega}$ seconds. Then for σ_R = 15 meters and N = $\frac{\pi}{120\omega}$ = 31 observations in 1/4 period, we obtain the desired covariance matrix by inverting the information matrix C:

$$\text{Cov}(\hat{a}_i, \hat{a}_j) = \frac{\sigma_R^2}{N} C^{-1},$$

$$\text{Cov}(\hat{a}_i, \hat{a}_j)_R = \begin{array}{c} \begin{matrix} (x_o) & (y_o) & (\dot{x}_o) & (\dot{y}_o) \end{matrix} \\ \begin{pmatrix} 3.143 \times 10^4 m^2 & 1.15 \times 10^3 m^2 & -28.14 & 21.37 \\ 1.15 \times 10^3 m^2 & 98.0 m^2 & -960 \frac{m^2}{sec.} & .684 \frac{m^2}{sec.} \\ -28.14 \frac{m^2}{sec.} & -.960 \frac{m^2}{sec.} & .0258 \frac{m^2}{sec.^2} & -.0194 \frac{m^2}{sec.^2} \\ 21.37 \frac{m^2}{sec.} & .684 \frac{m^2}{sec.} & -.0194 \frac{m^2}{sec.^2} & .0147 \frac{m^2}{sec.^2} \end{pmatrix} \end{array}$$

From Apollo Note No. 101, the covariance matrix for range-rate observations is:

$$\text{Cov}(\hat{a}_i, \hat{a}_j)_{\dot{R}} = \begin{array}{c} \begin{matrix} (y_o) & (\dot{x}_o) & (\dot{y}_o) \end{matrix} \\ \begin{pmatrix} 2226.0\ m^2 & -3.4836 \frac{m^2}{sec.} & -0.6841 \frac{m^2}{sec.} \\ -3.4836 \frac{m^2}{sec.} & 55.340 \times 10^{-4} \frac{m^2}{sec.^2} & 9.9362 \times 10^{-4} \frac{m^2}{sec^2} \\ -0.6841 \frac{m^2}{sec.} & 9.9362 \times 10^{-4} \frac{m^2}{sec.^2} & 2.9501 \times 10^{-4} \frac{m^2}{sec.^2} \end{pmatrix} \end{array}$$

where it will be recalled that the x_o covariance terms could not be computed, since the corresponding terms in the $\dot{R}$ information matrix were zero.

APOLLO NOTE NO. 103

H. Dale
12 September 1963

STATISTICS OF MINIMUM RENDEZVOUS RANGE

Previous Apollo notes have been concerned with estimating the error in LEM position at the time of nominal rendezvous (see Notes 85, 95 and 100). Although the relative range is a minimum (in fact zero) at the time of nominal rendezvous for no errors in the LEM orbit, some other time may yield minimum range when errors exist. A sketch of such a situation is shown below.

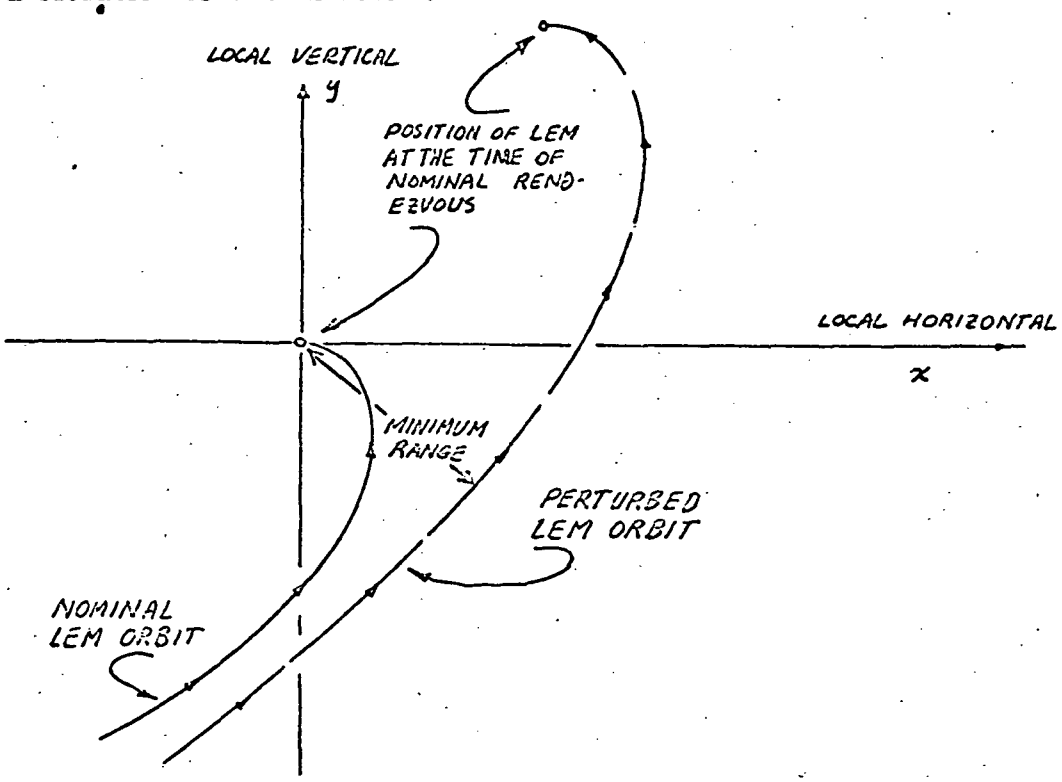

Sketch of LEM position in CM/SM Centered Coordinates for Nominal and Off-Nominal LEM Trajectory

It is the purpose of this note to calculate the variance in the minimum miss or range as a function of the covariance matrix of the errors in the orbit parameters at the termination of ascent boost, (LEM perilune).

Defining:

t = time since perilune

t_o = nominal time of rendezvous

τ = time since nominal rendezvous

$R(\tau)$ = relative range between LEM and CM/SM at τ.

ΔV = nominal horizontal injection velocity at rendezvous

ω = angular velocity of the CM/SM orbit

Then from Note 7 an expression for the nominal position of the LEM with respect to the CM/SM can be written:

$$\overrightarrow{N(\tau)} = \frac{2\,\Delta V}{\omega}\left(\frac{3\omega\tau}{2} - 2\sin\omega\tau\right)\hat{i} + \frac{2\,\Delta V}{\omega}(\cos\omega\tau - 1)\hat{j} + o\,\hat{k} \qquad (1)$$

Where the i , j , and k directions correspond to range along the local horizontal, altitude, and track respectively in a right-handed system. The parameter of the LEM orbit are $a_1, a_2, \ldots, a_6$ as defined in Note No. 82, and thus errors in these parameters may be defined as Δa_1, Δa_2, $\Delta a_3, \ldots, \Delta a_6$. These errors will cause errors in the position and velocity of the LEM at the nominal time of rendezvous, $J(t_o)\,\Delta a_i$.

Thus

$$J(t_o)\,ai = \begin{bmatrix} \frac{\partial x(t_o)}{\partial a_1}, & \frac{\partial x(t_o)}{\partial a_2} \text{ ----- } & \frac{\partial x(t_o)}{\partial a_6} \\ \frac{\partial y(t_o)}{\partial a_1}, & \text{----------} & \\ \frac{\partial z(t_o)}{\partial a_1}, & \text{----------} & \\ \frac{\partial \dot{x}(t_o)}{0\, a_1}, & \text{----------} & \\ \frac{\partial \dot{y}(t_o)}{\partial a_1}, & \text{----------} & \\ \frac{\partial \dot{z}(t_o)}{\partial a_1}, & \text{----------}, & \frac{\partial z(t_o)}{\partial a_6} \end{bmatrix} \begin{bmatrix} \Delta a_1 \\ \Delta a_2 \\ \Delta a_3 \\ \Delta a_4 \\ \Delta a_5 \\ \Delta a_6 \end{bmatrix} = \begin{bmatrix} x_o \\ y_o \\ z_o \\ \dot{x}_o \\ \dot{y}_o \\ \dot{z}_o \end{bmatrix} \tag{2}$$

Where $J(t_o)$ is a Jacobian evaluated at the nominal time of rendezvous and x_o, -------$\dot{z}_o$ are the errors in position and velocity of the LEM at the nominal time of rendezvous, t_o. Now for any time, τ, later than t_o(or earlier for - τ) the components x_o, --- $\dot{z}_o$ may be used as initial conditions to calculate the position of the LEM with respect to the nominal position of the LEM at τ through the use of Equations (11) and (12) from Note No. 7.

$$\left.\begin{aligned} \overrightarrow{M(\tau)} = &\left\{\left[\frac{4\dot{x}_o}{\omega} + 6y_o\right]\sin\omega\tau + \frac{2\dot{y}_o}{\omega}\cos\omega\tau - \left[6y_o + \frac{3\dot{x}_o}{\omega}\right]\omega\tau + x_o - \frac{2y_o}{\omega}\right\}\hat{i} \\ &+\left\{\frac{\dot{y}_o}{\omega}\sin\omega\tau - \left[\frac{2\dot{x}_o}{\omega} + 3y_o\right]\cos\omega\tau + 4y_o = \frac{2\dot{x}_o}{\omega}\right\}\hat{j} \\ &+\left\{\dot{z}_o = \frac{\dot{z}_o}{\omega}\sin\omega\tau\right\}\hat{k} \end{aligned}\right\} \tag{3}$$

Now

$$\overrightarrow{R(\tau)} = \overrightarrow{N(\tau)} + \overrightarrow{M(\tau)} \tag{4}$$

or

$$\overrightarrow{R(\tau)} = \left\{\left[\frac{4(\dot{x}_o - \Delta V)}{\omega} + 6y_o\right]\sin\omega\tau + \frac{2\dot{y}_o}{\omega}\cos\omega\tau - \left[6y_o + \frac{3(\dot{x}_o - \Delta V)}{\omega}\right]\omega\tau + x_o - \frac{2\dot{y}_o}{\omega}\right\}\hat{i}$$

$$+ \left\{\frac{\dot{y}_o}{\omega}\sin\omega\tau - \left[\frac{2(\dot{x}_o - \Delta V)}{\omega} + 3y_o\right]\cos\omega\tau + 4y_o + \frac{2(\dot{x}_o - \Delta V)}{\omega}\right\}\hat{i} \qquad (5)$$

$$+ \left\{z_o + \frac{\dot{z}_o}{\omega}\sin\omega\tau\right\}\hat{k}$$

Now $R(\tau)$ reaches $R_{min}(\tau)$ when $\frac{dR}{d\tau} = 0$, or when

$$\frac{dR(\tau)^2}{d\tau} = 0 = 2R\frac{dR}{dt} = 2(R_x\dot{R}_x + R_y\dot{R}_y + R_z\dot{R}_z) \qquad (6)$$

Where

$$\dot{R}_x = \left[4(\dot{x}_o - \Delta V) + 6y_o\omega\right]\cos\omega\tau - 2\dot{y}_o\sin\omega\tau - \left[6y_o\omega + 3x_o - \Delta V)\right]$$

$$\dot{R}_y = \dot{y}_o + \left[2(\dot{x}_o - \Delta V) + 3y_o\omega\right]\sin\omega\tau$$

$$\dot{R}_z = \dot{z}\cos\omega\tau$$

Making first order sine and cosine approximations for small $\omega\tau$ gives

$$R\frac{dR(\tau)}{d\tau} = \left[(\dot{x}_o - \Delta V)\tau + x_o\right]\left[(\dot{x}_o - \Delta V) - 2y_o\omega\tau\right] \qquad (7)$$

$$+ \left[y_o + \dot{y}_o\tau\right]\left[\dot{y}_o + \left\{2\left[\dot{x}_o - \Delta V\right] + 3y_o\omega\right\}\omega\tau\right]$$

$$+ \left[z_o + \dot{z}_o\tau\right]\left[\dot{z}_o\right] = 0$$

Now in general, this equation should be solved for $\tau = \tau_o$ should then be used to generate R_{min}. In actual practice x_o, y_o, and z_o would be on the order of 10^3 to 10^4 meters, while $\dot{x}_o$, $\dot{y}_o$, $\dot{z}_o$ would be less than a meter per second. $\omega\tau$ will, in practice, be less than one-hundredth of a radian. Thus an approximate solution of equation (7) is:

$$\tau \cong \frac{X_o}{\Delta V}$$

Using this expression in the first order approximations for R_x, R_y and R_z gives:

$$R^2_{min.} \simeq \left[(\dot{x}_o - \Delta V)\frac{x_o}{\Delta V} + x_o\right]^2 + \left[y_o + \dot{y}_o \frac{x_o}{\Delta V}\right]^2 + \left[z_o + \dot{z}_o \frac{x_o}{\Delta V}\right]^2 \tag{8}$$

Now since ΔV is about 30 meters/sec., while $\dot{x}_o$, $\dot{y}_o$, and $\dot{z}_o$ are less than a meter per second; and further since x_o, y_o, and z_o are all between 10^3 and 10^4 meters per second, then

$$R^2_{min} \simeq y_o^2 + z_o^2 \tag{9}$$

$$= \sum_{i,j=1}^{6} \left[\frac{\partial y(t_o)}{\partial a_i}\frac{\partial y(t_o)}{\partial a_j} + \frac{\partial z(t_o)}{\partial a_i}\frac{\partial z(t_o)}{\partial a_j}\right] \Delta a_i \Delta a_j$$

The variance, $\overline{R^2}_{min}$, of the minimum range is thus expressed either as the sum of y_o^2 and z_o^2 or as a function of the elements of the Jacobian and elements of the covariance matrix at time zero.

APOLLO NOTE NO. 104

J. R. Holdsworth
18 September 1963

THE CALCULATION OF THE COVARIANCE OF ESTIMATOR ERRORS FOR TWO CROSS CORRELATED DATA SOURCES

Apollo note 77 extended note 43 to the case where the orbit parameters were estimated from data obtained from several different sources. In that note it was assumed that the noise processes corrupting the data were statistically independent of one another and that the sources were sampled at equally spaced time intervals which were long with respect to the auto correlation time of the individual noise processes. In this note we consider the case where we have two data sources whose contaminating noise sources may be cross correlated for samples taken at the same instant of time. We do however retain the assumption that the auto correlation of the separate noise processes may be neglected as well as any cross correlation for non zero time lags. Furthermore, for notational ease we shall neglect any systematic bias errors which may exist in either the range or range-rate data.

Specifically we shall assume that there are certain parameters a_i, $i = 1, 2, \ldots 6$ which we wish to estimate on the basis of our observed data. We also assume that we have available range and range-rate data which we denote by R and $\dot{R}$ and that in the absence of noise that R and $\dot{R}$ may be written as invertible functions of the parameters of interest.

As in Apollo Note No. 77 we assume that we may write:

$$R_m(t) = R_c(a_i, t) + n_R(t)$$

$$\dot{R}_m(t) = \dot{R}_c(a_i, t) + n_{\dot{R}}(t) \qquad (1)$$

In Equation (1) the quantities subscripted m are the measured quantities, the quantities subscripted c refer to the correct functional values if the data were not corrupted by noise and $n_R(t)$, $n_{\dot{R}}(t)$ indicate the additive random noise.

We shall assume that $n_R(t)$, $n_{\dot{R}}(t)$ are zero mean gaussian processes with variances σ_R^2, $\sigma_{\dot{R}}^2$ respectively which are not auto-correlated in time. Furthermore, we assume that for a fixed instant of time that $n_R(t)$, $n_{\dot{R}}(t)$ are jointly distributed according to a bivariate gaussian distribution with cross-correlation coefficient ρ. We also assume that the correlation is memory-less in the sense that $n_R(t_i)$ and $n_{\dot{R}}(t_k)$ are not correlated unless $t_i = t_k$.

From what has just been said, it follows from Equation (1) that if we have N measurements of R and $\dot{R}$ that we may write the following expression for the joint likelihood function of the data:

$$L = \frac{1}{(2\pi)^N \sigma_R^N \sigma_{\dot{R}}^N (1-\rho^2)^{\frac{N}{2}}} \exp - \mathcal{L} \tag{2}$$

where:

$$\mathcal{L} = \frac{1}{2(1-\rho^2)} \sum_{k=1}^{N} \left[\left(\frac{R_m(t_k) - R_c(a_i t_k)}{\sigma_R} \right)^2 - 2\rho \left(\frac{R_m(t_k) - R_c(a_i, t_k)}{\sigma_R} \right) \left(\frac{\dot{R}_m(t_k) - \dot{R}_c(a_i, t_k)}{\sigma_{\dot{R}}} \right) + \left(\frac{\dot{R}_m(t_k) - \dot{R}_c(a_i, t_k)}{\sigma_{\dot{R}}} \right)^2 \right] \tag{3}$$

As before the maximum likelihood estimates of the parameters a_i are those functions of the data which maximize the likelihood function. They are obtained by solving the equations:

$$\frac{\partial \mathcal{L}}{\partial a_i} = 0 \qquad i = 1, \ldots 6 \tag{4}$$

for the parameters a_i as functions of the observed data R_m, $\dot{R}_m$.

Performing the indicated differentiations and substituting into Equation (4) we obtain:

$$\frac{1}{\sigma_R^2}\sum_{k=1}^{N}\left[R_m(t_k) - R_c(t_k)\right]\frac{\partial R_c(t_k)}{\partial a_i} - \frac{\rho}{\sigma_R \sigma_{\dot{R}}}\sum_{k=1}^{N}\left[\left[R_m(t_k) - R_c(t_k)\right]\frac{\partial \dot{R}_c}{\partial a_i}\right.$$

$$\left. + \left[\dot{R}_m(t_k) - \dot{R}_c(t_k)\right]\frac{\partial R_c(t_k)}{\partial a_i}\right] \qquad i = 1, 2 \ldots 6$$

$$+ \frac{1}{\sigma_{\dot{R}}^2}\sum_{k=1}^{N}\left[\dot{R}_m(t_k) - \dot{R}_c(t_k)\right]\frac{\partial \dot{R}_c(t_k)}{\partial a_i} = 0$$

The functional forms R_c, $\dot{R}_c$ are known as are the observed data points $R_m(t_k)$, $\dot{R}_m(t_k)$. The solutions $\hat{a}_i$ of this system of equations in terms of the observed data are the maximum likelihood estimators of the parameters a_i.

Assuming that N is sufficiently large we write:

$$\hat{a}_i = a_i + \Delta a_i .$$

where the Δa_i are sufficiently small so that only first order terms in these random perturbations need be retained in various series expansions. This assumption is asymptotically exact as the number of independent samples increases.

Utilizing the above assumptions we write the following approximations.

$$R_c(\hat{a}_i, t_k) = R_c(a_i, t_k) + \sum_{i=1}^{6}\frac{\partial R_c(t_k)}{\partial a_i}\Delta a_i$$

$$\dot{R}_c(a_i, t_n) = \dot{R}_c(a_i, t_n) + \sum_{i=1}^{6}\frac{\partial \dot{R}_c(t_k)}{\partial a_i}\Delta a_i$$

$$\frac{\partial R_c(\hat{a}_i, t_k)}{\partial a_i} \approx \frac{\partial R_c(a_i, t_k)}{\partial a_i}, \quad \frac{\partial \dot{R}_c(\hat{a}_i, t_k)}{\partial a_i} \approx \frac{\partial \dot{R}_c(a_i, t_k)}{\partial a_i}$$

Substituting Equation (7) into Equation (5) and performing some tedious but routine algebra yields the following system of equations which is linear in the random perturbation quantities Δa_i

$$C \ \Delta a = e$$

In Equation (8) Δa is the error column vector whose components are $\Delta a_1 \ldots \Delta a_6$. C is a 6 by 6 matrix whose i, j th element is

$$C_{ij} = \sum_{k=1}^{N} \left[\frac{1}{\sigma_R^2} \frac{\partial R_c(t_k)}{\partial a_i} \frac{\partial R_c(t_k)}{\partial a_j} - \frac{\rho}{\sigma_R \sigma_{\dot{R}}} \frac{\partial \dot{R}_c(t_k)}{\partial a_i} \frac{\partial R_c(t_k)}{\partial a_j} \right.$$

$$\frac{\rho}{\sigma_R \sigma_{\dot{R}}} \frac{\partial R_c(t_k)}{\partial a_i} \frac{\partial \dot{R}_c(t_k)}{\partial a_i}$$

$$\left. + \frac{1}{\sigma_{\dot{R}}^2} \frac{\partial \dot{R}_c(t_k)}{\partial a_i} \frac{\partial \dot{R}_c(t_k)}{\partial a_j} \right]$$

Similarly, e is a six-dimensional column matrix whose ith component is given by:

$$e_i = \sum_{k=1}^{N} \left[\frac{1}{\sigma_R^2} \frac{\partial R_c(t_k)}{\partial a_i} n_R(t_k) - \frac{\rho}{\sigma_R \sigma_{\dot{R}}} \frac{\partial \dot{R}_c(t_k)}{\partial a_i} n_R(t_k) \right.$$

$$\left. - \frac{\rho}{\sigma_R \sigma_{\dot{R}}} \frac{\partial R_c(t_k)}{\partial a_i} n_{\dot{R}}(t_k) + \frac{1}{\sigma_{\dot{R}}^2} \frac{\partial \dot{R}(t_k)}{\partial a_i} n_{\dot{R}}(t_k) \right]$$

Again as in Apollo Note No. 77 it follows that we may write our desired covariance matrix as:

$$\text{Cov}(\hat{a}_i, \hat{a}_j) = E\left[\Delta a \ \Delta a^T\right] = C^{-1} E(e e^T) C^{-1}$$

where the superscript T is matrix transposition and E is the expected value operator.

The assumptions we have made about the noise processes imply the following relations:

$$
\begin{aligned}
E\left[n_R(k)\, n_R(\ell)\right] &= \delta_{k\ell}\sigma_R^2 \\
E\left[\dot{n}_R(k)\, \dot{n}_R(\ell)\right] &= \delta_{k\ell}\dot{\sigma}_R^2 \\
E\left[n_R(k)\, \dot{n}_R(\ell)\right] &= \delta_{k\ell}\rho\,\sigma_R\dot{\sigma}_R
\end{aligned}
\tag{12}
$$

Using the above expressions and computing the expected value of the matrix $e\, e^T$ we find once again that

$$E\ (e\ e^T) = C \tag{13}$$

Thus we have the following expression for our desired covariance matrix:

$$\mathrm{Cov}\ (\hat{a}_i,\ \hat{a}_j) = C^{-1} \tag{14}$$

where the elements of C are given explicity by Equation (9).

APOLLO NOTE NO. 105

C. Siska
13 September 1963

NORMAL DISPLACEMENTS FROM RECTILINEAR TRAJECTORIES

Introduction

In Apollo Notes No. 87, 90 and 97, one observes that the preferred direction from the ΔV application to the Far-Side Relay is roughly perpendicular and to the left of the CSM velocity vector. At the time the CSM enters the LSOI (lunar sphere of influence), this ΔV application has caused the Far-Side Relay to be displaced approximately normal to the CSM position (i. e., the two locations have approximately the same radius magnitude from the Earth).

If one assumes that the CSM trajectory can be approximated by a rectilinear path, then the normal displacement of the Far-Side Relay can be described by a particularly simple expression. This is shown in the following analysis.

Analysis

The geometry of the situation is illustrated in Figure 1. When the radial distance of the CSM is r_o, a small velocity increment, ΔV, is applied normal to the CSM velocity vector V. Since the time history along the resulting paths is approximately the same, at a given time, the radial position on each trajectory is approximately the same. Consequently the normal displacement can be written (since the angle δ is quite small),

$$x \approx r_1 \delta \tag{1}$$

Since the eccentricity e of the Far-Side Relay trajectory is near unity, the phase angle from perigee can be written,

$$\cos \phi = \frac{1}{e} (p/r - 1) \approx \frac{p}{r} - 1 \tag{2}$$

However, the angle ϕ will be close to 180°, so that letting

$$\phi = \pi - w \tag{3}$$

and combining Equations (2) and (3) results in the approximate relation,

$$\cos(\pi - w) = -\cos w \approx -\left(1 - \frac{w^2}{2}\right) \approx -\left(1 - \frac{p}{r}\right)$$

or

$$w^2 \approx \frac{2p}{r} \tag{4}$$

Since the angle δ is $\phi_1 - \phi_o$, combining Equations (1), (3), and (4) yields,

$$x \approx r_1 (w_o - w_1) \approx r_1 \left(\sqrt{\frac{2p}{r_o}} - \sqrt{\frac{2p}{r_1}}\right) \tag{5}$$

In terms of the angular momentum,

$$\frac{p}{r_o} = \left(\frac{H^2}{u}\right)\left(\frac{1}{r_o}\right) \tag{6}$$

and since $H = r_o \Delta V$ and $u = g R^2$, Equation (6) becomes

$$\frac{p}{r_o} = \left(\frac{\Delta V}{\sqrt{gR}}\right)^2 \frac{r_o}{R} \tag{7}$$

Combining Equations (5) and (7), then yields the desired relation for normal displacement,

$$x = r_1 \sqrt{\frac{2r_1}{R}} \left(\frac{\Delta V}{\sqrt{gR}}\right) \sqrt{\frac{r_o}{r_1}} \left(1 - \sqrt{\frac{r_o}{r_1}}\right) \tag{8}$$

Note that the factor $\frac{r_1}{\sqrt{gR}} \sqrt{\frac{2r_1}{R}}$ is the approximate parabolic flight time to r_1, if $r_o << r_1$.

The maximum displacement, x_{max}, occurs when $\frac{r_o}{r_1} = \frac{1}{4}$ resulting in:

$$x_{max} = r_1 \sqrt{\frac{r_1}{8R}} \left(\frac{\Delta V}{\sqrt{gR}}\right) \tag{9}$$

Letting r_1 = 208,000 n.mi., the Earth-Moon radius yields a value $\frac{x_{max}}{\Delta V} \approx 22 \frac{\text{n.mi.}}{\text{ft/sec.}}$ at a value of r_o = 52,000 n.mi.

Figure 2 shows a comparison between the results of using Equation (8) and the values obtained using the nominal trajectory of Apollo Notes No. 87, 90, and 97. For the latter trajectory, the direction of ΔV is taken to be $\alpha = -90^\circ$, which yields a perpendicular direction to the left of the velocity vector at radius r_o.

The value of r_1 is taken to be 191,000 n.mi., approximately the radius when the CSM enters the LSOI.

It seems surprising that the best agreement in Figure 2 occurs at low values of r_o where the velocity vector for the nominal trajectory is oriented approximately 70° from the local vertical. On the other hand, at values of r_o around 50,000 n.mi., the orientation is but 15° from the local vertical which starts to approximate rectilinearity, but here, the comparison is poorest. Evidently the agreement at small r_o is fortuitous and the assumption of a rectilinear CSM trajectory is not adequate to calculate normal displacements for a range of initial conditions involving the application of ΔV.

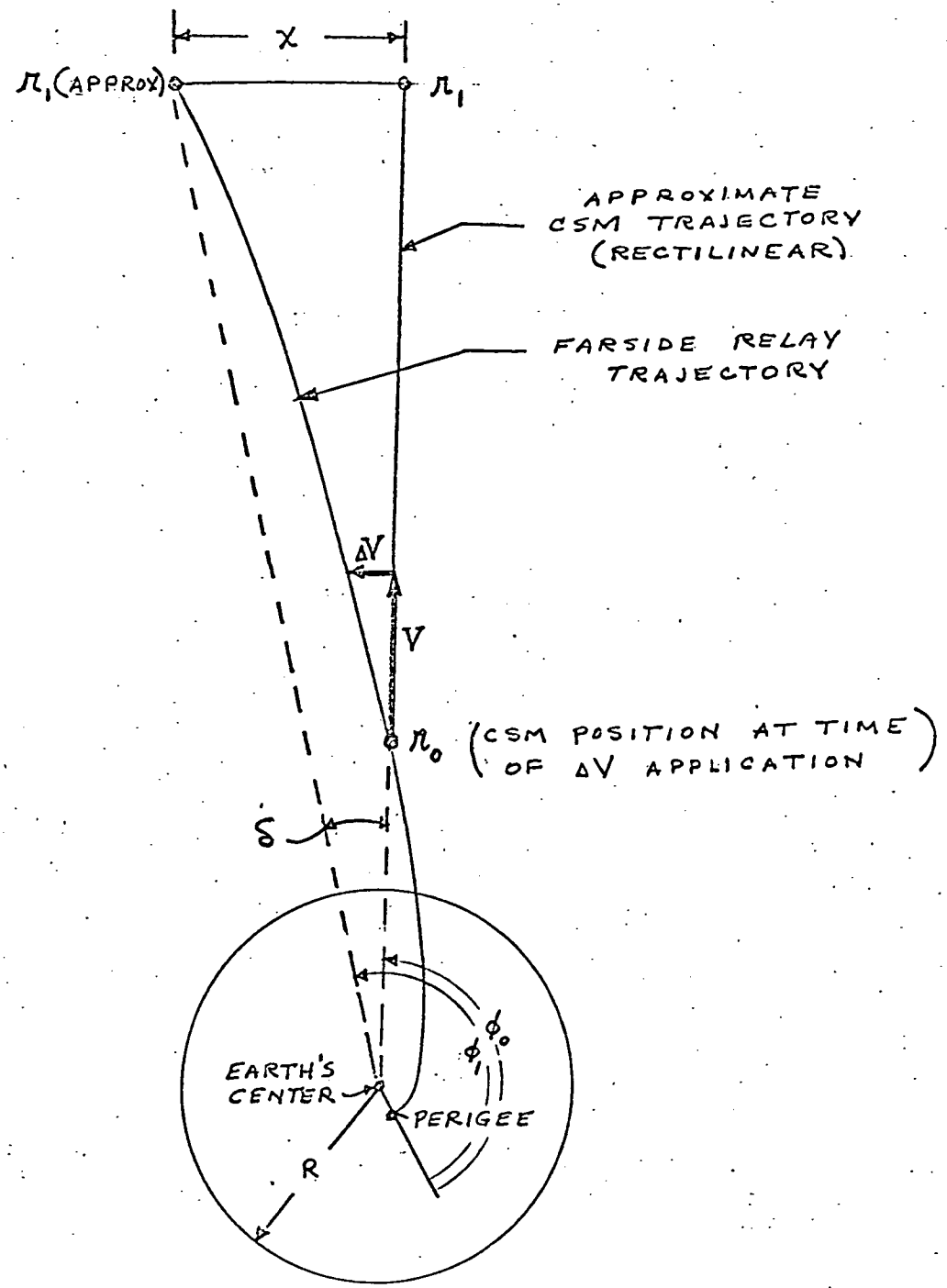

Figure 1.

Schematic Diagram of Trajectory Geometry

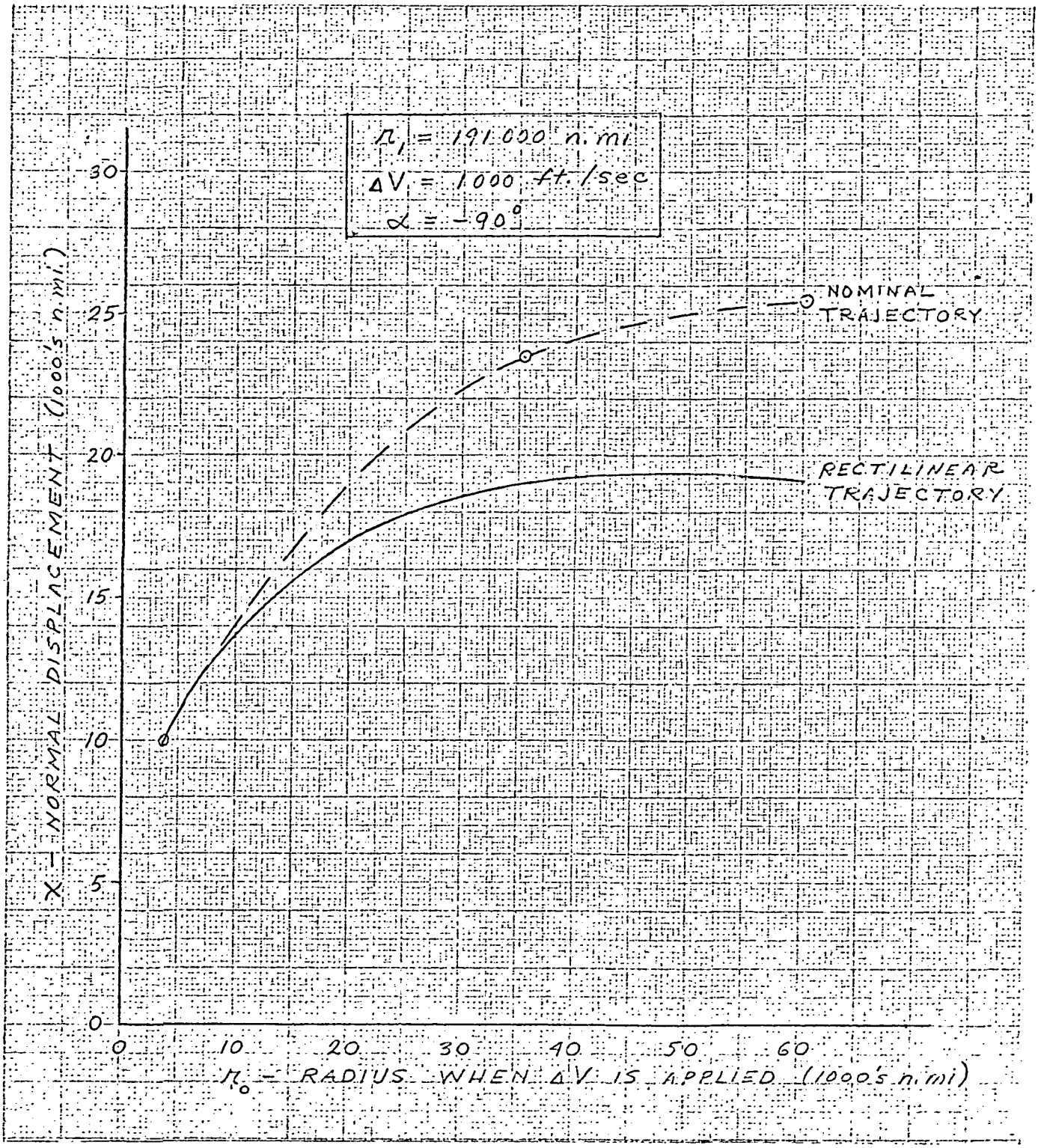

Figure 2.

Comparison of Far-Side Relay Displacements For Nominal and Rectilinear CSM Trajectories

APOLLO NOTE NO. 106

G. F. Floyd
16 September 1963

BISSETT-BERMAN (NASA) PRESENTATION
September 16, 1963

	1.	Bissett-Berman Study Effort.
	2.	Angle vs. Range Data.
Results	3.	Assumed Measurement Errors.
	4.	Measurement Errors.
	5.	First LEM Rendezvous Results.
	6.	1 Station Curves.
	7.	2 Station Curves.
	8.	3 Station Curves.
	9.	Mid-course Correction Case.
	10.	MSFN Conclusions Regarding LEM Rendezvous.
	11.	Best R $\dot{R}$ Station Locations.
	12.	Approximate CSM Return Results.
Computer Program	13.	Maximum Likelihood Estimates.
	14.	Calculation of $\frac{\partial f_i}{\partial a_j}$.
	15.	Computer Program.
	16.	Program Capabilities.
	17.	New Studies.

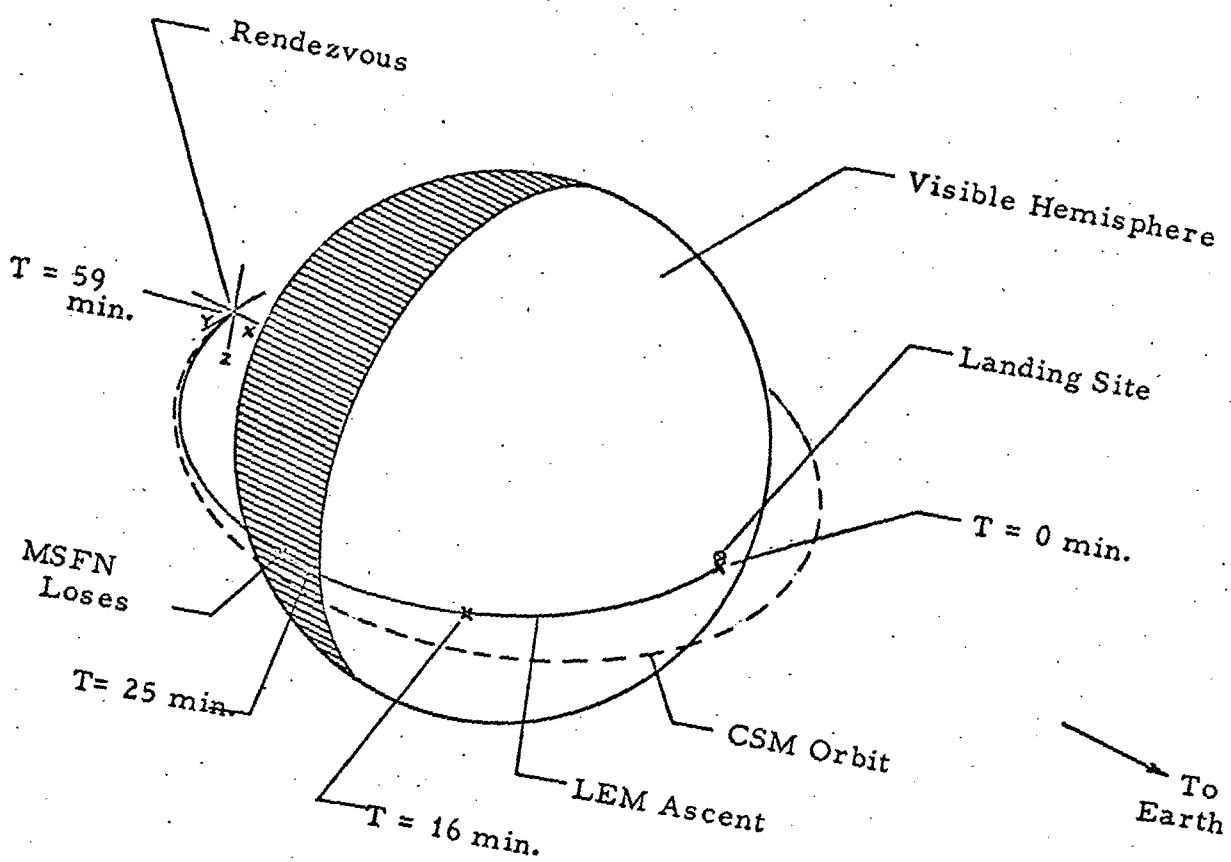
Rendezvous
Visible Hemisphere
T = 59 min.
Y
X
Z
Landing Site
T = 0 min.
MSFN Loses
T= 25 min.
CSM Orbit
To Earth
LEM Ascent
T = 16 min.

THE BISSETT-BERMAN STUDY

MAGNITUDE

10 men for 6 months

OBJECTIVE

Evaluate Capabilities of MSFN for

Apollo Guidance and Navigation

STATUS

1. R and R Program Working

2. First LEM Rendezvous Results

ANGLE VERSUS RANGE DATA

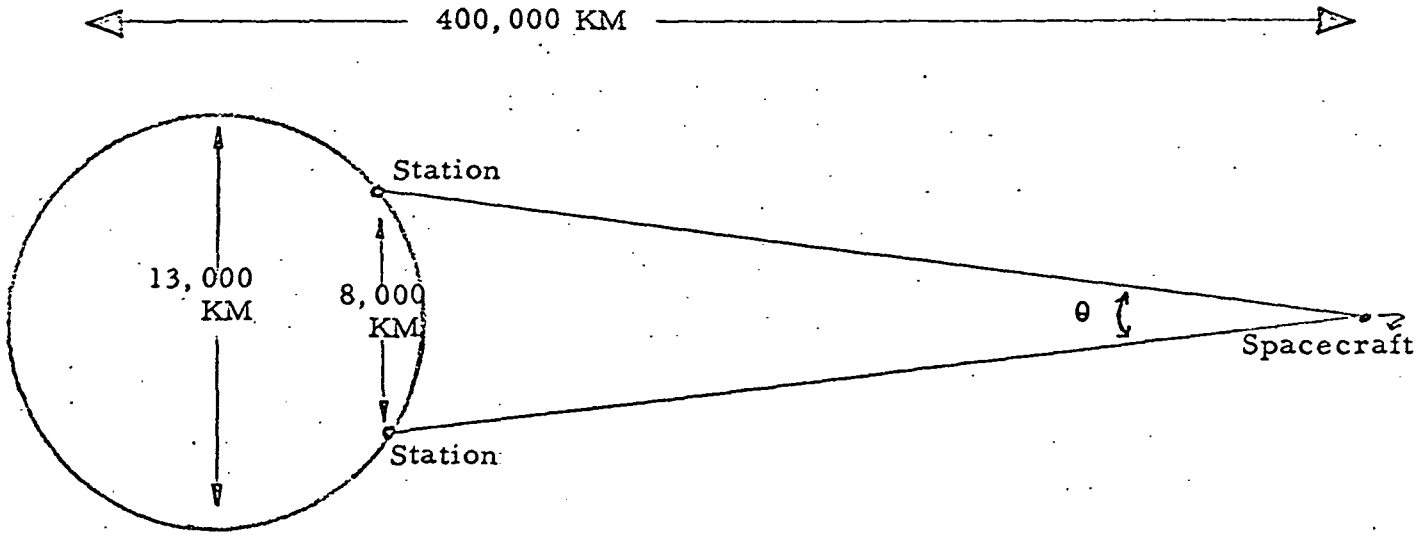

15 m Range $\quad \Delta P_R = \sqrt{2}\ \frac{\Delta R}{\sin\theta} = 21\ \frac{400,000}{8,000} = 1100\,m = 1\ KM$

0.1 mil Angle $\quad \Delta P_{angle} = R\,\delta = 400,000 \times 10^{-4} = 40\ KM$

$$\Delta P_{angle} \approx 40\ \Delta P_R$$

ASSUMED MEASUREMENT ERRORS (1 σ)

RANGE: 15 meters with 1 minute correlation time

RANGE-RATE: 3 cm/sec. with 1 minute correlation time

A Priori (telemetered) on each component:

- At Injection
  - Position: 1 km
  - Velocity: 3 m/sec.

Midcourse: 1 m/sec.

MEASUREMENT ERRORS

For Fixed Observation Time: Miss $\alpha\ \sigma_{meas.}\sqrt{t_{corr.}}$

	Range	Range-Rate
Used	15 m $\sqrt{60\ sec.}$ = 115	3 cm/sec. $\sqrt{60\ sec}$ = 23
SYNCOM I (Short Range)	19 $\sqrt{1.2}$ = 20 = 1/6 used	4 $\sqrt{1.2}$ = 4 1/2 = 1/5 used
MARINER II (Long Range L-Band)	Did not have	0.5 $\sqrt{60}$ = 4 = 1/5 used

FIRST LEM RENDEZVOUS RESULTS

1. Errors in all predicted velocity components negligible (less than 0.1 m/sec.).

2. Error in time of closest approach negligible (less than 30 sec.).

3. Predicted Miss error components in altitude and out-of-plane are of comparable magnitude.

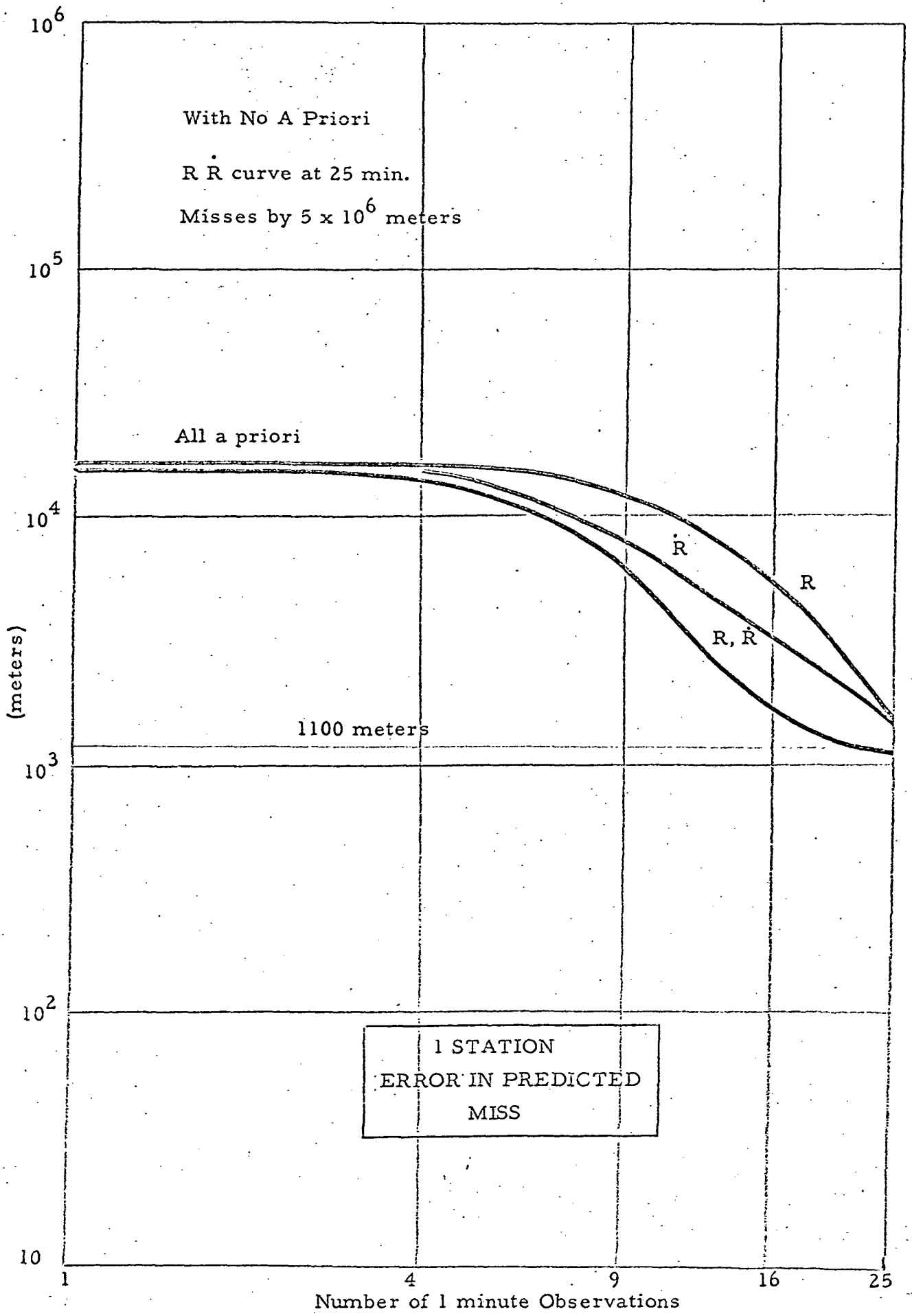
With No A Priori
$\dot{R}$ R curve at 25 min.
Misses by 5 x 10^6 meters
All a priori
$\dot{R}$
R
R, $\dot{R}$
1100 meters
1 STATION
ERROR IN PREDICTED
MISS
10^6
10^5
10^4
10^3
10^2
10
(meters)
1
4
9
16
25
Number of 1 minute Observations

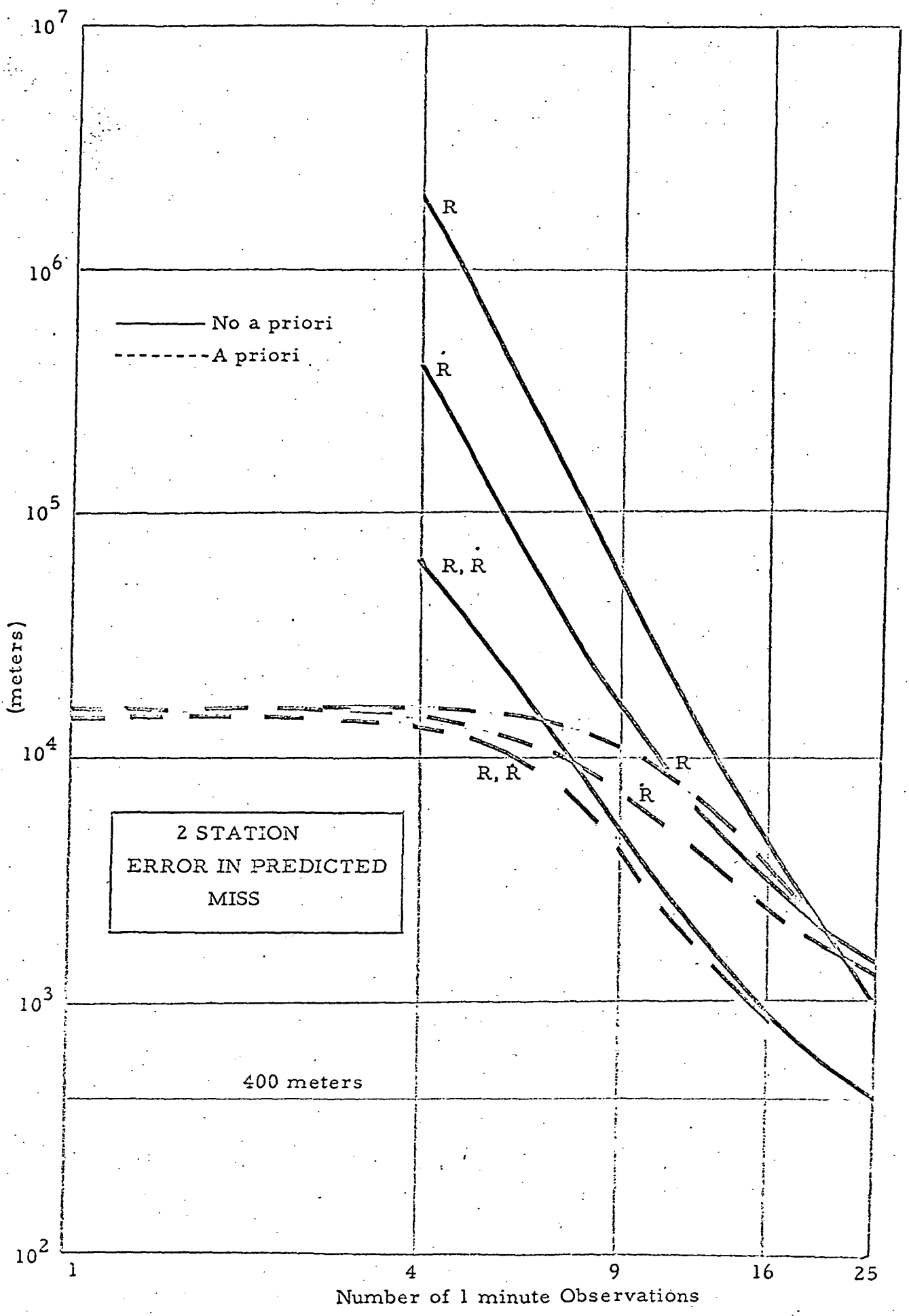
10^7
10^6
10^5
10^4
10^3
10^2
(meters)
No a priori
A priori
R
$\dot{R}$
R, $\dot{R}$
R, $\dot{R}$
R
$\dot{R}$
2 STATION
ERROR IN PREDICTED
MISS
400 meters
1
4
9
16
25
Number of 1 minute Observations

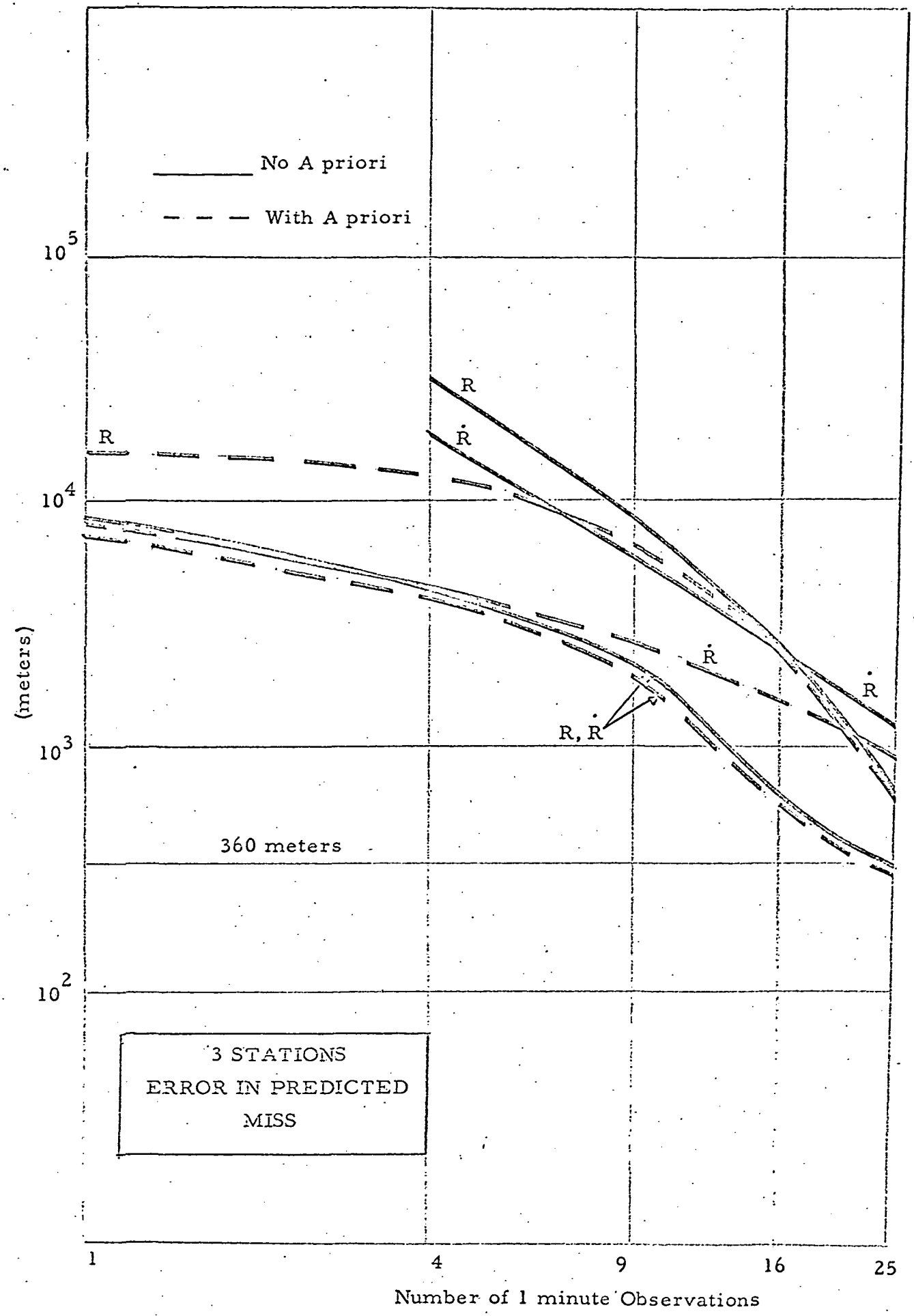
No A priori
With A priori
10^5
10^4
10^3
10^2
(meters)
R
$\dot{R}$
R
$\dot{R}$
$\dot{R}$
R, $\dot{R}$
$\dot{R}$
360 meters
3 STATIONS
ERROR IN PREDICTED
MISS
1
4
9
16
25
Number of 1 minute Observations

MID-COURSE CORRECTION CASE

ASSUMPTIONS:

3 R $\dot{R}$ Stations

Observe for 16 minutes

1 m/s Boost Error each component

Observe for 9 minutes more

Error in Predicted Miss = 790 m

MSFN CONCLUSIONS REGARDING LEM RENDEZVOUS

1. At assumed error values, R and $\dot{R}$ equally useful and combination (R $\dot{R}$) significantly better than either alone.

2. Single R $\dot{R}$ station marginal even with telemetered data.

3. Telemetered data not essential with 2 or more stations.

4. Velocity prediction better than 1/10 m/sec.

5. Two R $\dot{R}$ stations (North and South pair) good with docking boxes of 2000 meters after 12 minutes and 400 meters after 25 minutes.

6. Believe above numbers are 4 or 5 σ cases.

BEST R Ṙ STATION LOCATIONS

Goldstone	-	Pitcairn Island (British)
Guam	-	Canberra
Madrid	-	Ascension Island

APPROXIMATE CSM RETURN RESULTS

(1 Station, $\dot{R}$ only, 10% Execution Accuracy)

Time to go (hours)	MSFN Uncertainty in Re-entry Angle (degrees)	Error in Mid-Course Correction Execution m/sec.	Resultant Error in Re-entry Angle (degrees)
72	---	100	450
50	1.1	18	45
36	1.1	2	4.6
24	.7	0.3	.8
16	.3	0.1	.3
8	.09	0.05	.09
2	.02	- -	- -

MAXIMUM LIKELIHOOD ESTIMATES

$$\mathcal{L}(a) = K\, e^{-\frac{\sum_1^N (m_i - f_i(a))^2}{2\sigma_m^2}} \cdot e^{-\frac{(a' - a)^2}{2\sigma_p^2}}$$

$$\frac{\partial \mathcal{L}}{\partial a} = 0 = \frac{1}{\sigma_m^2} \sum_1^N (m_i - f_i(a)) \frac{\partial f_i}{\partial a} + \frac{a' - a}{\sigma_p^2}$$

Let

$$a \triangleq a_t + \Delta; \quad a' \triangleq a_t + \Delta',$$

$$f_i(a) = f_i(a_t) + \frac{\partial f_i}{\partial a_t} \Delta; \quad \frac{\partial f_i}{\partial a} = \frac{\partial f_i}{\partial a_t}$$

So,

$$m_i - f_i(a_t) = n_i$$

$$\Delta = \frac{\frac{\Delta'}{\sigma_p^2} + \frac{1}{\sigma_p^2} \sum_1^N n_i \frac{\partial f_i}{\partial a_t}}{\frac{1}{\sigma_p^2} + \frac{1}{\sigma_m^2} \sum_1^N \left(\frac{\partial f_i}{\partial a_t}\right)^2}$$

$$\boxed{\frac{1}{\sigma^2} = \frac{1}{\sigma_p^2} + \frac{1}{\sigma_m^2} \sum_1^N \left(\frac{\partial f_i}{\partial a_t}\right)^2}$$

CALCULATION OF $\frac{\partial f_i}{\partial a_j}$

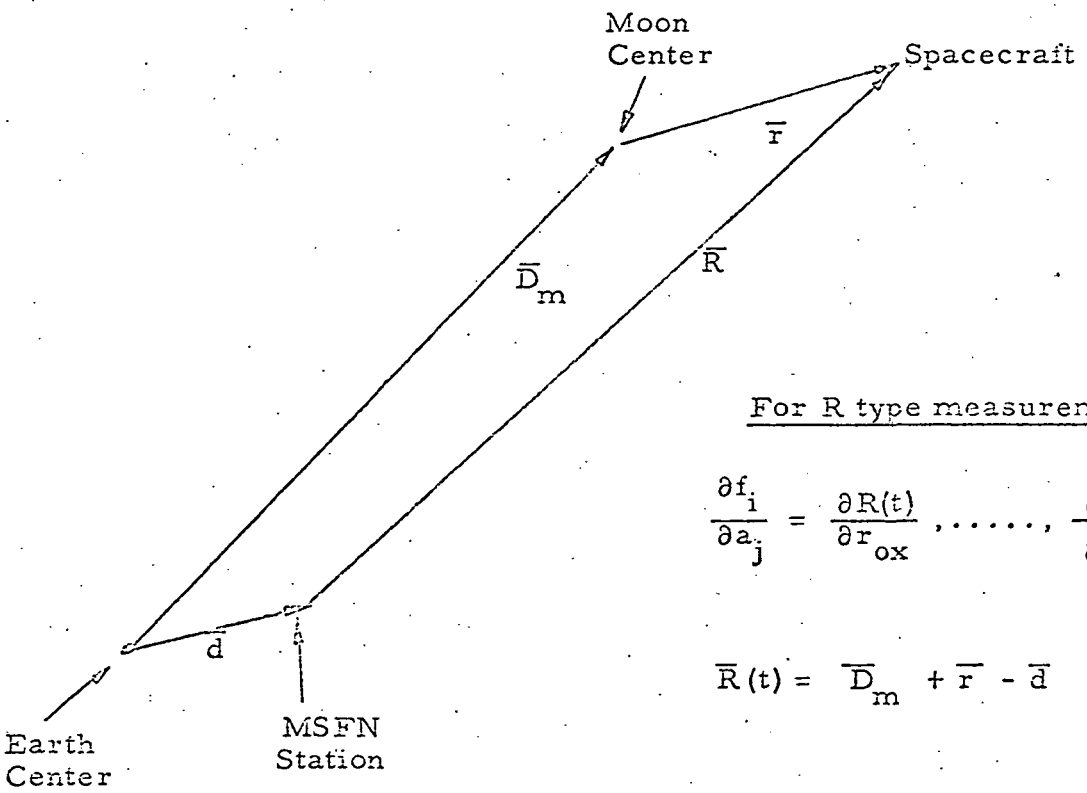

For R type measurements:

$$\frac{\partial f_i}{\partial a_j} = \frac{\partial R(t)}{\partial r_{ox}}, \ldots\ldots, \frac{\partial R(t)}{\partial \dot{r}_{oz}}$$

$$\bar{R}(t) = \bar{D}_m + \bar{r} - \bar{d}$$

$$\ddot{\bar{r}}(t) = -\frac{\mu}{r^3(t)}\,\bar{r}(t)$$

$$\bar{r}(t) = g(\bar{r}_o, \dot{\bar{r}}_o, t)$$

COMPUTER PROGRAM

1. Orbit calculation to get $\bar{r}\ (\bar{r}_o, \dot{\bar{r}}_o, t)$ and $\dot{\bar{r}}\ (r_o, \dot{\bar{r}}_o, t)$

2. Calculate information matrices for each station and each type of data (R, $\dot{R}$, α, β) as functions of observation time.

$$C_{ij} = \sum_t \frac{\partial f}{\partial a_i} \frac{\partial f}{\partial a_j} \quad (6 \times 6 \text{ or larger})$$

A priori information = inverse of a priori errors.

3. Sum weighted information matrices.

4. Inverse of sum = injection error matrix

5. Use (1) to extrapolate (4) to time T.

PROGRAM CAPABILITIES

1. Will evaluate usefulness of R, $\dot{R}$, 2 angle data from any number of stations, CM, and a priori or telemetered data.

2. Can be used to predict MSFN accuracy during any free-flight portion of Apollo mission.

NEW STUDIES

1. Use of angle data in rendezvous case.

2. Station Selection, Biases and Correlated Errors.

3. MSFN capabilities in other mission phases
   (Earth Orbit, To Moon, Lunar Orbit,
   LEM descent, Earth return).

4. R, $\dot{R}$ accuracy obtainable
   (theoretical and experimental).

5. MSFN Guidance and Navigation during re-entry.

APOLLO NOTE NO. 107

J. R. Holdsworth
12 September 1963

AN APPROXIMATE METHOD FOR DEALING WITH AUTO-CORRELATED NOISE IN THE ERROR ANALYSIS OF ORBIT PARAMETER ESTIMATORS

A long series of notes beginning with Apollo Note No. 3 has been written about the calculation of the errors in the maximum likelihood estimates of various orbit parameters. An assumption basic to the analyses in all of these notes is that the time interval between successive observations is long with respect to the correlation time of the noise so that successive noise samples may be assumed to have independent Gaussian distributions.

If this assumption is not valid, i. e. if the sampling rate is such that there exists an appreciable statistical dependence between successive noise samples, then the results in the aforementioned notes must be viewed with suspicion. This would be unfortunate since an exact treatment of the error analysis would involve cumbersome manipulations with auto covariance matrices of very large order.

The qualitative effect of non-negligible correlation between successive samples is that less information is obtained from each new piece of data because of the statistical dependence of successive samples in time. Equivalently, we might say that the effect of auto-correlated noise is such that it tends to reduce the effective sample size or number of observations.

The purpose of this note will be to suggest a way to compute an effective sample size from a knowledge of the auto-correlation function of the noise. That is, given that we base our estimates upon N observations of data contaminated by auto-correlated noise, we shall assume that the covariance matrix of our estimator errors is such that it may be adequately approximated by a matrix computed

by the method outlined in Apollo Note No. 43. That is, we assume that as far as the estimator errors are concerned, we may replace our original problem involving auto-correlated noise by the problem of estimating the parameters from N_{eff} pieces of data which are contaminated by uncorrelated noise where $N_{eff} < N$. The quantity of N_{eff} is the reduced sample size, and the difference between N and N_{eff} will reflect the deterioration of our information due to noise correlation. This note will describe a method for computing N_{eff} which is motivated by the fact that it yields exact results for a much simpler but somewhat related problem.

Assume first that N independent observations are made of a single quantity whose mean value is μ and that the variance of any observation is σ^2. Denote the observations by $X_1, \ldots X_N$. The usual estimator of the parameter μ, based upon the N observations is:

$$\hat{\mu} = \frac{1}{N} \sum_{i=1}^{N} X_i \tag{1}$$

Furthermore, it is well known that the variance of this estimator is given by:

$$\sigma_{\hat{\mu}}^2 = \frac{\sigma^2}{N} \tag{2}$$

Equation (2) says that when the successive observations are uncorrelated that the mean square error in the estimator decreases as the reciprocal of the number of observed data points.

Next, however, assume that we again have available N pieces of observed data $X_1, \ldots X_N$ all coming from a population with mean μ and variance σ^2. Instead of assuming the data to consist of independent observations, we assume that the observations are correlated with a coefficient of correlation $\rho(i, j)$ existing be-

tween the i-th and j-th measurement where:

$$\rho(i,j) = \frac{1}{\sigma^2} \; E\left[(X_i - \mu)(X_j - \mu)\right] \tag{3}$$

and where E denotes the expected value operator.

Now if we still estimate the parameter μ by the expression in Equation (1), an easy calculation shows that the variance of the estimator based upon correlated observations is give by:

$$\sigma_{\hat{\mu}}^2 = \frac{\sigma^2}{N} \left[\frac{1}{N \Big/ \sum_{i=1}^{N} \sum_{j=1}^{N} \rho(i,j)} \right] \tag{4}$$

Equation (4) is interesting because it indicates that the error in the estimator based upon N pieces of correlated data is exactly the same as if the estimation were based upon:

$$N_{eff} = \frac{N^2}{\sum_{j=1}^{N} \sum_{i=1}^{N} \rho(i,j)} \tag{5}$$

uncorrelated observations.

In light of this it might be a fruitful approach to account for the presence of auto-correlated noise in the orbit parameter estimation problem by proceeding as in the case of independent observations only replacing the actual number of observations N by N_{eff} rounded to the nearest integer as given in Equation (5).

Equation (5) is interesting in that, if the correlation is extremely weak, then we have approximately:

$$\rho(i,j) \approx \delta_{ij} \tag{6}$$

in which case

$$N_{eff} \approx N$$

as we know it must. On the other hand, if the correlation is extremely strong then several of the quantities $\rho(i, j)$ will be close to one and the equivalent sample size will be appreciably reduced.

If the sampling is done continuously instead of periodically, in time there is no reason why the foregoing remarks should fail to hold. In this case Equation (5) would be replaced by

$$N_{eff} = \frac{T^2}{\int_0^T \int_0^T \rho(t_1, t_2)\, dt_1\, dt_2} \tag{7}$$

where T is the total integration or observation time.

As a parting reminder we mention again that the method suggested is approximate rather than rigorously exact and at this time no numerical comparisons have been made with more exact but also more laborious methods. In view of this one should proceed with caution. One obvious restriction is that both N and N_{eff} should be much larger than the number of parameters to be estimated.

Numerical comparisons between approximate results using this method and more exact results obtained by properly treating the auto covariance matrix of the noise process will be the subject of further Apollo notes.

ADDENDUM TO APOLLO NOTE NO. 107

J. R. Holdsworth
24 September 1963

On page 3 of Apollo Note No. 107, in the sentence immediately preceding Equation (4), the following statement was made. "An easy calculation shows that the variance of the estimator based upon correlated observations is given by:

$$\sigma_{\hat{\mu}}^2 = \frac{\sigma^2}{N} \left[\frac{1}{N \Big/ \sum_{i=1}^{N} \sum_{j=1}^{N} \rho(i,j)} \right] \tag{8}$$

As several questions have been asked regarding the details of this calculation it is presented here. By definition we have:

$$\sigma_{\hat{\mu}}^2 = E\left[\left(\hat{\mu} - \mu \right)^2 \right] \tag{9}$$

$$= E\left(\hat{\mu}^2 \right) - \mu^2 \tag{10}$$

$$= E\left[\frac{1}{N} \sum_{i=1}^{N} X_i \frac{1}{N} \sum_{j=1}^{N} X_j \right] - \mu^2 \tag{11}$$

$$= \frac{1}{N^2} \sum_{i=1}^{N} \cdot \sum_{j=1}^{N} E\left(X_i X_j \right) - \mu^2 \tag{12}$$

However, from Equation (3) we see that

$$E\left(X_i X_j \right) = \sigma^2 \rho(i,j) + \mu^2 \tag{13}$$

Thus substituting the results of (13) into Equation (12) we have:

$$\sigma_{\hat{\mu}}^2 = \frac{\sigma^2}{N^2} \sum_{i=1}^{N} \sum_{j=1}^{N} \rho(i,j) \tag{14}$$

or:

$$\sigma_{\hat{\mu}}^2 = \frac{\sigma^2}{N} \left[\frac{1}{N \Big/ \sum_{i=1}^{N} \sum_{j=1}^{N} \rho(i, j)} \right] \tag{15}$$

I apologize for any confusion created by failing to include the details of this calculation in the body of the note.

APOLLO NOTE NO. 108

H. Engel
20 September 1963

STATION LOCATION ERRORS

Outline

Now that it appears that radar measurement errors will not result in large errors in the estimates of orbit parameters, it becomes necessary to examine the effect of station location errors.

Using the notation of previous Apollo Notes,

$$\bar{s} = \bar{X}_m + \bar{r} - \bar{X}_d$$

and

$$\frac{\partial \bar{s}}{\partial a_j} = - \frac{\partial \bar{X}_d}{\partial a_j} \qquad j = 7, 8, 9$$

in which a_7, a_8, and a_9 are components of station location.

Then

$$\frac{\partial s}{\partial a_j} = \frac{-\bar{s}}{s} \cdot \frac{\partial \bar{X}_d}{\partial a_j}$$

$$\frac{\partial \dot{\bar{s}}}{\partial a_j} = - \frac{\partial \dot{\bar{X}}_d}{\partial a_j}$$

$$\frac{\partial \dot{s}}{\partial a_j} = \frac{-1}{s} \left[\bar{s} \cdot \frac{\partial \dot{\bar{X}}_d}{\partial a_j} + \left(\dot{\bar{s}} - \frac{\dot{s}}{s} \bar{s} \right) \cdot \frac{\partial \bar{X}_d}{\partial a_j} \right]$$

$$\frac{\partial \phi_1}{\partial a_j} = \frac{1}{w^2 + v^2} \left(v \frac{dw}{\partial a_j} - w \frac{\partial v}{\partial a_j} \right)$$

and

$$\frac{\partial \phi_2}{\partial a_j} = \left[w^2 + v^2 \right]^{1/2} \left[\frac{\partial u}{\partial a_j} - \frac{u}{v} \frac{\partial w}{\partial a_j} - \frac{w u}{w^2 + v^2} \left(\frac{\partial w}{\partial a_j} - \frac{w}{v} \frac{\partial v}{\partial a_j} \right) \right]$$

in which u, v and w are components of $\hat{s}$ in the u, v, w directions.

The elements of the information matrices for range, range-rate or angle measurements, which depend on the above quantities, can now be evaluated.

APOLLO NOTE NO. 108

H. Engel
20 September 1963

STATION LOCATION ERRORS

Outline

Now that it appears that radar measurement errors will not result in large errors in the estimates of orbit parameters, it becomes necessary to examine the effect of station location errors.

Using the notation of previous Apollo Notes,

$$\bar{s} = \bar{X}_m + \bar{r} - \bar{X}_d$$

and

$$\frac{\partial \bar{s}}{\partial a_j} = - \frac{\partial \bar{X}_d}{\partial a_j} \qquad j = 7, 8, 9$$

in which a_7, a_8, and a_9 are components of station location.

Then

$$\frac{\partial s}{\partial a_j} = \frac{-\bar{s}}{s} \cdot \frac{\partial \bar{X}_d}{\partial a_j}$$

$$\frac{\partial \dot{\bar{s}}}{\partial a_j} = - \frac{\partial \dot{\bar{X}}_d}{\partial a_j}$$

$$\frac{\partial \dot{s}}{\partial a_j} = \frac{-1}{s} \left[\bar{s} \cdot \frac{\partial \dot{\bar{X}}_d}{\partial a_j} + \left(\dot{\bar{s}} - \frac{\dot{\bar{s}}}{s} \bar{s} \right) \cdot \frac{\partial \bar{X}_d}{\partial a_j} \right]$$

$$\frac{\partial \phi_1}{\partial a_j} = \frac{1}{w^2 + v^2} \left(v \frac{dw}{\partial a_j} - w \frac{\partial v}{\partial a_j} \right)$$

and

$$\frac{\partial \phi_2}{\partial a_j} = \left[w^2 + v^2 \right]^{1/2} \left[\frac{\partial u}{\partial a_j} - \frac{u}{v} \frac{\partial w}{\partial a_j} - \frac{w u}{w^2 + v^2} \left(\frac{\partial w}{\partial a_j} - \frac{w}{v} \frac{\partial v}{\partial a_j} \right) \right]$$

in which u, v and w are components of $\hat{s}$ in the u, v, w directions.

The elements of the information matrices for range, range-rate or angle measurements, which depend on the above quantities, can now be evaluated.

Means for Calculation

Let x", y", z" be an Earth-centered rectangular coordinate system rotating with the Earth such that z" is parallel to z, x" is in the meridian plane of the station and $y'' = z'' \times x''$, and let a_7, a_8 and a_9 be the x", y" and z" coordinates of the station.

Then

$$\frac{\partial x''_d}{\partial a_j} = \delta_{7j}$$

$$\frac{\partial y''_d}{\partial a_j} = \delta_{8j}$$

$$\frac{\partial z''_d}{\partial a_j} = \delta_{9j}$$

and

$$\frac{\partial \dot{x}''_d}{\partial a_j} = \frac{\partial \dot{y}''_d}{\partial a_j} = \frac{\partial \dot{z}''_d}{\partial a_j} = 0.$$

Now

$$\begin{bmatrix} x_d'' \\ y_d'' \\ z_d'' \end{bmatrix} = \begin{bmatrix} \cos(\omega_e T + \alpha) & \sin(\omega_e T + \alpha) & 0 \\ -\sin(\omega_e T + \alpha) & \cos(\omega_e T + \alpha) & 0 \\ 0 & 0 & 1 \end{bmatrix} \begin{bmatrix} x_d \\ y_d \\ z_d \end{bmatrix}$$

or

$$X''_d = \mathcal{A} X_d$$

Then

$$X_d = \mathcal{A}^{-1} X''_d$$

and

$$\frac{\partial X_d}{\partial a_j} = \mathcal{A}^{-1} \frac{\partial X''_d}{\partial a_j}$$

Now

$$\dot{X}_d = \begin{bmatrix} \dot{x}_d \\ \dot{y}_d \\ \dot{z}_d \end{bmatrix} = \begin{bmatrix} -\omega_e\, y_d \\ \omega_e\, x_d \\ 0 \end{bmatrix}$$

so

$$\frac{\partial \dot{X}_d}{\partial a_j} = \begin{bmatrix} \frac{\partial \dot{x}_d}{\partial a_j} \\ \frac{\partial \dot{y}_d}{\partial a_j} \\ \frac{\partial \dot{z}_d}{\partial a_j} \end{bmatrix} = \begin{bmatrix} -\omega_e \frac{\partial y_d}{\partial a_j} \\ \omega_e \frac{\partial x_d}{\partial a_j} \\ 0 \end{bmatrix}$$

Next

$$\frac{\partial X'_d}{\partial a_j} = L\,K\,\frac{\partial X_d}{\partial a_j}$$

and

$$\frac{\partial \dot{X}'_d}{\partial a_j} = L\,K\,\frac{\partial \dot{X}_d}{\partial a_j}$$

$\bar{s}$ and $\dot{\bar{s}}$ are already available in the x' y' z' coordinates as X'_s and $\dot{X}'_s$ so $\partial s/\partial a_j$ and $\partial \dot{s}/\partial a_j$ can be evaluated.

The components of s in the u, v, w system are:

$$Y_s{}^w = \begin{bmatrix} u \\ v \\ w \end{bmatrix} = \frac{1}{s}\; J\; K^{-1}\; L^{-1}\; X'_s$$

so

$$\frac{\partial Y_s{}^w}{\partial a_j} \begin{bmatrix} \frac{\partial u}{\partial a_j} \\ \frac{\partial v}{\partial a_j} \\ \frac{\partial w}{\partial a_j} \end{bmatrix} = \frac{1}{s}\; J\; K^{-1}\; L^{-1} \quad \frac{\partial X'_s}{\partial a_j}$$

Thus $\partial \phi_1/\partial a_j$ and $\partial \phi_2/\partial a_j$ can be evaluated. Having $\partial s/\partial a_j$, $\partial \dot{s}/\partial a_j$, $\partial \phi_1/\partial a_j$ and $\partial \phi_2/\partial a_j$, the information matrices can be found.

APOLLO NOTE NO. 109

H. Dale
23 September 1963

EFFECT OF THE LONGITUDE OF THE LEM LANDING SITE ON THE ERRORS IN DETERMINING RENDEZVOUS POSITION BY THE MSFN

It is apparent that if a simple 180° Hohmann transfer ascent trajectory is used, then the MSFN tracking time can be affected by the initial location of the ascending LEM. This is shown by the figure below in which α is the angle away from the Earth-Moon time which describes the initial (perilune) position of the LEM in its ballistic ascent trajectory.

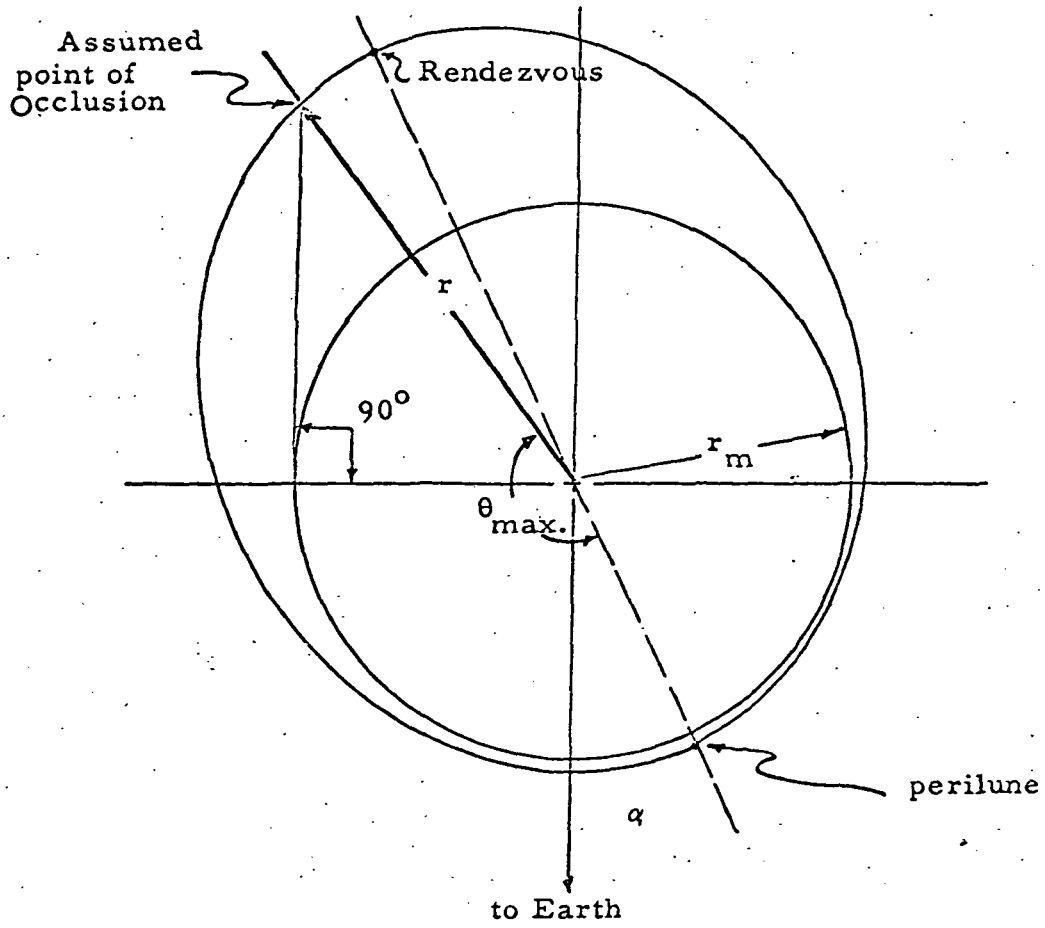

Figure 1. A Sketch of the Geometry

In order to calculate the period of visibility between perilune and lunar occlusion, it is first necessary to calculate the corresponding angle from perilune which measures this maximum time. From the figure it can be seen that occlusion occurs when:

$$r \cos \left(\theta_{max.} - \frac{\pi}{2} - \alpha \right) = r_m \tag{1}$$

where r is the distance from the center of the Moon to the LEM and r_m is the lunar radius. Now defining the semi-major axis, a, and the eccentricity, e, the above equation may be rewritten

$$\frac{a(1 - e^2)}{1 + e \cos \theta_{max.}} \cos \left(\theta_{max.} - \frac{\pi}{2} - \alpha \right) = r_m \tag{2}$$

By algebraic manipulation this equation may in turn be rewritten

$$- \left[r_m e + a(1 - e^2) \sin \alpha \right] \cos \theta_{max.} + \left[a(1 - e^2) \cos \alpha \right] \sin \theta_{max.} = r_m \tag{3}$$

or

$$A \cos \theta_{max.} + B \sin \theta_{max.} = r_m$$

from which $\theta_{max.}$ may be obtained

$$\sqrt{A^2 + B^2} \cos (\theta_{max.} - \ell) = r_m$$

$$\text{with } \cos \ell = \frac{A}{\sqrt{A^2 + B^2}} ; \quad \sin \ell = \frac{B}{\sqrt{A^2 + B^2}} \tag{4}$$

Now given $\theta_{max.}$, the eccentric anomaly, E, may be calculated.

$$\sin E = \frac{\sqrt{1 - e^2} \sin \theta_{max.}}{1 + e \cos \theta_{max.}} \tag{5}$$

This, in turn, may be used to calculate the observation time (time between perilune and occlusion).

$$t = \sqrt{\frac{a^3}{\mu}} \quad (E - e \sin E) \tag{6}$$

where μ is the lunar gravitational constant. This time is plotted below as a function of α.

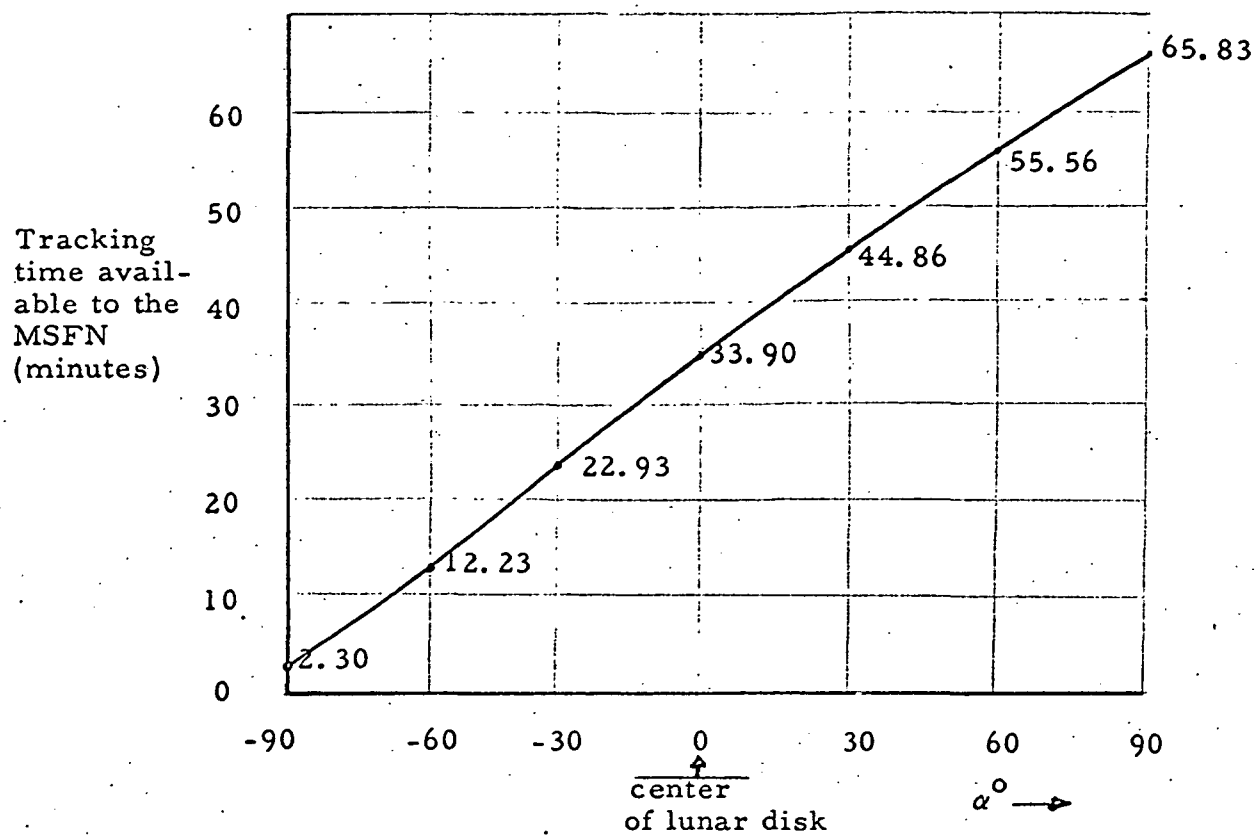

Figure 2 Tracking time vs. Perilune location with Rendezvous at 180° from perilune and at 80 n. mi. lunar altitude.

Now using the above tracking times and the computer program described in Apollo Note 82, the covariance matrix of the errors at rendezvous may be calculated. Since this program uses one minute intervals for uncorrelated data, the above times should be rounded off to the nearest minute. Since Rendezvous occurs at 58.05 minutes after perilune the $\alpha = 90^\circ$ case should be terminated at 58.05 minutes rather than the total time of 65.83 minutes. Figure 3 shows the three positional

error estimates (σ_x, σ_y, σ_z) at the nominal time of rendezvous (58.05 min after perilune) for two cases. The first utilizes range and range-rate data from the Madrid and Johannesburg stations. This is plotted as heavy lines and assumes σ_R = 15 meters and $\sigma_{\dot{R}}$ = 0.03 meters per second. The second case adds a priori data from the LEM IMU. This is plotted as dashed curves and assumes for a priori errors 1000 meter and 10 meters per second in each of three orthoganal directions. Figure 4 shows the RMS total error at the nominal time of rendezvous (58.05 min.) for the cases with and without a priori data.

$$\text{RMS total error} = \sqrt{\sigma_x^2 + \sigma_y^2 + \sigma_z^2}$$

Since for most cases the velocity errors are small near rendezvous, the actual RMS miss is due simply to x and z components of error (see Apollo Note No. 103). Thus Figure 5 is a plot of $\sqrt{\sigma_x^2 + \sigma_z^2}$ for the above two cases.

From Figure 5 one may conclude that most of the Lunar equator (-50° to $+90^\circ$) could be used as a perilune or landing site without exceeding a 1000 meter miss.

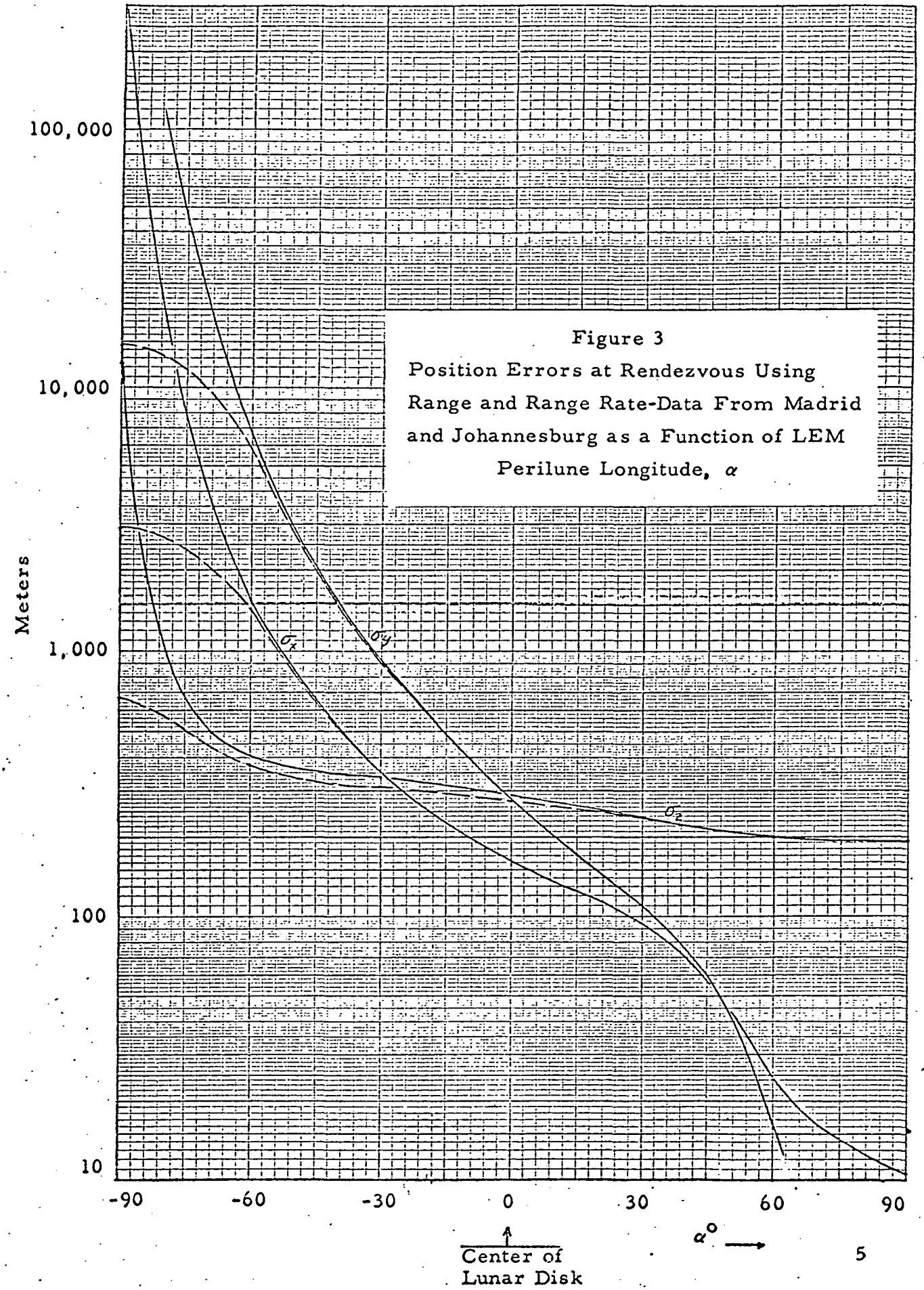

Figure 3
Position Errors at Rendezvous Using Range and Range Rate-Data From Madrid and Johannesburg as a Function of LEM Perilune Longitude, α

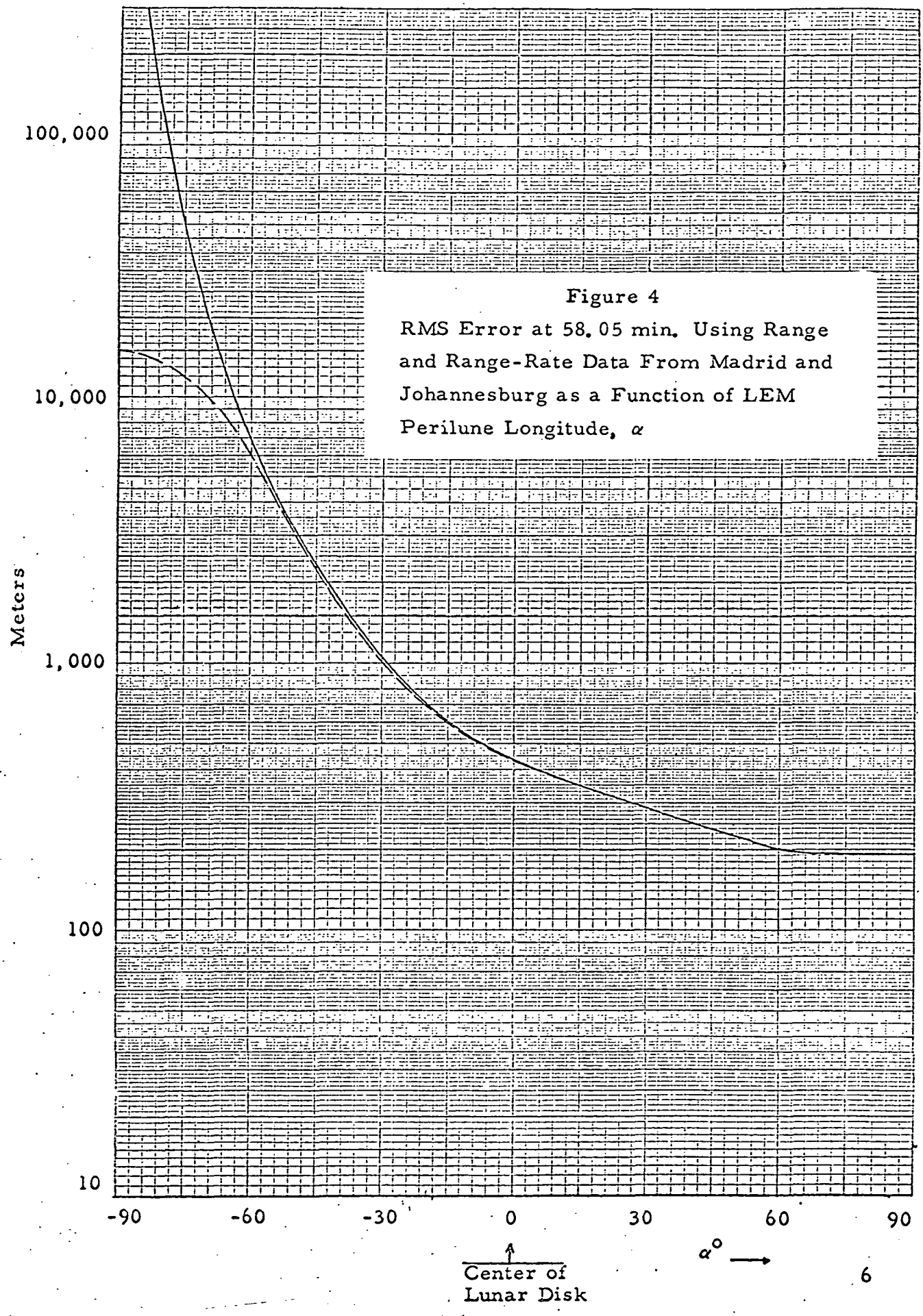

Figure 4

RMS Error at 58.05 min. Using Range and Range-Rate Data From Madrid and Johannesburg as a Function of LEM Perilune Longitude, α

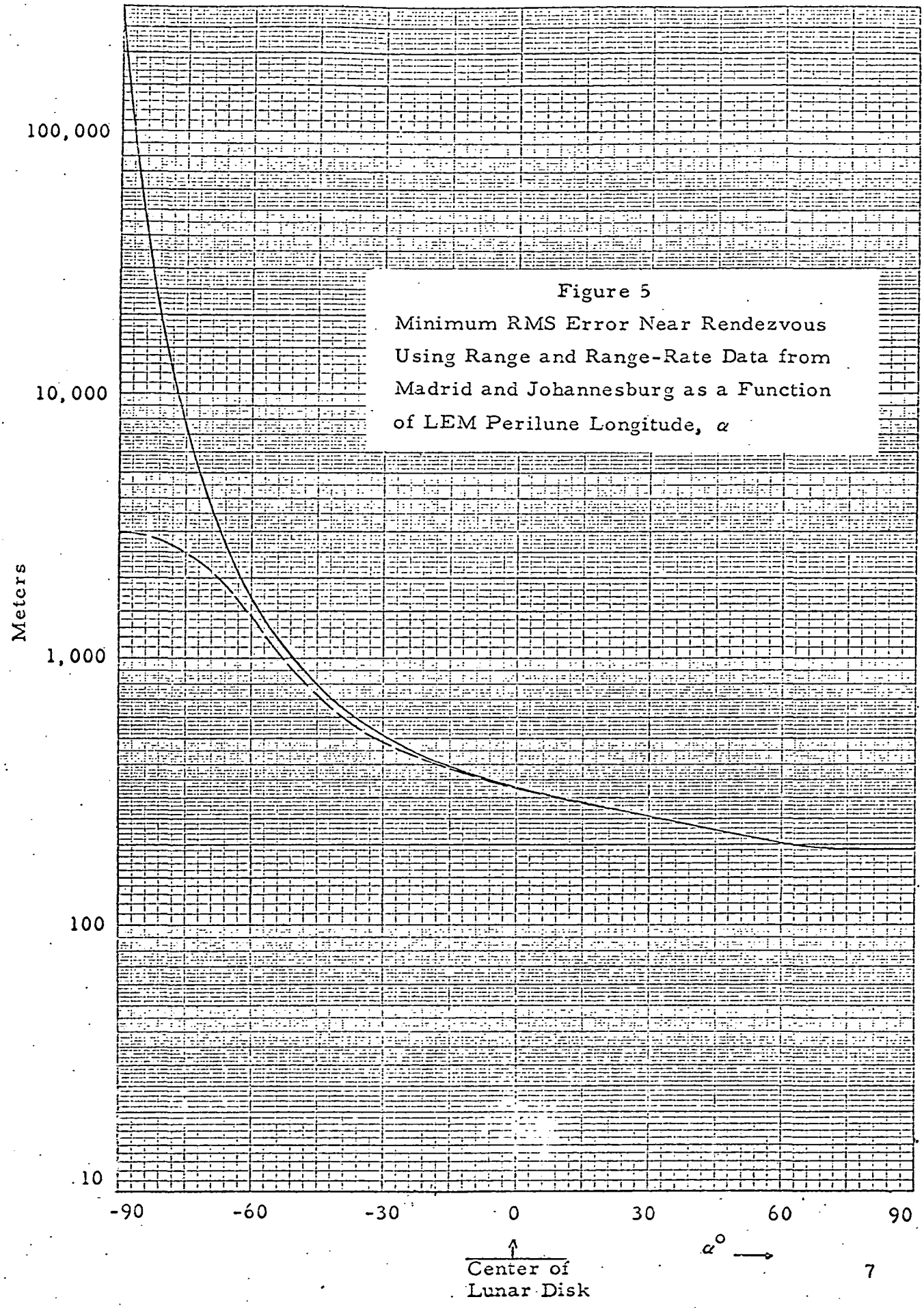

Figure 5

Minimum RMS Error Near Rendezvous Using Range and Range-Rate Data from Madrid and Johannesburg as a Function of LEM Perilune Longitude, α

APOLLO NOTE NO. 110

H. Epstein
25 September 1963

ERROR SOURCES FOR RANGE AND RANGE-RATE MEASUREMENTS

This note will treat a number of possibly significant error sources for range and for range-rate measurables. The objective of this note is to present these factors and to indicate efforts required to determine the magnitude of these effects. Measurables, orbit models, and calculated ephemeric are all considered as referenced to the velocity of light (e.g., measurables as time and frequency rather than range and range-rate respectively) for this purpose. Since for Apollo applications, we are dealing with precision comparable and even better than most well designed scientific experiments, effects that are normally considered negligible may be of great significance. For present purposes, it is convenient to regard errors in terms of their correlation time with respect to the individual sample measurement and the total measurement periods. Errors which have correlation times short as compared to the sample duration may be considered as smoothed both by the sampling techniques and by orbital smoothing over the measurement period. On the other hand, errors with correlation times long as compared to the measurement period should be considered as bias-type errors which are essentially unaffected by smoothing. These errors sources can typically be treated by increasing the number of unknown parameters to include an appropriate degree polynomial. Correlation times lying between these limits will be affected by smoothing and curve fitting techniques in terms of which correlation model is most appropriate.

It is of considerable importance (particularly, where only short smoothing times are available) that a number of fundamental constants be accurately established prior to the Apollo mission. This data can be obtained from Ranger, Surveyor, early Apollo missions, and other aerospace programs.

A number of accuracy factors need to be examined. A partial list includes:

1. Receiver Noise

Optimal processing of a waveform leads to a frequency uncertainty given by

$$\delta f = \frac{1}{\alpha \left(\frac{2E}{N_o}\right)^{\frac{1}{2}}}$$

For a CW waveform, $\alpha = \frac{\pi T}{\sqrt{3}}$

$$\delta f = \frac{\sqrt{3}}{\pi T \left(\frac{2E}{N_o}\right)^{\frac{1}{2}}} = \frac{\sqrt{3}}{\pi T \left[\frac{2S}{N} (BT)\right]^{\frac{1}{2}}}$$

This latter formulation represents a convenient expression for the determination of frequency uncertainty. A $\frac{S}{N}$ of about unity in the transponder phase-locked loop is a very conservative (in fact too conservative) estimate of the minimum $\frac{S}{N}$ to maintain phase-lock for long periods of time. For this situation, the $\frac{S}{N}$ at the receiving site will be degraded by the transmitter power ratio (transponder vs MSFN) while improved by the relative noise figures. Considering a very narrow bandwidth (such as 20 cps for Mariner II), 60 seconds of smoothing of noisy data, and a $\frac{S}{N}$ = - 30 db net, the frequency uncertainty would be about .006 cps. The corresponding $\dot{R}$ error would be .09 cm/sec. This clearly demonstrates that the primary role at least at this date of signal-to-noise ratio of this type is to insure good phase-lock loop tracking (to prevent loss of lock during the tracking time) and to minimize the effects of non-linearities on system performance. As a matter of interest, the range change error would be about 5.4 cm which is negligible with respect to assumed range errors for the Apollo program.

2. Oscillator Stability

Considering that Apollo will employ the most accurate and stable oscillators available, it must then be assumed that calibration of these oscillators can only be made relative to a similar standard to estimate stability and relative drift. Considering that no calibration can be made during the round-trip time between spacecraft and Earth, a frequency variation of 1 part in 10^{10} and 1 part in 10^{11} corresponding to range-rate errors of 1.5 and .15 cm/sec., respectively. For the Mariner mission this would correspond to doppler errors of about .1 and .01 cps respectively. After curve fitting of the doppler data for periods of about an hour, the doppler residue was primarily less than about .025 cps (1 σ). With typical transit times of several hundred seconds, it is quite possible that the oscillator (an atomic standard) could be the major contributor to error.

Efforts are presently underway to establish the nature of these errors both from measurement data and whatever analytical mechanisms can or have been predicated to account for the measured results.

3. Propagation Errors

Propagation effects can be considered in terms of whether uncharged particles or charged particles are associated with the variation of such parameters as index of refraction.

The Earth's troposphere and ionosphere are major contributors to these effects.

Very crude range variation through the troposphere may be approximated by

$$\Delta R = \frac{N_s H}{\cos \phi}$$

N_s = surface refraction index variation from unity $\simeq 3 \times 10^4$

H = effective depth of the troposphere ~ 7 KM

ϕ = angle of incidence with respect to the Earth's surface

Then $\Delta R \simeq \frac{2}{\cos \phi}$ meters,

and the corresponding range-rate error could be associated with the variation of ϕ with time for particular satellites.

Much more detailed analyses and presentations of experimental results are contemplated including not only ionospheric effect but also dealing with cislunar space characteristics.

4. Spaceborne Transponder Errors

A number of errors sources need to be considered of possible significance for Apollo applications. An example of a linear type error can be associated with the dynamic lag of the phase-locked loop. The correlation function and/or spectrum of the error can be determined from the trajectories of interest. Non-linear effects are typified by the phase detector and discriminator employed as well as to the multiplier networks.

5. Antenna Motion With Respect to the Vehicle Center of Gravity

This effect introduces both range and range-rate errors which are related to the antenna motion with respect to the attached point on the airframe and the motion of the attached point to the center of gravity.

6. Exospheric Effect

Such effect as gravitational gradient, solar pressure, the charge density and particle density of cislunar space needs to be examined.

7. Model Errors

The influence of the errors due to model deficiencies such as errors in gravitational potential, uncertainties in fundamental constants, and uncertainties in station locations. Included in this effort should be a treatment of computational errors compatible with allowable computational time.

Summary

In summary, the results from Mariner *II* and Syncom are such as to make it quite clear that considerable ephemeris accuracy improvement can be derived from a better understanding leading to better equipment design. Therefore, it becomes necessary to establish the relevant error sources.

APOLLO NOTE NO. 111

G. F. Floyd
25 September 1963

SUGGESTED MSFN OPERATION FOR LEM RENDEZVOUS

Have one S-band phase-lock transponder in LEM and CSM operating at different transmitting frequencies so will transmit CW from single Earth station and receive return from both CSM and LEM at as many Earth stations as can see the Moon. Transmitter and receiving stations will all use the same type of frequency standard. This standard is assumed to be the best available with short and long term drifts of about 1 part in 10^{10}. All receiving stations beat the received CW signal against their own frequency standards and with phase-lock loops count the number of doppler cycles received from both the CSM and LEM. This number of doppler cycles is then transmitted at 1 second intervals to the MCC via a low frequency data link, such as the USN low frequency world-wide system.

Ground communications plans are available. (R.T.Th)

At the central computing station, the doppler count data received on the CSM is used to determine individual oscillator drifts and changes in actual wave velocity (both in space and through the Earth's atmosphere), and correct the LEM received doppler count data for these effects. This correction procedure is done continuously all the time the LEM and CSM are visible from the Earth. The system is kept on all the time that the LEM is resting on the Moon in order to calculate very precise values of the initial scalar range at take-off from individual MSFN stations to the LEM. The system is also kept on during the LEM boost-off so that counts of the number of doppler cycles received by all the operable stations are fed into the central computer throughout the boost phase. RTCC

Each doppler cycle count corresponds to a total path length change of λ = 10 cm at S-band or about 5 cm in distance from the Earth station with the initial value of scalar range determined very well during the 24 hour Moon-landing phase. Also, since the two

signals travel almost the same path, the use of the CSM count data can correct for the errors caused by oscillator drifts which at 1 part in 10^{10} would be $10^{-10} \frac{c}{2}$ = 1.5 cm/sec. as well as changes in the effective value of c due to ionization changes.

On the other hand, errors in the LEM-CSM transponders are uncorrelated and $\pm$ 3° of phase angle jitter at 19 mc is equivalent to $\pm$ 470° = $\pm$ 1.3 counts = $\pm$ 6 cm at 3 kmc. Further tracking "noise" will be introduced by attitude oscillation of the LEM or CSM since the transponders will probably not be located at the c.g. and so attitude oscillations will change the count and be confused with transponder jitter. The correlation times of these noise sources will probably be between 1 and 10 seconds which then sets the desired receiving station readout time of about once per second.

The orbit determination program is then to use as the measurable the change in scalar range, (the term, $(S - S_o)$ in the note notation), and from these determine the LEM orbit parameters. Actually, by tracking during the 24 hour Moon landing and throughout the ascent phase, S_o will be well known as well. In evaluating the MSFN rendezvous miss uncertainty resulting with this system, the use of CSM return makes it seem reasonable to use a σ for the LEM range change measurement which does not grow with observation time, and since for fixed observation time the quantity $(\sigma\sqrt{t_{correlation}})$ is simply the scale factor of the final miss uncertainty, I would suggest the values:

$$\sigma = 10 \text{ cm}, \; t_{correlation} = 1 \text{ sec.}$$

as being reasonable for the range change accuracy at this stage of our knowledge as to what could be obtained with such a ground system.

APOLLO NOTE NO. 112

H. Epstein
25 September 1963

DIFFERENTIAL RANGE ACCURACY

This note will treat the noise characteristics of differential range measurements. It is convenient to consider the situation as though the range is actually a constant and that the differential range is zero for noise considerations. Actual target dynamics present additional constraints. It will be contended here that CW waveforms are ideal without rigorous mathematical proof. However, it will be shown that unmodulated CW types are superior to bandwidth limited ranging techniques which directly measure range. Several other practical advantages are present in the CW type that further verify the intuitive feeling that unmodulated CW is the proper waveform for differential range measurement such as: one, equipment simplicity; two, frequency is the most accurate and stable quantity that may be obtained; and, three, differential range accuracy is substantially independent of target dynamics during the measurement period.

But we have accepted the pseudo random noise codes

The required equations for noise performance will be taken from the excellent paper of M. I. Skolnik [1]. The basic equations are as follows employing Mr. Skolnik's notation.

$$\delta T_r = \frac{1}{\beta \left(\frac{2E}{N_o} \right)^{1/2}} \tag{1}$$

$$\beta^2 = \frac{(2\pi)^2 \int_{-\infty}^{\infty} f^2 \left| S(f) \right|^2 df}{\int_{-\infty}^{\infty} \left| S(f) \right|^2 df} \tag{2}$$

---

(1) Merrill I. Skolnik, Theoretical Accuracy of Radar Measurement, (IRE Transactions on Aeronautical and Navigational Electrics - December 1960, pp. 123-129).

$$S(f) = \int_{-\infty}^{\infty} s(t)\, e^{-j2\pi ft}\, dt \tag{3}$$

$$\delta f = \frac{1}{\alpha \left(\frac{2E}{N_o}\right)^{1/2}} \tag{4}$$

$$\alpha^2 = \frac{(2\pi)^2 \int_{-\infty}^{\infty} t^2 s^2(t)\, dt}{\int_{-\infty}^{\infty} s^2(t)\, dt} \tag{5}$$

where

δT_r = rms time error

E = total energy in the received signal

N_o = noise power density (noise assumed as white noise)

$s(t)$ = signal modulation on the carrier frequency

t = time (with the time origin as the mean epoch)

Case I - Unmodulated CW

It can readily be shown that

$$\alpha = \frac{\pi T}{\sqrt{3}} \tag{6}$$

and

$$\delta f = \frac{\sqrt{3}}{\pi T \left(\frac{2E}{N_o}\right)^{1/2}} \tag{7}$$

The error in range-rate ($\delta \dot{R}$) and the resultant error in range (δR) for a two-way system is then given by

$$\delta \dot{R} = \frac{\lambda \delta f}{2} = \frac{c \delta f}{2 f} \tag{8}$$

$$\delta R = T \delta \dot{R} = \frac{1}{f} \left[\frac{c \sqrt{3}}{2\pi \left(\frac{2E}{N_o} \right)^{1/2}} \right] \tag{9}$$

Equation (9) yields the final desired result for the unmodulated CW case.

Case II - Bandwidth Limited Modulation

$$\beta = \frac{\pi B}{\sqrt{3}}$$

Considering that two range measurements are required to measure differential range, it can readily be shown that

$$\delta R = \frac{\sqrt{2}}{B} \left[\frac{c \sqrt{3}}{2\pi \left(\frac{2E}{N_o} \right)^{1/2}} \right] \tag{10}$$

Maintaining the same total energy for both systems (1/2 energy in each range measurement) and from Equations (9) and (10), the ratio of the error for the bandwidth limited case to the unmodulated CW case for differential range measurement (ρ) is given simply by:

$$\rho = \frac{2f}{B} \tag{11}$$

This clearly demonstrates the case for superiority of the unmodulated CW transmission. One further remark should be made. Equation (9) indicates the desirability for the utilization of higher carrier frequency operation.

APOLLO NOTE NO. 113

H. Engel
26 September 1963

MSFN DIRECTED LEM ASCENT

Introduction

With no on-board attitude control system other than a pilot observing the stars and horizon, and rate gyros that appear to be required for stable flight, it appears likely that an excellent ascent orbit injection can be made. With an operative IMU and ground assistance, of course, even better injection is possible.

Further investigation is needed.

Procedure

Continuous observation of the LEM on the Moon for 24 hours from three MSFN stations (not always the same three) with zero mean random range errors having a standard deviation of 15 m for one-minute observations, allows the range to the LEM to be determined to 0.23 m (= 15 m x 1 min/ [60 x 24 min x 3 stations]), and the orthogonal components of position to about 100 times this. (This ignores station location errors.)

Prior to the start of boost the ground stations switch to the JPL 2-way Doppler mode, and this is used to measure changes in range thereafter. The change in range from each station measured in this fashion appears to be accurate to 1.0 m over a period of a good fraction of an hour. Thus, at any time during boost the range component of position is known to the order of 0.6 m (= 1.0 m / $\sqrt{3}$), and the other two orthogonal components to 60 m.

If the LEM takes off from near 0^{o} latitude and 0^{o} longitude on the Moon, this means that with one second of observation the altitude rate can be determined to the order of 1.2 m/sec. (= 0.6 m x 2/1 sec). In the same time the horizontal components of velocity can be found to about 120 m/sec.

Let us say that the pilot is given a programmed elevation and azimuth to fly as functions of time, using the stars or horizon and a grid on the port as a reference. Further, let us say that on the basis of radar observations during boost the MSFN advises the pilot of deviations he should fly from the preprogrammed course. Now let us find out how the MSFN may direct the pilot, and the accuracy of orbit injection attainable.

Let us define $\overline{V}_c(\overline{R}, t)$ as the velocity the LEM should have at position $\overline{R}$ at time t in order to intercept the CM/SM at the nominal rendezvous point in free fall. Let $\overline{V}$ be the LEM velocity, and define $\overline{V}_g$, the velocity to be gained, as

$$\overline{V}_g \triangleq \overline{V}_c - \overline{V}.$$

If the LEM thrust is directed so as to reduce $\overline{V}_g$ to 0 and then terminated, the LEM will reach the rendezvous point at the same time as the CM/SM.

A simple way of reducing $\overline{V}_g$ to zero is to direct the LEM thrust along $\overline{V}_g$. This, however, may not result in an economical use of propellant. To obtain a more efficient boost trajectory we may write

$$\overline{V}_g = \overline{V}_c + \overline{V}_a - \overline{V}$$

in which $\overline{V}_a$ is an additional term the purpose of which is to shape the boost trajectory. $\overline{V}_a$ has the property that it goes to 0 as the correct velocity is approached.

$\overline{V}_a$ and $\overline{V}_c$ are computed before takeoff from the Moon. The MSFN determines $\overline{R}$ and $\overline{V}$ from radar measurements, computes $\overline{V}_g$ and the angle between $\overline{V}_g$ and the preprogrammed elevation and azimuth angles in the possession of the pilot, and transmits these differences to the pilot as corrections to steering. These correction angles should be small and slowly varying. Delays in transmission therefore should not seriously affect performance of the guidance system. In order to insure that cut-off velocity is correct, however, it is necessary to transmit the time of cut-off ahead of time.

Errors

The problem of finding the covariance matrix of errors in position and velocity after some period of powered flight is a difficult one, and will probably require computer runs for solution. In order to determine whether it is worthwhile to expend that much effort, we can obtain the solution to a simpler problem directly. Consider the one-dimensional case in which the range 'x' to the vehicle is measured at 1 second intervals with standard deviation σ_m, and the vehicle has a known thrust history, the thrust acceleration 'a' in any interval having a standard deviation σ_a.

Letting y_n and $\dot{y}_n$ be the estimates of range and range-rate after the measurement x_n, and letting z_n and $\dot{z}_n$ be these same estimates before measurement x_n, we can write

$$\begin{bmatrix} z_{n+1} \\ \dot{z}_{n+1} \end{bmatrix} = \begin{bmatrix} 1 & 1 \\ 0 & 1 \end{bmatrix} \begin{bmatrix} y_n \\ \dot{y}_n \end{bmatrix} + a_n \begin{bmatrix} \frac{1}{2} \\ 1 \end{bmatrix}$$

or

$$Z_{n+1} = M_n \; Y_n + A_n$$

Assuming unbiased estimates, and letting Z_n^* be the exact values of range and range-rate, and A_n^* the exact value of A_n,

$$\text{cov}\,(Z_{n+1},\, Z_{n+1}) = E\left[(Z_{n+1} - Z^*_{n+1})(Z_{n+1} - Z^*_{n+1})^T\right]$$

$$= E\left[\left\{M_n(Y_n - Z^*_n) + (A_n - A^*_n)\right\}\left\{M_n(Y_n - Z^*_n) + (A_n - A^*_n)\right\}^T\right]$$

$$= M_n \,\text{cov}\,(Y_n,\, Y_n)\; M_n^T + \text{cov}\,(A_n, A_n)$$

We assume, further, that cov (A_n, A_n) is time independent, so

$$\text{cov}\,(Z_{n+1}, Z_{n+1}) = M_n \,\text{cov}\,(Y_n,\, Y_n)\; M_n^T + \text{cov}\,(A,\, A)$$

Denote the elements of the covariance matrix of any 2 dimensional vector B by b_{ij}.

Then

$$\operatorname{cov}(Z_{n+1}, Z_{n+1}) = \begin{bmatrix} 1 & 1 \\ 0 & 1 \end{bmatrix} \begin{bmatrix} y_{11} & y_{12} \\ y_{21} & y_{22} \end{bmatrix} \begin{bmatrix} 1 & 0 \\ 1 & 1 \end{bmatrix} + \sigma_a^2 \begin{bmatrix} \frac{1}{4} & \frac{1}{2} \\ \frac{1}{2} & 1 \end{bmatrix}$$

$$= \begin{bmatrix} y_{11} + y_{12} + y_{21} + y_{22} + \frac{\sigma_a^2}{4} & y_{12} + y_{22} + \frac{\sigma_a^2}{2} \\ y_{21} + y_{22} + \frac{\sigma_a^2}{2} & y_{22} + \sigma_a^2 \end{bmatrix}$$

Now

$$Y_{n+1} = \operatorname{cov}(Y_{n+1}, Y_{n+1}) \left[\operatorname{cov}^{-1}(Z_{n+1}, Z_{n+1}) Z_{n+1} + \operatorname{cov}^{-1}(X_{n+1}, X_{n+1}) X_{n+1} \right]$$

and

$$\operatorname{cov}^{-1}(Y_{n+1}, Y_{n+1}) = \operatorname{cov}^{-1}(Z_{n+1}, Z_{n+1}) + \operatorname{cov}^{-1}(X, X)$$

In the limit, after infinitely many measurements,

$$\operatorname{cov}(Y_{n+1}, Y_{n+1}) = \operatorname{cov}(Y_n, Y_n)$$

so, in the limit,

$$\operatorname{cov}(Y, Y) = \left[\operatorname{cov}^{-1}(Z, Z) + \operatorname{cov}^{-1}(X, X) \right]^{-1}$$

Denoting the elements of cov (Z, Z) by

$$\operatorname{cov}(Z, Z) = \begin{bmatrix} A & B \\ C & D \end{bmatrix}$$

for convenience, we have

$$\operatorname{cov}^{-1}(Z, Z) = \frac{1}{AD - BC} \begin{bmatrix} D & -B \\ -C & A \end{bmatrix}$$

$$\operatorname{cov}^{-1}(X, X) = \frac{1}{\sigma_m^2} \begin{bmatrix} 1 & 0 \\ 0 & 0 \end{bmatrix}$$

$$\operatorname{cov}^{-1}(Z, Z) + \operatorname{cov}^{-1}(X, X) = \frac{1}{AD - BC} \begin{bmatrix} D + \frac{AD - BC}{\sigma_m^2} & -B \\ -C & A \end{bmatrix}$$

and

$$\left[\text{cov}^{-1}(Z, Z) + \text{cov}^{-1}(X, X)\right]^{-1} = \frac{1}{1 + \frac{A}{\sigma_m^2}} \begin{bmatrix} A & B \\ C & D + \frac{AD - BC}{\sigma_m^2} \end{bmatrix}$$

The covariance matrices are symmetric. Taking them term by term, we can write

$$y_{11} = \frac{1}{1 + \frac{A}{\sigma_m^2}} \quad A$$

$$y_{12} = \frac{1}{1 + \frac{A}{\sigma_m^2}} \left(y_{12} + y_{22} + \frac{\sigma_a^2}{2}\right)$$

$$y_{22} = \frac{1}{1 + \frac{A}{\sigma_m^2}} \left(y_{22} + \sigma_a^2\right)$$

in which

$$A = y_{11} + 2\, y_{12} + y_{22} + \frac{\sigma_a^2}{4}$$

or, multiplying through by $1 + \frac{A}{\sigma_m^2}$

$$\frac{A}{\sigma_m^2}\, y_{11} = A - y_{11}$$

$$\frac{A}{\sigma_m^2}\, y_{12} = y_{22} + \frac{\sigma_a^2}{2}$$

$$\frac{A}{\sigma_m^2}\, y_{22} = \sigma_a^2$$

Then

$$\frac{\sigma_m^2}{A} = \frac{y_{22}}{\sigma_a^2}$$

and

$$y_{12} = \frac{y_{22}}{\sigma_a^2}\left(y_{22} + \frac{\sigma_a^2}{2}\right)$$

$$= y_{22}\left(\frac{y_{22}}{\sigma_a^2} + \frac{1}{2}\right)$$

$$y_{11} = \frac{y_{22}}{\sigma_a^2}\left(2\,y_{12} + y_{22} + \frac{\sigma_a^2}{4}\right)$$

$$= \frac{y_{22}}{\sigma_a^2}\left[2\,y_{22}\left(\frac{y_{22}}{\sigma_a^2} + \frac{1}{2}\right) + y_{22} + \frac{\sigma_a^2}{4}\right]$$

$$= y_{22}\left[2\left(\frac{y_{22}}{\sigma_a^2}\right)^2 + 2\,\frac{y_{22}}{\sigma_a^2} + \frac{1}{4}\right]$$

Further,

$$\sigma_m^2 = A\,\frac{y_{22}}{\sigma_a^2}$$

$$= \frac{y_{22}}{\sigma_a^2}\left(y_{11} + 2\,y_{12} + y_{22} + \frac{\sigma_a^2}{4}\right)$$

$$\frac{\sigma_m^2}{\sigma_a^2} = \frac{y_{22}}{\sigma_a^2}\left[\frac{y_{22}}{\sigma_a^2}\left\{2\left(\frac{y_{22}}{\sigma_a^2}\right)^2 + 2\left(\frac{y_{22}}{\sigma_a^2}\right) + \frac{1}{4}\right\}\right.$$

$$\left. + \frac{y_{22}}{\sigma_a^2}\left\{2\left(\frac{y_{22}}{\sigma_a^2}\right) + 1\right\} + \left(\frac{y_{22}}{\sigma_a^2}\right) + \frac{1}{4}\right]$$

Letting

$$u = y_{22}/\,\sigma_a^2$$

we have

$$2u^4 + 4u^3 + \frac{9}{4}u^2 + \frac{1}{4}u - \frac{\sigma_m^2}{\sigma_a^2} = 0$$

Now, the vehicle thrust acceleration is of the order of 7 m/sec^2. Assuming a 5 percent uncertainty in the value, yields a σ_a of the order of 0.35 m/sec^2. We take σ_m to be 100 m. Then σ_m^2/σ_a^2 is 8.2×10^4 sec^4, and u is approximately 14. It follows that

$$y_{22} = \sigma_a^2 u$$

$$= .122 \times 14 = 1.71 \quad m^2/sec^2$$

$$y_{11} = 1.71 \left[2 (14)^2 + 2 (14) + \frac{1}{4} \right]$$

$$= 383. \quad m^2$$

The standard deviations in position and velocity are then 20 m. and 1.3 m/sec in the limit. These values compare with the limiting values of 0 m and 0 m/sec that would result if there were not thrust acceleration uncertainties. Before takeoff the position is known to about 23 m and the velocity to essentially 0 m/sec. It therefore appears that position can be monitored to of the order of 20 to 40 m and the velocity to 1.3 to 3 m/sec during boost. It therefore seems worthwhile to expend the effort to perform a three-dimensional analysis.

In three dimensions, letting the 1 direction be the direction of accurate radar measurement, the 2 direction be down range, and the 3 direction be cross range.

$$Z^* = \begin{bmatrix} z_1^* \\ z_2^* \\ z_3^* \\ \dot{z}_1^* \\ \dot{z}_2^* \\ \dot{z}_3^* \end{bmatrix}$$

and

$$M^* = \begin{bmatrix} 1 - \frac{u}{2(R^*)^3} & 0 & 0 & 1 & 0 & 0 \\ 0 & 1 - \frac{u}{2(R^*)^3} & 0 & 0 & 1 & 0 \\ 0 & 0 & 1 - \frac{u}{2(R^*)^3} & 0 & 0 & 1 \\ -\frac{u}{(R^*)^3} & 0 & 0 & 1 & 0 & 0 \\ 0 & -\frac{u}{(R^*)^3} & 0 & 0 & 1 & 0 \\ 0 & 0 & -\frac{u}{(R^*)^3} & 0 & 0 & 1 \end{bmatrix}$$

in which the time of prediction is 1 second. We assume that the gravity vector does not change appreciably during 1 second, and that $M = M^*$. Further, so far as the covariance matrix of errors in position and velocity is concerned, we can neglect the gravity terms, so that

$$M = \begin{bmatrix} 1 & 0 & 0 & 1 & 0 & 0 \\ 0 & 1 & 0 & 0 & 1 & 0 \\ 0 & 0 & 1 & 0 & 0 & 1 \\ 0 & 0 & 0 & 1 & 0 & 0 \\ 0 & 0 & 0 & 0 & 1 & 0 \\ 0 & 0 & 0 & 0 & 0 & 1 \end{bmatrix}$$

For the covariance of the thrust acceleration, we assume that the standard deviation of thrust acceleration magnitude is 0.35 m/sec^2 and the standard deviation of thrust acceleration in each of the two orthogonal directions is also 0.35 m/sec^2. Since the thrust acceleration is of the order of 7 m/sec^2, this corresponds to a thrust acceleration magnitude error of 5 percent, and elevation and azimuth pointing error standard deviations of about 3 degrees. By choosing the standard deviations equal in the three orthogonal directions we simplify the computations.

We are aware that there is a high correlation between the thrust acceleration errors at successive instants, but for this first analysis we assume these errors are uncorrelated. Then

$$\text{cov}(A, A) = \sigma_a^2 \begin{bmatrix} 1/4 & 0 & 0 & 1/2 & 0 & 0 \\ 0 & 1/4 & 0 & 0 & 1/2 & 0 \\ 0 & 0 & 1/4 & 0 & 0 & 1/2 \\ 1/2 & 0 & 0 & 1 & 0 & 0 \\ 0 & 1/2 & 0 & 0 & 1 & 0 \\ 0 & 0 & 1/2 & 0 & 0 & 1 \end{bmatrix}$$

Only range measurements are made. Resolving these into the 1, 2, 3 directions, the information matrix corresponding to one set of measurements is

$$\text{cov}^{-1}(X, X) = \begin{bmatrix} 0.36 & 0 & 0 & 0 & 0 & 0 \\ 0 & 3600 & 0 & 0 & 0 & 0 \\ 0 & 0 & 3600 & 0 & 0 & 0 \\ 0 & 0 & 0 & 0 & 0 & 0 \\ 0 & 0 & 0 & 0 & 0 & 0 \\ 0 & 0 & 0 & 0 & 0 & 0 \end{bmatrix}$$

Starting with

$$\text{cov}(Y_o, Y_o) = \begin{bmatrix} 0.053 & 0 & 0 & 0 & 0 & 0 \\ 0 & 530 & 0 & 0 & 0 & 0 \\ 0 & 0 & 530 & 0 & 0 & 0 \\ 0 & 0 & 0 & 0 & 0 & 0 \\ 0 & 0 & 0 & 0 & 0 & 0 \\ 0 & 0 & 0 & 0 & 0 & 0 \end{bmatrix}$$

we compute cov (Y_n, Y_n) iteratively, using

$$\text{cov}(Z_{n+1}, Z_{n+1}) = M \text{ cov } (Y_n, Y_n)\ M^T + \text{cov } (A, A)$$

and

$$\text{cov}(Y_{n+1}, Y_{n+1}) = \left[\text{cov}^{-1}(Z_{N+1}, Z_{n+1}) + \text{cov}^{-1}(X, X)\right]^{-1}$$

This must be performed on a digital computer.

APOLLO NOTE NO. 114

H. Dale
30 September 1963

CALCULATION OF COVARIANCE MATRICES FOR HYPERBOLIC ORBITS

(A Revision of Apollo Note No. 82)

Apollo Note No. 82 presents a means for finding the covariance matrix when Doppler observations of a vehicle in an elliptic or circular orbit about a moving Moon are made from a MSFN facility on the surface of the Earth. This note extends the analysis to cover the hyperbolic case, that is, for the case of eccentricity, e, greater than unity.

In Apollo Note No. 82 the important relationships are denoted by placing them in boxes. This note presents the corresponding relationships only where changes occur due to the eccentricity of the orbit.

Starting on page 8 of Apollo Note No. 82:

The eccentric anomaly, defined as $\mathcal{E}$ for the elliptic case, must be redefined as F. Thus the initial value of the eccentric anomaly, F_o, is given by its sinh and cosh:

$$\sinh F_o = \frac{(e^2 - 1)^{1/2} \sin \theta_o}{1 + e \cos \theta_o}$$

$$\boxed{\sinh F_o = \frac{\sqrt{2E}\, \sin \theta_o}{a_5}}$$

and

$$\cosh F_o = \frac{e + \cos \theta_o}{1 + e \cos \theta_o}$$

$$\boxed{\cosh F_o = \frac{e + \cos \theta_o}{\left(\frac{H a_5}{\mu}\right)}}$$

The mean anomaly at the initial condition is:

$$M_o = e \sinh F_o - F_o$$

and the mean motion is:

$$n = \frac{2E\sqrt{2E}}{\mu}$$

so that time, t_o, from perilune to the initial point, T = 0, is

$$t_o = M_o/n$$

also

$$\frac{\partial n}{\partial a_j} = \frac{3n}{2E} \frac{2E}{\partial a_j}$$

Then,

$$e \sinh F_o = \frac{(e^2 - 1)^{1/2} e \sin \theta_o}{1 + e \cos \theta_o}$$

$$\frac{\partial (e \sinh F_o)}{\partial a_j} = \frac{e \sinh F_o}{2(e^2 - 1)} \frac{\partial e^2}{\partial a_j} + \frac{(e^2 - 1)^{1/2}}{1 + e \cos \theta_o} \frac{\partial (e \sin \theta_o)}{\partial a_j} - \frac{e \sinh F_o}{1 + e \cos \theta_o} \frac{\partial (e \cos \theta_o)}{\partial a_j}$$

and

$$e \cosh F_o = \frac{e^2 + e \cos \theta_o}{1 + e \cos \theta_o}$$

$$\frac{\partial (e \cosh F_o)}{\partial a_j} = \frac{1}{1 + e \cos \theta_o} \frac{\partial e^2}{\partial a_j} + \frac{(1 - e^2)}{(1 + e \cos \theta_o)^2} \frac{\partial (e \cos \theta_o)}{\partial a_j}$$

The next correction occurs since

$$F_o = \tanh^{-1} \left(\frac{e \sinh F_o}{e \cosh F_o} \right)$$

from which it follows that

$$\frac{\partial F_o}{\partial a_j} = \frac{1}{1 - \tanh^2 F_o} \left[\frac{e \cosh F_o \dfrac{\partial (e \sinh F_o)}{\partial a_j} - e \sinh F_o \dfrac{\partial (e \cosh F_o)}{\partial a_j}}{(e \cosh F_o)^2} \right]$$

so

$$\boxed{e \frac{\partial F_o}{\partial a_j} = \cosh F_o \frac{\partial (e \sinh F_o)}{\partial a_j} - \sinh F_o \frac{\partial (e \cosh F_o)}{\partial a_j}}$$

Since

$$M_o = e \sinh F_o - F_o$$

it follows that:

$$\boxed{e \frac{\partial M_o}{\partial a_j} = (e \cosh F_o - 1)\left(e \frac{\partial F_o}{\partial a_j}\right) + \frac{\sinh F_o}{2} \frac{\partial e^2}{\partial a_j}}$$

The eccentric anomaly must be computed by solution of the equation

$$\boxed{M = e \sinh F - F}$$

and the values of sinh F and cosh F found from F.

Then the trigonometric functions of the control angle are

$$\boxed{\sin \theta = \frac{(e^2 - 1)^{1/2} \sinh F}{e \cosh F - 1}}$$

and

$$\boxed{\cos \theta = \frac{e - \cosh F}{e \cosh F - 1}}$$

Now,

$$\tanh F = \frac{\sinh F}{\cosh F} = \frac{(e^2 - 1)^{1/2} \sin \theta}{e + \cos \theta}$$

so

$$\frac{\partial F}{\partial a_j} = \frac{e \cosh F - 1}{(e^2 - 1)^{1/2}} \frac{\partial \theta}{\partial a_j} + \frac{\sinh F}{2e(e^2 - 1)} \frac{\partial e^2}{\partial a_j}$$

Then from

$M = e \sinh F - F$

it follows that

$$\frac{\partial M}{\partial a_j} = (e \cosh F - 1) \frac{\partial F}{\partial a_j} + \frac{\sinh F}{2e} \frac{\partial e^2}{\partial a_j}$$

$$= \frac{(e \cosh F - 1)^2}{(e^2 - 1)^{1/2}} \frac{\partial \theta}{\partial a_j} + \frac{\sinh F}{2e} \left[\frac{e \cosh F - 1}{e^2 - 1} + 1 \right] \frac{\partial e^2}{\partial a_j}$$

$$e \frac{\partial M}{\partial a_j} = \frac{(e \cosh F - 1)^2 e}{(e^2 - 1)^{1/2}} \frac{\partial e}{\partial a_j} + \frac{\sinh F}{2} \frac{\partial e^2}{\partial a_j} + \frac{\sinh F (e \cosh F - 1)}{2(e^2 - 1)} \frac{\partial e^2}{\partial a_j}$$

Following Apollo Note No. 82 to the bottom of page 13:

$$e \frac{\partial \theta}{\partial a_j} = \frac{(e^2 - 1)^{1/2}}{(e \cosh F - 1)^2} \left\{ \frac{3(M - M_o)}{2E} e \frac{\partial E}{\partial a_j} + e \frac{\partial M_o}{\partial a_j} - \frac{\sinh F}{2} \left(\frac{e \cosh F - 1}{e^2 - 1} + 1 \right) \frac{\partial e^2}{\partial a_j} \right\}$$

Setting F, θ, and M equal to F_o, θ_o, and M_o, we find

$$\frac{\partial (\theta - \theta_o)}{\partial a_j} = (e^2 - 1)^{1/2} \left\{ \frac{\frac{3(M - M_o)}{2E} \frac{\partial E}{\partial a_j} - \sinh F \left(\frac{e \cosh F - 1}{e^2 - 1} + 1 \right) \frac{\partial e}{\partial a_j}}{(e \cosh F - 1)^2} + \frac{\sinh F \left(\frac{e \cosh F_o - 1}{e^2 - 1} + 1 \right) \frac{\partial e}{\partial a_j}}{(e \cosh F_o - 1)^2} + \frac{(\cosh F - \cosh F_o) \left[2 - e(\cosh F + \cosh F_o) \right]}{(e \cosh F - 1)^2 (e \cosh F_o - 1)^2} \left(e \frac{\partial M_o}{\partial a_j} \right) \right\}$$

The remainder of Apollo Note No. 82, beginning with the second equation on page 15, remains unchanged for hyperbolic orbits.

APOLLO NOTE NO. 115

J. R. Holdsworth
30 September 1963

THE CALCULATION OF THE COVARIANCE MATRIX OF THE ERRORS IN THE ESTIMATORS OF THE ORBIT PARAMETERS WHEN THE ESTIMATES ARE BASED UPON DATA WHICH IS CONTAMINATED BY AUTO-CORRELATED NOISE

The purpose of this note is to extend the analysis of Apollo Note No. 43 to the case where the data are contaminated by additive noise which is correlated in time so that the successive samples may no longer be considered to be statistically independent pieces of data. Apollo Note No. 107 offered an approximate method for accounting for this correlation which was very convenient as it permitted the use of computer programs which are already in existence. The present note is an honest treatment of the error analysis problem with auto-correlated observations and hence may be used as a standard of comparison to determine the regime of numerical validity of the approximate method described in Apollo Note No. 107.

The analysis in the present problem becomes notationally vexing unless heavy use is made of vector and matrix methods. Thus it will be convenient for us to depart somewhat from the notation employed in Apollo Notes No. 3, 43, and subsequent notes. To facilitate the notational change, we list below some of the quantities which will be frequently used.

N = the number of pieces of observed data.

M = the number of orbit parameters under consideration whose values must be estimated. Usually $M = 6$ or 7 depending upon whether a bias error exists or not.

σ^2 = the variance of the noise process.

$\rho(i, j)$ = the normalized auto-correlation between the ith and jth noise sample.

A = the auto-covariance matrix of the noise process whose i, jth element is given by $a_{ij} = \sigma^2 \rho(i,j)$.

$\bar{p}$ = the M dimensional parameter vector, i.e., the column matrix whose components are to be estimated from the data.

$\hat{\bar{p}}$ = the M dimensional estimator vector whose ith component is the maximum likelihood estimate of the ith component of the vector $\bar{p}$.

$\Delta\bar{p} = \hat{\bar{p}} - \bar{p}$ is the M dimensional vector of estimator errors.

$\bar{d}_m$ = the N dimensional measurement vector the kth component of which corresponds to the measurement made at the kth sampling instant.

$\bar{n}$ = the N dimensional noise vector the kth component of which is the value of the kth noise sample.

$\bar{d}_a$ = the actual N dimensional trend vector which would be observed if there were no noise. $\bar{d}_a$ is a function of $\bar{p}$ hence accounts for any systematic non-fluctuating bias which may exists.

E = the expected value operator or integration with respect to the joint distribution of the N noise samples.

We assume that the contaminating noise process is gaussian with auto-covariance A as indicated above. Furthermore, since we have defined our parametric vector $\bar{p}$ so that it consists of all parameters which must be estimated including a bias and possibly other parameters which might appear in a systematic time variation

of the mean noise, there is no loss of generality in assuming that the noise process $\bar{n}$ has a zero mean. It is of some interest to note that had this been done in Apollo Notes 3 and 43, i.e., if the function $\tilde{f}_c(t) = f_c(t) + b$ had been used instead of f_c, then the notational inconveniences arising from the appearance of the bias would not have occurred and Equation (6) of that note need not have been written.

From our preceding remarks it follows that we may write the following vector equation where all vectors are assumed to be column vectors except when transposition is explicitly indicated.

$$\bar{d}_m = \bar{d}_a + \bar{n} \tag{1}$$

The joint likelihood or probability density function of all of the data may be written:

$$L = \frac{1}{(2\pi)^{\frac{N}{2}} (\det A)^{\frac{N}{2}}} \exp \frac{1}{2} \mathcal{L} \tag{2}$$

where $\mathcal{L}$ is given by the quadratic form

$$\mathcal{L} = \bar{n}^T A^{-1} n \tag{3}$$

where in Equation (3), the T denotes matrix transposition.

From Equation (1), we may write

$$\mathcal{L} = (\bar{d}_m - \bar{d}_a)^T A^{-1} (\bar{d}_m - \bar{d}_a) \tag{4}$$

We note from (2) that L is a monotonically decreasing function of $\mathcal{L}$ and hence that the likelihood function L will be maximized if the function $\mathcal{L}$ is minimized.

We recall that the trend vector $\bar{d}_a$ is a function of the parametric vector to be estimated $\bar{p}$. That is:

$$\bar{d}_a = \bar{d}_a(\bar{p}) \tag{5}$$

The vector $\bar{p}$ is what we wish to estimate as a function of the measurement vector $\bar{d}_m$. The maximum likelihood estimators of the components of $\bar{p}$ are obtained by considering these components variable and by equating the partial derivative of $\mathcal{L}$ with respect to each of the components to zero. This yields a system of M equations in the M unknown components of $\bar{p}$. The vector solution of this equation is the maximum likelihood estimator $\hat{\bar{p}}$ of the unknown vector $\bar{p}$ based on the available data.

Differentiating Equation (4) with respect to the components p_i and equating the resulting expression to zero, and performing a small amount of simplification allows us to write the following vector expression for the M scalar likelihood equations.

$$\left(\frac{\partial \bar{d}_a}{\partial \bar{p}} \right)^T A^{-1} \left[\bar{d}_m - \bar{d}_a(\hat{\bar{p}}) \right] = 0 \tag{6}$$

Equation (6) requires some comment. The quantity denoted by $\frac{\partial \bar{d}_a}{\partial \bar{p}}$ is actually an N x M matrix with components as indicated below.

$$\frac{\partial \bar{d}_a}{\partial \bar{p}} = \begin{pmatrix} \frac{\partial d_a(1)}{\partial p_1} & \cdots & \frac{\partial d_a(1)}{\partial p_M} \\ \vdots & & \\ \frac{\partial d_a(N)}{\partial p_1} & & \frac{\partial d_a(N)}{\partial p_M} \end{pmatrix} \tag{7}$$

That is, the i, jth element of the matrix $\frac{\partial \bar{d}_a}{\partial \bar{p}}$ is the partial derivative of the ith component of the vector $\bar{d}_a$ with respect to the jth component of the parametric vector $\bar{p}$. The superscript T as usual denotes the operation of matrix transposition. Furthermore,

to emphasize the nature of the estimation problem we have explicitly exhibited the dependence of $\bar{d}_a$ upon the estimator vector $\hat{\bar{p}}$. That is $\hat{\bar{p}}$ is the vector solution obtained from solving the system of equations in (6) for the parametric vector $\bar{p}$ as a function of the data $\bar{d}_m$.

From our list of definitions we may write the following relationship connecting the parametric vector, the estimator vector and the estimator error vector.

$$\hat{\bar{p}} = \bar{p} + \Delta\bar{p} \tag{8}$$

Substitution of Equation (8) into Equation (6) yields:

$$\left(\frac{\partial \bar{d}_a}{\partial \bar{p}} \right)^T A^{-1} \left(\bar{d}_m - \bar{d}_a \left(\bar{p} + \Delta \bar{p} \right) \right) = 0 \tag{9}$$

Now as in previous notes, we assume that the sample size is sufficiently large and the noise variance sufficiently small so that the components of the error vector $\Delta \bar{p}$ may be expected to be small with respect to the components of $\bar{p}$. This assumption was asymptotically valid with the number of observations for the earlier cases involving independent noise. It is asymptotically true in the present case with correlated noise samples also providing that the total sampling time extends over several noise correlation times and that all N sampling times are not sandwiched into some short time interval which is small with respect to the noise correlation time. At any rate we shall assume that these conditions have been sufficiently well met to justify the following linearization.

$$\bar{d}_a \left(\bar{p} + \Delta \bar{p} \right) = \bar{d}_a \left(\bar{p} \right) + \frac{\partial \bar{d}_a}{\partial \bar{p}} \Delta \bar{p} \tag{10}$$

In Equation (10) $\frac{\partial \bar{d}_a}{\partial \bar{p}}$ is the matrix defined in Equation (7) and all partial derivatives are assumed to be evaluated at the parametric

value $\bar{p}$.

Substitution of (10) into (9) yields:

$$\left(\frac{\partial \bar{d}_a}{\partial \bar{p}}\right)^T A^{-1} \left(\bar{d}_m - \bar{d}_a(\bar{p}) - \frac{\partial \bar{d}_a}{\partial \bar{p}} \Delta \bar{p} \right) = 0 \qquad (11)$$

Since $\bar{n} = \bar{d}_m - \bar{d}_a(\bar{p})$

then from Equation (11) we obtain the following linear equation for the estimator error vector.

$$\left(\frac{\partial \bar{d}_a}{\partial \bar{p}}\right)^T A^{-1} \frac{\partial \bar{d}_a}{\partial \bar{p}} \Delta \bar{p} = \left(\frac{\partial \bar{d}_a}{\partial \bar{p}}\right)^T A^{-1} \bar{n} \qquad (12)$$

Solving Equation (12) for $\Delta \bar{p}$ yields

$$\Delta \bar{p} = \left(\frac{\partial \bar{d}_a}{\partial \bar{p}}^T A^{-1} \frac{\partial \bar{d}_a}{\partial \bar{p}} \right)^{-1} \frac{\partial \bar{d}_a}{\partial \bar{p}}^T A^{-1} \bar{n} \qquad (13)$$

Taking the transpose of both sides of (13) gives,

$$\Delta \bar{p}^T = \bar{n}^T A^{-1} \frac{\partial \bar{d}_a}{\partial \bar{p}} \left(\frac{\partial \bar{d}_a}{\partial \bar{p}}^T A^{-1} \frac{\partial \bar{d}_a}{\partial \bar{p}} \right)^{-1} \qquad (14)$$

where in passing from (13) to (14) we have used the fact that the matrices A^{-1} and $\frac{\partial \bar{d}_a}{\partial \bar{p}}^T A^{-1} \frac{\partial \bar{d}_a}{\partial \bar{p}}$ are both symmetric.

Now by definition the covariance matrix of the estimator errors is $E(\Delta \bar{p} \; \Delta \bar{p}^T)$. Thus if we pre-multiply Equation (14) by Equation (13) and use the fact that

$$E(\bar{n}\ \bar{n}^T) = A \tag{15}$$

we obtain the following expression for the covariance matrix of our estimator errors.

$$E(\Delta\bar{p}\ \Delta\bar{p}^T) = \left(\frac{\partial \bar{d}_a}{\partial \bar{p}}^T A^{-1} \frac{\partial \bar{d}_a}{\partial \bar{p}}\right)^{-1} \tag{16}$$

Formula (16) thus generalizes the approach used in all of the earlier notes to the case where the noise samples are auto-correlated.

It may be worthwhile to mention that the auto-covariance matrix is known once the power spectral density function of the noise is known. Also, the present analysis does not require the assumption that the noise process is stationary. This is no real generalization however since the analysis in Note 43 may be easily modified to account for non-stationary noise.

APOLLO NOTE NO. 116

G. F. Floyd
30 September 1963

MSFN LUNAR COVERAGE

Preliminary analysis dealing with station locations for precision Earth-based tracking during the lunar rendezvous is summarized in the figure.

The figure shows as a function of the location of the sub-lunar point (Moon's declination varies between 28 North and 28 South), the MSFN stations which can see the Moon at least 5° above their respective horizons. The stations used are those which are receiving attention from the point of view of proper location during injection as well as the political stability of the country in which they are located. As shown on the figure, we have selected three stations: Goldstone, Carnarvon (Australia) and Ascension Island as the transmit and receive stations and six receive-only stations: Cape Canaveral, Canberra (Australia), Guam Island, Madrid, Johannesburg and Antiqua Island (British West Indies). The choice of these three for the transmitting stations was primarily based on obtaining a large overlap to permit both easy hand-over and shift between the illuminating transmitter and larger horizon angles without loss of system coverage. In this connection, we note that the motion of the sub-lunar point is primarily due to Earth spin at 15° per hour so that the minimum overlap of 30° allows a minimum of two hours to shift over, or 20° horizons. Many other choices for the 3 transmitting stations are satisfactory.

The coverage of the system shown is very good in terms of a large and almost constant number of observing stations, (there are never less than three and most of the time there are four). On the other hand, the computer studies indicate the desirability of a large North/South separation in order to determine accurately the out-of-plane rendezvous miss. In this regard the system is weak, when the sub-lunar point is between 100° and 130° West. During

this period the most southerly receiving station would be Antiqua Island which is only 18° South of Goldstone. The degradation in system operation resulting from this small latitude separation is currently being investigated on the computer. Throughout the remaining 330° of possible sub-lunar points, the system geography appears to be good with latitude differences of the order of 40°.

MSFN LUNAR COVERAGE WITH 5° HORIZON

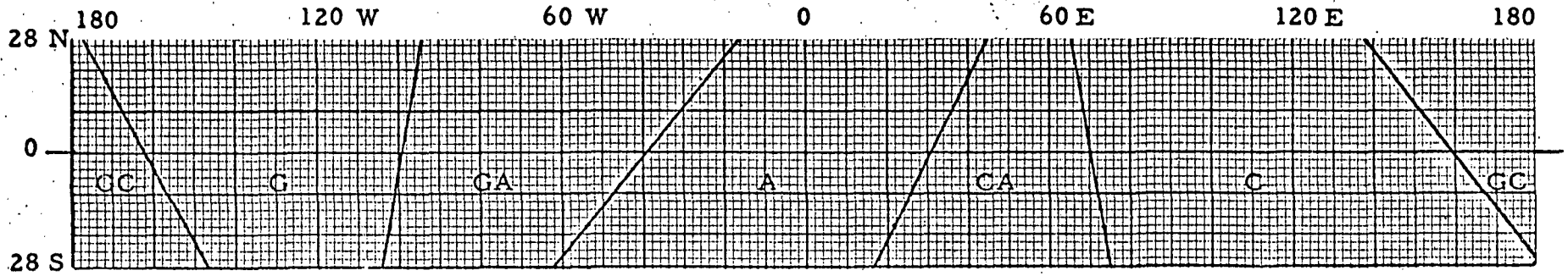

3 Transmit-Receive Stations:

Goldstone (G); Carnarvon (C); Ascension (A).

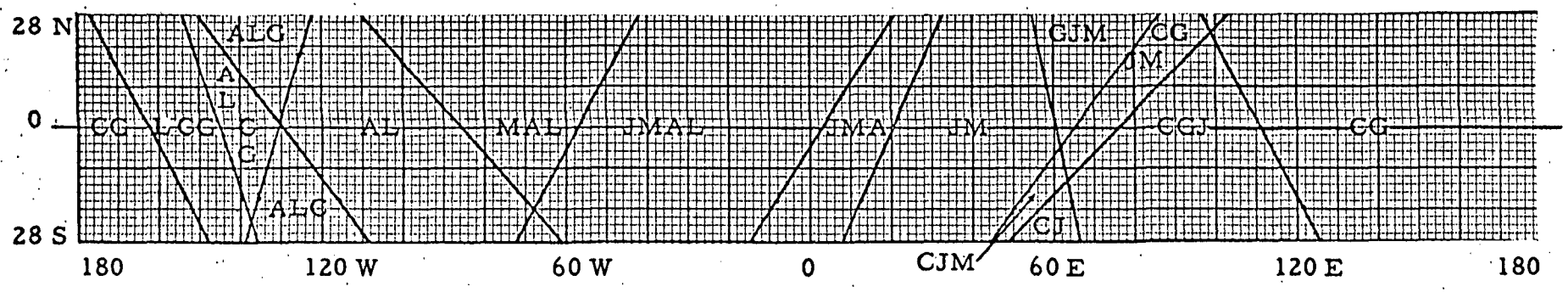

6 Receiving Stations:

Canaveral (L); Canberra (C); Guam (G); Madrid (M);

Johannesburg (J); Antiqua (A).

APOLLO NOTE NO. 117

H. Engel
3 October 1963

EARTH-MOON AND MOON-EARTH TRAJECTORIES

The object of this note is to describe a means for computing approximate trajectories and for obtaining error covariance matrices for points on these trajectories. The notation is that of earlier Apollo notes, especially Apollo Note No. 82.

The equation of the LSOI* (which is not really a sphere) is

$$\frac{m_M}{m_E}\,\frac{\left|\dfrac{\bar{r}}{r^3}+\dfrac{\bar{X}_m}{X_m^3}\right|}{\dfrac{1}{R^2}} = \frac{m_E}{m_M}\,\frac{\left|\dfrac{\bar{h}}{h^3}-\dfrac{\bar{X}_m}{X_m^3}\right|}{\dfrac{1}{R^2}}$$

in which m_m and m_E are the masses of the Moon and Earth and

$$\bar{R} = \bar{X}_m + \bar{r}\,.$$

The radius of the lunar sphere of influence varies with direction, but is approximately 0.13 times the Earth-Moon distance. The radius of the LSOI where an Earth-Moon or Moon-Earth trajectiory pierces it can be determined by substituting the values of $\bar{r}$ or $\bar{R}$, obtained on the Moon-centered or Earth-centered portions of the trajectory into the equation for the LSOI and determining when it is satisfied.

If a slightly different trajectory is employed the same radius may be used for the LSOI without causing any appreciable error since the accelerations in the vicinity of the surface of the LSOI are small. Thus, in determining the error covariance matrix, the radius of the LSOI may be considered constant.

---

* Reference Apollo Note No. 12.

Earth-Moon Trajectories

Having the orbit parameters of the Earth-centered portion of the Earth-Moon trajectory, the time of piercing the LSOI can be computed. From Apollo Note No. 82 the eccentricity and mean motion can be computed from the initial position and velocity, asterisks denoting Earth-centered portion of trajectory,

$$H^* = a_1^* \, a_5^*$$

$$2E^* = \frac{-2\mu_E}{a_1^*} + a_4^{*2} + a_5^{*2}$$

$$e^* \cos \theta_o^* = \frac{H^* a_5^*}{\mu_E} - 1$$

$$e^* \sin \theta_o^* = \frac{H^* a_4^*}{\mu_E}$$

$$\theta_o^* = \tan^{-1} \left(\frac{e^* \sin \theta_o^*}{e^* \cos \theta_o^*} \right)$$

$$e^{*2} = (e^* \cos \theta_o^*)^2 + (e^* \sin \theta_o^*)^2$$

$$e^* = \sqrt{e^{*2}}$$

$$n^* = \frac{-2E^* \sqrt{-2E^*}}{\mu_E}$$

$$\sin \xi_o^* = \frac{\sqrt{-2E^*}}{a_5^*} \sin \theta_o^*$$

$$\cos \xi_o^* = \frac{e^* + \cos \theta_o^*}{\left(\frac{H^* a_5^*}{\mu_E} \right)}$$

$$\xi_o^* = \tan^{-1}\left(\frac{e^* \sin E_o^*}{e^* \cos E_o^*}\right)$$

$$M_o^* = \xi_o^* - e^* \sin \xi_o^*$$

$$t_o^* = M_o^* / n^*$$

$$T_o = 0$$

At any later time T,

$$t^* = T + t_o^*$$

$$M^* = n^* t^*$$

ξ^* is computed from

$$M^* = \xi^* - e^* \sin \xi^*$$

Then

$$\sin \theta^* = \frac{(1 - e^{*2})^{1/2} \sin \xi^*}{1 - e^* \cos \xi^*}$$

$$\cos \theta^* = \frac{\cos \xi^* - e^*}{1 - e^* \cos \xi^*}$$

$$R = \frac{H^{*2}}{\mu_E (1 + e^* \cos \theta^*)}$$

$$\dot{R} = \frac{\mu_E e^*}{H^*} \sin \theta^*$$

The Earth-centered portion of the orbit is in the $x'^* y'^*$- plane, the quantity ρ_m^* having been taken as zero. The orientation of the orbit with respect to the Earth is described in terms of the angles L, ℓ, β, ξ^* η^* and ζ^*, and the coordinate systems are x y z, $\tilde{x}$ $\tilde{y}$ $\tilde{z}$ and x'^*, y'^*, z'^*.

The position and velocity of the Moon with respect to the Earth are given by

$$\tilde{X}_m = \begin{bmatrix} \rho_m \cos \omega_m T \\ \rho_m \sin \omega_m T \\ 0 \end{bmatrix}$$

and

$$\dot{\tilde{X}} = \begin{bmatrix} -\omega_m \tilde{y}_m \\ \omega_m \tilde{x}_m \\ 0 \end{bmatrix}$$

and the components in the x y z system are given by

$$X_m = K^T \tilde{X}_m$$

$$\dot{X}_m = K^T \dot{\tilde{X}}$$

The vehicle position and velocity in the same coordinate system are found from

$$\mathbb{R}'^* = \begin{bmatrix} R \cos \theta^* \\ R \sin \theta^* \\ 0 \end{bmatrix}$$

$$\dot{\mathbb{R}}'^* = \begin{bmatrix} \frac{-H^*}{R} \sin (\theta^* - \theta_o^*) + \dot{R} \cos (\theta^* - \theta_o^*) \\ \frac{H^*}{R} \cos (\theta^* - \theta_o^*) + \dot{R} \sin (\theta^* - \theta_o^* \\ 0 \end{bmatrix}$$

$$\mathbb{R} = K^T L^{*T} \mathbb{R}'^*$$

$$\dot{\mathbb{R}} = K^T L^{*T} \dot{\mathbb{R}}'^*$$

and then, since

$$\bar{r} = \bar{X}_m - \bar{R}$$

it follows

$$X = X_m - \mathbb{R} .$$

The time T can be varied until the equation for the boundary of the LSOI is satisfied. For this particular value of T, called T_L, the position and velocity of the vehicle with respect to the Moon are computed from

$$X = X_m - \mathbb{R}$$

and

$$\dot{X} = \dot{X}_m - \dot{\mathbb{R}} .$$

The components of these quantities in $\tilde{x}\,\tilde{y}\,\tilde{z}$ coordinates are obtained from

$$\tilde{X} = K X$$

and

$$\dot{\tilde{X}} = K \dot{X} .$$

Then

$$r^2 = X^T X$$

and

$$(\dot{r})^2 = \dot{X}^T \dot{X}$$

$$H^2 = r_o^2 (\dot{r}_o)^2 - (X^T \dot{X})^2$$

$$H = \sqrt{H^2}$$

$$2E = - \frac{2\mu_m}{r_o} + (\dot{r}_o)^2$$

$$e^2 = 1 + \frac{2E\ H^2}{\mu_m^2}$$

$$e = \sqrt{e}$$

$$r_p = \frac{H^2}{\mu_m (1 + e)}$$

$$\cos \theta_o = \frac{1}{e} \left[\frac{H^2}{\mu_m r} - 1 \right] .$$

$$\theta_o = \cos^{-1}(\cos\theta_o) \quad , \begin{cases} -\pi < \theta_o < 0 \text{ if } X^T\dot{X} < 0 \\ 0 < \theta_o < \pi \text{ if } X^T\dot{X} > 0 \end{cases}$$

The components of H in $\tilde{x}\tilde{y}\tilde{z}$ coordinates are

$$\tilde{H} = \begin{bmatrix} \tilde{y}\dot{\tilde{z}} - \dot{\tilde{y}}\tilde{z} \\ \tilde{z}\dot{\tilde{x}} - \dot{\tilde{z}}\tilde{x} \\ \tilde{x}\dot{\tilde{y}} - \dot{\tilde{x}}\tilde{y} \end{bmatrix}$$

and the components of $\hat{z}'$ in $\tilde{x}\tilde{y}\tilde{z}$ coordinates are $\tilde{H}/H$ and denoted by $(z'_{\tilde{x}}, z'_{\tilde{y}}, z'_{\tilde{z}})$. The components of $\hat{r}_o$ in $\tilde{x}\tilde{y}\tilde{z}$ coordinates are $\tilde{X}/r$ and denoted by $(r_{o\tilde{x}}, r_{o\tilde{y}}, r_{o\tilde{z}})$ Define $\hat{\gamma}$

$$\hat{\gamma} = \hat{z}' \times \hat{r}_o$$

Then

$$\hat{x}' = \hat{r}_o \cos\theta_o - \hat{\gamma} \sin\theta_o$$

and

$$\hat{y}' = \hat{r}_o \sin\theta_o + \hat{\gamma} \cos\theta_o$$

so the components of $\hat{x}'$ and $\hat{y}'$ in $\tilde{x}\tilde{y}\tilde{z}$ coordinates can be found, and in the x' y' z' coordinate system y' = z' = 0 at perilune. The parameters of the lunar portion of the orbit, expressed in terms of the conditions at perilune, are

$$a_1 = r_p$$

$$a_2 = a_3 = 0$$

$$a_5 = H/a_1$$

$$a_4 = a_6 = 0$$

The time of perilune, T_p, is T_L plus the time from entry into the LSOI until perilune.

In order to find the nominal launch conditions to place the vehicle in an orbit with desired perilune altitude, orbit inclination with respect to the Moon, and time of flight, these quantities may be calculated using the above procedure and the launch parameters varied until the desired orbit is obtained.

Thereafter, for observations in the Earth-centered portion of the orbit the covariance matrix at T_o may be calculated, and the corresponding covariance matrix at T_L computed from

$$\text{cov}\left[x'^*(T_L),\ x'^*(T_L)\right] = Q_L'^* \,\text{cov}\left[a^*,\ a^*\right]\, Q_L'^{*T}$$

in which $Q_L'^*$ is the Jacobian matrix with elements

$$Q'^*_{L,i,j} = \frac{\partial\, x_i'^*(T_L)}{\partial\, a_j^*}$$

the elements of which are normally computed in the program for finding the covariance matrices.

The Jacobian matrix relating the Moon-centered coordinates to the Earth-centered coordinates at the surface of the LSOI is Q_L' with components obtained by use of the rotation matrices L^*, Γ and Λ which take x'^*, y'^*, z'^* into $\tilde{x}$, $\tilde{y}$, $\tilde{z}$, take $\tilde{x}$, $\tilde{y}$, $\tilde{z}$ into r_o, γ, z', and take r_o, γ, z' into x', y', z'. L^* has already been mentioned,

$$\Gamma = \begin{bmatrix} r_{o\tilde{x}} & r_{o\tilde{y}} & r_{o\tilde{z}} \\ (z'_{\tilde{y}} r_{o\tilde{z}} - z'_{\tilde{z}} r_{o\tilde{y}}) & (z'_{\tilde{z}} r_{o\tilde{x}} - z'_{\tilde{x}} r_{o\tilde{z}}) & (z'_{\tilde{x}} r_{o\tilde{y}} - z'_{\tilde{y}} r_{o\tilde{x}}) \\ z'_{\tilde{x}} & z'_{\tilde{y}} & z'_{\tilde{z}} \end{bmatrix}$$

$$\Lambda = \begin{bmatrix} \cos\theta_o & -\sin\theta_o & 0 \\ \sin\theta_o & \cos\theta_o & 0 \\ 0 & 0 & 1 \end{bmatrix}$$

Then

$$Q'_L = \begin{bmatrix} \Lambda & 0 \\ 0 & \Lambda \end{bmatrix} \begin{bmatrix} \Gamma & 0 \\ 0 & \Gamma \end{bmatrix} \begin{bmatrix} L^{*T} & 0 \\ 0 & L^{*T} \end{bmatrix}$$

and

$$\text{cov}\left[x'(T_L),\ x'(T_L)\right] = Q_L\ \text{cov}\left[x'^{*}(T_L),\ x'^{*}(T_L)\right] Q_L^T$$

Now, the Jacobian matrix Q_{pL} with components

$$Q_{pL,i,j} = \frac{\partial x'_i(T_L)}{\partial a_j}$$

is computed as part of the computer program, and may be used to find the covariance matrix of the errors in the parameters a_i. We have

$$\text{cov}\left[x'(T_L),\ x'(T_L)\right] = Q_{pL}\ \text{cov}_1\left[a_i,\ a_j\right] Q_{pL}^T$$

so

$$\text{cov}_1\left[a_i, a_j\right] = Q_{pL}^{-1}\ \text{cov}\left[x'(T_L),\ x'(T_L)\right] Q_{pL}^{-1T}$$

If there are additional observations within the LSOI which, by themselves, result in a covariance matrix $\text{cov}_2\left[a_i,\ a_j\right]$, then the covariance matrix of the combined observations is

$$\text{cov}\left[a_i,\ a_j\right] = \left\{\text{cov}_1^{-1}\left[a_i,\ a_j\right] + \text{cov}_2^{-1}\left[a_i,\ a_j\right]\right\}^{-1}$$

$$= \left\{Q_{pL}\ \text{cov}^{-1}\left[x'(T_L),\ x'(T_L)\right] Q_{pL}^T + \text{cov}_2^{-1}\left[a_i,\ a_j\right]\right\}^{-1}$$

Moon-Earth Trajectories

Having the orbit parameters of the portion of the Moon-Earth trajectory within the LSOI, the time of piercing the LSOI, the position and velocity of piercing the LSOI, and the covariance matrix of position and velocity errors at the nominal time of piercing the LSOI can be computed according to Apollo Note No. 82. Calling this time T_L, we have $X'(T_L)$ and $\text{cov}\left[x'(T_L),\ x'(T_L)\right]$.

For the remainder of the trajectory, we must find the position and velocity of the vehicle in Earth-centered coordinates at T_L. These are simply

$$\tilde{R} = \tilde{X}_m - \tilde{X}$$

and

$$\dot{\tilde{R}} = \dot{\tilde{X}}_m - \dot{\tilde{X}}$$

From these quantities, the x'^*, y'^*, z'^* coordinate system can be found by a method similar to that employed for finding the x', y', z' coordinates in the Earth-Moon trajectory, and the perigee conditions can be found by a like method.

In the case of Earth return, however, the reentry conditions rather than the perigee conditions are of prime interest. That is, the x'^*, y'^*, z'^* coordinates should be selected to correspond to reentry rather than perilune. This is not difficult to do. The covariance matrix of errors in position and velocity at the nominal time of reentry can then be calculated. Call this cov (a^*, a^*).

The dive angle δ is

$$\delta = \tan^{-1} \frac{-a_4}{a_5}$$

The partial derivatives of the dive angle with respect to the parameters are

$$\frac{\partial \delta}{\partial a_j} = 0 \qquad j = 1, 2, 3, 6$$

$$\frac{\partial \delta}{\partial a_4} = \frac{-a_5}{a_4^2 + a_5^2}$$

$$\frac{\partial \delta}{\partial a_5} = \frac{a_4}{a_4^2 + a_5^2}$$

Let M_p and M_c be the misses in the plane of the trajectory and normal to the plane of the trajectory at the time the reentry altitude is actually reached. Then, according to Figure 1,

$$\frac{\partial M_p}{\partial a_1} = - \frac{a_5}{a_4}$$

$$\frac{\partial M_p}{\partial a_2} = 1$$

$$\frac{\partial M_p}{\partial a_j} = 0 \qquad j = 3, 4, 5, 6$$

$$\frac{\partial M_c}{\partial a_j} = \delta_{3j}$$

Now, it is not the misses along and across in inertial coordinates that are of interest, but the errors on the rotating Earth. In order to compute these it is necessary to know the error in time of reentry. This is given by

$$\frac{\partial t}{\partial a_j} = - \delta_{j1} / a_4 .$$

The miss parallel and miss cross can be resolved into components in the latitude and longitude directions by finding the angle ψ^* between the a_z direction and the meridian at the nominal reentry point. Then letting M_L and M_ℓ denote the misses in latitude and longitude,

$$\frac{\partial M_L}{\partial a_j} = \frac{\partial M_p}{\partial a_j} \cos\psi^* + \frac{\partial M_c}{\partial a_j} \sin\psi^*$$

$$\frac{\partial M_\ell}{\partial a_j} = \frac{- \partial M_p}{\partial a_j} \sin\psi^* + \frac{\partial M_c}{\partial a_j} \cos\psi^* + \delta_{1j} \frac{\omega_e a_1 \cos\lambda^*}{a_4}$$

in which λ^* is the latitude of the reentry point. Then letting Z be

$$Z = \begin{bmatrix} \frac{\partial M_L}{\partial a_1} & \frac{\partial M_\ell}{\partial a_1} & \frac{\partial \delta}{\partial a_1} \\ \frac{\partial M_1}{\partial a_2} & \frac{\partial M_\ell}{\partial a_2} & \frac{\partial \delta}{\partial a_2} \\ \vdots & \vdots & \vdots \\ \frac{\partial M_L}{\partial a_6} & \frac{\partial M_L}{\partial a_6} & \frac{\partial \delta}{\partial a_6} \end{bmatrix}$$

the covariance matrix of M_L, M_ℓ and δ is

$$Z^T \text{ cov } (a^*, a^*)\ Z$$

APOLLO NOTE NO. 118

C. Black
7 October 1963

EFFECT OF THE SOLAR PLASMA ON THE DOPPLER MEASUREMENTS FOR MARINER II

One of the experiments performed aboard Mariner II was the measurement of the positive component of the plasma radiating from the sun. The equipment was sensitive to protons with the energy range from 240 to 8400 electron volts. During the course of the flight from Earth to Venus protons were detected with energy range from 750 to 2500 electron volts with a density of 10 to 20 protons per cubic inch. The velocity of the particles were in the range from 200 to 500 miles per second and the velocities were found to vary from 20 to 100% over periods of 24 to 48 hours.[1/]

Since a density of ions in free space reduces the dielectric constant of free space by an amount proportional to the density, it is intended to calculate the effect on the Doppler data that the measured density of solar plasma will produce. It is assumed that the plasma is neutral in charge so that an equivalent number of electrons accompany the protons and other positive components of the plasma.

Following Mitra[2/] the change in dielectric constant, K, produced by a charge density N_e is given by the equation

$$\Delta K = -4\pi N_e \times \frac{e^2}{m\omega^2}$$

The phase velocity, u, in free space with the ion density, N_e,

---

1/ Mariner - Mission to Venus, McGraw Hill, N. Y. (1963).

2/ S. K. Mitra, The Upper Atmosphere, Second Edition (1952), Hafner Publishing Co., New York, p. 179.

is given by

$$u = c\left(1 - \frac{4\pi N_e e^2}{m\omega^2}\right)^{-1/2}$$

$$\cong c\left(1 + 2\pi N_e \times \frac{e^2}{m\omega^2}\right)$$

Using the values for the ion density of 10 electrons per cubic inch and 20 electrons per cubic inch and a value for ω of 6×10^9 radians per second we obtain the magnitude of a fractional change in the range rate determination given by

$$\frac{\Delta u}{c} = 2.6 \text{ to } 5.2 \times 10^{-11}$$

This is equivalent to a velocity error of approximately 1 centimeter per second.

The conclusion of the above calculation is that the error introduced by the solar plasma along the transmission path between the Mariner vehicle and Earth is comparable to the errors expected in oscillator stability (about 1 part in 10^{10}). It is of interest to note that the correlation time for the errors introduced by the solar plasma is of the order of 6 hours or more. This results from the fact that difference in the orbital radius between Venus and Earth is approximately 25,000,000 miles and the velocity of the solar plasma is of the order of 1000 feet per second or less. Therefore a burst of plasma emitted from the solar surface and proceeding radially from the sun would require a minimum of 6 hours to clear the line of sight between the Earth and the Mariner. The solar plasma effect can therefore not account for the short term fluctuations observed in the Doppler data.

In applying results of this calculation to an understanding of the errors that might exist in a Lunar mission, it is well to keep

in mind that the plasma density in the Earth-Lunar region can be somewhat different from that in inner-planetary space. One would expect velocity errors due to the solar plasma to be a value at least 1 centimeter per second but this error can be proportionately larger as the ion density between the Earth and Moon increases. A velocity error of 1 centimeter per second provides a cumulative position error of approximately 1 kilometer per day or 100 kilometers in 100 days. It is unlikely therefore that we can specify the position of the Mariner vehicle near the Venus crossing to better than 100 kilometers unless we take account of the plasma induced effects.

In short term Lunar navigation problems, however, the position errors will be proportionately smaller. On the other hand, the correlation time of the solar plasma induced errors can be appropriately smaller because of the smaller distance over which any burst of plasma must travel. If the moon is in the first or third quarter during the period of measurement, this correlation time could be very small depending on the thickness of the plasma wave emanating from the Sun.

APOLLO NOTE NO. 119

H. Dale
7 October 1963

LUNAR ASCENT AND RENDEZVOUS USING A REALISTIC ESTIMATE OF THE SUB-LUNAR POINT AND AVAILABLE TRACKING STATIONS

Apollo Note No. 99 presents computer results for some assumed geometries. No attempt was made to rationalize the choice of geometry. This note presents essentially the same sort of data only an attempt has been made to choose a realistic sub-lunar point.

A number of trajectory plans have assumed that the Moon-Earth injection occurs at 4 degrees North latitude and 15 degrees West longitude in Earth coordinates. It would then be reasonable to assume that the perilune of the ascent trajectory occurred 3 or 5 hours earlier (lunar period equals 2 hours). This would place the sub-lunar point of the initiation of tracking at 30 degrees East for the 3 hour case and 60 degrees East for the 5 hour case.

Further assuming that the Johannesburg station is unused results in only two stations being within line-of-sight for the 3 hour case. These stations are Madrid and Ascension. For the 5 hour case (60°E sub-lunar initial point) a third station, Carnarvon can also be used. The following figure shows these stations.

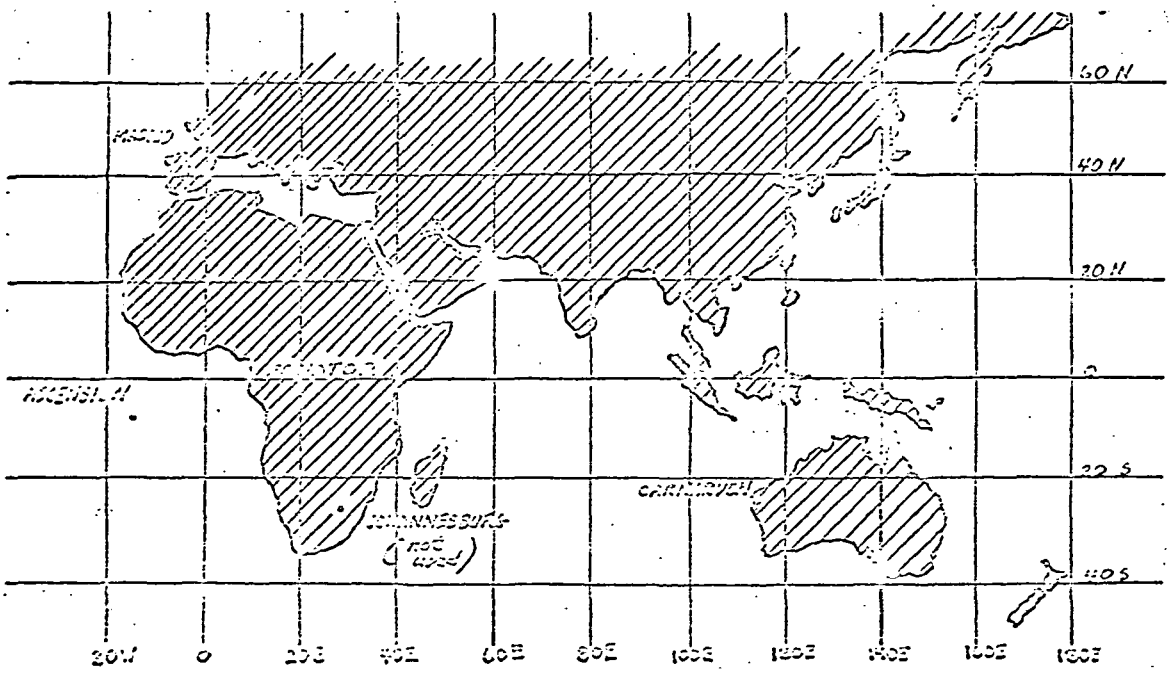

MSFN Station Location

From Apollo Note No. 109 it can be seen that about 34 minutes of tracking are available for each of these cases. Assumed values for σR and $\sigma \dot{R}$ for one-minute intervals are 15 meters and 0.03 meters per second respectively.

The results for the 3 hour case (Madrid and Ascension, $4^{\circ}N$-$30^{\circ}E$ sub-lunar point, range and range-rate data) are:

$\sigma_x = 158.7$ meters $\qquad \sqrt{\sigma_x^2 + \sigma_y^2 + \sigma_z^2} = 500$ meters

$\sigma_y = 274.3$ $\qquad \sqrt{\sigma_x^2 + \sigma_z^2} = 416.5$

$\sigma_z = 398.0$

This compares quite favorably with the Madrid and Johannesburg case reported in Apollo Note No. 109 in which the minimum miss was:

$$\sqrt{\sigma_x^2 + \sigma_z^2} = 325 \text{ meters}$$

For the 5 hour case (Carnarvon added and sub-lunar point at $4^{\circ}N$-$60^{\circ}E$) only a slight improvement is seen:

$\sigma_x = 122.8$ meters $\qquad \sqrt{\sigma_x^2 + \sigma_y^2 + \sigma_z^2} = 461.5$ meters

$\sigma_y = 211.5$ $\qquad \sqrt{\sigma_x^2 + \sigma_z^2} = 410.3$

$\sigma_z = 390.3$

APOLLO NOTE NO. 120

L. Horowitz/
W. Iwata
9 October 1963

BIAS EFFECTS ON ORBIT PARAMETER DETERMINATION

Introduction

Using the perturbation techniques of Apollo Note No. 102, this study considers the effect of fixed bias on the "measurables" (R or $\dot{R}$) insofar as it affects the covariance matrices of the maximum likelihood orbit parameter estimators. Again using the simplified two-dimensional model of Apollo Note No. 102 with one measurement per minute over $\frac{1}{4}$ period for a total of 31 observations, it is shown that no significant changes in the covariance matrices are induced by addition of fixed bias.

This study assumes no a priori knowledge of the bias itself, so that the conclusions obtained are conservative. The technique used for inverting the n + 1 x n + 1 matrices from the inverses of the corresponding n x n matrices is due to H. Engel.

Bias Terms in the Information Matrix

From Apollo Note No. 43, bias terms in the information matrix are:

$$C_{M+1,j} = \frac{1}{N} \sum_{k=1}^{N} \frac{\partial f_c}{\partial a_j}(k), \qquad 1 \leq j \leq M$$

$$C_{M+1,\,M+1} = 1$$

where f_c is R or $\dot{R}$, as the case may be. Apollo Note No. 101

and 102 derive these information matrices for $\dot{R}$ and R respectively, with zero bias assumed. Then the bias terms (1) of the information matrix are:

$$R: \qquad C_{4,j} = \frac{2\omega}{\pi} \int_0^{\pi/2\omega} \frac{\partial V_D(t)}{\partial a_i} \, dt; \quad 1 \leq j \leq 3$$

$$C_{4,4} = 1,$$

where $\frac{\partial V_D}{\partial a_i}$ are given by Equation (6) of Apollo Note No. 101.

$$R: \qquad C_{5,j} = \frac{2\omega}{\pi} \int_0^{\pi/2\omega} \frac{\partial u}{\partial a_i} \, dt; \; 1 \leq j \leq 4$$

$$C_{5,5} = 1,$$

where $\frac{\partial u}{\partial a_i}$ are given by Equation (5) of Apollo Note No. 102.

Inversion of Information Matrices

The covariance matrices for R and $\dot{R}$ data are given on page 7 of Apollo Note No. 102 for the case of zero bias. To compute the inverses of the "enlarged" information matrices $C_{i,j}$ containing non-zero bias information terms, we use H. Engel's technique to observe that if an "enlarged" matrix A* is partitioned as shown:

$$A^* = \left(\begin{array}{c|c} A_{11} & A_{12} \\ \hline A_{21} & A_{22} \end{array}\right), \text{ where}$$

A_{11} is the original matrix whose inverse we already happen to know, and A_{12}, A_{21} and A_{22} comprise the "adjoined" information, then the inverse of A^* is:

$$(A^*)^{-1} = \left(\begin{array}{c|c} B_{11} & B_{12} \\ \hline B_{21} & B_{22} \end{array}\right), \text{ where}$$

$$B_{11} = A_{11}^{-1} + X\, B_{22}\, X^T$$

$$B_{12} = -X B_{22}$$

$$B_{21} = B_{12}^T$$

$$B_{22} = \Delta^{-1}$$

Here, the superscript T denotes matrix transposition, and we have defined

$$X = A_{11}^{-1} A_{12}$$

$$\Delta = A_{22} - A_{12}^{T} X$$

$$\Delta^{-1} = \frac{1}{\Delta}$$

Conclusions

Performing the indicated computations, the new covariance matrices corresponding to non-zero bias are:

$$\text{Cov}\,(\hat{a}_i, \hat{a}_j)_R = \begin{array}{c} \begin{array}{ccccc} (x_o) & (y_o) & (\dot{x}_o) & (\dot{y}_o) & (b) \end{array} \\ \left(\begin{array}{ccccc} 3.143 \times 10^4 m^2 & 1.14 \times 10^3 m^2 & -28.15 \frac{m^2}{sec} & 21.40 \frac{m^2}{sec} & 2.80 \\ 1.14 \times 10^3 m^2 & 102\ m^2 & -.950 \frac{m^2}{sec} & .664 \frac{m^2}{sec} & -2.64 \\ -28.15 \frac{m^2}{sec} & -.950 \frac{m^2}{sec} & .0258 \frac{m^2}{sec^2} & -.0194 \frac{m^2}{sec^2} & -.0042 \\ 21.40 \frac{m^2}{sec} & .664 \frac{m^2}{sec} & -.0194 \frac{m^2}{sec^2} & .0148 \frac{m^2}{sec^2} & .0119 \\ 2.80 & -2.64 & -.0042 & .0119 & .157 \end{array} \right) \end{array}$$

$$\text{Cov}(\hat{a}_i, \hat{a}_j)_R = \begin{array}{c} \begin{matrix} (y_o) & (\dot{x}_o) & (\dot{y}_o) & (b) \end{matrix} \\ \begin{bmatrix} 2279.\ m^2 & -3.487\ \frac{m^2}{sec} & -.6990\ \frac{m^2}{sec} & -.01321 \\ -3.487\ \frac{m^2}{sec} & 55.34 \times 10^{-4}\ \frac{m^2}{sec^2} & 9.946 \times 10^{-4}\ \frac{m^2}{sec^2} & 8.235 \times 10^{-7} \\ -.6990\ \frac{m^2}{sec} & 9.946 \times 10^{-4}\ \frac{m^2}{sec^2} & 2.992 \times 10^{-4}\ \frac{m^2}{sec^2} & .3723 \times 10^{-5} \\ -.01321 & 8.235 \times 10^{-7} & .3723 \times 10^{-5} & .3306 \times 10^{-5} \end{bmatrix} \end{array}$$

Comparing these new covariance matrices for R and $\dot{R}$ respectively with those given on page 7 of Apollo Note No. 102 (where zero bias was assumed), it can be seen that the effect of bias errors on the maximum likelihood estimators is clearly negligible. It is emphasized that these conclusions are conservative, since no a priori knowledge of bias was assumed.

APOLLO NOTE NO. 121

G. F. Floyd
10 October 1963

SIMPLIFIED EVALUATION OF MSFN ERRORS

The rigorous evaluation of MSFN orbit prediction errors and comparison of the worth of different types of data sources, (ground-based: R, $\dot{R}$, angle, and relative spacecraft R, $\dot{R}$, angle), is being accomplished using a rather elaborate digital computer program. The purpose of this note is then to perform a very simple analytical analysis to get approximate results which should check the conclusions reached on the computer.

Consider first the relative trajectory of the CSM with respect to the perfectly launched LEM. Since the two satellites are going to collide at LEM apogee, we can draw the trajectory of the CSM relative to the LEM as the solid lines in Figure 1.

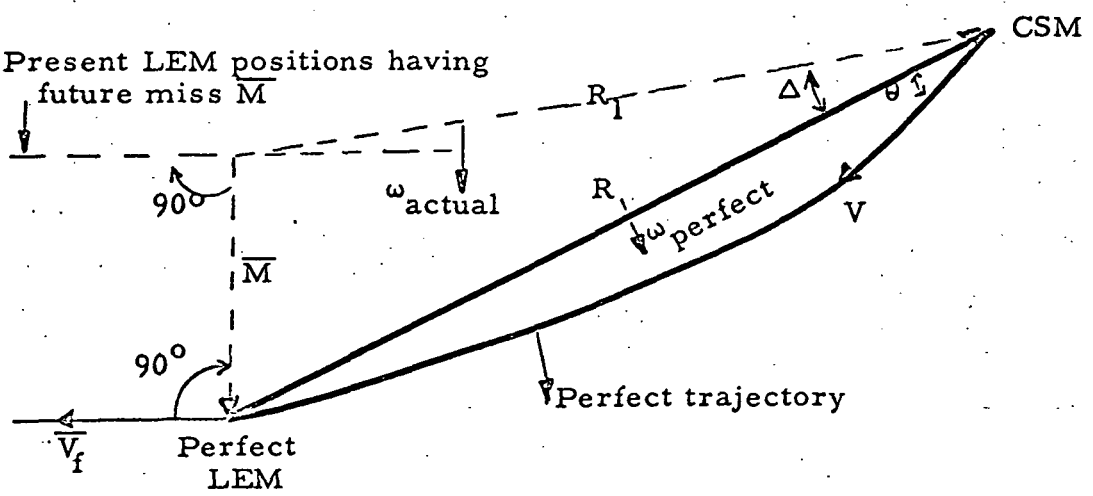

Figure 1.

The perfect trajectory is, of course, curved since there is relative acceleration between the two vehicles due to the vector difference in gravity at the CM and LEM positions.

Now consider the locus of all LEM positions which will result in miss $\overline{M}$ (distance of closest approach). The present position

locus of the LEM which will result in future miss $\overline{M}$ is shown dotted in the figure, where the figure neglects the gravitational difference along the zero and finite miss LEM trajectories, since this is very small at 1/2 n.mi. misses compared with the gravity difference between the LEM and CSM at 70 n.mi. separation.

With Figure 1, we can now compute the difference between the actual and ideal angular rates of the line-of-sight. From the figure,

$$\omega_{perfect} = \frac{V \sin \phi}{R} \tag{1}$$

$$\omega_{actual} = \frac{V \sin (\phi + \Delta)}{R_1} \approx \frac{V \sin \phi}{R} + \frac{V \Delta}{R} \tag{2}$$

$$\Delta \approx \frac{M}{R_1} \approx \frac{M}{R}$$

Thus,

$$\omega_{actual} - \omega_{perfect} \approx \frac{M V}{R^2}$$

or if we steer the actual LEM on the basis of computed ω_{L_S} and make an error ($\delta \omega$) in the measurement we have

$$\boxed{M = \frac{R^2 (\delta \omega)}{V}} \tag{4}$$

Equation (4) is the familiar miss equation used for years in fire control and guided missile studies and so applies equally well to satellite interceptors except that now a "collision course" does not have $\omega = 0$ at large separations. However, for computing the uncertainty in the miss the same equation holds whether or not there is a relative acceleration.

Even though the foregoing derivation is trivially easy, the result is quite useful in estimating the effects of different MSFN errors

since it says that the MSFN uncertainty in the future miss is found by first calculating the uncertainty in the present CM-LEM sight line rate ($\delta\omega$) and then simply multiplying this by the square of the present range (R^2) divided by the magnitude of the present relative velocity (V). Since (R^2/V) is known as a function of time for the nominal trajectory, it is just the scale factor used to convert ($\delta\omega$) into future miss uncertainty and, more important, it is only ($\delta\omega$) which is important in determination of the miss uncertainty. The remainder of the note will be devoted to the use of Equation (4) to evaluate different sources of MSFN errors.

Station Location Errors and Range Biases

Station location in errors and range biases change the measured positions by constant amounts and so to a first order will not change the computed sight line angular rate, hence we would expect these errors to have small effects.

Ground-based Angle versus Range Data

In computing line-of-sight rates we need vector position changes divided by relative range, so the comparison here may be made on the basis of absolute positional accuracy. For a single range and angle station the right left positional accuracy is D ($\delta\theta$) while for 2 R only, stations separated by (B), (see Figure 2), the positional accuracy is ($\frac{D}{B}$ dR).

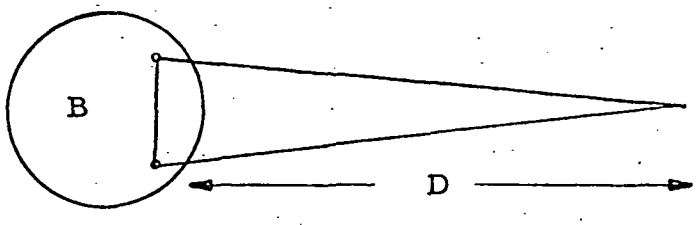

Figure 2.

Letting

$B = 30^{\circ}$ latitude = 2000 miles

$D = 250,000$ miles (Earth-Moon distance)

$\delta R = 15$ meters

$\delta \theta = 2 \times 10^{-4}$ radians

$D(\delta \theta) = 2.5 \times 10^{5} \times 2 \times 10^{-4} = 50$ miles

$\frac{D}{B} dR = \frac{250,000}{2,000} \times 15 = 750$ m = 1/2 mile

Thus the range data is 100 times more accurate in determining ω and, hence, the miss. Thus ground-based angle data should not be worthwhile processing.

LEM/CSM Relative Data

Here we have the possibilities of relative range, range-rate and angular data. However, Equation (4) shows that it is only inertial angular rate which is important, hence relative range or range-rate should not be much help.

To evaluate the potential usefulness of sight line observations, we turn Equation (4) around to calculate the effective angular rate accuracy of the R, $\dot{R}$ MSFN. For this, we use the 3 R $\dot{R}$ station curve on page 8 of Apollo Note No. 106 for miss uncertainty and approximate computations of R and V at the plotted times to go. From these and the formula $MV = R^2 (\Delta \omega)$ we get the table below:

Observation Time (Min)	$\Delta \omega$ Rad/sec
4	4×10^{-6}
9	3×10^{-6}
16	1.5×10^{-6}
25	2×10^{-6}

Thus with the assumed R, $\dot{R}$ accuracy, (15 m at 1 min. and 3 cm/sec at 1 min), the MSFN equivalent angular rate accuracy is about .003 mils/sec., and at the present time we believe the assumed errors to be high by a factor of 4. Thus, it is not unreasonable to set a goal of .001 mils/sec. for the equivalent MSFN angular rate accuracy. If precise angular measurements could be made from the LEM of the CSM against the star background, we might get 1 mil measurement and several of these over a 10 min (600 sec) period would produce inertial rates of about the same accuracy as the MSFN. Thus, it would appear that on-board angular sightings will not significantly improve the straight MSFN R, $\dot{R}$ results.

MSFN R versus $\dot{R}$ Data

This comparison has already been begun in Apollo Notes 111 and 112 with the conclusion that the doppler count data (which gives changes in scalar range), will have very small variance and so be very accurate R data with a bias, and on the basis of the preceding discussion it does not appear that the miss uncertainty will be overly sensitive to biases. Therefore, the tentative conclusion is that the MSFN will do better in the straight CW doppler cycle count mode than in the pseudo-random precise ranging mode.

Therefore, the tentative conclusions are:

1. The most accurate data for rendezvous miss prediction will result from the use of the MSFN in its simple CW Doppler cycle counting mode.

2. Other data sources: Range or angle data from either the ground or the spacecraft will not appreciably improve the ground-based CW data.

3. Since the on-board inertial system has an uncertainty of about 10 km in the rendezvous miss, the MSFN in its CW doppler mode will know the rendezvous miss about an order of magnitude better than the on-board system except during boost and the actual docking.

APOLLO NOTE NO. 122

H. Dale
10 October 1963

ESTIMATE OF EARTH-MOON INJECTION ERRORS USING TWO MSFN STATIONS

This note presents an estimate of the injection errors assuming two stations track the Apollo between ten and twenty minutes after injection into the trans-lunar orbit.

As of this writing many possible Earth-Moon injections seem equally likely. These are presented in "Trajectory Studies for Use in Determining Tracking Requirements for Project Apollo" dated August 30, 1963 and prepared by the Flight Operations Division of the NASA Manned Spacecraft Center. For the purposes of the following analysis an injection during the first orbit was chosen that allowed at least two MSFN stations to track the vehicle. Figure 14 (c) of the above report shows such an injection which causes the Apollo to move Eastwardly over Australia during the first ten minutes. By twenty minutes after injection the ground trace has just past the New Hebrides Islands. The inclination of the Earth parking orbit for this injection is 32 degrees. The injection altitude is 107 nautical miles. The injection occurs at 30°S Latitude and 100° E Longitude. The two stations that can see the vehicle(at least before the ten-minute-after-injection point) are Carnarvon Australia (24.87°S, 113.7°E) and Canberra (35.4°S, 148.8°E).

The exact trajectory used in the above report is not known and thus an approximate trajectory was analytically obtained and used. Actually small differences in the position of the Apollo trajectory should make no difference in the ability of the MSFN, to obtain orbit estimators. The trajectory used the above injection point as perigee, the lunar distance as apogee and had an inclination of 30°.

The reasons for the chosen end points of the tracking time, 10 minutes and 20 minutes after injection, are detailed in the referenced report. Basically 10 minutes and 1000 n. mi. altitude occur coincidently and the DSIF radars can not track well below 1000 n. mi.. Transposition and docking is done by having the CM/SM separate from the LEM/SIV-B combination (the SIV-B providing attitude control for the LEM)

and re-attaching, CM to LEM. The SIV-B is vent-free limited to 60 minutes after injection, and 40 minutes is estimated as the maximum time required for docking. Thus separation should occur at 20 minutes after injection.

Using estimated radar errors of σ_R = 15 meters and $\sigma_{\dot{R}}$ = 0.03 meters/sec. for one minute uncorrelated samples, the following covariance matrix results at 20 minutes after tracking (given in meters^2 and(meters/sec)^2):

x - y plane — defined as the plane of the orbit.

x — defined along the Earth-center to initial vehicle position line, positive away from the Earth (initial position is perigee.

y — defined such that $\dot{y}_o$ is positive.

	x	y	z	$\dot{x}$	$\dot{y}$	$\dot{z}$
x	$.2077 \times 10^6$	$.4060 \times 10^5$	$-.5988 \times 10^5$	$.1988 \times 10^3$	$.1598 \times 10^3$	$-.1359 \times 10^2$
y	$.9060 \times 10^5$	$.3954 \times 10^5$	$-.2617 \times 10^5$	$.8668 \times 10^2$	$.6969 \times 10^2$	$-.5990 \times 10^1$
z	$-.5988 \times 10^5$	$-.2617 \times 10^5$	$.1792 \times 10^5$	$-.5742 \times 10^2$	$-.4609 \times 10^2$	$.4752 \times 10^1$
$\dot{x}$	$.1988 \times 10^3$	$.8668 \times 10^2$	$-.5742 \times 10^2$	.1908	.1530	$-.1362 \times 10^{-1}$
$\dot{y}$	$.1598 \times 10^3$	$.6969 \times 10^2$	$-.4609 \times 10^2$	.1530	.1229	$-.1062 \times 10^{-1}$
$\dot{z}$	$-.1359 \times 10^2$	$-.5990 \times 10^1$	$.4752 \times 10^1$	$-.1362 \times 10^{-1}$	$-.1062 \times 10^{-1}$	$.2464 \times 10^{-2}$

Now since the error in velocity is all that is required, an easy number to talk about is the square root of the average value of the square of the velocity error, defined as

$$\sqrt{\overline{\sigma V^2}} = \sqrt{\sigma_{\dot{x}}^2 + \sigma_{\dot{y}}^2 + \sigma_{\dot{z}}^2}$$

or from the last three diagonal terms of the covariance matrix

$$= \sqrt{.1908 + .1229 + .0025} = .562 \text{ meters/sec.}$$

This is quite close to the "one or two feet per second (one sigma)" stated as a requirement in the above referenced report. However, the σ_R and $\sigma_{\dot{R}}$ values used in this analysis are probably a bit conservative.

APOLLO NOTE NO. 123

L. S. Lustick
11 October 1963

ORBIT DETERMINATION WITH RANGE CHANGE AS THE MEASURABLE

Introduction

Previous analyses have used instantaneous doppler measurements as the measurable for determining the orbit parameters. More recent analysis of the doppler mode of operations has indicated that actually what is measured is a change in range for a specified time interval. The error in this range change is the result of random fluctuations in the rate of the clock. If a time interval in which the range change is measured is chosen that is large compared to the correlation time of the random fluctuations in the clock rate each of the measured range changes can be assumed independent with zero mean and the same variance. The following note describes the manner in which the errors for a system using range change can be established.

Method

In Apollo Note No. 43, it is shown that the covariance matrix defining the errors in the estimation of the orbit parameters can be found from the inverse of the following matrix.

$$(\text{cov}) = \sigma^2 \left(C_{ij}\right)^{-1}$$

where:

$$C_{ij} = \sum_{k=1}^{N} \frac{\partial M}{\partial a_i}(k) \frac{\partial M}{\partial a_j}(k) \qquad 1 \leq i \leq 6$$

M = functional form of the measurable

σ^2 = variance in the error in the measurable

$a_{i=1-6}$ = orbit parameters to be estimated

This formulation applies for any measurable as long as the error in each measurement is normally distributed and independent with zero mean and the same variance.

The measurable of interest in this note is the difference in scalar range during the time interval $(T_{k+1} - T_k)$. The element of the information matrix (C_{ij} matrix) for this case is given by the equation below.

$$C_{ij} = \sum_{k=1}^{N-1} \left[\left(\frac{\partial S_{k+1}}{\partial a_i} - \frac{\partial S_k}{\partial a_i} \right) \left(\frac{\partial S_{k+1}}{\partial a_j} - \frac{\partial S_k}{\partial a_j} \right) \right]$$

where:

$S = f(a_1 \ldots a_6)$ is the functional form for the scalar range

$T_{k+1} - T_k = \tau$ for all k

T_1 = Time at which observations begin

Modification to Computer Program

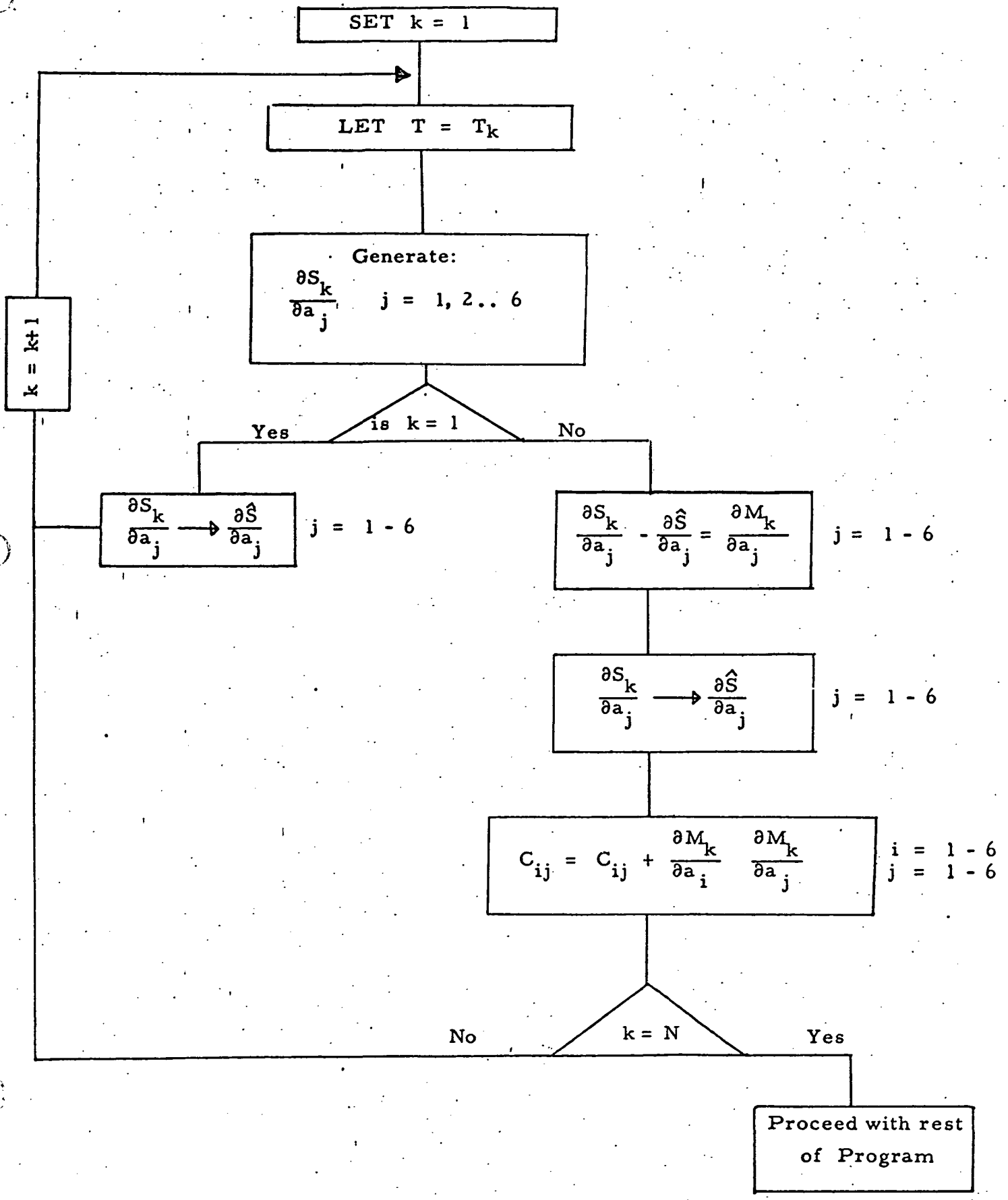
SET k = 1
LET T = T_k
Generate:
$\frac{\partial S_k}{\partial a_j}$ j = 1, 2.. 6
k = k+1
is k = 1
Yes
No
$\frac{\partial S_k}{\partial a_j} \rightarrow \frac{\partial \hat{S}}{\partial a_j}$ j = 1 - 6
$\frac{\partial S_k}{\partial a_j} - \frac{\partial \hat{S}}{\partial a_j} = \frac{\partial M_k}{\partial a_j}$ j = 1 - 6
$\frac{\partial S_k}{\partial a_j} \rightarrow \frac{\partial \hat{S}}{\partial a_j}$ j = 1 - 6
$C_{ij} = C_{ij} + \frac{\partial M_k}{\partial a_i} \frac{\partial M_k}{\partial a_j}$ i = 1 - 6 j = 1 - 6
k = N
No
Yes
Proceed with rest of Program

APOLLO NOTE NO. 124

H. Engel
11 October 1963

ERRORS IN PREDICTED POSITION AND VELOCITY

This note indicates a way of reducing the amount of computation required to find the elements of interest in the covariance matrices of errors in future position and velocity.

We have

$$\text{cov}\left[x(t),\ x(t)\right] = Q(t)\ \text{cov}\left[x(o), x(o)\right]\ Q^T(t)$$

There are six components of position and velocity, but each of the matrices above may be larger by the number of fixed biases in the measurables (See Apollo Note No. 98).

We can partition the Q and covariance matrices as shown:

$$Q(t) = \begin{bmatrix} A & 0 \\ 0 & I \end{bmatrix}$$

$$\text{cov}\left[x(o),\ x(o)\right] = \begin{bmatrix} a & b \\ b^T & d \end{bmatrix}$$

$$\text{cov}\left[x(t),\ x(t)\right] = \begin{bmatrix} \alpha & \beta \\ \beta^T & \delta \end{bmatrix}$$

Here A, a and α are 6 x 6 matrices (6 orbit parameters), I, d, and δ are k x k matrices, where k is the number of fixed biases in the measurables. I is the identity matrix.

By matrix multiplication we find that

$$\alpha = A\,a\,A^T$$
$$\beta = A\,b$$
$$\delta = d$$

Thus, if we are interested only in errors in future position and velocity and their covariance we need calculate only α, which involves only the multiplication of 6 x 6 matrices no matter how many biases there are.

The value of "a", however, does depend on the number of biases in a fashion that we describe below:

Consider a measurable, m_i, with an associated constant bias. The information matrix corresponding to a number of measurements of this measurables at different times can be written as

$$m_{i,b} = \begin{bmatrix} m_i & \rho_i \\ \rho_i^T & r_i \end{bmatrix}$$

in which m_i is the information matrix that would result if there were no bias associated with this measurable, and q_i is a number. We may then write

$$m_{i,b} = m_{i,o} + \mu_i$$

in which $m_{i,o}$ is m_i augmented by an additional row and column of zeros, and

$$\mu_i = \begin{bmatrix} 0 & \rho_i \\ \rho_i^T & r_i \end{bmatrix}$$

Now in order to combine the information matrices corresponding to measurements on ℓ different measurables, k of which have associated biases we must form a $(6 + k) \times (6 + k)$ information matrix, S_b,

$$S_b = \sum_{g=1}^{\ell} M_i$$

where

$$M_i = \begin{bmatrix} m_i & 0 & 0 & \cdots & 0 & r_i & 0 & \cdots & 0 \\ 0 & 0 & 0 & & 0 & 0 & 0 & & 0 \\ \vdots & & & & & & & & \\ 0 & 0 & 0 & & 0 & 0 & 0 & & 0 \\ r_i^T & 0 & 0 & & 0 & q_i & 0 & & 0 \\ 0 & 0 & 0 & & 0 & 0 & 0 & & 0 \\ \vdots & & & & & & & & \\ 0 & 0 & 0 & & 0 & 0 & 0 & & 0 \end{bmatrix} \begin{matrix} \} 6 \\ \} i-1 \\ \\ \} k-i \end{matrix}$$

$$\underbrace{\quad}_{6} \quad \underbrace{\quad\quad}_{i-1} \quad \underbrace{\quad\quad}_{k-i}$$

S_b, in turn, may be written as

$$S_b = \begin{bmatrix} S & 0 \\ 0 & 0 \end{bmatrix} + \begin{bmatrix} 0 & P \\ P^T & R \end{bmatrix}$$

where

$$S = \sum_{g=1}^{\ell} m_i$$

Let U_b be the covariance matrix that is the inverse of S_b. The upper left 6 x 6 portion of U_b, which we call "a", can be written as

$$a = S^{-1} + S^{-1} P \left[R - P^T S^{-1} P \right]^{-1} P^T S^{-1}$$

indicating how the bias terms affect the covariance of the errors in the coefficients.

APOLLO NOTE NO. 125

H. Engel
14 October 1963

RANGE OBSERVATIONS OF LEM FROM MADRID AND CSM

The covariance matrices of errors in position and velocity at nominal LEM/CSM rendezvous have been computed on the basis of zero bias range-only measurements from Madrid and the CSM using a standard deviation of 15 m. The CSM is in an orbit at 80 n. mi. and the LEM uses a Hohmann transfer from 8 n. mi., starting at the center of the visible face of the Moon.

The standard deviations of the x, y and z components of miss, and of the minimum r.m.s. miss near rendezvous have been plotted. This minimum error is very nearly the same as for range observations from Madrid and Johannesburg. The components, however, are different. In the present case the maximum error is out of plane. In the Madrid-Johannesburg case the maximum errors are in the in-plane components.

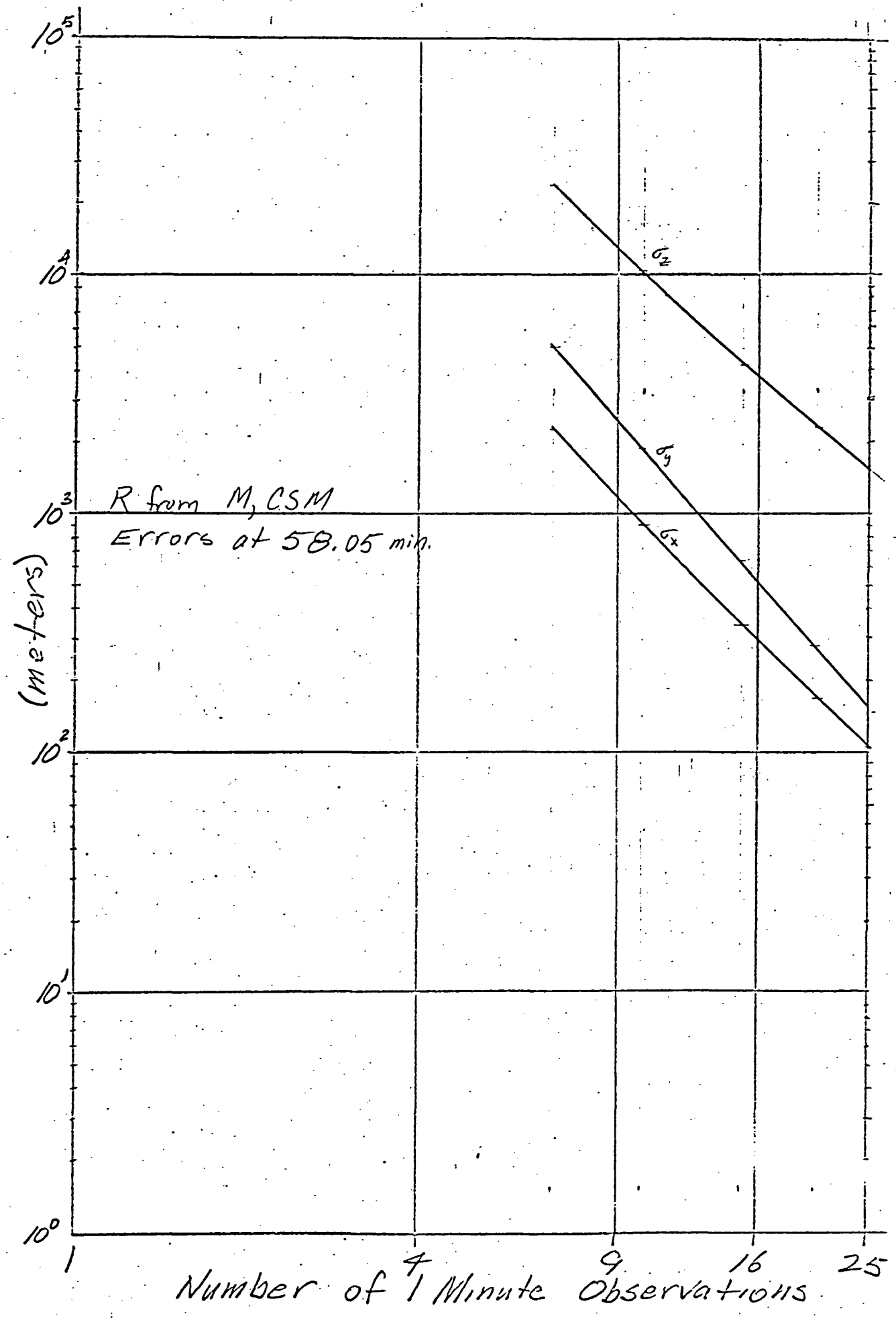
10^5
10^4
10^3
10^2
10^1
10^0
σ_z
σ_y
σ_x
R from M, CSM
Errors at 58.05 min.
(meters)
1
4
9
16
25
Number of 1 Minute Observations

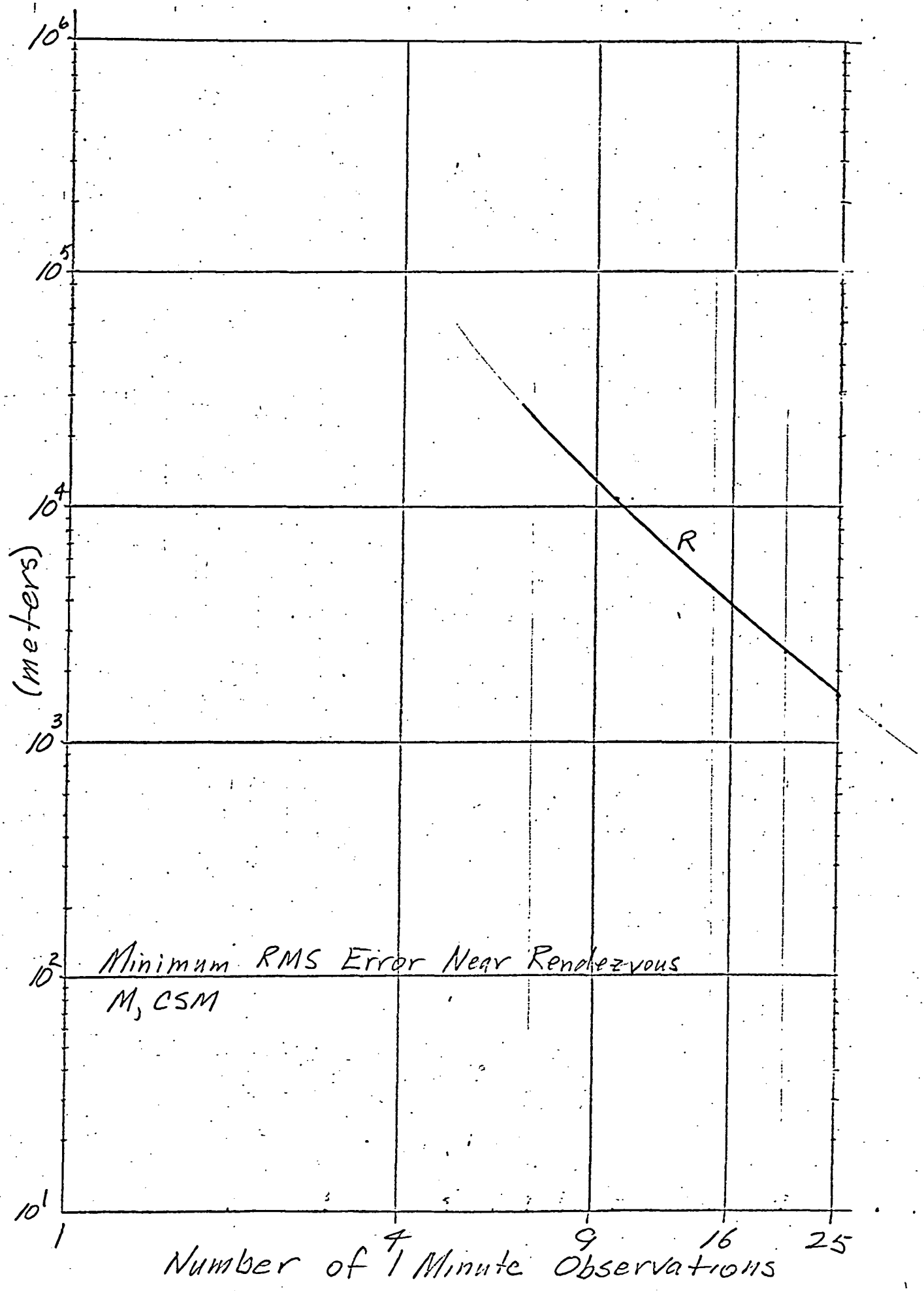
10^6
10^5
10^4
10^3
10^2
10^1
(meters)
R
Minimum RMS Error Near Rendezvous
M, CSM
1
4
9
16
25
Number of 1 Minute Observations

APOLLO NOTE NO. 126

L. Horowitz
18 October 1963

CANONICAL DIAGONALIZATION OF COVARIANCE MATRICES

Introduction:

As before, we assume that N measurements of some measureable quantity $f_m(t)$ (R, $\dot{R}$, etc.) are made in the presence of noise $n(t)$ and bias b so that

$$f_m(t) = f_c(t) + b + n(t),$$

where $f_c(t)$ is the computed value of the measured quantity obtained as some function of the orbit parameters $a_1, \ldots, a_m$ and time t. Then Apollo Note No. 43 et al show how to determine the accuracy to which the orbit parameters $a_1, \ldots, a_m$ may be estimated by computing the covariance matrix cov $(\hat{a}_i, \hat{a}_j)$ of the maximum likelihood estimators $\hat{a}_1, \ldots, \hat{a}_m$. In general, the off-diagonal terms cov $(\hat{a}_i, \hat{a}_j)$ $(i \neq j)$ are not zero, since the orbit parameter estimators are computed as functions of the same observed data; hence correlated.

Now the fact that covariance matrices are always real and symmetric permits the introduction of a new orthogonal coordinate system (the so-called "normal" coordinates, obtained by a pure rotation of the original coordinate system) in which the same covariance matrix, referred to the new coordinate system, is rendered diagonal (all off-diagonal terms are zero).

The utility of this representation lies in the following: at each point of the vehicle trajectory in phase space (the six dimensional space spanned by the position and velocity coordinates of the vehicle) corresponding to a particular time t, an "error ellipsoid" may be constructed with the property that expected errors in estimated position and velocity lie on the boundary of the phase volume so defined. Expected errors in a particular direction are then proportional to the distance to the error ellipsoid in the given direction. For this construction, the semi-principal axes of the error ellipsoid are simply

the square roots of the main diagonal terms of the diagonalized covariance matrix.

This note shows how the error ellipsoid is obtained and illustrates the general method for diagonalizing covariance matrices. The transformation to normal coordinates is also given so that the orientation of the error ellipsoid in phase space may be determined.

Canonical Diagonalization:

If A is a real symmetric matrix of order n, the zeros of determinant $|A - \lambda I|$ are called the eigenvalues of A, where I is the identity matrix. The non-zero vectors X satisfying

$$AX = \lambda X \tag{1}$$

are called the eigenvectors of A. Since the eigenvectors X of A satisfy (1), it is clear that any scalar multiple of X is also an eigenvector of A. Hence without loss of generality, in all that follows we may take the eigenvectors of A to be normalized: $|X| = 1$. Two matrices A and B are said to be similar if there exists a nonsingular matrix P such that $B = P^{-1} A P$; the passage from A to B is called a similarity transformation. Since PB = AP, a physical interpretation of similar matrices is simply that the matrices represent the same linear transformation relative to two different bases.

The following are well-known properties of real symmetric matrices A: 1/

(i) the eigenvalues of A are real

(ii) the eigenvectors of A are mutually orthogonal

(iii) there exists an orthogonal matrix P (i.e., $PP^T = I$ where T denotes matrix transposition) such that $P^{-1} A P$ is a diagonal matrix

---

1/ See e.g. D. C. Murdock, Linear Algebra (Wiley, 1957), p. 144 ff.

(iv) if λ is an eigenvalue of A of multiplicity p (i.e., if λ is a root of multiplicity p of the equation $\det |A - \lambda I| = 0$), then there are exactly p mutually orthogonal eigenvectors of of A corresponding to λ

(v) the orthogonal matrix P is precisely the matrix whose column vectors are the normalized eigenvectors of A.

(vi) the diagonal matrix similar to A is precisely the diagonal matrix whose non-zero elements are the eigenvalues of A.

Hence all that is required to diagonalize the real symmetric matrix A is a knowledge of the eigenvalues of A; (vi) then provides the required diagonal form. The order in which the eigenvalues appear is as yet immaterial, since the new coordinate system to which this diagonal matrix is referred has not been fully specified.

Error Ellipsoid:

With each real symmetric matrix A we associate a quadratic form $X^T AX$, where X is the vector with components $x_1, \ldots, x_m$. Equating this quadratic form to 1 defines a quadric surface Q:

$$\sum_{i,\ j}^{m} a_{ij}\, x_i\, x_j = 1 \qquad (2)$$

where $A = (a_{ij})$. Since A is always positive definite for the case of covariance matrices, Q is always an ellipsoid. Two quadratic forms are said to be reciprocal if their corresponding matrices are inverse to each other. We note in particular that up to the multiplicative constant $\frac{\sigma^2}{N}$, the quadratic forms corresponding to the covariance matrix and the information matrix respectively are reciprocal. Both reciprocal forms have the same eigenvectors, and the corresponding eigenvalues are reciprocals of each other.

Now the ellipsoid (2) is in general obliquely oriented in the coordinate system of the x_i due to the presence of the "cross terms" $a_{ij}\, x_i\, x_j$ $(i \neq j)$. By (ii), the eigenvectors of A are mutually orthogonal. But by (1), $AX_i = \lambda_i X_i$ so that the quadratic form (2) reduces to $\lambda_i \sum_{j=i}^{m} x_j^2 = 1$; just the equation of an m-sphere of radius $\frac{1}{\sqrt{\lambda_i}}$.

Then since

$$\sum_{i,j}^{m} a_{ij}\, x_i\, x_j = \lambda_i \sum_{j}^{m} x_j^2 = 1,$$ the sphere and ellipsoid are tangent at the points $X = X_i$ $(i = 1, \ldots, m)$, which means that the m eigenvectors X_i are precisely the principal axes of the ellipsoid. We note in particular that the principal axes of Q are mutually orthogonal.

For each of the eigenvalues λ_i of A, there corresponds precisely one eigenvector X_i, i.e., the solution X_i to the m simultaneous equations $AX = \lambda_i X$. It is customary to speak of λ_i as the eigenvalue belonging to the eigenvector X_i.

Construction of the error ellipsoid:

1. Obtain the eigenvalues of the covariance matrix $\operatorname{cov}(\hat{a}_i, \hat{a}_j)$ by solving for the m zeros of the secular polynomial $\det|A - \lambda I|$. These are the <u>squares</u> of the principal axes of the error ellipsoid.

2. Obtain the m eigenvectors X_i of $\operatorname{cov}(\hat{a}_i, \hat{a}_j)$ by solving for the nontrivial solutions X_i of

$$AX = \lambda_i X ; \quad i = 1, \ldots, m$$

3. Normalize these eigenvectors: $|X_i| = 1$.

The six dimensional error ellipsoid in phase space corresponding to cov $(\hat{a}_i, \hat{a}_j)$ evaluated at time t then has semi-principal axes of length $\sqrt{\lambda_i}$, and is oriented so that these principal axes are aligned with the corresponding eigenvectors belong to the λ_i. The transformation between the normal coordinate system and the original coordinate system is then simply the matrix P whose column vectors are the normalized eigenvectors of cov $(\hat{a}_i, \hat{a}_j)$, appearing in the same order as the eigenvalues λ_i. If it is desired to construct an equivalent three dimensional ellipsoid in ordinary x-y-z space, it is only necessary to follow the above procedure, considering only the first three diagonal terms of the diagonalized matrix.

APOLLO NOTE NO. 127

H. Engel
18 October 1963

COMPARISON OF $\dot{R}$ AND ΔR DATA

There has been some concern over the fact that the error analysis program assumes that the radar measures radial rate $\dot{R}$, whereas the radar actually counts Doppler cycles and thus measures changes in range over the measurement interval. This note shows that for nearly circular lunar orbits, at least, the error resulting from the assumption that the radar uses $\dot{R}$ is small,

This demonstration uses the expressions for perturbations from a circular orbit derived in Apollo Note No. 7 to calculate the difference between the partial derivative of ΔR with respect to the orbit parameters and Δt times the partial derivative of $\dot{R}$ with respect to the orbit parameters.

From Apollo Note No. 7, the perturbations x and y from a particle moving in a circular orbit at radius r are

$$x = \left[\frac{4\dot{x}_o}{\omega} + 6y_o\right]\sin\theta + \frac{2\dot{y}_o}{\omega}\cos\theta - \left[6y_o + \frac{3\dot{x}_o}{\omega}\right]\theta + \left[x_o - \frac{2\dot{y}_o}{\omega}\right]$$

$$y = \frac{\dot{y}_o}{\omega}\sin\theta - \left[\frac{2\dot{x}_o}{\omega} + 3y_o\right]\cos\theta + \left[4y_o + \frac{2\dot{x}_o}{\omega}\right]$$

$$\theta = \omega t$$

in which $\dot{y}$ is measured always in the radial direction, x is measured perpendicular to y in the general direction of motion, and ω is the angular rate of a particle in the circular orbit.

It is more convenient to write

$$x = A\sin\theta + B\cos\theta + C\theta + D$$

$$y = E\sin\theta + F\cos\theta + G$$

We assume the Earth-Moon distance to be so large that the line-of-sight does not change direction. Letting the measured distance from the Earth to the vehicle be u,

$$u = K + (r + y)\cos\theta - x\sin\theta$$

and

$$u(t+\Delta t) - u(t-\Delta t) = \left[r + y(t+\Delta t)\right]\cos(\theta+\Delta\theta) - x(t+\Delta t)\sin(\theta+\Delta\theta)$$
$$- \left[r + y(t-\Delta t)\right]\cos(\theta-\Delta\theta) - x(t-\Delta t)\sin(\theta-\Delta\theta)$$
$$= -2r\sin\theta\sin\Delta\theta$$
$$+\frac{E}{2}\sin 2(\theta+\Delta\theta) + \frac{F}{2}\left[1+\cos 2(\theta+\Delta\theta)\right] + G\cos(\theta+\Delta\theta)$$
$$-\frac{E}{2}\sin 2(\theta-\Delta\theta) - \frac{F}{2}\left[1+\cos 2(\theta-\Delta\theta)\right] - G\cos(\theta-\Delta\theta)$$
$$-\frac{A}{2}\left[1-\cos 2(\theta+\Delta\theta)\right] - \frac{B}{2}\sin 2(\theta+\Delta\theta) - C(\theta+\Delta\theta)\sin(\theta+\Delta\theta) - D\sin(\theta+\Delta\theta)$$
$$+\frac{A}{2}\left[1-\cos 2(\theta+\Delta\theta)\right] + \frac{B}{2}\sin 2(\theta-\Delta\theta) + C(\theta-\Delta\theta)\sin(\theta-\Delta\theta) + D\sin(\theta-\Delta\theta)$$
$$= -2r\sin\theta\sin\Delta\theta - 2C\theta\cos\theta\sin\Delta\theta - 2C\Delta\theta\sin\theta\cos\Delta\theta - 2D\cos\theta\sin\Delta\theta$$
$$+(E-B)\cos 2\theta\sin 2\Delta\theta - (A+F)\sin 2\theta\sin 2\Delta\theta - 2G\sin\theta\sin\Delta\theta$$

$$u\left(t+\frac{\Delta t}{2}\right) - u\left(t-\frac{\Delta t}{2}\right) = -2r\sin\theta\sin\frac{\Delta\theta}{2} - C\theta\cos\theta\sin\Delta\theta - C\Delta\theta\sin\theta\cos\Delta\theta - D\cos\theta\sin\Delta\theta$$
$$+(E-B)\cos 2\theta\sin\Delta\theta - (A+F)\sin 2\theta\sin\Delta\theta - 2G\sin\theta\sin\frac{\Delta\theta}{2}$$

Also, we have that

$$\dot{u}(t) = (\dot{y} - \omega x)\cos\theta - (\dot{x} + \omega r + \omega y)\sin\theta$$
$$= (E\omega\cos\theta - F\omega\sin\theta - A\omega\sin\theta - B\omega\cos\theta - C\omega\theta - D\omega)\cos\theta$$
$$- (A\omega\cos\theta - B\omega\sin\theta + C\omega + r\omega + E\omega\sin\theta + F\omega\cos\theta + G\omega)\sin\theta$$
$$= \omega\left[(E-B)\cos 2\theta - (A+F)\sin 2\theta - (r+C+G)\sin\theta - C\theta\cos\theta - D\cos\theta\right]$$
$$\Delta t\,\dot{u}(t) = \Delta\theta\left[(E-B)\cos 2\theta - (A+F)\sin 2\theta - (r+C+G)\sin\theta - C\theta\cos\theta - D\cos\theta\right]$$

Letting

$$\phi = u\left(t + \frac{\Delta t}{2}\right) - u\left(t - \frac{\Delta t}{2}\right) - \dot{u}(t)\ \Delta t$$

we have

$$\phi = (E-B)\cos 2\theta\,(\sin\Delta\theta - \Delta\theta) - (A+F)\sin 2\theta\,(\sin\Delta\theta - \Delta\theta)$$

$$- (G+r)\sin\theta\left(2\sin\frac{\Delta\theta}{2} - \Delta\theta\right) - D\cos\theta\,(\sin\Delta\theta - \Delta\theta)$$

$$- C\theta\cos\theta\,(\sin\Delta\theta - \Delta\theta) - C\sin\theta\,(\Delta\theta\cos\Delta\theta - \Delta\theta)$$

$$= \left[(E-B)\cos 2\theta - (A+F)\sin 2\theta - (C\theta + D)\cos\theta\right](\sin\Delta\Delta - \Delta\theta)$$

$$- (G+r)\sin\theta\left(2\sin\frac{\Delta\theta}{2} - \Delta\theta\right) - C\sin\theta\ \Delta\theta\,(\cos\Delta\theta - 1)$$

Now

$$\sin\Delta\theta - \Delta\theta = -\frac{(\Delta\theta)^3}{3!} + O(\Delta\theta)^5$$

$$2\sin\frac{\Delta\theta}{2} - \Delta\theta = -\frac{(\Delta\theta)^3}{4.3'} + O(\Delta\theta)^5$$

and

$$\Delta\theta\,(\cos\Delta\theta - 1) = -\frac{(\Delta\theta)^3}{2!} + O(\Delta\theta)^5$$

Thus

$$\phi \cong \left[-(E-B)\cos 2\theta + (A+F)\sin 2\theta + (C\theta + D)\cos\theta + \frac{(G+r)\sin\theta}{4} + \frac{C\sin\theta}{2}\right]\frac{(\Delta\theta)^3}{3!}$$

Now

$$E-B = -\frac{\dot{y}_o}{\omega}$$

$$\frac{\partial(E-B)}{\partial a_i} = -\frac{\delta_{i5}}{\omega}$$

$$A+F = \frac{2\dot{x}_o}{\omega} + 3y_o$$

$$\frac{\partial(A + F)}{\partial a_i} = \frac{2}{\omega} \delta_{4j} + 3 \delta_{2j}$$

$$C\theta + D = -\left(6 y_o + \frac{3 \dot{x}_o}{\omega}\right)\theta + x_o - \frac{2 \dot{y}_o}{\omega}$$

$$\frac{\partial(C\theta + D)}{\partial a_i} = \delta_{1j} - 6 \theta \delta_{2j} - \frac{3 \theta}{\omega} \delta_{4j} - \frac{2}{\omega} \delta_{5j}$$

$$G + r = 4 y_o + \frac{2 \dot{x}_o}{\omega} + r$$

$$\frac{\partial(G + r)}{\partial a_i} = 4 \delta_{2j} + \frac{2}{\omega} \delta_{4j}$$

$$C = -\left(6 y_o + \frac{3 \dot{x}_o}{\omega}\right)$$

$$\frac{\partial C}{\partial a_i} = 6 \delta_{2j} + \frac{3}{\omega} \delta_{4j}$$

Then

$$\frac{\partial \phi}{\partial a_i} = \cos \theta \frac{(\Delta\theta)^3}{3!}$$

$$\frac{\partial \phi}{\partial a_2} = \left[3 \sin 2\theta - 6\theta \cos \theta - 2 \sin \theta\right] \frac{(\Delta\theta)^3}{3!}$$

$$\frac{\partial \phi}{\partial a_4} = \left[\frac{2}{\omega} \sin 2\theta - \frac{3\theta}{\omega} \cos \theta + \frac{1}{\omega} \sin \theta\right] \frac{(\Delta\theta)^3}{3!}$$

$$\frac{\partial \phi}{\partial a_5} = \left[\frac{1}{\omega} \cos 2\theta - \frac{2}{\omega} \cos \theta\right] \frac{(\Delta\theta)^3}{3!}$$

and

$$\frac{\partial(\dot{u} \Delta t)}{\partial a_i} = -\cos \theta \, \Delta\theta$$

$$\frac{\partial(\dot{u}\,\Delta t)}{\partial a_2} = \left[-3 \sin z\theta + 2 \sin\theta + 6\theta \cos\theta \right]\Delta\theta$$

$$\frac{\partial(\dot{u}\,\Delta t)}{\partial a_4} = \left[\frac{-2}{\omega} \sin 2\theta + \frac{3\theta}{\omega} \cos\theta + \frac{1}{\omega} \sin\theta \right] \Delta\theta$$

$$\frac{\partial(\dot{u}\,\Delta t)}{\partial a_5} = \left[-\frac{1}{\omega} \cos 2\theta + \frac{2}{\omega} \cos\theta \right]\Delta\theta$$

so

$$\frac{\partial\phi}{\partial a_i} = -\frac{(\Delta\theta)^2}{3!} \frac{\partial(\dot{u}\,\Delta t)}{\partial a_i}$$

The error in taking $\dot{u}\,\Delta t$ instead of $u(t + \frac{\Delta t}{2}) - u(t - \frac{\Delta t}{2})$ is a scalar error!

For $\Delta\theta$ small,

$$\frac{\partial\phi}{\partial a_i} \Big/ \frac{\partial(\dot{u}\,\Delta t)}{\partial a_i} = -\frac{(\Delta\theta)^2}{3!}$$

Since for low altitude lunar obrits ω is approximately 10^{-3} rad/sec, it follows that for 1 minute observations the fractional error resulting from the use of $\dot{u}\,\Delta t$ is 6×10^{-4}.

APOLLO NOTE NO. 128

H. Dale/
H. Engel

PRELIMINARY RESULTS OF THE EFFECT OF RANGE BIAS ERRORS

As is well known the MSFN may well measure range with an unknown bias along with zero mean, Gaussian noise. Apollo Note No. 98 analytically describes the technique for handling this situation, and the computer program which generated the data in Apollo Note No. 99 has been programed to handle biased range data.

Computer Results

The following computations have been performed, and the results are presented graphically. In all these cases the parameters used are:

$a_1 = 1.7525 \times 10^6$ m

$a_4 = 0$ m/sec.

$a_5 = 1.70172 \times 10^3$ m/sec

$\xi = 0^\circ$

$\eta = 180^\circ$

$\zeta = 180^\circ$

$\omega_e = .7291160 \times 10^{-4}$ rad/sec

$\omega_m = .42360 \times 10^{-6}$ rad/sec

$\rho_e = 6.3781 \times 10^6$ m

$\rho_m = 3.85 \times 10^8$

$\mu = 4.896 \times 10^{12}$ m^3/sec^2

$L = 15^\circ$

$\ell = 90^\circ$

Stations:

Madrid ($\lambda = 41^\circ$, $\alpha = -4^\circ$)
Johannesburg ($\lambda = -26^\circ$, $\alpha = 28^\circ$)
Woomera ($\lambda = -30^\circ$, $\alpha = 138^\circ$)

Computations were made for all three stations and for just two stations (Madrid and Johannesburg) using: range data only, range data with a priori data, range and range-rate data, and finally range and range rate-data with a priori data. The minimum miss near rendezvous, defined as $\sqrt{\sigma_x^2 + \sigma_y^2}$ (see Apollo Note No. 103), and the time between minimum miss and nominal rendezvous are plotted in the following figures. The a priori data used was

$$\sigma_{a_1} = \sigma_{a_2} = \sigma_{a_3} = 10^3 \text{ m}; \quad \sigma_{a_4} = \sigma_{a_5} = \sigma_{a_6} = \sqrt{10} \text{ m/sec.}$$

Conclusions

Since the inputs (above)are identical to those of Apollo Note No. 99, a comparison between results with and without bias errors is easy to make by simply copying the older data on the new figures (see Figure 1 through 4).

Two Stations (Figure 1 and 2)

- Without a priori data unknown bias errors tend to degrade the minimum miss by a factor of 5 or 10.
- At long tracking times (16 to 25 minutes) a priori data reduces the degradation to a factor of 2.
- At short tracking times (less than about 7 minutes) a priori data seems to "take out" the bias error effects.

Three Stations (Figure 3 and 4)

- The above general comments for two stations apply although the third station generally improves the errors.

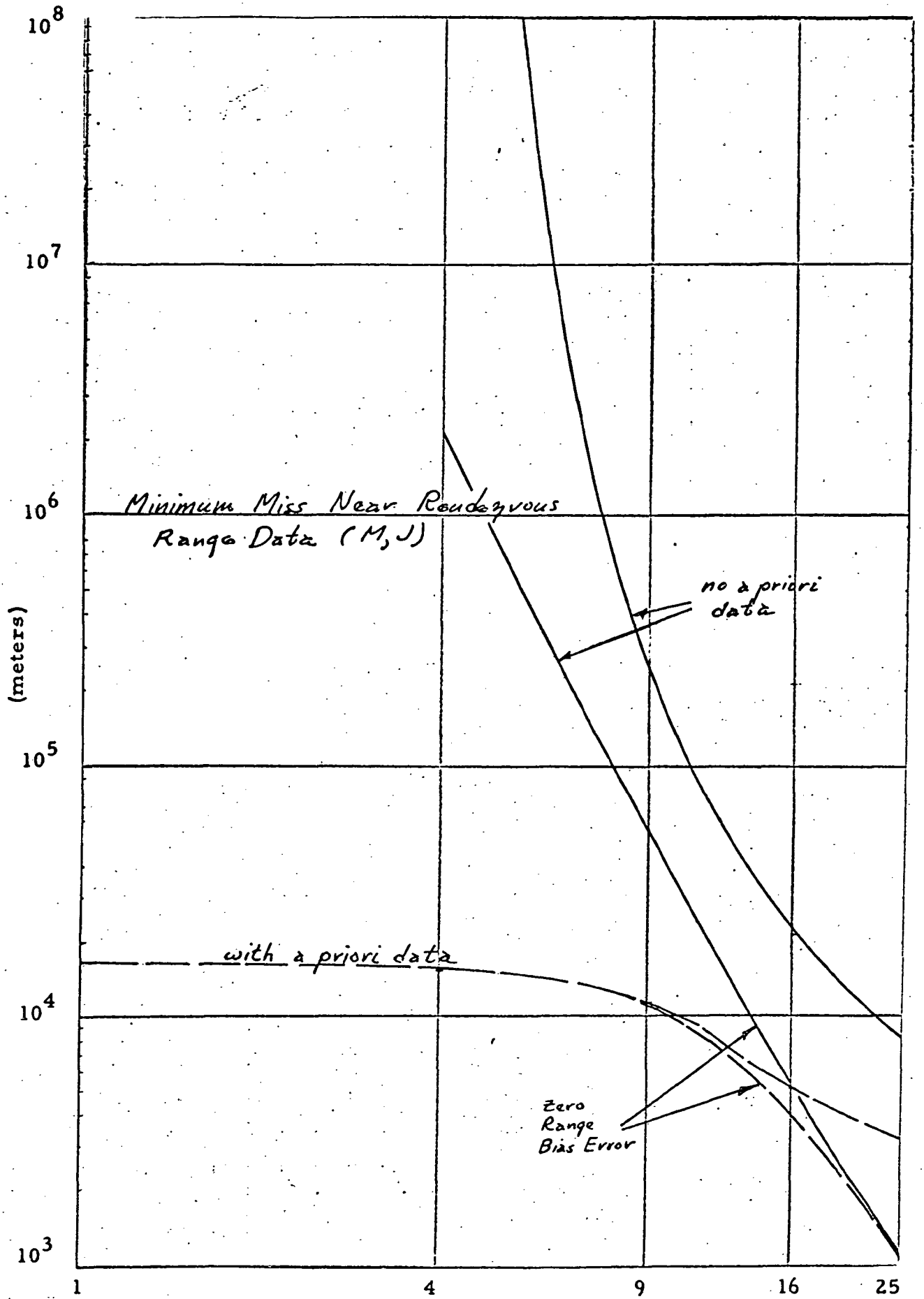
10^8
10^7
10^6
10^5
10^4
10^3
(meters)
Minimum Miss Near Rendezvous
Range Data (M, J)
no a priori data
with a priori data
Zero Range Bias Error
1
4
9
16
25
Number of 1 Minute Observations

Figure 1.

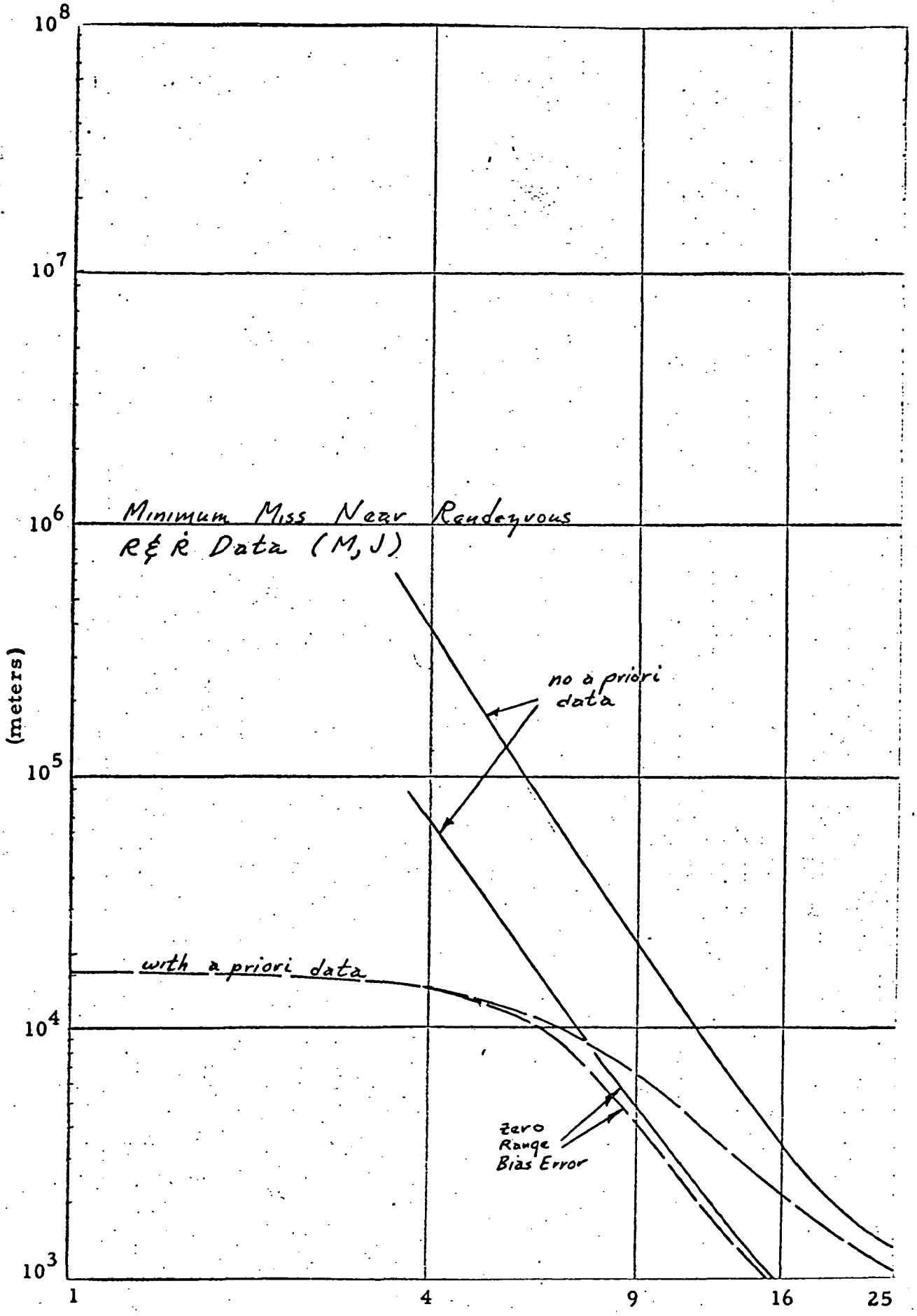

Figure 2.

Number of 1 Minute Observations

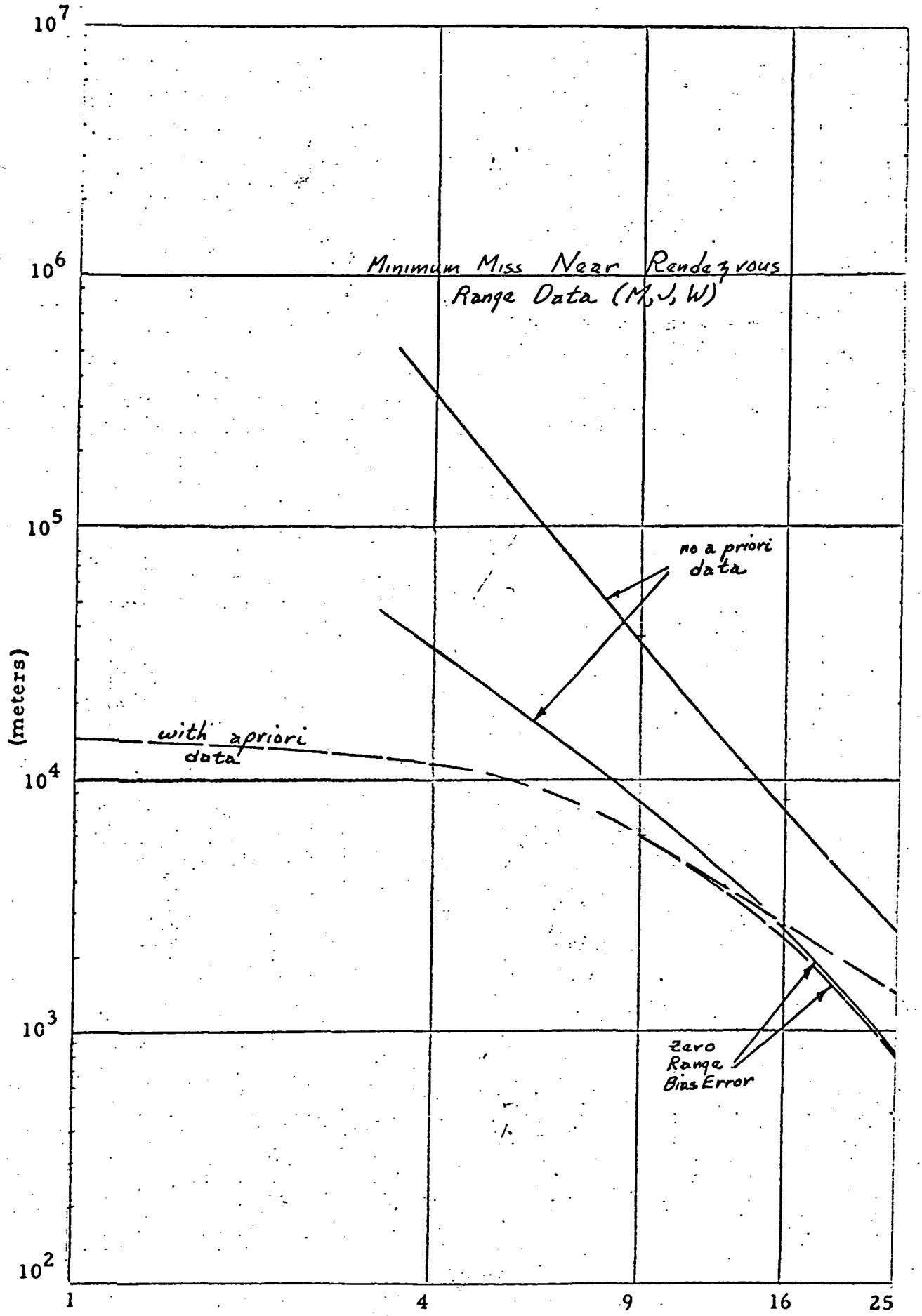

Figure 3.
Number of 1 Minute Observations

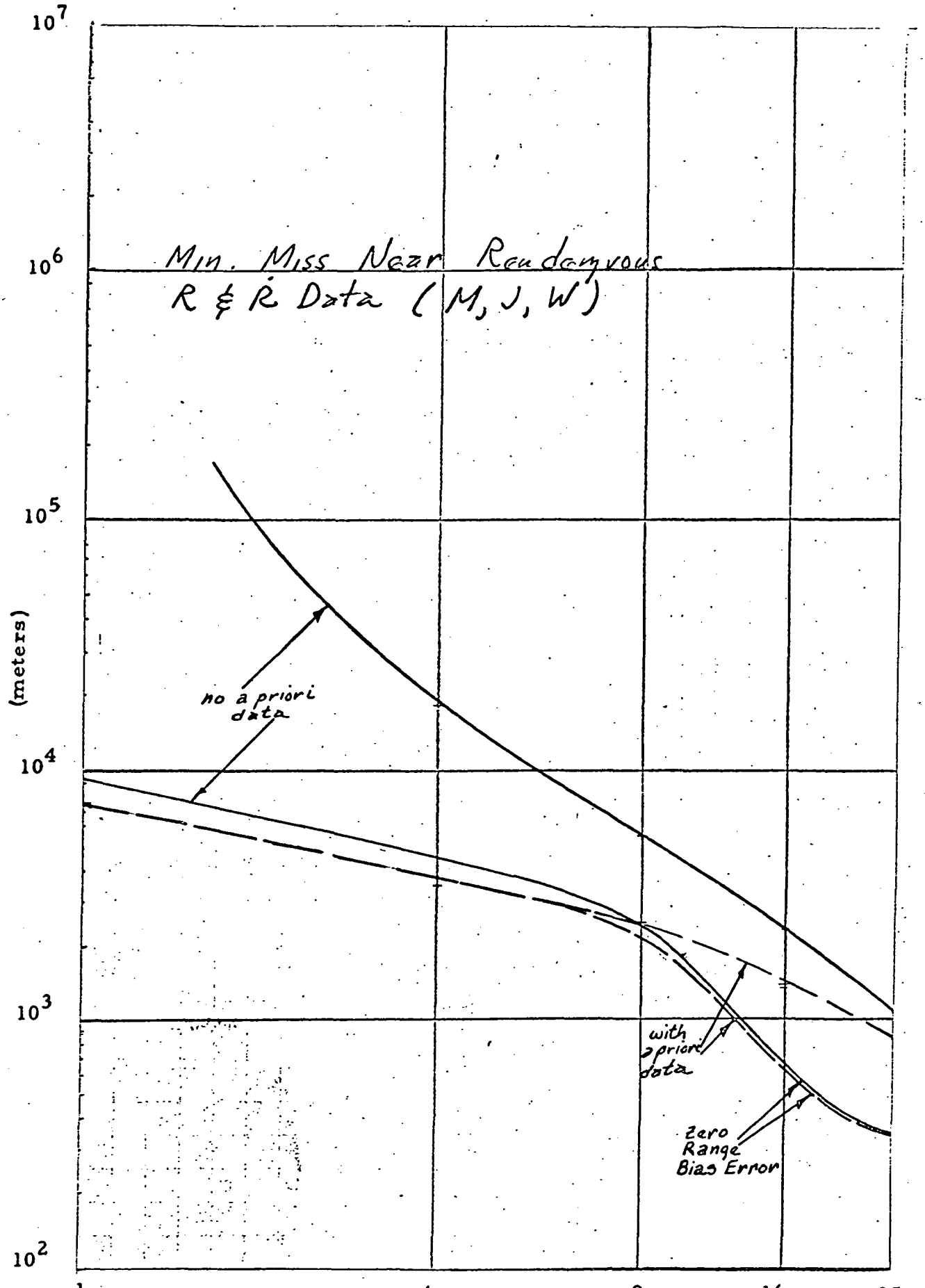

Figure 4.

Number of 1 Minute Observations

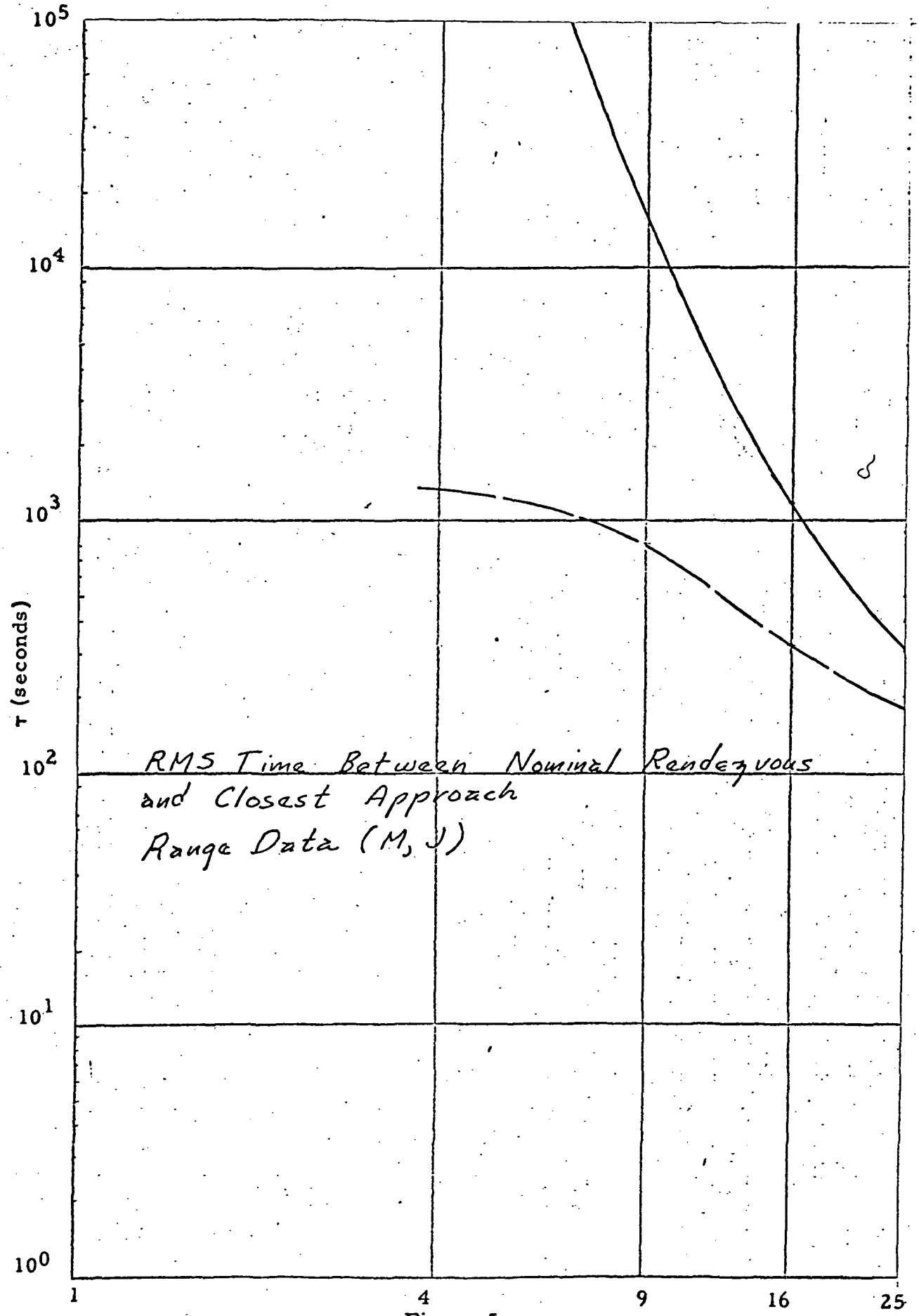

Figure 5.

Number of 1 Minute Observations

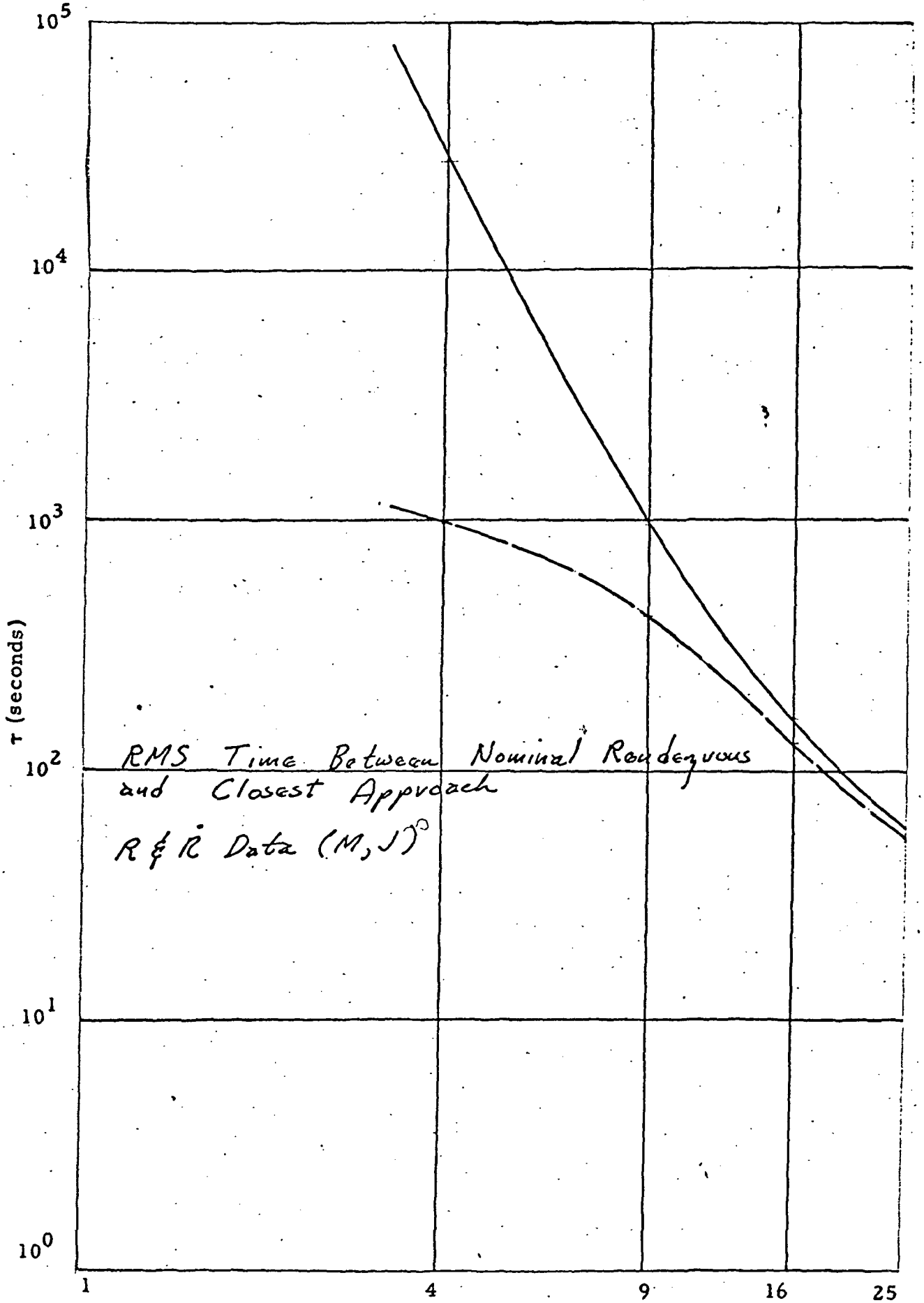

Figure 6.

Number of One Minute Observations

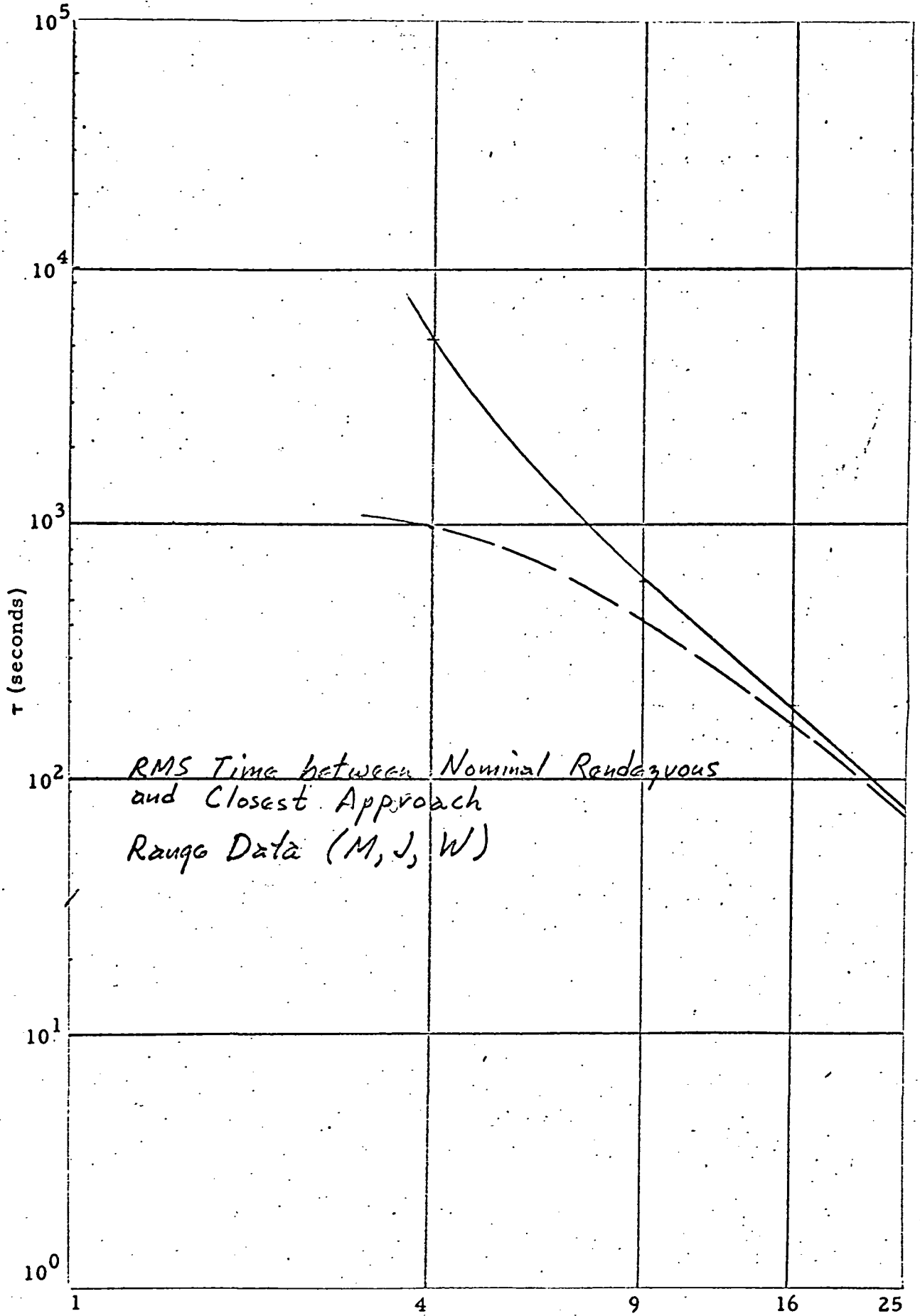

Figure 7.

Number of 1 Minute Observations

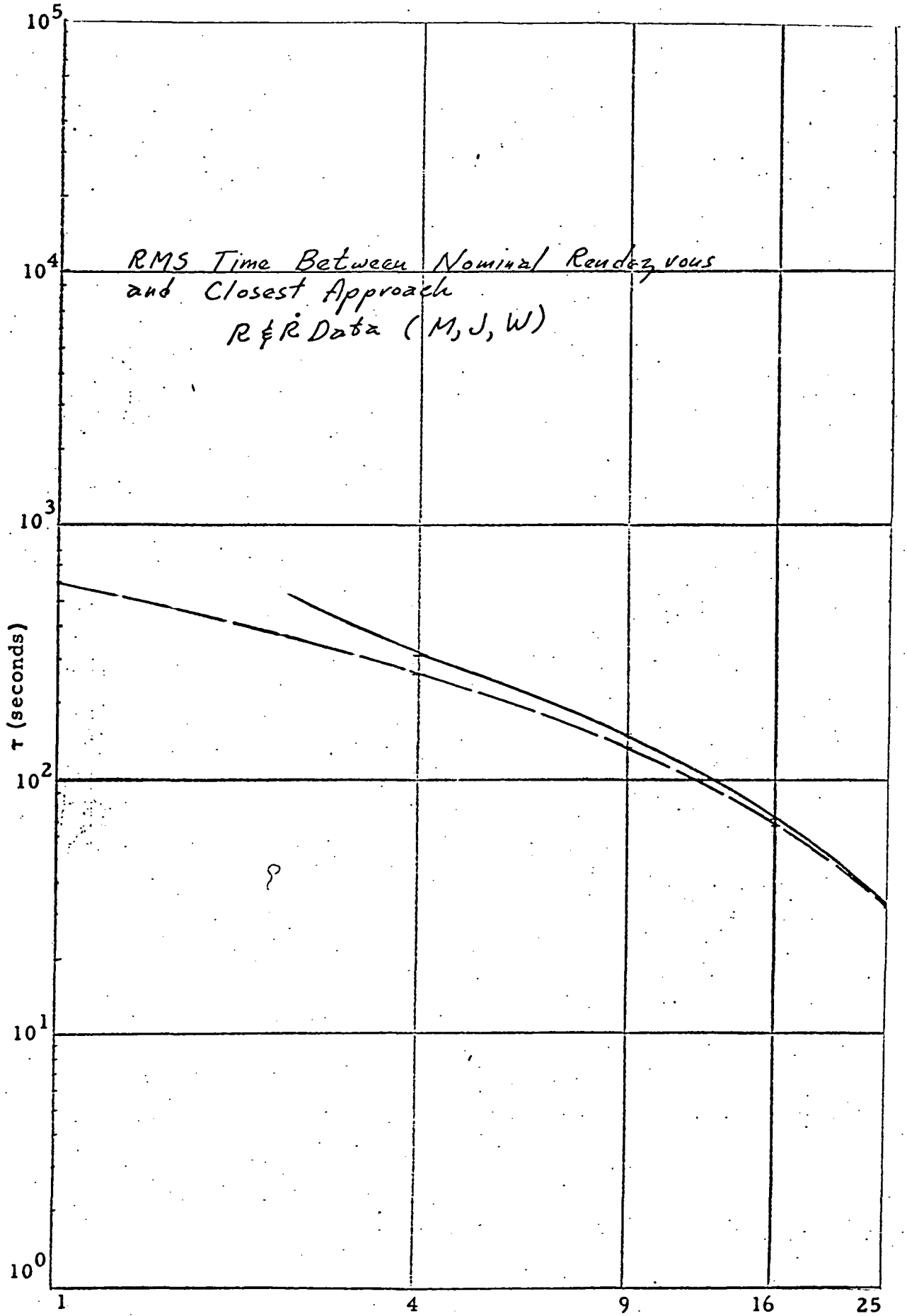

Figure 8.

Number of 1 Minute Observations

APOLLO NOTE NO. 129

G. F. Floyd
25 October 1963

EXPERIMENTAL PRECISION DOPPLER ACCURACY

During the Mariner II Venus probe flight, JPL measured doppler data in a three-way mode (one Goldstone station transmitting, the phase-lock transponder in the probe repeating, and another Goldstone station receiving and counting doppler cycles). They used a Varian rubidium frequency standard with stability of a few parts in 10^{11}. The counts were read once per minute on 11 different days for between 2 and 9 hours per day. The data was then curve fitted at one hour intervals with a third degree polynomial and then the residuals computed. On the basis of 4330 observations, the average 1 σ error in doppler frequency was .016 cps with a maximum of .023 cps. The transmitter was operating at 10^9 cps (L-Band) so:

$$\text{JPL:} \quad \frac{\Delta f}{f} = 2 \times 10^{-11} = \text{Frequency Standard Accuracy} \qquad (1)$$

When the Syncom I satellite was launched, Goddard had a phase-lock transponder aboard and measured doppler counts with a frequency standard which they quote as good to 5×10^{-10}. From 180 sec. of 1 sec. samples with 2nd degree curve fit, they then computed a 1 σ $\dot{R}$ fluctuation of 3.9 cm/sec. Thus, since

$$\Delta \dot{R} = \frac{\Delta f}{f} \frac{c}{2} \qquad (2)$$

we have,

$$\text{Goddard:} \quad \frac{\Delta f}{f} = \frac{3.9}{1.5 \times 10^{10}} \approx 3 \times 10^{-10} \approx \text{Frequency Standard Accuracy} \qquad (3)$$

Thus, in both cases, the measured doppler accuracy equals the frequency standard accuracy which means that with present day coherent 3-way doppler system, the only important source of error is the standard and accuracy of a part in 10^{11} or .2 cm/sec with 3-way

modes is reasonable for the Apollo time period.

The correlation time of the Goddard data was about 1.3 sec., and the JPL data was uncorrelated at the sampling time (1 minute). Beat frequencies between two STL rubidium standards have been taken and will be correlated. Also, experimental data is being obtained on the Varian and General Technology standards.

If the correlation time were to come out about 10 sec., then the effective doppler noise would be $.2\sqrt{10} = .6$ cm/sec.$^{1/2}$ as compared with the value of $3\sqrt{60} = 23$ cm/sec.$^{1/2}$ that was used in the first computer runs. This would reduce the miss uncertainty with $\dot{R}$ data by a factor of 38 so that with 3 $\dot{R}$ stations and no a priori data, using the results plotted in Apollo Note No. 106, we would get the table below.

Observation Time (minutes)	Miss Uncertainty (meters)
4	10,000
9	500
16	80
25	35

APOLLO NOTE NO. 130

John R. Holdsworth
28 October 1963

THE EFFECT OF NOISE AUTO-CORRELATION ON THE ACCURACY OF THE ESTIMATORS OF THE ORBIT PARAMETERS

Current computer programs are able to calculate the estimator errors in the orbit determination problem when the data is corrupted by additive gaussian noise which is uncorrelated from sample to sample. Two other notes, i.e., Apollo Notes 107 and 116 have dealt with the problem of auto-correlated noise. Apollo Note No. 116 was a reasonably rigorous treatment of the problem for correlated noise similar to that in Note 43 for uncorrelated noise. Note 107, however, described an approximate method for performing the computations involving correlated noise which would permit the use of computer programs already in existence. It is the unpleasant purpose of this Note to show that the conclusions drawn in Note 107 were faulty and hence that the method suggested there may be of little or no use.

Apollo Note No. 107 developed a possible method of accounting for a lack of statistical independence in consecutive noise samples by postulating that the effect of the noise auto-correlation was such that it degraded the data in a particular way. Specifically it was assumed that the presence of auto-correlated noise was such that its effect on the estimator errors of the orbit parameters based on N observations was equivalent to assuming that the parameters had been estimated from pieces of data which were contaminated by independent additive noise of the same variance as the correlated noise samples. An analytic expression for effective sample size N_{eff}, which was generally less than the number of pieces of correlated data N, was then derived as a function of the auto-correlation function of the noise.

As was mentioned in Apollo Note No. 107, the analysis was rigorously exact when the sampling was done from a stationary population and where the one parameter to be estimated was the population mean. It was suggested, however, that for numerical purposes the analogy could possibly be considerably extended to

situations where the systematic trend of the data was a rather arbitrary function of time and the orbit parameters of interest. This suggestion, however, implies an interesting inconsistency.

Namely, our postulate assumed the essential equivalence of the estimation problem with N pieces of correlated data to another one involving N_{eff} pieces of independent data where $N_{eff} \leq N$. This however implies the conclusion that the effect of auto-correlation on the additive noise corrupting the data is such that the accuracies in the estimators of all of the parameters are degraded. This, however, is not the case since we will exhibit an example where auto-correlated noise greatly improves the accuracy of the estimators of some parameters.

Consider the following simplified situation. We assume that we are observing a time series composed of a deterministic linear trend corrupted by additive zero mean stationary gaussian noise with normalized auto-correlation function $\rho(\tau)$ where τ is the time lag between successive observations. To simplify things even more we assume that we have two observations from which we must estimate the two parameters appearing in the linear trend.

That is, we assume that the data may be represented in the form

$$x(t) = b + at + n(t) \tag{1}$$

where n (t) is the additive noise and is assumed to be stationary and have zero mean. If we have only two observations, say $x(t_1)$ and $x(t_2)$, then an obvious estimate for the parameter a is given by:

$$\hat{a} = \frac{x(t_2) - x(t_1)}{t_2 - t_1} \tag{2}$$

If we assume that the noise is uncorrelated then the mean square error in the estimator $\hat{a}$ is given by:

$$\sigma^2_{\hat{a}} = \frac{2\sigma^2}{(t_2 - t_1)^2} \tag{3}$$

where σ^2 is the variance of the additive noise.

On the other hand, if the noise is correlated, then the mean square error of the estimator $\hat{a}$ is given by:

$$\sigma_{\hat{a}}^2 = \frac{2\sigma^2 \left(1 - \rho\,(t_2 - t_1)\right)}{(t_2 - t_1)^2} \tag{4}$$

Comparison of Equation (4) with (3) shows that if the errors at times t_1 and t_2 are positively correlated then the variance of the estimator calculated from correlated data is smaller than that of the estimator computed on the basis of independent data. In fact as the correlation becomes extremely strong we may estimate the parameter a with arbitrary accuracy.

Thus we have exhibited a situation where auto-correlation in the noise samples increases rather than decreases the accuracy with which certain parameters may be estimated. More generally if the time series may be represented in the form

$$x(t) = b + \sum_{k=1}^{n} a_k t^k + n(t) \tag{5}$$

and if at least n + 1 samples are available within some time interval in which all of pairs of successive noise samples are very strongly correlated, then it may be shown that the parameters $a_1, \ldots a_n$ can be estimated with far greater accuracy than if they were estimated from independent data.

The significant point for our consideration is that over reasonable smoothing intervals the data function for our estimation problem should at least approximately representable as a polynomial, and hence from what we have said in this note, there will exist cases in which auto-correlated noise will increase rather than decrease the accuracy of the estimators which is directly contrary to the implications of Apollo Note No. 107. Thus, it would perhaps be best if Apollo Note No. 107 were ignored in practice.

APOLLO NOTE NO. 131

W. Iwata
29 October 1963

A METHOD OF MANUFACTURING A PROPER ROTATION MATRIX WHICH CONVERTS THE COVARIANCE MATRIX TO DIAGONAL FORM

The following problem is posed by L. Lustick. * Given an arbitrary random variable $x = \text{col}\,(x_1, \ldots, x_n)$ with a given probability function defined relative to a basis $e_1, \ldots, e_n$ of an n-dimensional space R_n find a method of calculating a proper orthogonal (rotation) matrix B such that the n-random variables $y_1, \ldots, y_n$ defined by $\text{col}\,(y_1, \ldots, y_n) = Bx$ are uncorrelated. Stated geometrically, this means find a proper rotation of the basis $e_1, \ldots, e_n$ into a new basis $f_1, \ldots, f_n$ such that a principal semi-axes of the ellipsoid of concentration of the random variable x is coincident with each f_i, $i=1, \ldots, n$. In matrix rotation this amounts to:

(i) a proper rotation B: $BB^T = I$, $\det B = 1$,
where B^T denotes the transpose of B;

(ii) $\text{cov}\,(y_i, y_j) = \text{Diag}\,(d_1, \ldots, d_n)$ or equivalently,
$BAB^T = \text{Diag}\,(d_1, \ldots, d_n)$, where
$A = \text{cov}\,(x_i, x_j)$;

(iii) $y = BHB^T \text{col}\,(f_1, \ldots, f_n)$, where H is defined by
$x = H \text{col}\,(e_1, \ldots, e_n)$ and $y = \text{col}\,(y_1, \ldots y_n)$.

Any introductory text in matrix theory will tell us that a matrix satisfying these conditions exists (since A is a positive definite symmetric matrix), and also evidence can be amassed, cited possibly

---

* Received August 1963.

from the same source, to persuade us to believe how plausible the construction of such a matrix should be--but regrettably for us citations taken alone are nothing more than reassuring aphorisms. The most cogent reason for the omission of a method of constructing matrix B, aside fromthe impractical method of solving an homogeneous system of linear equations (see (ii)), is that B is not uniquely defined; for example any row permutation of B will satisfy the three foregoing conditions and similarly with any matrix of the form BE where E is an arbitrary orthogonal matrix of determinant 1 permutable with A. Indeed, the problem is further complicated by the fact there are generally a non-trivial number of real non-orthogonal matrices P for which the relation $P^{-1}AP = \text{Diag}\,(d_1, \ldots, d_n)$ holds. Luckily, however, the Gram Schmidt process obviates the most objectionable aspects of this problem and makes the actual calculation relatively straightforward.

The factors which motivate its use here are conditions i) and ii), the former of which implies that columns $B_1, \ldots, B_n$ of the matrix B^T form an orthonormal system of n eigenvectors of the matrix A which because of the latter belong to the eigenvalues $d_1, \ldots, d_n$ respectively. This observation is directly applicable via the Gram Schmidt process to the columns of any real similarity transformation P which diagonalizes A into the form

$$P^{-1}AP = \text{Diag}\,(\lambda_1, \ldots, \lambda_n)$$

Here, we presume that P and its eigenvalues $\lambda_1, \ldots, \lambda_n$ are obtainable by standard computer methods. (If not, we shall propose an alternative method in another Apollo Note).

Let $P_1, \ldots, P_m$ denote the columns of the n x n matrix P and let the symbol (u, v) stand for the dot product of vectors u and v in R_n. Since P is a non-singular matrix the set $P_1, \ldots, P_n$ is a basis for the space R_n, so that the Gram Schmidt process admits an orthonormal system of n vectors $Q_1, \ldots, Q_n$ in terms of the P_i in the following manner.

Let

$$Q_1 = P_1 / (P_1, P_1)^{1/2} \tag{1}$$

and for any k, $1 \leq k < n$, let

$$Q_{k+1} = Q'_{k+1} \Big/ (Q'_{k+1}, Q'_{k+1}) \tag{2}$$

where

$$Q'_{k+1} = P_{k+1} - (a_k Q_k + \ldots + a_1 Q_1) \tag{3}$$

where

$$a_i = (P_{k+1}, Q_i), \quad i = 1, \ldots, k.$$

Clearly $Q'_{k+1} \neq 0$, since the vector difference, $Q'_{k+1} - P_{k+1}$, is obviously representable as a linear combination of the linearly independent set of k vectors, $P_1, \ldots, P_k$. Hence $(Q'_{k+1}, Q'_{k+1}) \neq 0$ and moreover, our choice of (P_{k+1}, Q_i) for the scalar quantity a_i forces $(Q'_{k+1}, Q_i) = 0$, $i=1, \ldots, k$. This shows Q_{k+1} to be a well-defined normal vector, orthogonal to any predecessor Q_i, $1 \leq i \leq k$, which proves therefore, by induction, that $Q_1, \ldots, Q_n$ is an orthonormal system.

The crucial point not covered by the Gram Schmidt process is the fact that for each $i = 1, \ldots, n$, Q_i is an eigenvector of A belonging to the eigenvalue λ_i. The following argument, good for symmetric matrices only, shall confirm this assertion. Surely Q_1 is an eigenvector of A corresponding to λ_1. Since it differs from P_1 by a scalar; and for any other k, where $1 < k < n$, assume Q_k is an eigenvector of A corresponding to λ_k and consider the meaning of the equation:

$$AQ_{k+1} = \left(A\ P_{k+1} - (a_k Q_k + \ldots + a_1 Q_1)\right) \Big/ (Q'_{k+1}, Q'_{k+1})^{1/2}$$

Since $A P_{k+1} = \lambda_{k+1} P_{k+1}$ and since for each $i=1, \ldots, k$

$$A Q_i = \lambda_i Q_i, \text{ we have,}$$

$$(P_{k+1}, A Q_i) = \lambda_i (P_{k+1}, Q_i)$$

$$(A P_{k+1}, Q_i) = \lambda_{k+1} (P_{k+1}, Q_i).$$

But $(P_{k+1}, A Q_i) = (P_{k+1}, A Q_i)$ since A is symmetric, and therefore, $(\lambda_{k+1} - \lambda_i)(P_{k+1}, Q_i) = 0$. Consequently, for $i=1, \ldots, k$, $a_i \neq 0$ iff $\lambda_i = \lambda_{k+1}$. In other words, the dot product of any two eigenvectors of a symmetric matrix is non-trivial iff their eigenvalues are equal. On account of this, simple computation shows that by Equation (3), we get,

$$A Q_{k+1} = \lambda_{k+1} \left[P_{k+1} - (a_k Q_k + \ldots + a_1 Q_1) \right] \Big/ (Q'_{k+1}, Q'_{k+1})^{1/2}$$

$$= \lambda_{k+1} Q_{k+1}.$$

This proves that in addition to the fact that $Q_1, \ldots, Q_n$ is an orthonormal system, it is also a set of n eigenvectors of the covariance matrix A with their eigenvalues being precisely $\lambda_1, \ldots, \lambda_n$ respectively.

Construction of a proper orthogonal matrix now becomes a relatively simple matter. Let Q be the matrix with columns $Q_1, \ldots, Q_n$ and according as det Q = 1 or -1 we may set $B = Q^T$ or $B = (QK)^T$, where $k = \text{diag}(-1, 1, \ldots, 1)$. Obviously then, $BB^T = I$, det B = 1 and $BAB^T = \text{Diag}(\lambda_1, \ldots, \lambda_n)$ so that B is indeed a proper rotation matrix with $f_i = Be_i$, $i=1, \ldots, n$. In particular, f_i are simply the columns of B if $e_i = \text{col}(0, \ldots, \underset{i}{1}, \ldots, 0)$, and hence are ortho-normal with $y_i = x_i \text{ col}(B)_i$, $i=1, \ldots, n$.

Scheme for a Computer

Preliminary:

Let $e_1, \ldots, e_n$ be a basis for the n-dimensional space R_n in question, where e_i is written as a column vector and let $x = \text{col}\,(x_1, \ldots, x_n)$ be the random variable whose covariance matrix $A = \text{cov}\,(x_i, x_i)$ is to be diagonalized.

Computer Calculations:

Use any computer scheme that will diagonalize the given covariance matrix A but in doing so keep track of the matrix, say $P = (P_{i,j})$, $1 \leq i, j \leq n$ which effects this diagonalization. Suppose the diagonal terms are $\lambda_1, \ldots, \lambda_n$. In matrix notation this is equivalent to

$$P^{-1} A P = \text{diag}\,(\lambda_1, \ldots, \lambda_n).$$

If any of the λ_i's equal zero start over again with double precision. Assuming that the condition $\lambda_i = 0$ does not obtain for any $1 \leq i \leq n$, let P_i denote the ith column of the n x n matrix P and for any pair of vectors u and v, let the symbol (u, v) stand for their dot product. Use the Gram Schmidt process described by Equations (1), (2), and (3) to convert $P_1, \ldots, P_n$ into a set of n vectors $Q_1, \ldots, Q_n$. Let Q be the matrix whose columns are given by $Q_1, \ldots, Q_n$. If det Q = 1, let $B = Q^T$ and if det Q = -1 let B be the matrix whose rows are given by $-Q_1^T, Q_2^T, \ldots, Q_n^T$. B is the proper rotation matrix and the new basis $f_1, \ldots, f_n$ is defined by $f_i = Be_i$, $i=1, \ldots, n$.

APOLLO NOTE NO. 132

L. Horowitz
29 October 1963

CONVERGENCE OF SUCCESSIVE ITERATION ON THE ORBIT PARAMETER ESTIMATORS

Introduction

The covariance matrix of the orbit parameter maximum likelihood estimators provides an asymptotic lower bound on the accuracy to which these parameters may be estimated. Actual estimation of these parameters requires an entirely separate computational procedure however. In general, local linearization of the measurable function is effected, and some sort of iteration technique utilized to estimate the orbit parameters by repeated comparison of the computed values of the measurable with observed values.

This note attempts to investigate the rate of convergence of such an iteration technique in order to estimate in turn the computation time required for determination of orbit parameters to a given accuracy.

This study assumes iterations are performed by the Newton-Raphson method, although the method described is readily adapted to other iteration techniques. Results are summarized in the concluding section.

Determination of the Maximum Likelihood Estimators

As explained in Apollo Note No. 43, we begin with N measurements of some measurable quantity $f_m(t_i) \equiv f_m(i)$, $i = 1, \ldots N$, and some more or less educated initial guesses a_j^o of the orbit parameters a_j; $j = 1, \ldots, m$. Now the equations of motion of the vehicle permit the actual computation of $f_c(i) = f_c(a_1, \ldots, a_m; t_i)$ as a parametric function of the a_j. The N initial values of $f_c(i)$ are then just $f_c^o(i) = f_c(a_1^o, \ldots, a_m^o; t_i)$, as determined by our original guesses a_j^o of the "m" orbit parameters a_j. We then wish to make better estimates of the a_j by modifying our original guesses a_j^o to provide for an optimum agreement between the $f_c(i)$ and the $f_m(i)$ in some sense. If we choose this sense so as to force optimum agreement by minimizing the sum of the squares

of the differences between the $f_c(i)$ and the $f_m(i)$ (Apollo Note No. 43 shows that this is tantamount to maximizing the likelihood of our observing the N measurements $f_m(i)$ which we have, in fact, observed. That is, this simply supposes that the N observations we made were, in fact, the most likely ones, in view of the presence of bias and random noise), we are led to better estimates $\hat{a}_j$ of the orbit parameters a_j.

Following Apollo Note No. 43, the technique is as follows: We introduce the functional $\psi = \psi(a_1, \ldots, a_m)$ to represent the sum of the squared differences:

$$\psi = \sum_{i=1}^{N} \left[f_c(a_1, \ldots, a_m; t_i) - f_m(i) \right]^2. \tag{1}$$

Then ψ is minimized when $\frac{\partial \psi}{\partial a_j} = 0$. Let $\phi_j = \phi_j(a_1, \ldots, a_m; f_m) = \frac{\partial \psi}{\partial a_j} = 0$.

Then

$$\phi_j = 2 \sum_i \left[f_c(i) - f_m(i) \right] \frac{\partial f_c(i)}{\partial a_j} = 0; \; j = 1, \ldots, m. \tag{2}$$

Recalling that a_j^o, $j = 1, \ldots, m$, were our original guesses of the orbit parameters, we make new estimates a_j^1 by letting

$$a_j^1 = a_j^o + \Delta_1 a_j. \tag{3}$$

Let us then evaluate ϕ_j on these new estimates a_i^1:

$$\phi_j(a_1^o + \Delta_1 a_1, \ldots\ldots, a_m^o + \Delta_1 a_m; f_m) = 0 \tag{4}$$

Expand ϕ_j in a Taylor Series about $a_1^o, \ldots, a_m^o$:

$$\phi_j(a_1^o + \Delta_1 a_1, \ldots\ldots, a_m^o + \Delta_1 a_m; f_m) = \phi_j(a_1^o, \ldots, a_m^o; f_m)$$

$$+ \sum_k \frac{\partial \phi_j}{\partial a_k} \Bigg|_{\substack{\Delta_1 a_k + \frac{1}{2} \sum_\ell \sum_m \frac{\partial^2 \phi_j}{\partial a_\ell \, \partial a_m} \\ a_k = a_k^o}} \Bigg|_{\substack{\Delta_1 a_\ell \Delta_1 a_m + \ldots\ldots, \\ a_\ell = a_\ell^o \\ a_m = a_m^o}}$$

and assume the $\Delta_1 a_i$ sufficiently small so that higher order terms containing the products $\Delta_1 a_2\ \Delta_1 a_m \ldots$ can be neglected. This yields a system of "m" simultaneous equations linear in the $\Delta_1 a_i$:

$$\phi_j (a_1^o, \ldots, a_m^o ; f_m) + \sum_{k=1}^{m} \frac{\partial \phi_j}{\partial a_k} \Bigg|_{a_k = a_k^o} \Delta_1 a_k = 0. \qquad (6)$$

Solving this simultaneous linear system for the $\Delta_1 a_i$ gives new estimates a_i^1 by (3):

$$a_i^1 = a_i^o + \Delta_1 a_i. \qquad (3)$$

We then repeat this same procedure, taking for our new estimates of the orbit parameters the a_i^1 instead of the a_i^o. Iteration on the a_i continues until the $\Delta_n a_i$ are sufficiently small; we call the resulting a_i^n the maximum likelihood estimators of the orbit parameters and denote them by $\hat{a}_i$. This technique for finding the "m" zeros Δa_i of ϕ_j is just the well-known Newton-Ralphson iteration method applied to functions ϕ_j of "m" variables.

Convergence of the Estimator Iterations

We first observe that if our original estimates a_i^o are too far off, it is entirely possible that the Newton-Raphson iteration need not converge at all. Hence, in all that follows, we exclude this contingency by assuming that our initial guesses are close enough to guarantee convergence. This is surely true if the ϕ_j are in fact linear in the a_i, for then the higher order mixed partial derivatives of (5) vanish identically so that (6) is no longer an approximation. From (2), we see that this assumption in turn requires that f_c be linear in the a_i so that $\frac{\partial f_c}{\partial a_i}$ are all constant for $i = 1, \ldots, m$. Thus, we restrict the following analysis to require that the f_c be linear in the region of interest.

This crucial assumption guarantees not only that the Newton-Raphson iteration converges, but also that the covariance matrix of the maximum likelihood estimators is identically constant in the region of interest (since its terms are derived from quantities of the form $\sum_i \frac{\partial f(i)}{\partial a_j} \frac{\partial f(i)}{\partial a_k}$; all constants under this assumption).

Now the covariance matrix cov $(\hat{a}_i, \hat{a}_j)$ indicates how well the orbit parameters can be estimated in the presence of unknown bias and random noise. From this information, we would like to be able to determine which of the parameters a_i dominates in the computation of f_c (i.e., we wish to determine to which of the a_i the computation of f_c is most sensitive), for by studying the convergence of the Newton-Raphson iteration on just this one ("worst") variable (i.e., with the other a_i held fixed) we can estimate the over-all convergence of the multi-variable iteration. Unfortunately, the general covariance matrix does not provide this information directly, since the non-zero covariance terms show that errors in any one parameter are correlated with errors in the others, and hence, that this "worst" parameter cannot be singled out by inspection of cov $(\hat{a}_i, \hat{a}_j)$ in its general form.

To surmount this difficulty, we use the technique of Apollo Note No. 126 to refer cov $(\hat{a}_i, \hat{a}_j)$ to a new coordinate system (the "normal" or "principal axis" system) in which the covariance terms $\sigma_{x_i x_j}$ $(i \neq j)$ all vanish, so that cov $(\hat{a}_i^*, \hat{a}_j^*)$ is rendered diagonal. Here, the asterisks indicate quantities referred to the normal coordinates, in which all subsequent calculations are performed. Note that the transformation between these two systems is always linear:

$$a_i^* = \sum_{j=1}^{m} \alpha_{ij} a_j \text{ (Apollo Note 126, p. 5).}$$

Now in the normal coordinate system, terms in the information matrix are:

$$C_{jk} = \frac{1}{\sigma^2} \sum_{i=1}^{N} \frac{\partial f_c(i)}{\partial a_j^*} \frac{\partial f_c(i)}{\partial a_k^*} , \qquad (7)$$

where

$C_{jk} = 0$ for $j \neq k$. (The information and covariance matrices are both diagonal in this system). Thus, the main diagonal terms of the information matrix reduce to

$$C_{kk} = \frac{1}{\sigma^2} \sum_{i=1}^{N} \left(\frac{\partial f_c(i)}{\partial a_k^*} \right)^2 , \tag{8}$$

so that the largest term on the main diagonal of the information matrix (equivalently, the smallest term on the main diagonal of the now diagonalized covariance matrix) is precisely that term for which the sum of the squares of the $\frac{\partial f_c(i)}{\partial a_k^*}$ is maximum. But this is precisely what we mean by the dominating (i.e., "worst") parameter, call it a^*. Hence, the dominating parameter a^* can be determined by diagonalizing cov $(\hat{a}_i, \hat{a}_j)$ and then selecting the parameter corresponding to the smallest diagonal element.

Convergence of the Newton-Raphson iteration on one variable is then estimated as follows: For the case in point (all the parameters a_i^* fixed except for the dominating variable a^*), the iterations on a^* are simply:

$$a^*(k+1) = a^*(k) - \frac{\phi\left[a^*(k)\right]}{\frac{\partial \phi\left[a^*(k)\right]}{\partial a^*}} , \tag{9}$$

as can be seen from (6); where we have now written $a^*(k)$ to denote the k^{th} iterate of a^*. Hildebrand [1/] has shown that if the Newton-Raphson iteration converges to a^*, the error at the $k+1^{st}$ iteration is given approximately by:

1/ F. B. Hildebrand, Introduction to Numerical Analysis, (McGraw-Hill, 1956), p. 448.

$$a^* - a^*(k+1) \approx -\frac{1}{2}\,\frac{\phi''(a^*)}{\phi'(a^*)}\left[a^* - a^*(k)\right]^2 \qquad (10)$$

where the primes denote differentiation with respect to the argument. For this computation, ϕ is no longer taken as a linear function of the a_i^*. Note that if ϕ just happened to be truly linear in the a_i^*, $\phi(a^*)$ would vanish identically, and the iterations would converge in just one step, as expected. When our estimates a_k^* are sufficiently close to the iteration limit a^*, we may rewrite (10) as:

$$e \approx -\frac{1}{2}\,\frac{\phi''(a^*(k))}{\phi'(a^*(k))}\left[a^*(k) - a^*(k-1)\right]^2, \qquad (11)$$

where e represents the accuracy to which we wish to determine a^*. Then the number of iterations required to force this accuracy e is given by the simultaneous solution of the finite difference system (9) and (11).

We observe in particular that by (10), the error $a^* - a^*(k+1)$, call it $\Delta a^*(k+1)$, tends to be proportional to the square of the error in $a^*(k)$, and hence that accuracies good to the second order result from this technique, guaranteeing rapid convergence for small values of $\Delta a^*(k+1)$. Finally, Hildebrand [2/] shows that for simultaneous systems of nonlinear equations in several variables, errors in the $k+1^{st}$ iterates tend to become linear in the squares of the k^{th} iterates, so that if one term does in fact dominate (as we have assumed throughout), then the assumed second order errors in the remaining variables contribute to the net error (11) only up to fourth order; surely negligible for purposes of this analysis.

A check on the convergence of the Newton-Raphson method may be performed by examining the Jacobian of the ϕ_i:

2/ Hildebrand, loc. cit., p. 451.

$$J \equiv \begin{vmatrix} \frac{\partial \phi_1}{\partial a_1^*} & \frac{\partial \phi_1}{\partial a_2^*} & \cdots & \frac{\partial \phi_1}{\partial a_m^*} \\ \vdots & & & \\ \frac{\partial \phi_m}{\partial a_1^*} & \frac{\partial \phi_m}{\partial a_2^*} & \cdots & \frac{\partial \phi_m}{\partial a_m^*} \end{vmatrix} \tag{12}$$

If J vanishes at a_i^*, $i = 1, \ldots, m$, then (2) does not possess a unique solution. If J vanishes near a_i^*, slow convergence or divergence of the iteration may be anticipated. 3/

Conclusions

By employing the techniques of Apollo Note 43, this study has shown how the Newton-Raphson iteration method may be used to compute the maximum likelihood estimators $\hat{a}_i$ of the orbit parameters. An estimate of the rate of convergence of this procedure was then performed by examining iterations on the "dominating" variable a^*; obtained in turn from inspection of the diagonalized covariance matrix. The number of iterations required to achieve a specified accuracy was then shown to result from the solution of a simultaneous system of finite-difference equations (9) and (11). Justification for performing this analysis on the "dominating" parameter a^* alone was then provided by showing that higher order errors induced through the remaining parameters contributed only up to the fourth order in the convergence of the iterations, and hence, that their effects could be neglected. Finally, a second check on the convergence of the Newton-Raphson

---

3/ Hildebrand, loc. cit., p. 451.

iteration was provided by an examination of the Jacobian of the system, evaluated on the maximum likelihood estimators $\hat{a}_i^*$.

It is emphasized that the crucial assumption in this analysis lies in the linearization (6) of the computed function f_c over the region of interest, since this guarantees convergence of the iterations on (2), as well as constancy of the covariance matrix over the entire region of interest. Under this assumption, the "dominating" parameter a^* remains the dominating parameter throughout the entire sequence of iterations. Note that this would probably not be the case were the linearization not valid over the region of interest, since the role of dominating parameter would generally change hands at various levels of the successive iterations.

We have also assumed that there is, in fact, only one "dominating" parameter a^*, corresponding to a patently smallest term on the main diagonal of $\mathrm{cov}(\hat{a}_i^*, \hat{a}_j^*)$. Although this should generally be the case, upper bound estimates on the rate of convergence can also be obtained for the case of "M" dominating parameters $(a^*)_k$; k=1,...,M. It is only necessary to determine the number of iterations "n" required on any <u>one</u> of the parameters $(a^*)_k$ (with all the other parameters held fixed) to drive the "accuracy" $\Delta(a^*)_k$ to the specified tolerance e. Then an upper bound on the number of multi-variable iterations required is clearly just "nM," since the convergence of simultaneous iterations on all "m" variables surely cannot be any worse than if iteration on each variable is performed separately.

APOLLO NOTE NO. 133

G. F. Floyd
5 November 1963

CLOCK ACCURACY

What is the expected error in the reading of a clock if it has been set at t = 0, allowed to run for (t_r) seconds and its reading at (t_r) corrected for its average error rate?

At time (t) let r (t) be the difference between the actual clock rate and its average error rate, so

$$E\,(r\,(t)) \;=\; 0 \tag{1}$$

We then set the clock at times (t_n) and run until ($t_n + t_r$), read the error, correct for the average rate and call the difference

$e\,(t_n + t_r)$. Thus,

$$e\,(t_n + t_r) = \int_{t_n}^{t_n+t_r} r\,(t)\,dt \;=\; \int_{o}^{t_r} r\,(t_n + \mu)\,d\mu \tag{2}$$

and by Equation (1)

$$E\,(e\,(t_n + t_r)) = \;0 \tag{3}$$

Now denote the variance of $e\,(t_n + t_r)$ by $\sigma_e^2\,(t_r)$ so from (2)

$$\left.\begin{aligned} \sigma_e^2\,(t_r) &= E\left(\int_o^{t_r} r\,(t_n + x)\,dx \int_o^{t_r} r\,(t_n + y)\,dy\right) \\ &= \int_o^{t_r} dx \int_o^{t_r} dy \quad E\Big(r(t_n + x)\; r\,(t_n + y)\Big) \\ &= \int_o^{t_r} dx \int_o^{t_r} dy \quad \phi_r\,(y-x) \end{aligned}\right\} \tag{4}$$

where

$$\phi_r\,(t) \;=\; \text{autocorrelation of } r\,(t) \tag{5}$$

Now letting:

$$y - x = \mu, \quad dy = d\mu \tag{6}$$

$$\sigma_e^2 (t_r) = \int_0^{t_r} dx \int_{-x}^{t_r - x} \phi_r (\mu)\, d\mu$$

$$= \int_0^{t_r} dx \left[\int_{-x}^{0} \phi_r (\mu)\, d\mu + \int_0^{t_r - x} \phi_r (\mu)\, d\mu \right]. \tag{7}$$

Since $\phi_r(t)$ is always an even function

$$\int_{-x}^{0} \phi_r (\mu)\, d\mu = \int_0^{x} \phi_r (\mu)\, d\mu \tag{8}$$

and letting $t_r - x = y$, $dx = -dy$, we have

$$\int_0^{t_r} dx \int_0^{t_r - x} \phi_r (\mu)\, d\mu = -\int_{t_r}^{0} dy \int_0^{y} \phi_r (\mu)\, d\mu = \int_0^{t_r} dy \int_0^{y} \phi_r (\mu)\, d\mu \tag{9}$$

Using Equations (8) and (9) in (7), we get,

$$\sigma_e^2 (t_r) = 2 \int_0^{t_r} dx \int_0^{x} \phi_r (\mu)\, d\mu \tag{10}$$

Now integrating (10) by parts with $dv = dx$ we have

$$\sigma_e^2 (t_r) = 2x \int_0^{x} \phi_r (\mu)\, d\mu \Big]_0^{t_r} - 2 \int_0^{t_r} x\ \phi_r (x)\, dx$$

$$= 2 t_r \int_0^{t_r} \phi_r (\mu)\, d\mu - 2 \int_0^{t_r} x\ \phi_r (x)\, dx \tag{11}$$

So $$\sigma_e^2(t_r) = 2\int_0^{t_r} (t_r - x)\,\phi_r(x)\,dx \tag{12}$$

and dividing by t_r,

$$\frac{\sigma_e^2(t_r)}{t_r} = 2\int_0^{t_r} \left(1 - \frac{\tau}{t_r}\right)\,\phi_r(\tau)\,d\tau \tag{13}$$

which relates the variance in the clock error to the running time and the basic random rate error r (t).

Now let t_r become large, so from Equation (13):

$$\lim_{t_r \to \infty}\left(\frac{\sigma_e^2(t_r)}{t_r}\right) = 2\int_0^{\infty} \phi_r(\tau)\,d\tau = \int_{-\infty}^{\infty} \phi_r(\tau)\,d\tau \tag{14}$$

Thus $\left(\frac{\sigma_e^2(t_r)}{t_r}\right)$ approaches a constant which is equal to the square root of the area under the autocorrelation function of the clock's random error rate (the zero frequency power density of the rate noise), and we will denote the square root of this number by (k) so

$$k = \sqrt{\int_{-\infty}^{\infty} \phi_r(\tau)\,d\tau} \tag{15}$$

and so has the units of sec.$^{1/2}$, and we have the simple result,

$$\lim_{t_r \to \infty}\left(\frac{\sigma_e}{\sqrt{t_r}}\right) = k \tag{16}$$

This result is, of course, nothing but the statement that in a random walk, the distance away from the mean increases as the square root of time which, of course, is easily seen for the case where the random process consists of selecting rate (r_n) every (t_c) seconds. Then the error at (t_r) is simply

$$e(t_r) = r_1 t_c + r_2 t_c + \ldots + r_n t_c; \quad n = \frac{t_r}{t_c} \tag{17}$$

Squaring Equation (17) and taking expected values we have for the simple discrete case,

$$\sigma_e^2 = E(r_1^2 t_c^2 + r_2^2 t_c^2 + \ldots + r_n^2 t_c^2 + \text{cross products})$$

$$= n \sigma_r^2 t_c^2 = \frac{t_r}{t_c} \sigma_r^2 t_c^2$$

or

$$\frac{\sigma_e}{\sqrt{t_r}} = \sigma_r \sqrt{t_c} = \text{constant}$$

The constant (k) of Equations (16) and (19) is the number which completely describes the so-called "long-term stability" of the clock, and allows calculation of the expected clock error over run times large compared with the correlation time of $\phi_r(\tau)$.

The behavior of $\sigma_e(t_r)$ at very short run times is also of interest (the so-called "short-term stability"). To calculate this we use (12) and let t_r be very small. Then since the upper limit of the integration is approaching zero, we expand $\phi_r(x)$ in a power series as

$$\phi_r(x) = \phi_r(o) + x^2 \ddot{\phi}_r(o) + \ldots \tag{20}$$

with no linear (x) term since $\phi_r(\tau)$ is even. Substituting (20) in

in (12) and integrating we get for short (t_r):

$$\sigma_e^2(t_r) = 2\int_0^{t_r}(t_r - x)\left(\phi_r(o) + x^2\,\ddot{\phi}_r(o) + \ldots\right)dx \tag{21}$$

$$= 2\left[\left(t_r^2 - \frac{1}{2}t_r^2\right)\phi_r(o) + \left(\frac{1}{3}t_r^4 - \frac{1}{4}t_r^4\right)\ddot{\phi}_r(o) + \ldots\right.$$

hence, since $\phi_r(o) = \sigma_r^2$,

$$\sigma_e^2(t_r) \to \sigma_r^2\, t_r^2 \tag{22}$$

In terms of the function $(\sigma_e/\sqrt{t_r})$ which becomes constant at large (t_r) we then have

$$\boxed{\frac{\sigma_c}{\sqrt{t_r}} \to \sigma_r\sqrt{t_r} \quad \text{as } t_r \to o.} \tag{23}$$

The forms of (23) and (16) then suggest that we plot the function $(\sigma_e/\sqrt{t_r})$ as ordinate with the variable $(\sqrt{t_r})$ as abscissa. Then at short run times the curve should go through the origin with straight line slope (the slope being (σ_r)) and at large values of $\sqrt{t_r}$ the function should approach the constant value (k).

To get an idea of the correlation time, we return to (12) and assume that,

$$\phi_r(x) = o \quad \text{for } x > t_c \tag{24}$$

and let (t_r) be greater than (t_c). For this case then,

$$\sigma_e^2 = 2\int_0^{t_c}(t_r - x)\,\phi_r(x)\,dx = 2\,t_r\int_0^{t_c}\phi_r(x)\,dx - 2\int_0^{t_c}x\,\phi_r(x)\,dx$$

$$= k^2 t_r - B. \qquad \text{with A, B = constant}$$

For this case,

$$\frac{\sigma_c}{\sqrt{t_r}} = \frac{\sqrt{k^2 t_r - B}}{\sqrt{t_r}} = k \sqrt{1 - \frac{B}{k^2 t_r}} \tag{26}$$

So calling $\sigma_c / \sqrt{t_r} = y$ and $\sqrt{t_r} = x$, the curve goes toward

$$y = k \sqrt{1 - \frac{B}{k^2 x^2}} \tag{27}$$

when t_r becomes greater than the correlation time of $\phi_r(\tau)$.

Thus the "knee" of the function $\sigma_c/\sqrt{t_r}$ versus $\sqrt{t_r}$ gives the correlation time of the error rate.

Also by differentiating (12) we have

$$\frac{d\,\sigma_e^2\,(t_r)}{dt_r} = 2 \int_0^{t_r} \phi_r\,(\tau)\, d\tau \tag{28}$$

Now $\phi_r\,(\tau)$ starts at a positive value (its maximum value also), and the area under the curve is the zero frequency power density and so is non-negative. Thus, the integral $\phi_r\,(\tau)$ is positive for almost all decent correlation functions. When this is true the $\sigma_e^2\,(t_r)$ is monotonic in t_r and so is $\sigma_e\,(t_r)$ and $\sigma_e/\sqrt{t_r}$ also. Thus we would expect the function $\sigma_e/\sqrt{t_r}$ plotted versus $\sqrt{t_r}$ to rise monotonically from zero to its final value (k).

Thus for a clock we would say that the number (k) essentially describes the clock accuracy for times longer than the correlation time of the rate error so that (k), together with an idea of the correlation time, are about all we really need to know and these numbers can be found by plotting $\sigma_e/\sqrt{t_r}$ versus $\sqrt{t_r}$.

APOLLO NOTE NO. 134

C. F. Black
5 November 1963

DOPPLER PROPAGATION ERRORS IN LUNAR NAVIGATION FROM THE EARTH

Introduction

Orbits and trajectories of the Command Module and Lunar Excursion Module in the vicinity of the Moon can be determined at the Earth's surface by measurement of the doppler shift in a signal transmitted from the Earth to the space vehicle and returned by means of a transponder to the Earth. This doppler shift information as a function of time can be fitted to the orbital equations determining the ephemeris to a high degree of accuracy. This technique proved highly successful in the Mariner II flight to Venus and should prove equally successful for the various Lunar missions. The frequency used in the Mariner flight was approximately 1 kmc and that proposed for the Lunar flights is approximately 2 kmc.

Errors are present in the doppler measurement giving an imperfect determination of the orbits and trajectories. These errors are due to a number of sources. First, there is an error in the velocity of light in a vacuum to about one part in 10^7. This can be considered as an unknown scale factor in the range. Second, there are errors in the atomic frequency standard and other instrumentation of a noise-like and bias-like nature. Finally, there is an error in the doppler shift induced during propagation of the signal from the Earth to the vehicle and back again, traversing the various media with different and changing dielectric constants.

These propagation media can be grouped as follows: the troposphere, the ionosphere, the magnetosphere, the exosphere, and the lunar atmosphere. This note will consider the propagation errors introduced by the first two media listed above, the troposphere and the ionosphere. This information was obtained primarily at the Bureau of Standards Laboratory at Boulder, Colorado. The information was obtained from R. S. Kirby, R. S. Lawrence, Moody Thompson, and Harris Janes. Error contributions due to the ions present between the ionosphere and Lunar surface will be considered in another note. In addition, a further note will discuss the errors in the atomic frequency standards.

Troposphere Effects

Many experiments have been conducted by the Bureau of Standards to measure the phase shift through the atmosphere over horizontal paths of many miles length. Since the phase shifts were measured between stationary points, any change in the phase shift can be considered as an error in the doppler rate which should be zero. Experimental data on the power spectrum of the range-rate errors are in very close agreement with theoretical calculations based on the assumption that the errors are induced by atmospheric turbulence. Both experiment and theory indicate that the mean square range-rate error per unit bandwidth should decrease with frequency approximately inversely as the two-thirds power of the frequency. Experiments further indicate that the large changes in the range-rate measurements are very closely correlated with changes in atmospheric

density and index of refraction. Extreme changes in the troposphere induced range-rate errors can then be corrected largely by monitoring index of refraction over the path of the line-of-sight from the Earth to the vehicle.

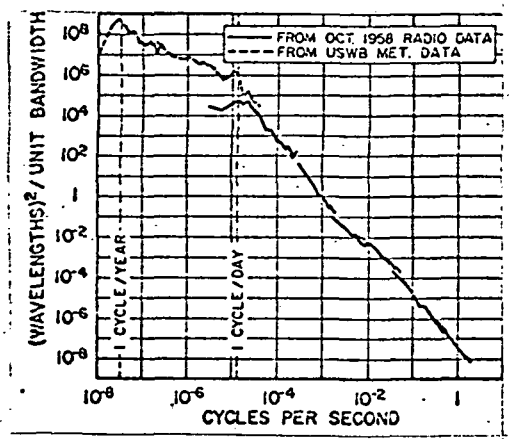

Figure 1.

Spectrum of Electrical Path Length Variations.

Green Mt. Mesa - Table Mesa Path

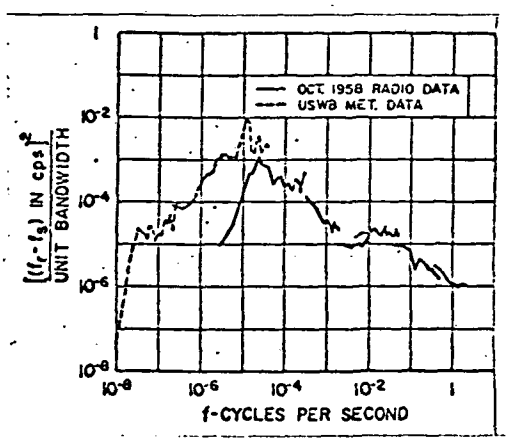

Figure 2.

Spectrum of Fluctuations in Received Signal
Frequency, $f_r - f_s$ = 9400 Mc, 15.2 -km Path, Boulder, Colo.

Experimental measurements made at Boulder [1/, 2/] over a nearly horizontal path at 5,700 feet altitude and 9.4 miles in length were used to determine the power spectrum showin in Figures 1 and 2.

The power spectrum fits very closely a straight line on a log-log scale for periods less than a day as would be expected from the theory. The spectrum for the mean square phase shift in wavelengths can be found to be

$$\phi(\lambda^2) = Af^{-2.6}$$

where

$A = 3 \times 10^{-8}$

f = in cycles per second

ϕ = in wavelengths squared per cycle per second

and the measurements were made at 9.4 kmc. This can be converted to a power spectrum for range-rate by multiplying by the square of frequency. Changing the units to radians per second, we have

$$\phi(\dot{r}^2) = 1.6 \times 10^{-8} \ \omega^{-.6} \ (\text{cm}^2/\text{sec}^2)\ (\text{radians/sec})^{-1}.$$

1/ Norton Barrows, Thompson, and Janes. IRE Transaction on Instrumentation, December 1962, p. 153.

2/ Thompson and Janes. Journal of Research of the National Bureau of Standards, Section D, Radio Propagation, Volume 63 D, July 1959, p. 45.

This value for the power spectrum was found to vary from day to day depending on the weather conditions. Although it is given as a typical value it can be a factor of 10 larger during stormy weather. The horizontal path is equivalent approximately to a 45^{o} path from sea level up through the atmosphere in terms of grams/cm^2 of atmosphere.

It can be seen that this power spectrum is a rather small quantity in terms of range-rate errors even at frequencies as low as 1 cycle/day. Calculations based on meteorological data indicate that the range-rate power spectrum decreases for longer periods than 1 day. It should be noted that the largest excursion ever observed in range over the 9.4 mile path length was a 56 cm excursion which occurred in approximately 30 minute time interval, yielding a range-rate of approximately 3/10 of a millimeter per second. This observation was made during the transition of a very strong cold front across the measuring site and was readily predictable from index of refraction measurements made at the site.

As indicated, the measurements were made at a specific frequency of 9.4 kmc,but it is found both theoretically and experimentally that the range shift in centimeters and range-rate shift in centimeters per second should be independent of carrier frequency to the first order. This data then is directly applicable to analysis of the doppler system at 2 kmc and 1 kmc. The errors measured represent a fractional range change over the path used of 3×10^{-5}. The measurements were made using an oscillator of stability of 1 part in 10^{8} so that these errors can be ascribed entirely to the tropospheric effects.

In extending this data to interpret the behavior of the atmosphere over a path which passes completely through the atmosphere two factors should be considered. It is expected that there will be less turbulence at high altitudes than was observed over the horizontal path used for the measurements. Therefore, the measured power spectrum can be considered as a conservative assumption in terms of error size. On the other hand, no determination of the effects of variations in the

height of the atmosphere are included in these measurements. A theoretical examination suggests that variations in the atmospheric height will partly compensate the variations observed at sea level since high atmosphere density at low altitude is probably accompanied by a lower height to the atmosphere tending to keep the total mass per square centimeter along the line-of-sight in a vertical direction relatively constant.

Ionospheric Effects

The nature of the ionosphere varies in three distinct ways. First of all there is a variation in the total ion content with time on a daily and seasonal basis. See Figure 3. There is also a change in the altitude distribution (Figure 4) of the ions with similar periods. This change in ion content can be expressed either as a change in the number of ions per cubic centimeter at various altitudes or as the number of ions per square centimeter looking out through the ionosphere over a fixed line-of-sight. It is found to be closely correlated with the temperature changes in the ionosphere induced by solar radiation. Therefore, one expects and it is actually observed that the ion content is greatest at noon and a minimum at midnight. On the other hand, the ion content is greater during the winter season and lesser during the summer season. This is probably due to the longer ionizing path of solar radiation in the ionosphere during the winter.

The diurnal variations in the ion density can be as large as a factor of 10 during the spring and winter months and as large as a factor of 3 or 4 during the summer months. Since there is a seasonal variation of the ion content one would also expect a latitude variation. This also is observed.

The second pronounced effect in the variation of the ion content of the ionosphere is a spatial variation. The total content is greatest along the magnetic equator and decreases somewhat as the magnetic poles are approached. A more interesting structural

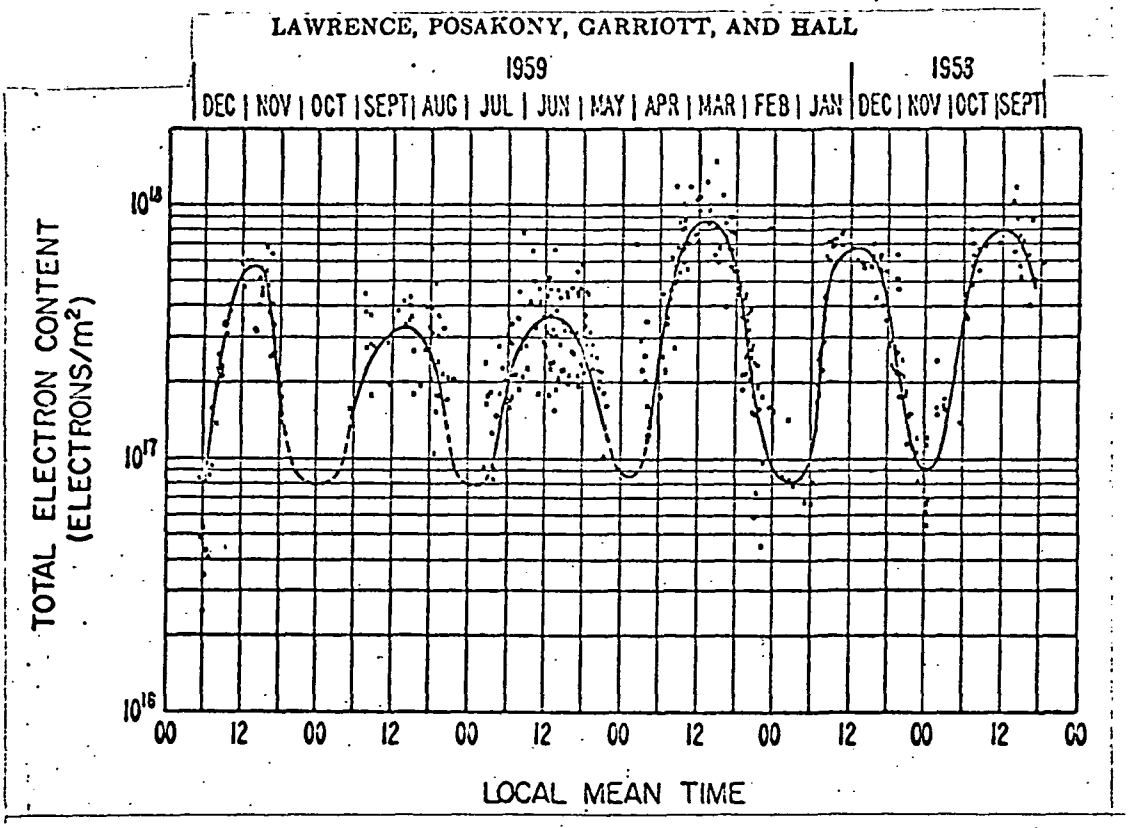
LAWRENCE, POSAKONY, GARRIOTT, AND HALL
1959
1958
DEC | NOV | OCT | SEPT | AUG | JUL | JUN | MAY | APR | MAR | FEB | JAN | DEC | NOV | OCT | SEPT
TOTAL ELECTRON CONTENT (ELECTRONS/m²)
10¹⁸
10¹⁷
10¹⁶
00 12 00 12 00 12 00 12 00 12 00 12 00
LOCAL MEAN TIME

Figure 3.

The total electron content of the ionosphere as deduced from Faraday rotation observations of 1958 δ_2. The circles represent observations at Stanford; the crosses are those at Boulder. Local time increases toward the right, going through six cycles in order to separate observations made in different seasons.

phenomenon is the fact that the ionosphere has ridges in it. It has been found from radio star and satellite measurements that there is a rib-like structure to the ionosphere producing variations in density along the magnetic equator with a wavelength of the order of 400 kilometers. These ridges are somewhat cigar-shaped with a width of 400 kilometers and a length oriented in a North-South direction of several thousand kilometers. These ridges and waves along the top of the ionosphere are not permanent in structure and will shift from day to day so that they cannot be predicted in advance. They result in a variation of the ion density expressed in ions/cm^2

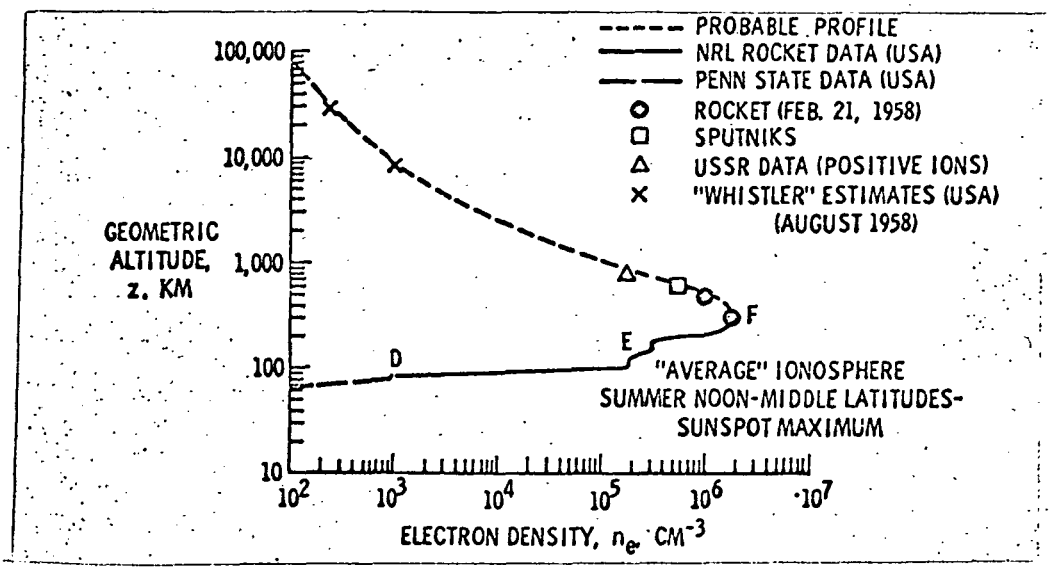
PROBABLE PROFILE
NRL ROCKET DATA (USA)
PENN STATE DATA (USA)
ROCKET (FEB. 21, 1958)
SPUTNIKS
USSR DATA (POSITIVE IONS)
"WHISTLER" ESTIMATES (USA)
(AUGUST 1958)
100,000
10,000
1,000
100
10
GEOMETRIC ALTITUDE, z, KM
D
E
F
"AVERAGE" IONOSPHERE
SUMMER NOON-MIDDLE LATITUDES-
SUNSPOT MAXIMUM
10^2
10^3
10^4
10^5
10^6
10^7
ELECTRON DENSITY, n_e, CM^{-3}

Figure 4.

along a path through the ionosphere of approximately 1% of the total ion content. See Figure 5. The height of these variations is such that if a line-of-sight from point on the Earth to a fixed star were established the rotation of the Earth would carry this line-of-sight through a 400 kilometer width of the ridge valley structure in approximately 20 minutes.

The third form of the change in the ionospheric structure is both a variation in time and in space. This comes about due to the presence of geomagnetic storms induced by solar flares and sun spots. These effects are difficult to predict in advance but are observed to be somewhat correlated with sunspot activity. The fluctuations are found to take place over periods of the order of a few days and are of a magnitude such that the total ion content of the ionosphere is changed by a factor of the order of 50%. Most of the time the concentration of the ions in the ionosphere is decreased by the magnetic storms, but this is not always true. In addition to reducing the total electron content of the ionosphere, the maximum electron density is depressed and the scale height of the altitude distribution of the density is increased.

Effect of the Ionosphere on Doppler Measurements

Whereas the troposphere reduces the phase velocity of a wave passing through it, the ionosphere increases this phase velocity to a value greater than the velocity of light. This increase in phase velocity is directly proportional to the density of electrons in the medium and inversely proportional to the square of the frequency. Therefore, the power spectrum of errors introduced by the ionosphere and other ionized media must be specified at a particular frequency. Its value can be corrected, therefore, to other frequencies by multiplication of a suitable factor. The density of ions in the ionosphere is found to vary [3/] between 10^{13} electrons per square centimeter and 10^{14}

3/ Lawrence, Posakony, Garriott, and Hall, Journal Geophysical Research, Vol. 68, No. 7, p. 1889 (April 1963).

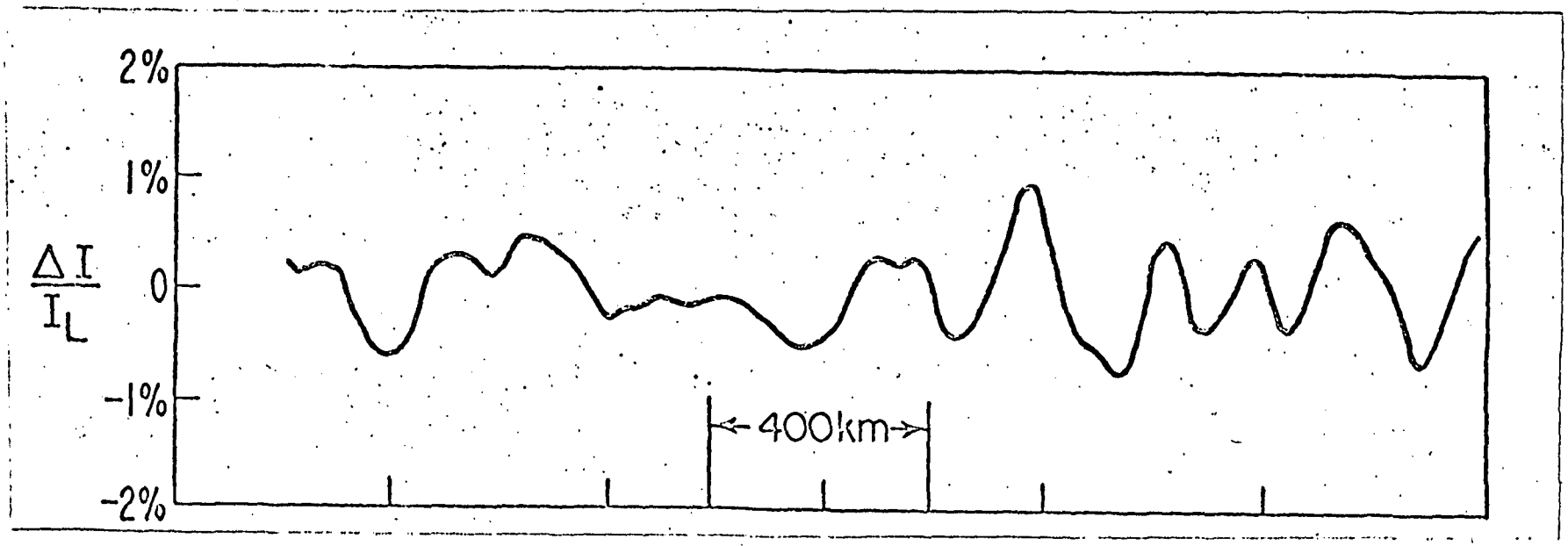

Figure 5.

Irregularities in ionospheric electron content 0834 MST, September 4, 1958.

$\frac{\Delta I}{I_L}$ is the percentage variation of the integrated electron content, $\int N \, dh$, relative to its smooth, slowly-changing value.

electrons per square centimeter along a vertical ray through the ionosphere. It can be shown that this* induces a range shift in a microwave signal at 1 kmc of 400 cm to 4000 cm. In addition to the variation described which occurs from midnight to noon, there are additional variations which can take place as a function of latitude and season. These additional variations are of the order of factors of 3.

The horizontal gradient effect provides a 1% change in the range shift at any one time over a 20 minute period.**

Interpreting both of these effects in terms of a range-rate error one finds that the maximum range-rate error with a 24 hour period due to the diurnal variations of the ionosphere is approximately 3/10 of a centimeter per second whereas the range-rate error due to the line-of-sight passing through the horizontal gradients with the Earth's rotation has a period of 20 minutes and a maximum value in the region of 2/10 of a centimeter per second, slightly less than the diurnal variations. Whereas the diurnal variation is very well defined in frequency, the horizontal gradients are not so nearly periodic and a spectrum of range-rate errors will exist with the peak of the spectrum occurring at the 20 minute period.

An additional effect of the ionosphere on doppler measurements is that caused by scintillation of the signal. This is an amplitude effect due to the diffraction of the signal by the ionosphere's non-uniform structure. These scintillations are not expected to be important, however, at large frequencies since the doppler measurements are made not on the amplitude of the signal but by amplifying the signal sufficiently that the amplitude variations can be removed.

The effect of geomagnetic storms should not be important

---

* A range shift will also occur due to the increased path length through the ionosphere due to refraction. Experiment and calculation indicate this is small compared to the effect considered.

** This is for a line-of-sight which is stationary. If a vehicle is being tracked near the Earth the period will be shorter (in most cases) and the range-rate errors will be larger.

compared to the diurnal ionospheric effects because of their long period in comparison with the size of the change in ion density. The predicted ionospheric errors in the doppler signal indicates a doppler shift of the order of 1 part in 10^{11} for a 1 kmc signal. This would be a factor of four smaller for a 2 kmc beacon in the Lunar program. The observed doppler data for the Mariner II flight to Venus indicates a residual with approximately a 20 second period at a value of 2 or 3 parts in 10^{11}. Since there is no discernible diurnal variation on this signal, however, it is unlikely that it is due to ionospheric effects.

Conclusions

Both the ionospheric effects and tropospheric effects appear to introduce errors small compared to those actually observed for the Mariner II flight. The ionospheric effects would be smaller still for the Lunar flight which operates at a higher microwave frequency. Although the errors do appear to be small compared to the errors introduced by the atomic frequency standard they may be significant in evaluating how much effort should be put into improving the atomic frequency standard beyond its present capability. There is no point in improving its accuracy much beyond the limitation imposed by the propagation errors. For smoothing times of 2 minutes or longer the uncorrectable propagation errors will be of the order of 3 parts in 10^{12} with a 2 kmc transponder.

APOLLO NOTE NO. 135

H. Dale
4 November 1963

COMPUTER RESULTS FOR LUNAR ASCENT USING RANGE AND RANGE RATE DATA FROM 1, 2, AND 3 STATIONS

This note presents computer results of Lunar ascent tracking (see Figures 1 through 18). Three stations were used in the following combinations: Madrid only; Madrid and Ascension; Madrid, Ascension, and Carnarvon. Two types of data were taken from each station: Range (with σ_R = 15 and 1.5 meters) and Range-Rate (with $\sigma_{\dot{R}}$ = .03 and .0015 meters/sec). Bias errors were not included because of conclusions reached in Apollo Note No. 128, i.e. that bias effects may be estimated given that the bias free estimates are known.

The parameters used for the Madrid station were (using notation) similar to Apollo Notes 82, 99, and 128):

A_1	=	.17525 + 07	meters
A_4	=	.0	meters/sec
A_5	=	.170172 + 04	meters/sec
GAM IND	=	1.	
BETA	=	.18308 + 02	deg.
XI	=	0	deg.
ETA	=	.180 + 3	deg.
ZETA	=	.180 + 3	deg.
LAMBDA	=	.404 + 2	deg.
ALPHA	=	-.370 + 01	deg.
OMEGA E	=	.729116 - 04	rad/sec
OMEGA M	=	.4236 - 06	rad/sec
RHO E	=	.63781 + 07	meters
RHO M	=	.385 + 09	meters
MU M	=	.4896 + 13	$meters^3/sec^2$
T(initial)	=	0	min.
T(interval)	=	1	min.

T(rendezvous)=		58.05	min.
BIG L	=	.40 + 1	deg.
SMALL L	=	.60 + 2	deg.
For Ascension:			
LAMBDA	=	-.79 + 01	deg.
ALPHA	=	.143 + 02	deg.
For Carnarvon:			
LAMBDA	=	-.2487 + 2	deg.
ALPHA	=	.1137 + 3	deg.

Two assumed a priori covariance matrices were used. The first, denoted by A_1 in the figures, assumed a 1000 meter error for each position and a $\sqrt{10}$ meter per second error for each velocity. The second a priori matrix, denoted by A_2 assumed a 1 meter per second error in each velocity; the assumed error in position remained unchanged from A_1.

Computations including the effect of range biases were not performed since from Apollo Note No. 128 the general effect can be rather well predicted.

One of the conclusions that can be drawn from this analysis is the small effect of a priori data for tracking times longer than about 10 minutes and for the assumed values of σ_R and $\sigma_{\dot{R}}$.

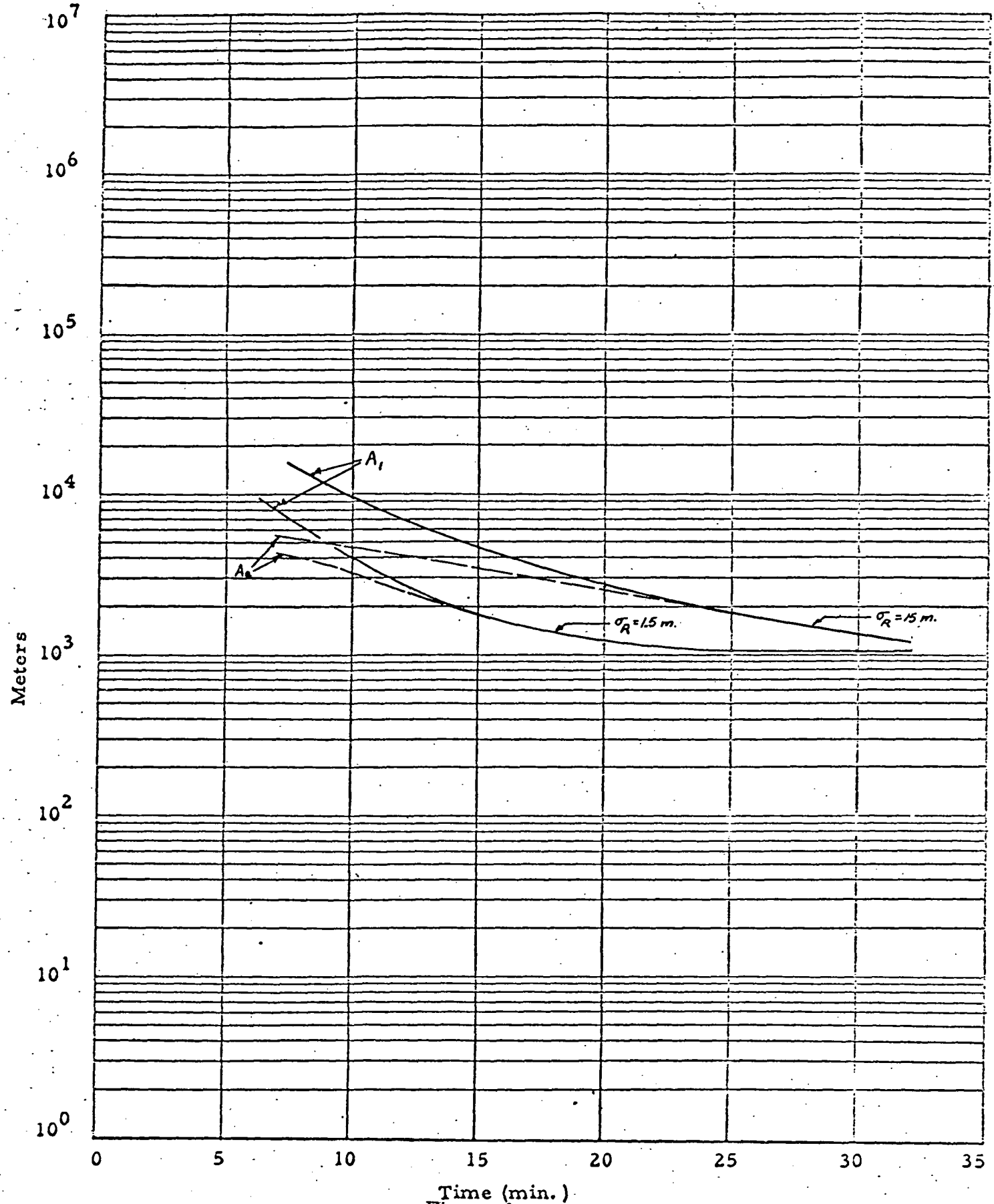

Figure 1

Minimum Miss, Madrid Only
Range Data without Bias

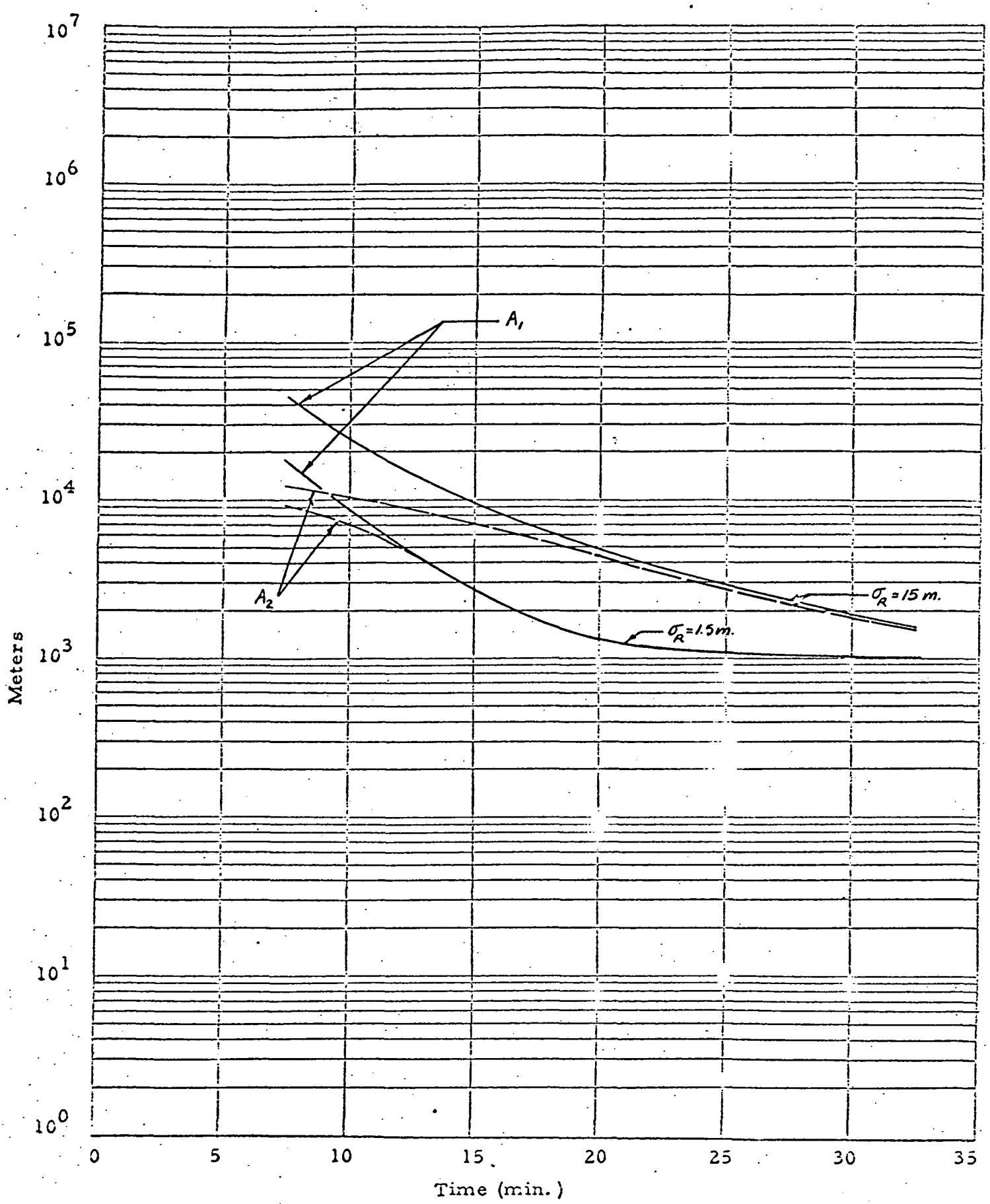

Figure 2

Rendezvous Miss, Madrid Only
Range Data without Bias

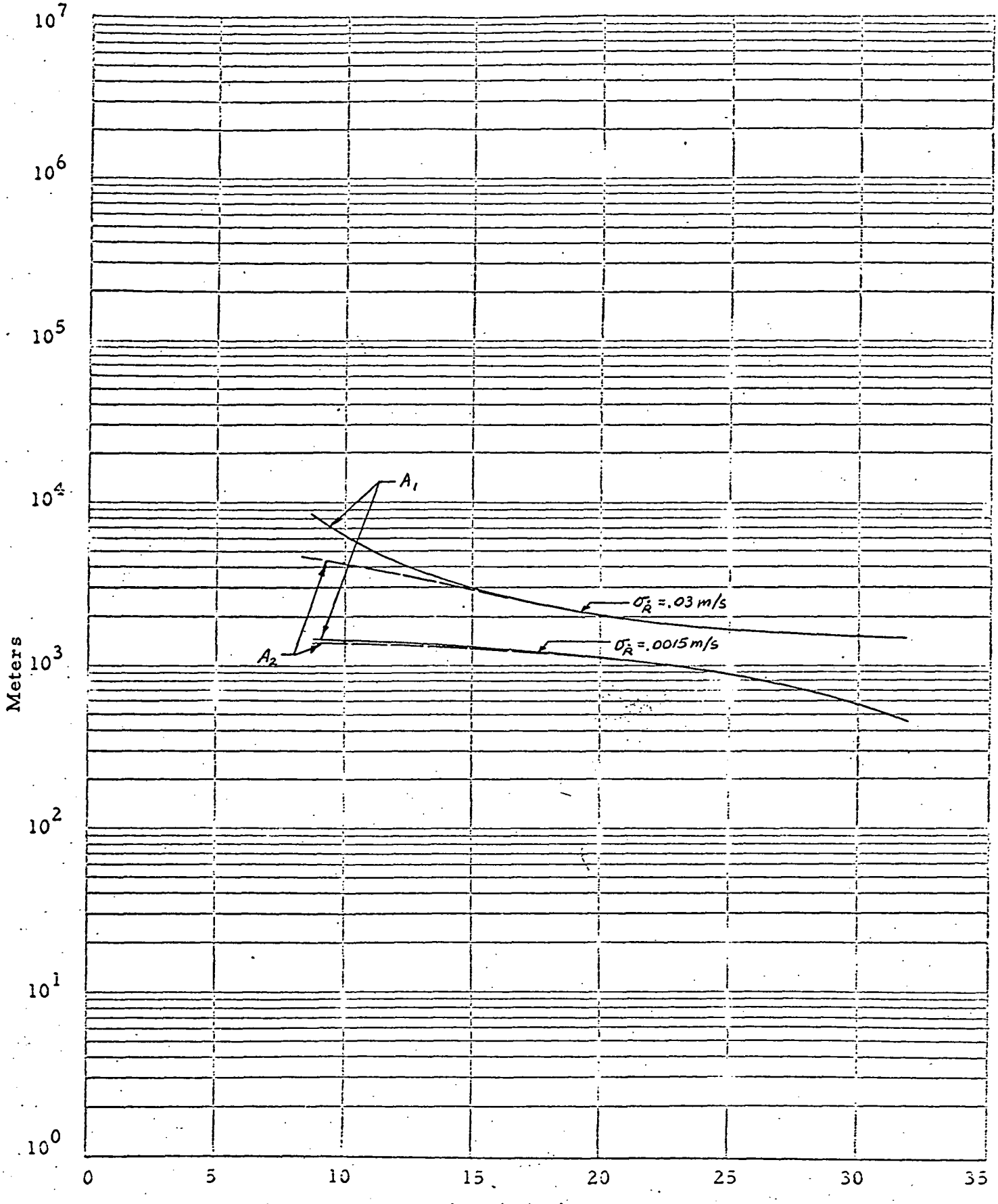

Figure 3

Minimum Miss, Madrid Only
Range-Rate Data

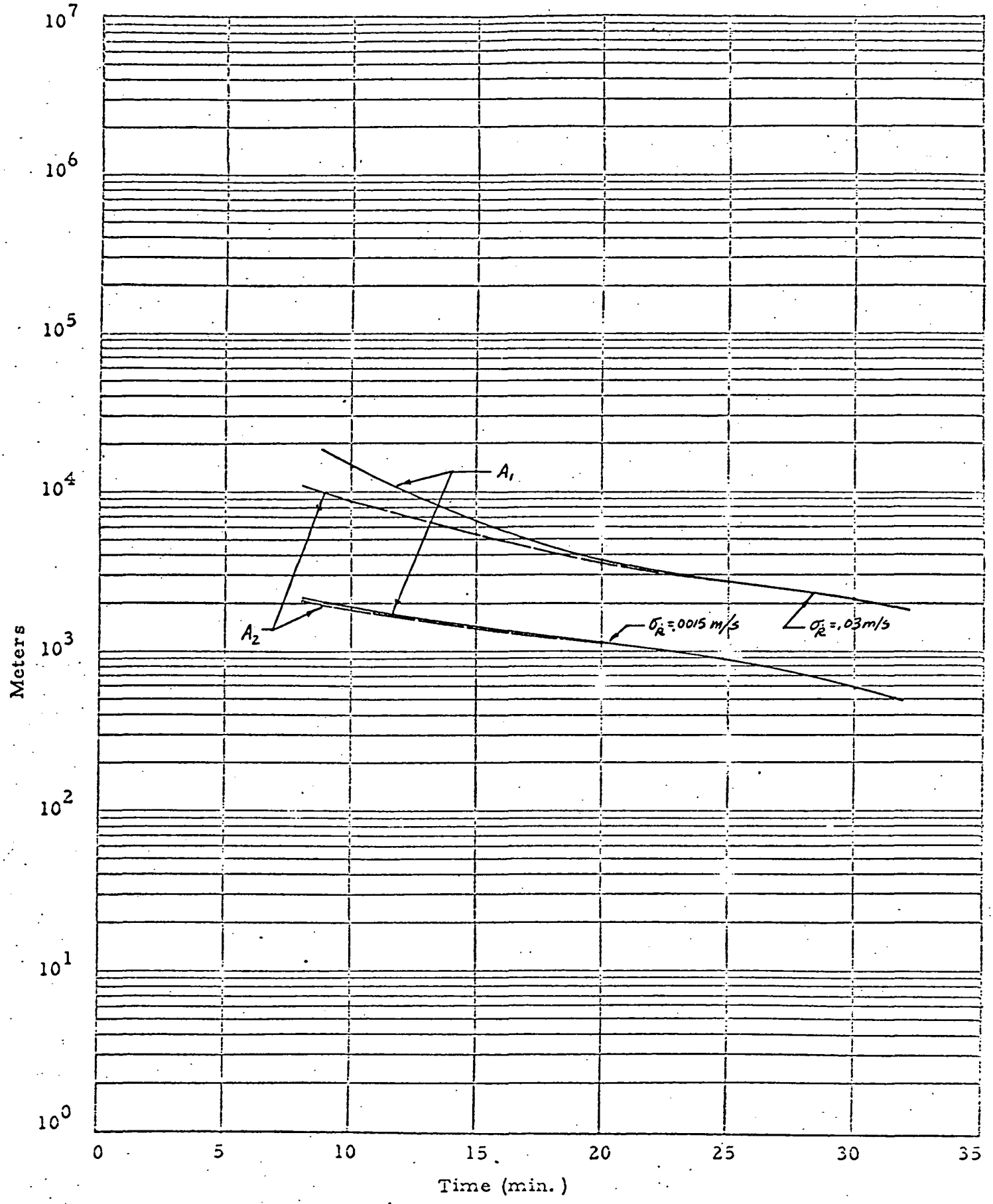

Figure 4

Rendezvous Miss, Madrid Only
Range-Rate Data

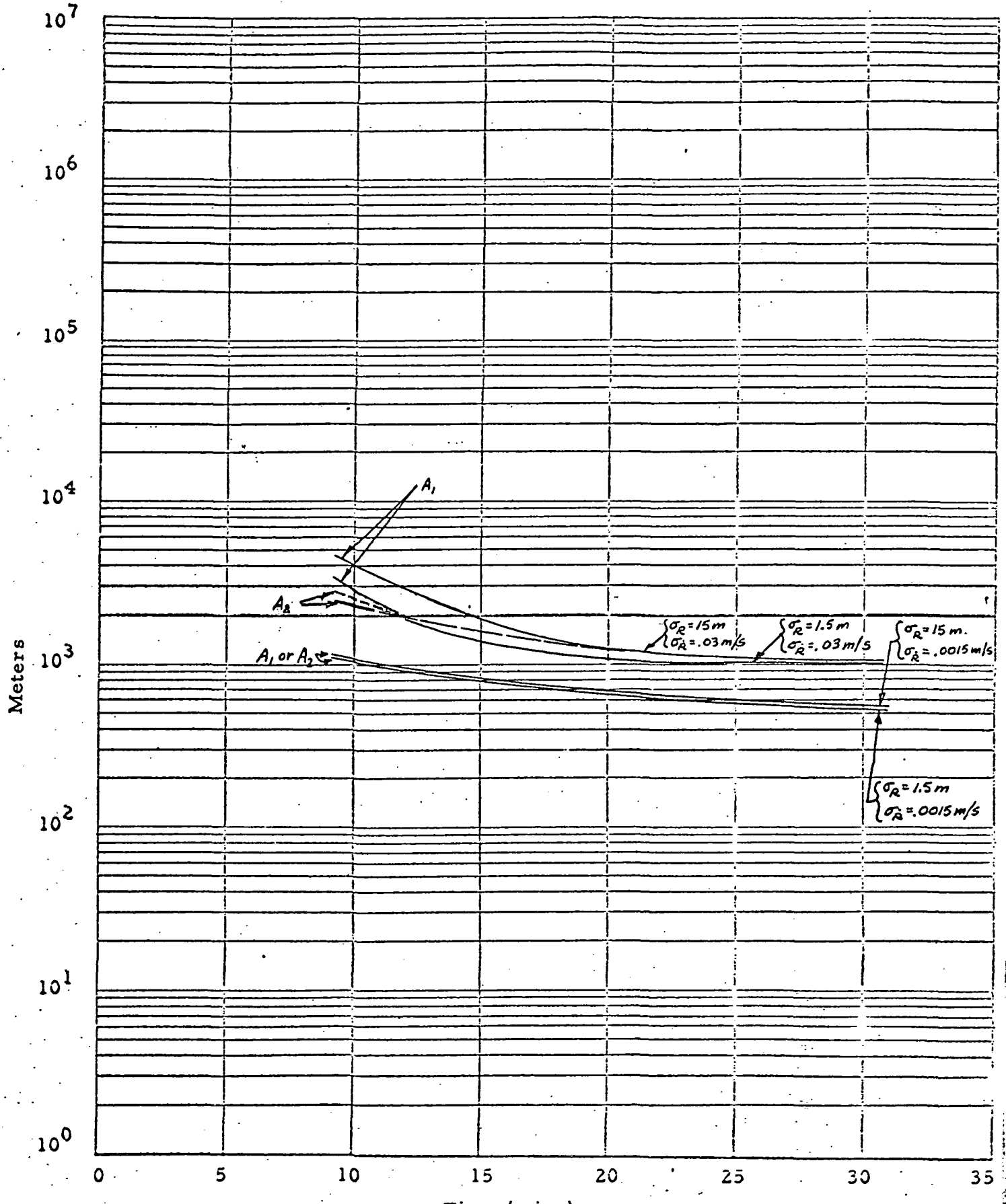

Figure 5

Minimum Miss, Madrid Only
Range and Range-Rate without Bias

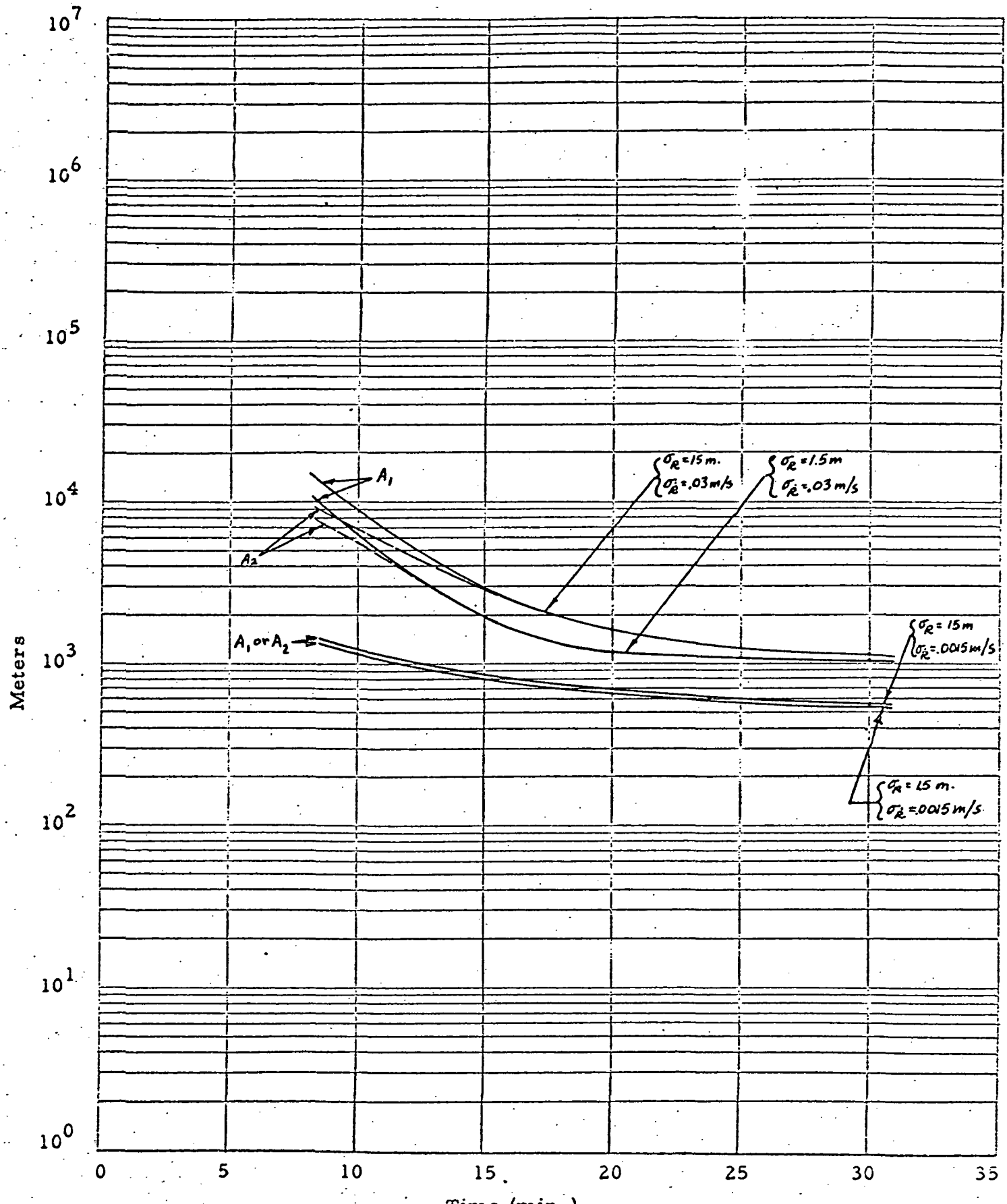

Figure 6

Rendezvous Miss, Madrid Only
Range and Range-Rate without Bias

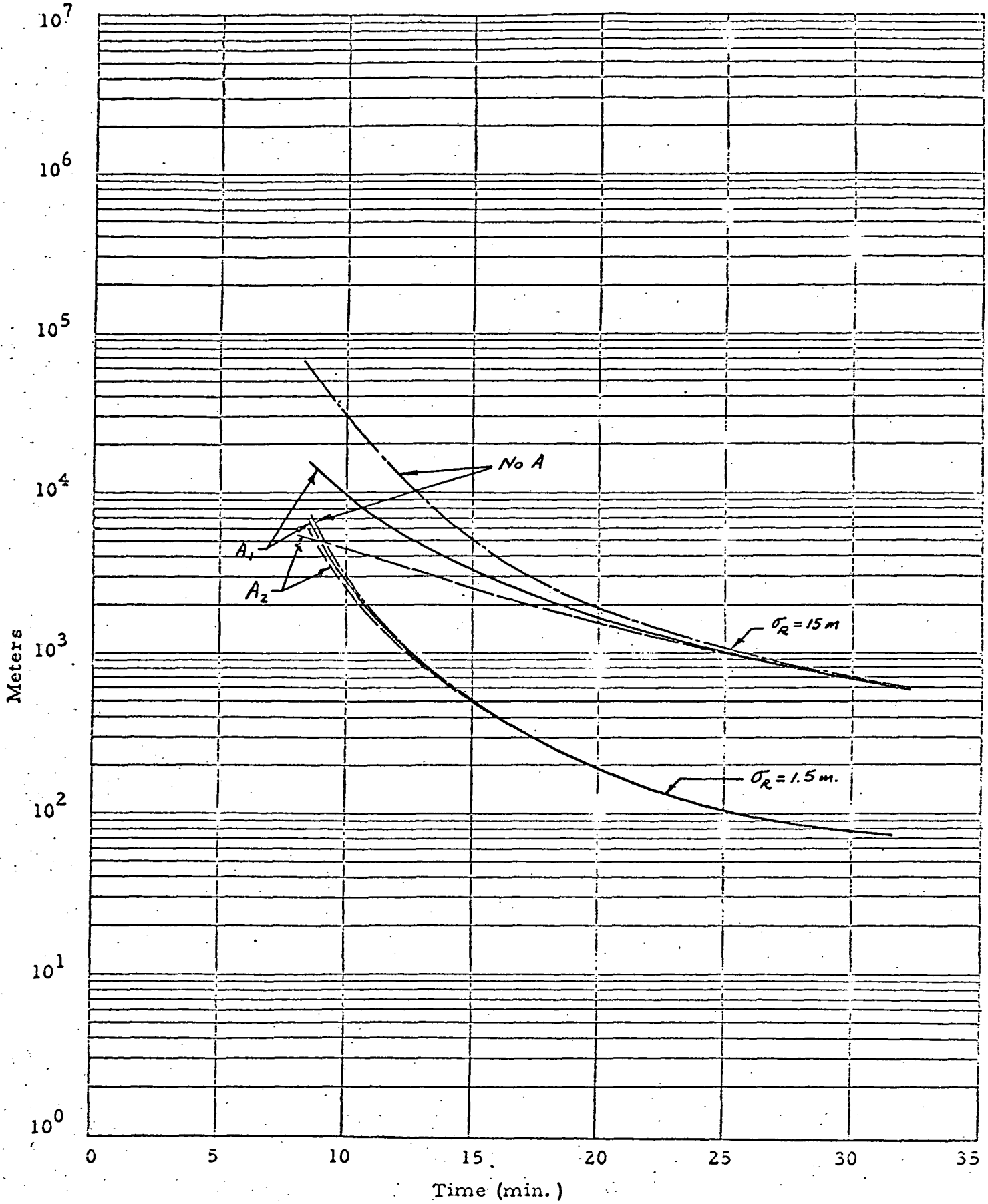

Figure 7

Minimum Miss, Madrid and Ascension

Range Data without Bias

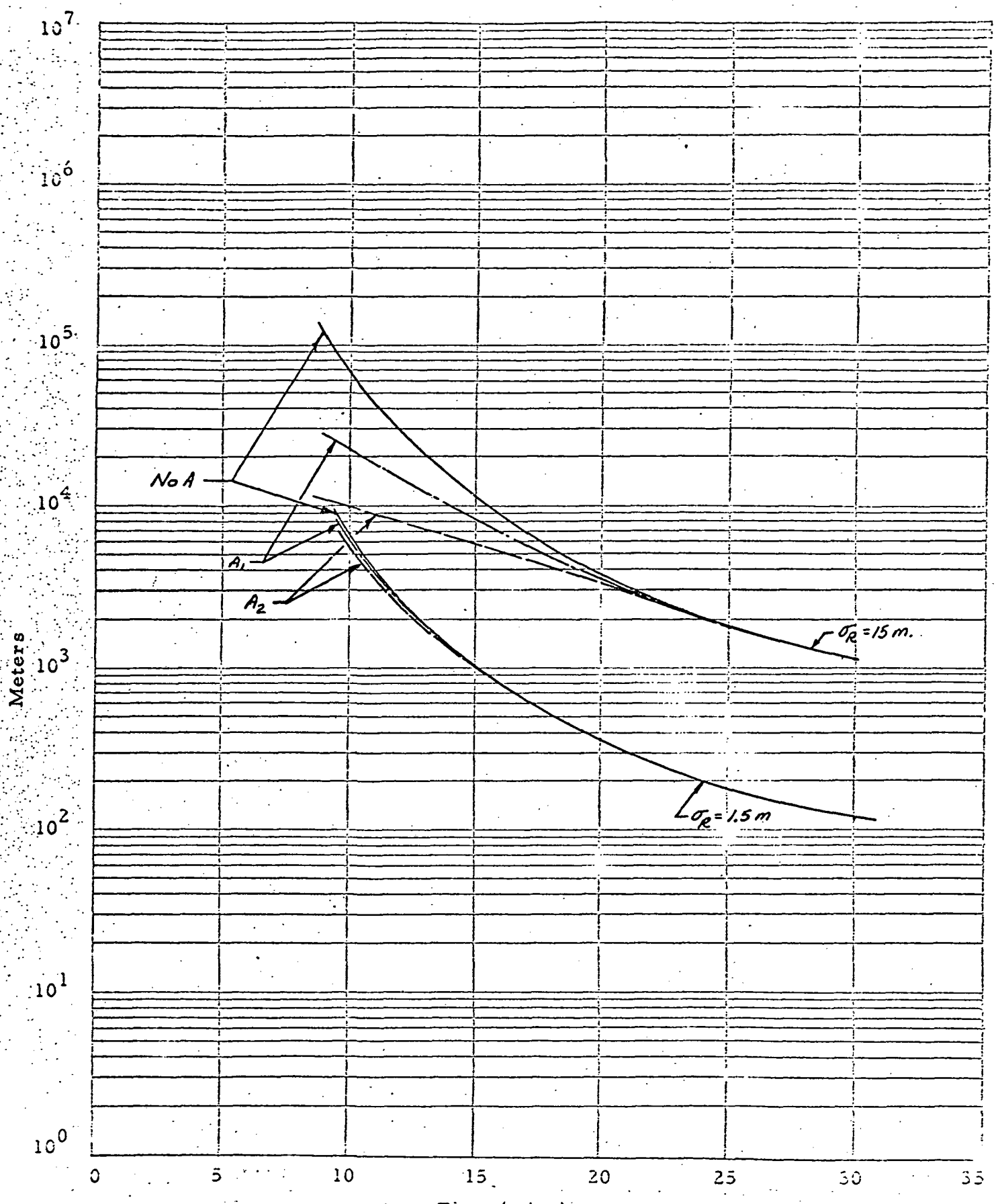

Figure 8

Rendezvous Miss, Madrid and Ascension
Range Data without Bias

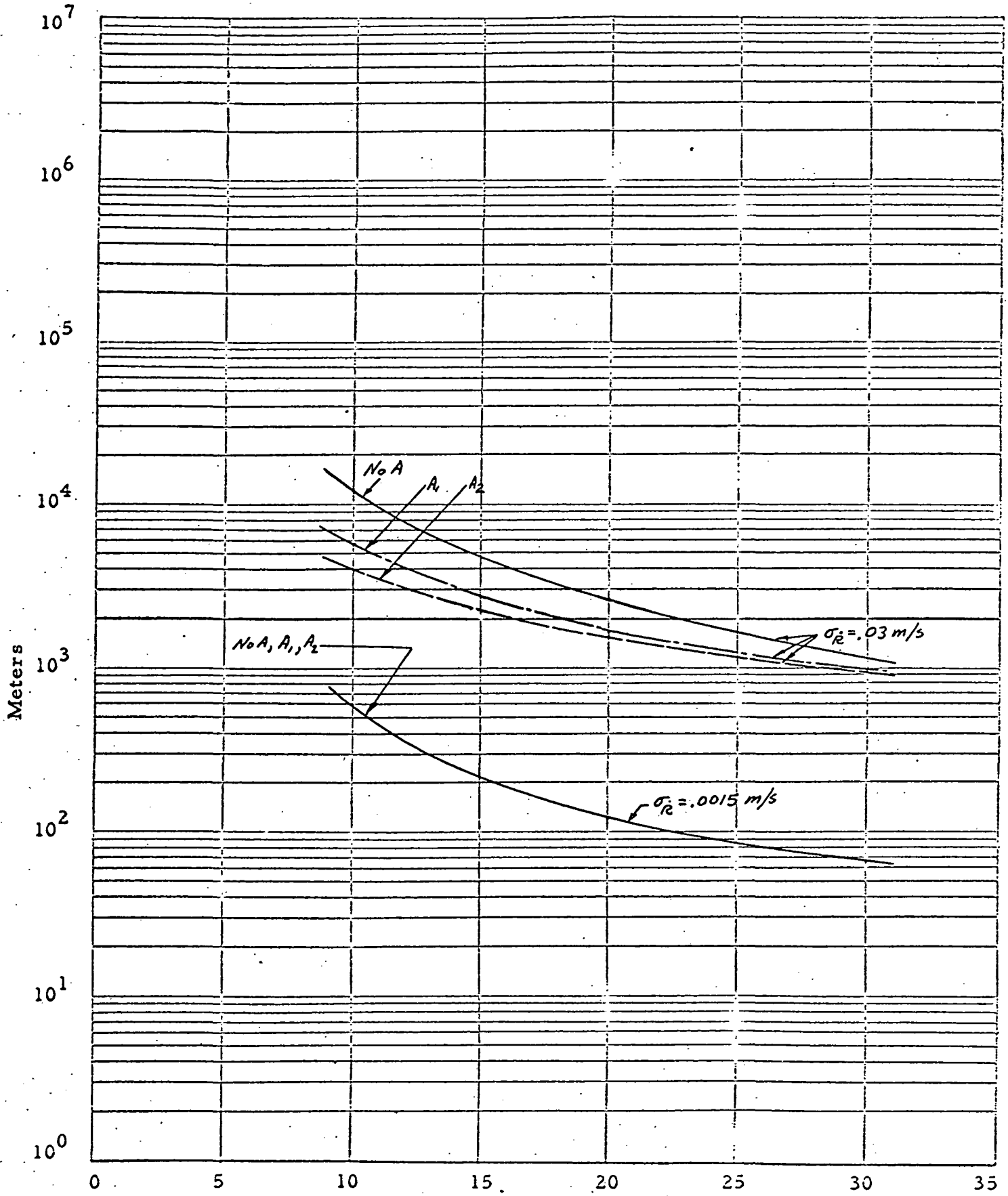

Figure 9

Minimum Miss, Madrid and Ascension Range-Rate Data

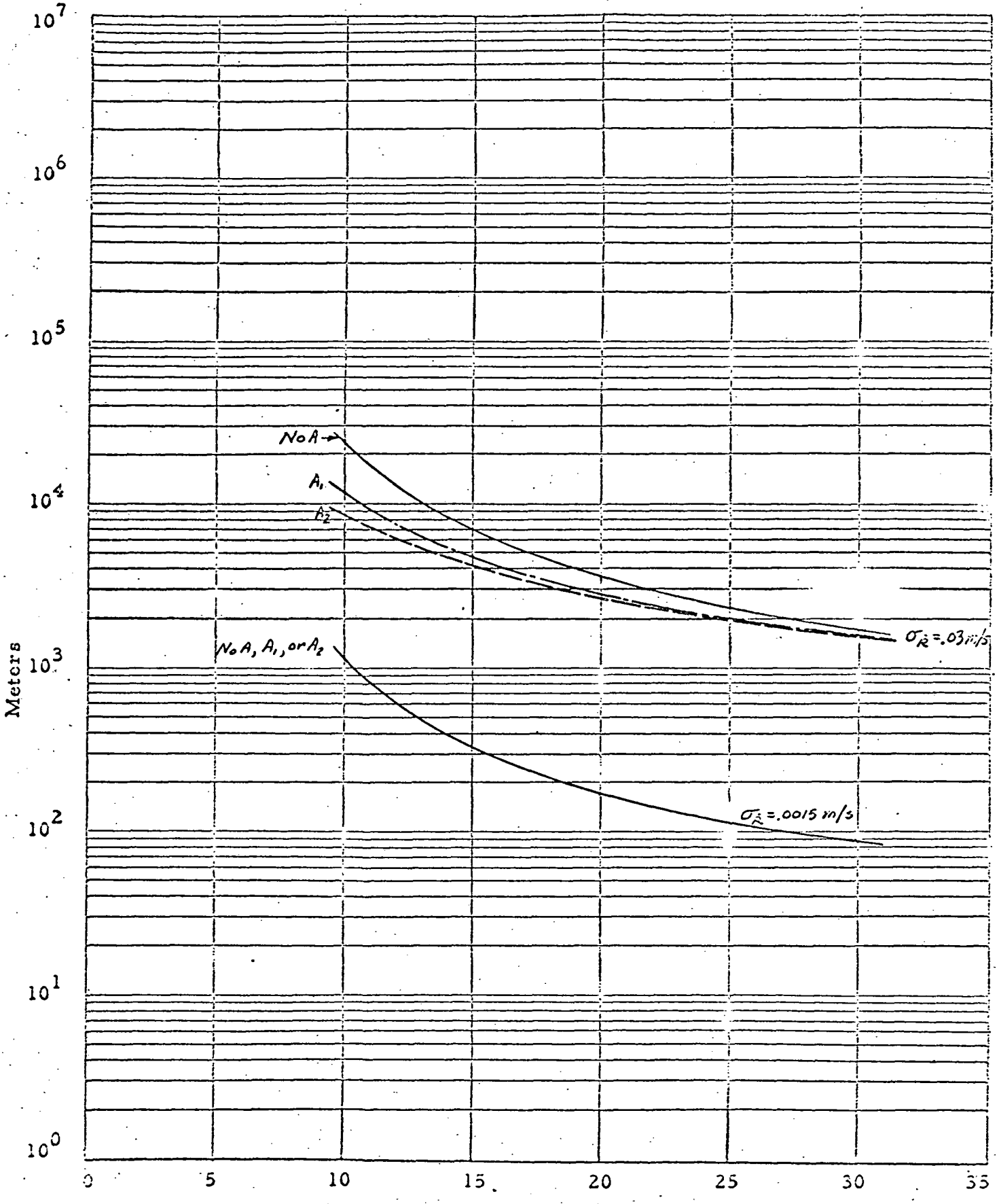

Figure 10

Rendezvous Miss, Madrid and Ascension Range-Rate Data

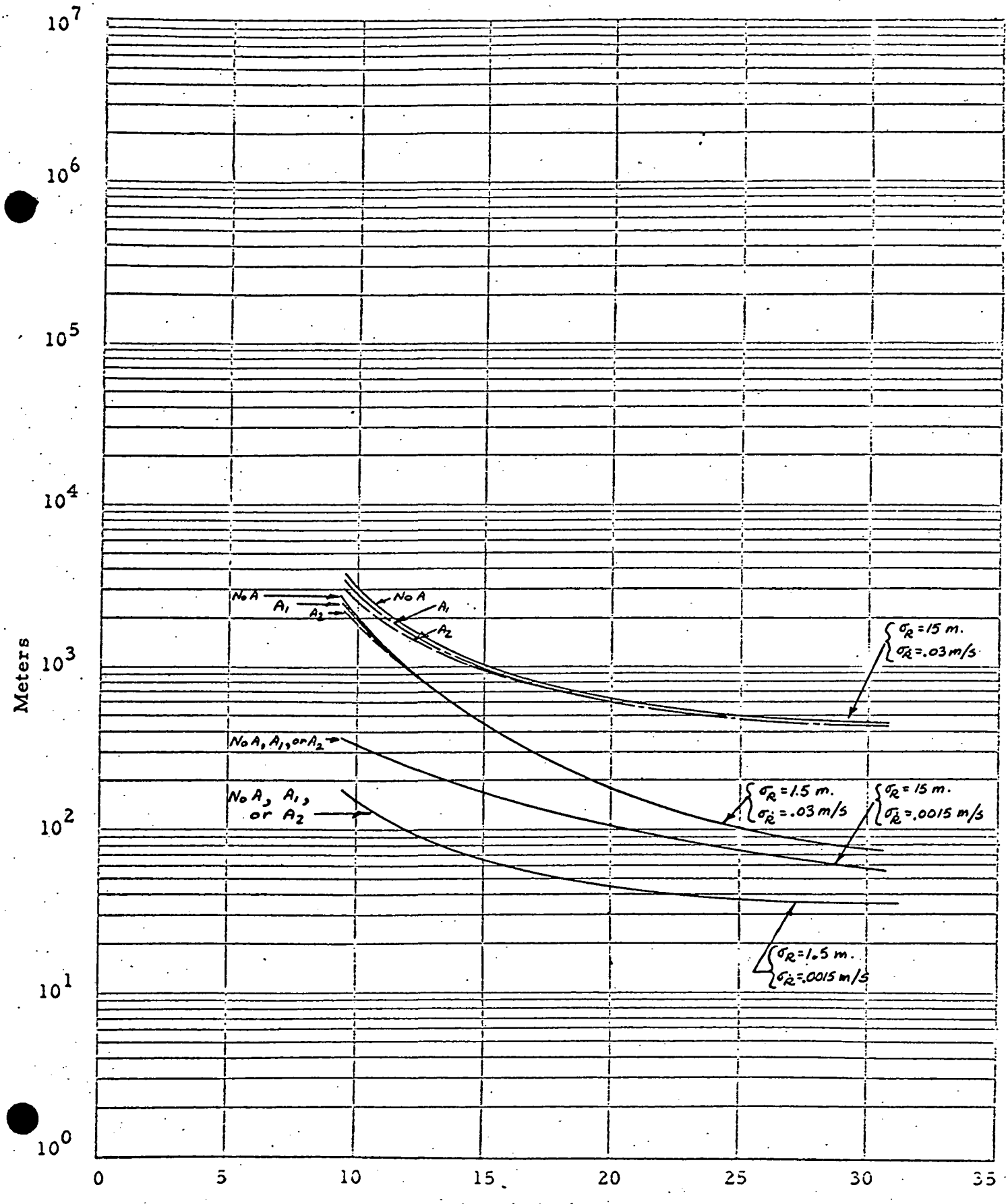

Figure 11

Minimum Miss, Madrid and Ascension
Range and Range-Rate without Bias

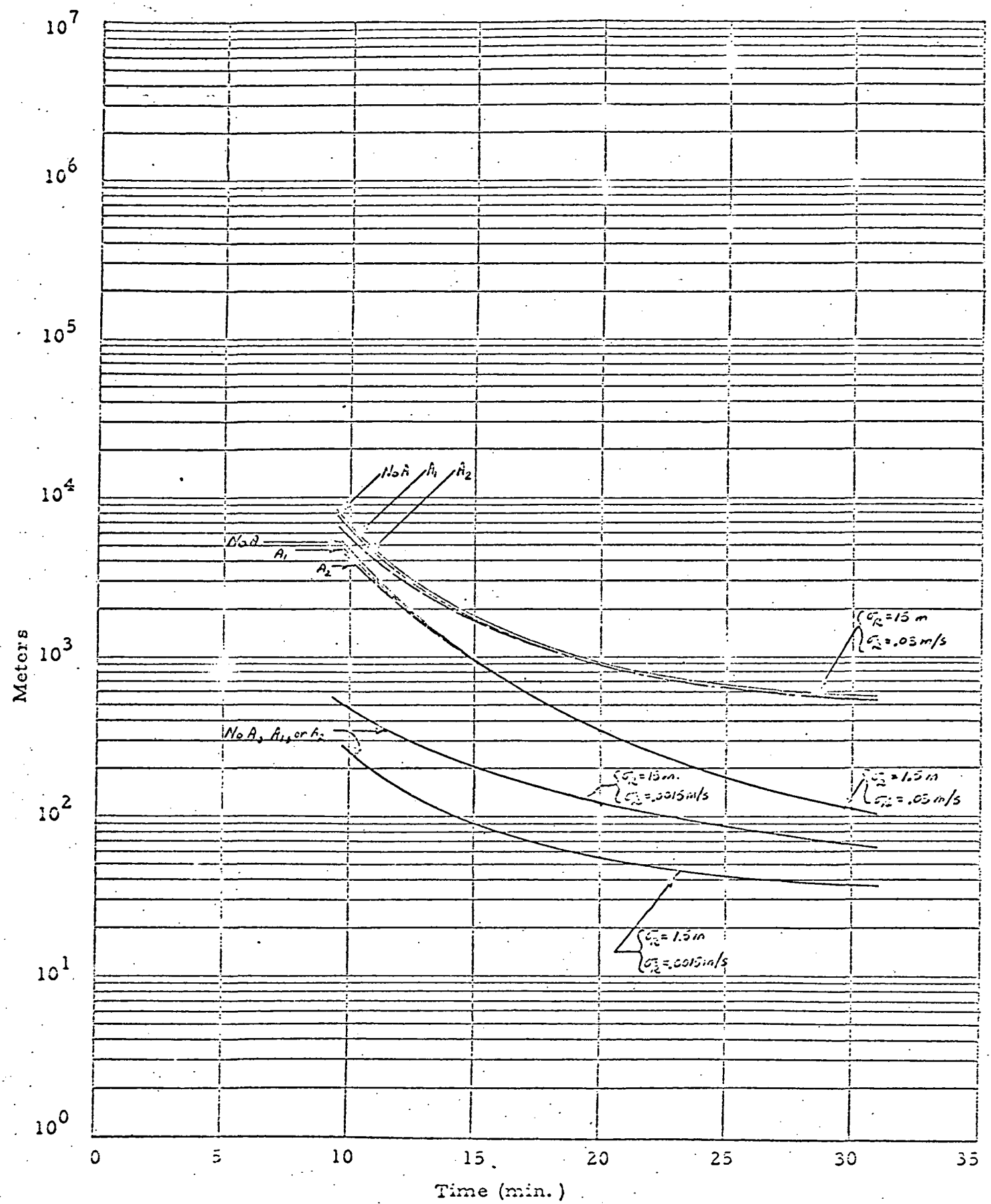

Figure 12

Rendezvous Miss, Madrid and Ascension
Range and Range-Rate without Bias

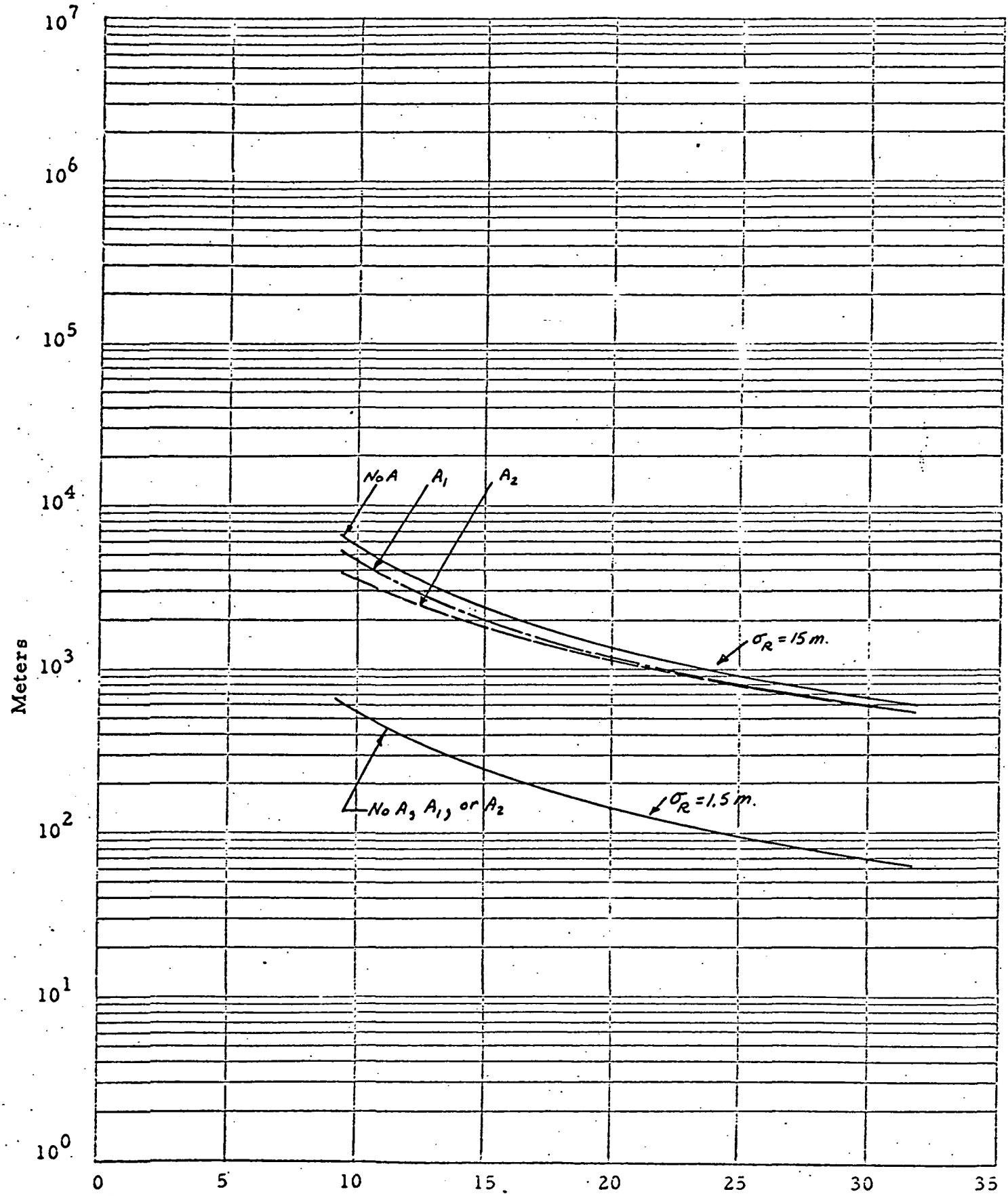

Figure 13

Minimum Miss, Madrid and Ascension and Carnarvon Range Data without Bias

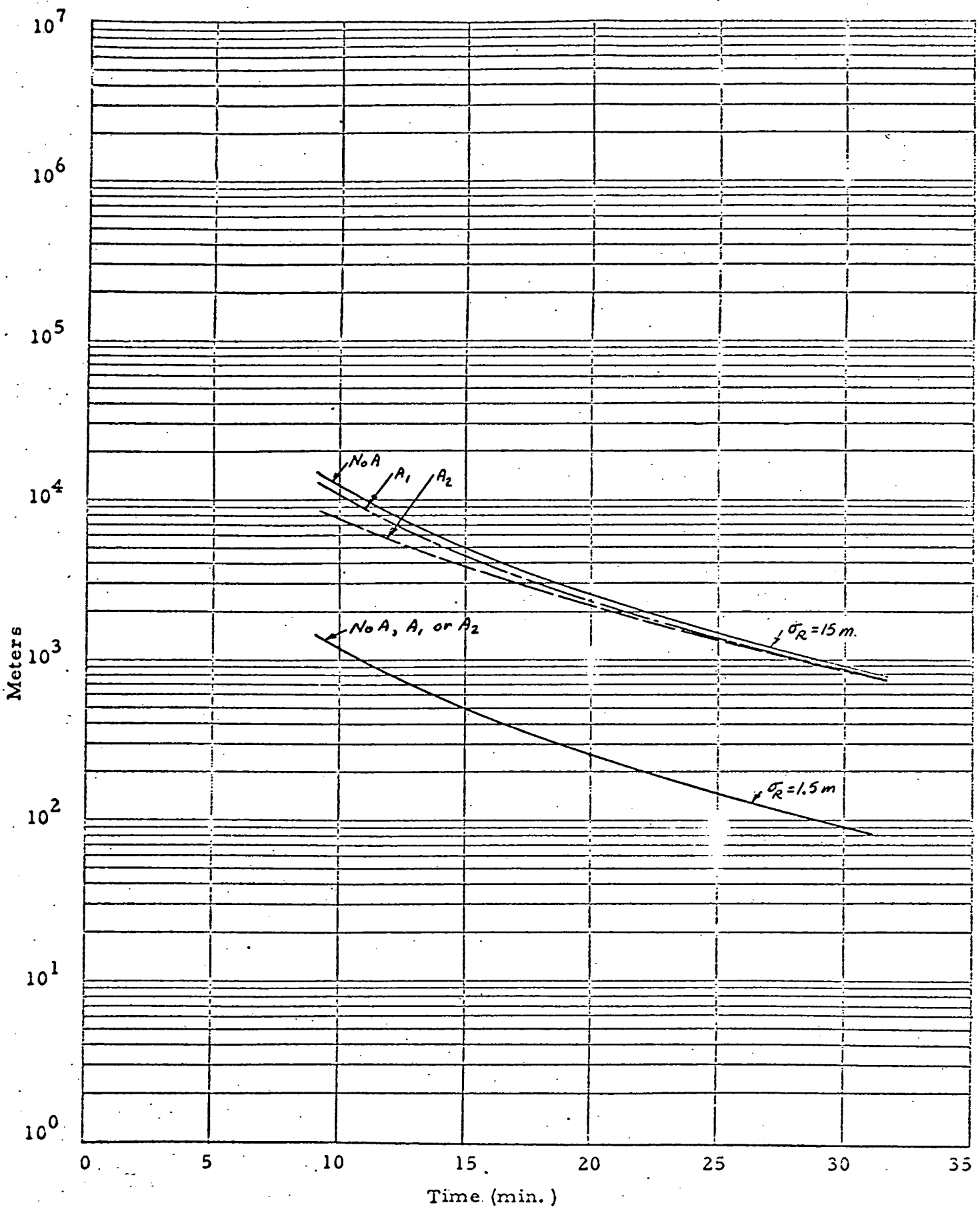

Figure 14

Rendezvous Miss, Madrid and Ascension and Carnarvon Range Data without Bias

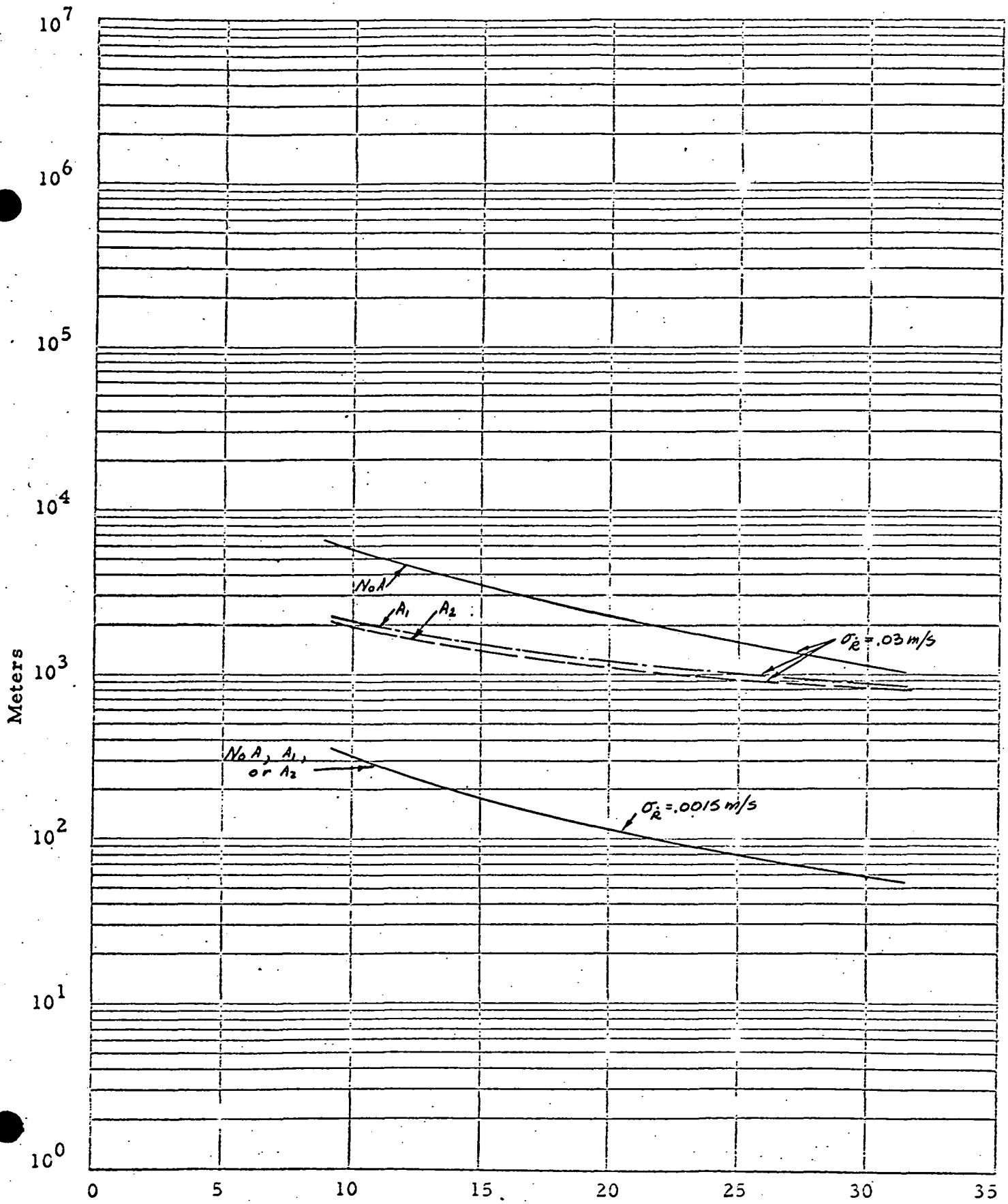

Figure 15
Minimum Miss, Madrid and Ascension and Carnarvon Range-Rate Data

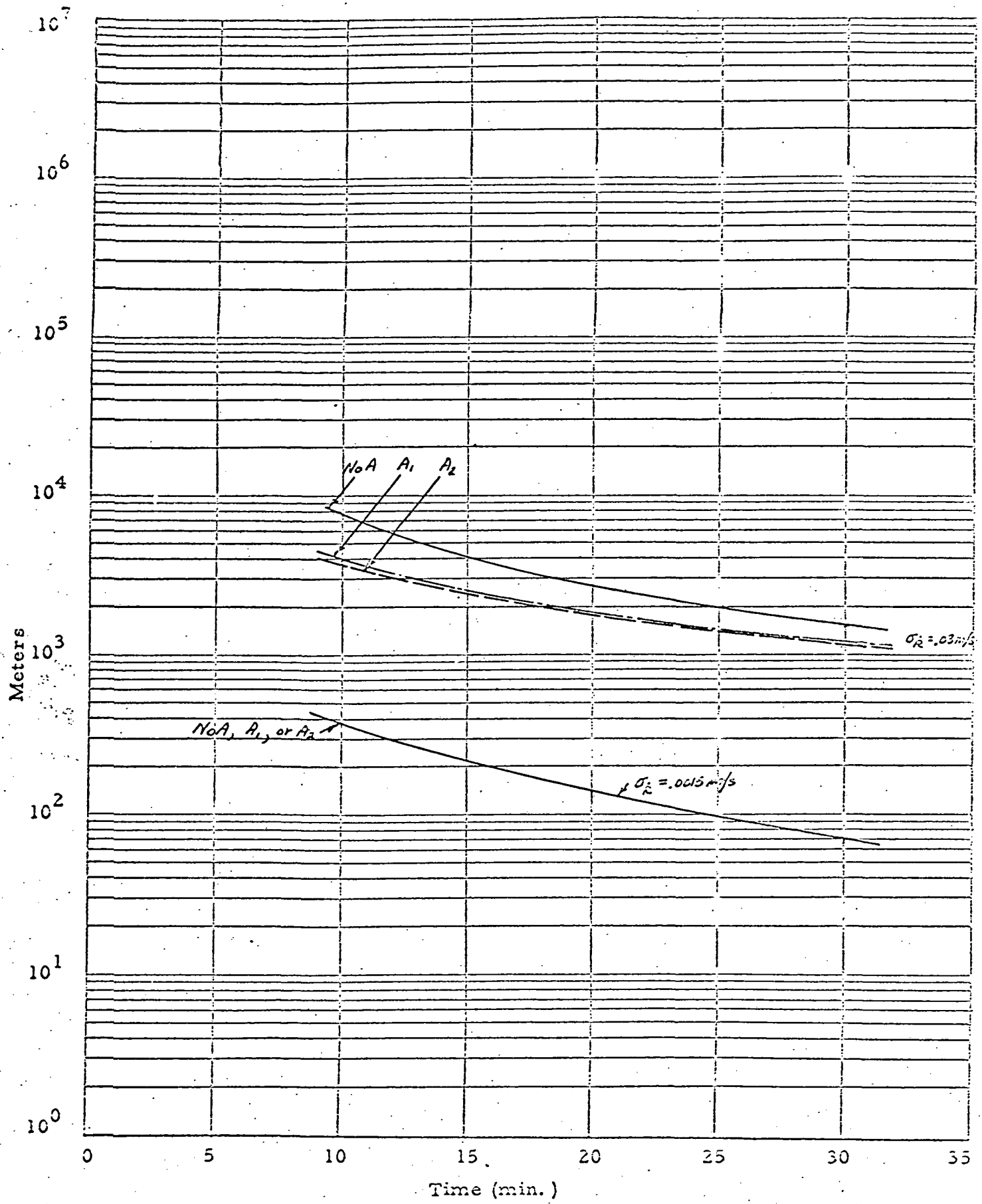

Figure 16

Rendezvous Miss, Madrid and Ascension and Carnarvon
Range-Rate Data

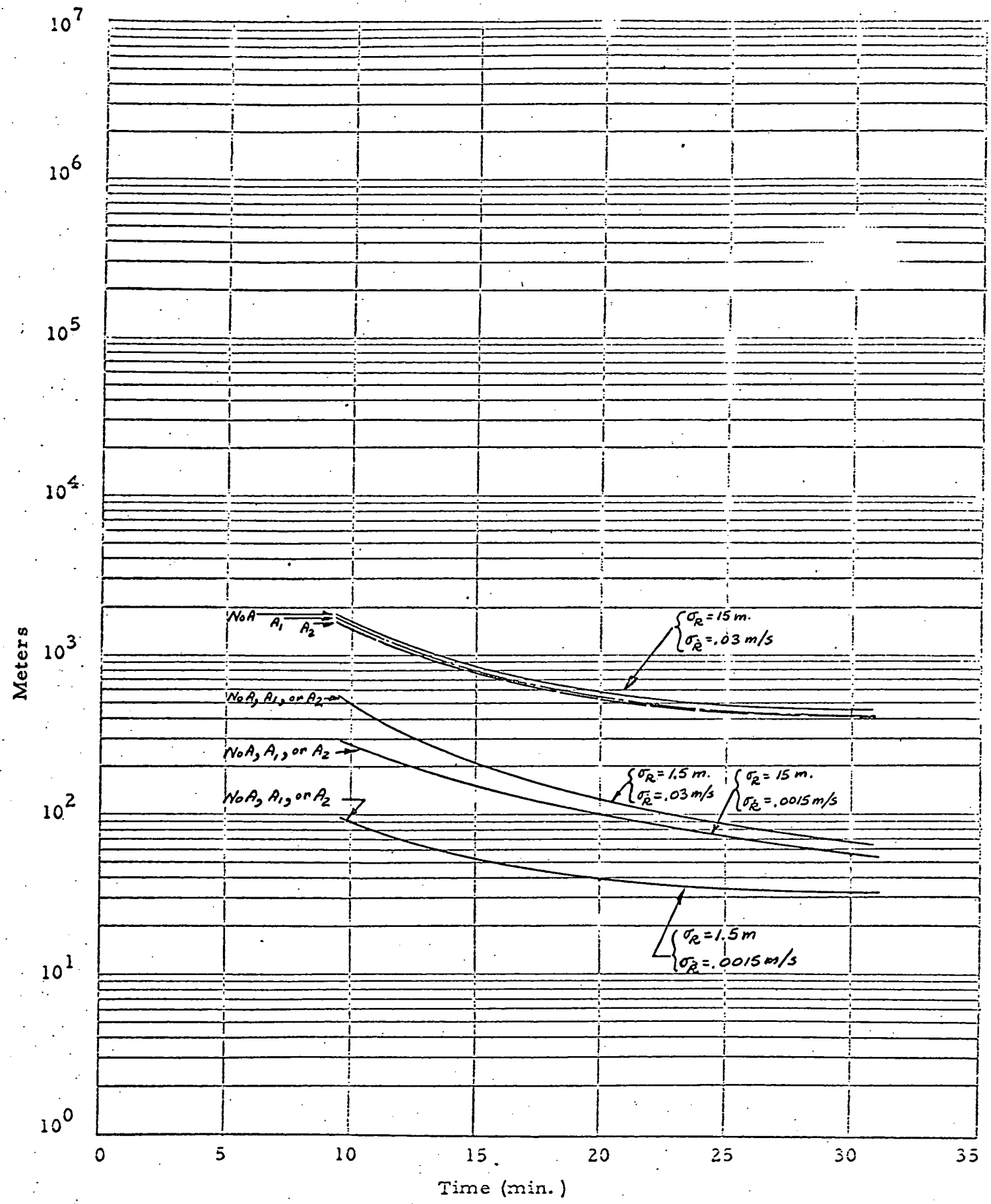

Figure 17

Minimum Miss, Madrid and Ascension and Carnarvon
Range and Range-Rate without Bias

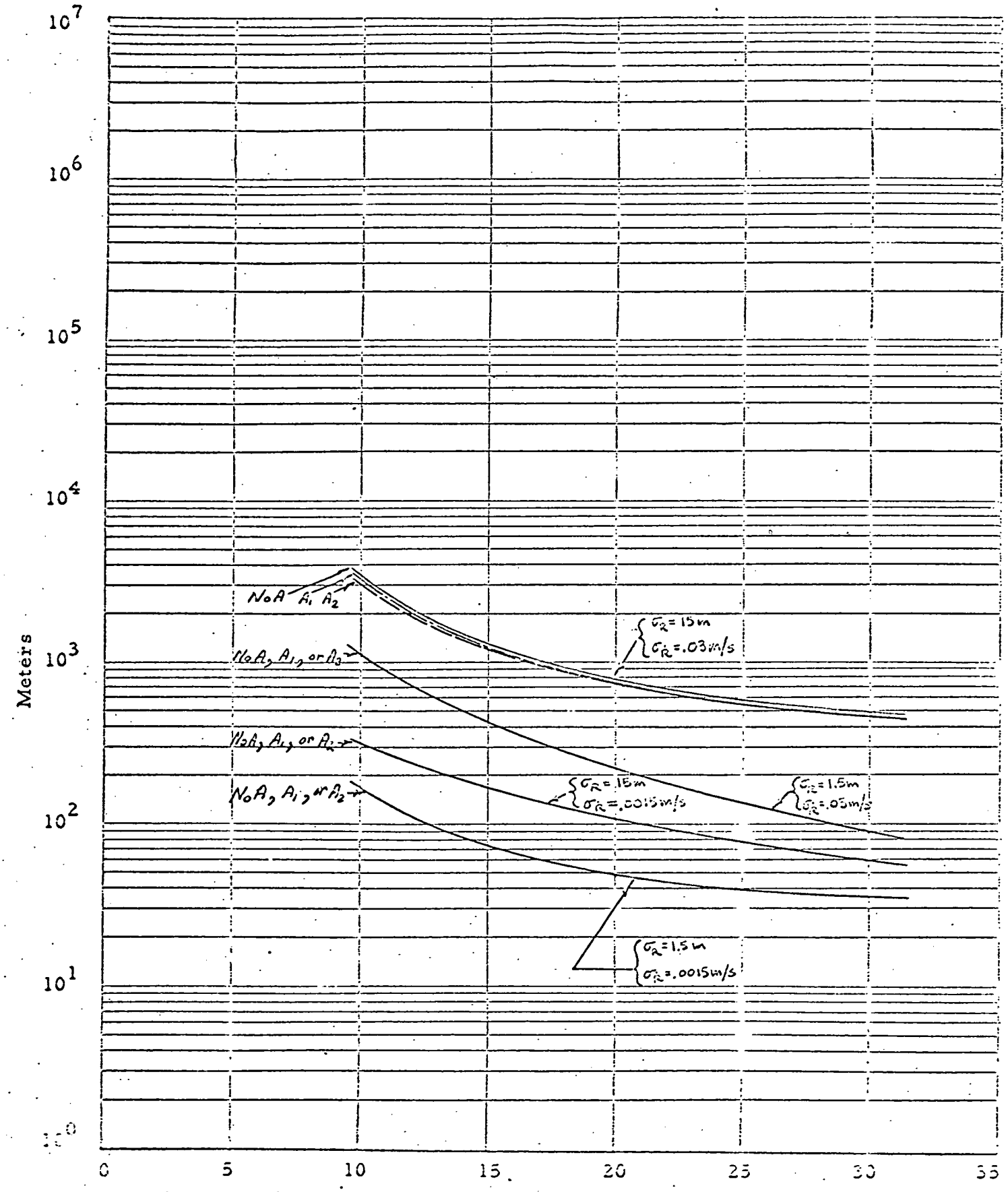

Figure 18

Rendezvous Miss, Madrid and Ascension and Carnarvon
Range and Range-Rate without Bias

APOLLO NOTE NO. 136

H. Engel
6 November 1963

MSFN RADAR ANGLE DATA IN LEM ASCENT

Introduction

The usefulness of MSFN radar angle data in determining the LEM ascent trajectory has been examined for a "standard" ascent trajectory by our error analysis computer program. It has been found that using range and angle data from one MSFN station or using range-rate and angle data from one MSFN station, the R.M.S. value of the error in the minimum distance between the LEM and CSM near the nominal time of rendezvous is considerably better than that obtainable from range or range-rate measurements alone from one station. On the other hand, if a priori data such as the position and velocity of the LEM at the end of boost are available from the on-board equipment, the angle data contributes a negligible improvement to the accuracy of prediction of rendezvous.

The effect of antenna angle biases has also been examined. Even if the antenna angle bias is completely unknown at the start of observation, its effect on the accuracy of predicted rendezvous position after 25 minutes of observation is negligible. At shorter times, in the absence of a priori LEM orbit data, angle bias errors can result in an order of magnitude degradation of the accuracy of prediction of rendezvous.

The computer results are displayed in accompanying figures.

Details

The "standard" ascent trajectory used here is a Hohmann transfer ellipse from 8 to 80 n.m. with perilune at the center of the visible face of the Moon and in the plane of Earth-Moon rotation. The inclination of the Moon's orbit is 18.3°, and at the start of observation

the sublunar point is at 4°N and 60°E.

The observing station is Madrid.

The radar is assumed to have standard deviations in range and range-rate of 15 m and 0.03 m/sec. The standard deviations of the radar angles are assumed to be 0.001 radians in the elevation direction and a like amount in the orthogonal direction normal to the line-of-sight.

The a priori data at the start of observation assumed accurate to 10^3 m and $\sqrt{10}$ m/sec in each direction.

No computations have been performed to evaluate the use of angle information from two or three MSFN stations. In such cases range and range-rate data are sufficient, and the angle information will contribute little to the accuracy of prediction.

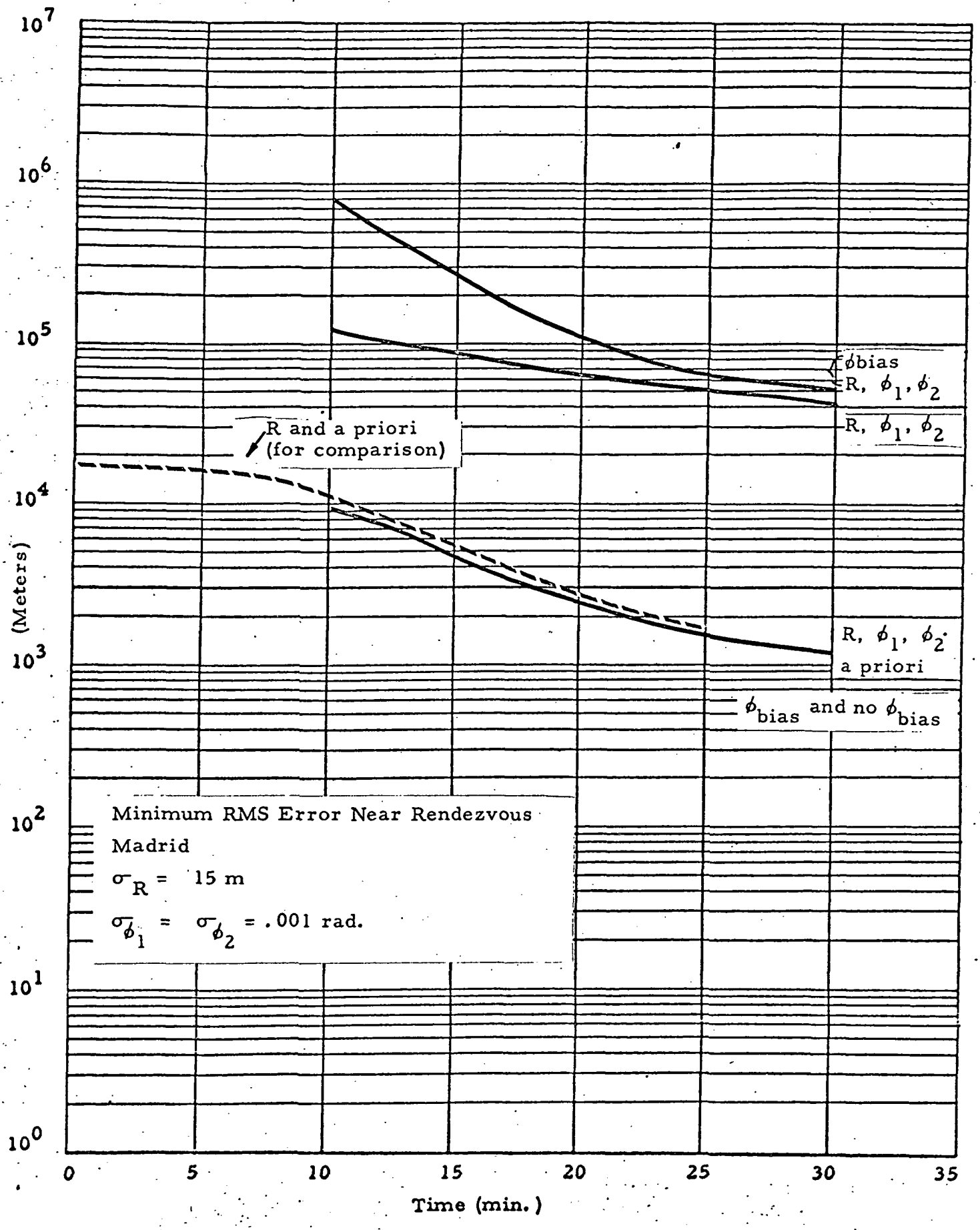
10^7
10^6
10^5
10^4
10^3
10^2
10^1
10^0
(Meters)
0
5
10
15
20
25
30
35
Time (min.)
ϕbias
R, ϕ_1, ϕ_2
R, ϕ_1, ϕ_2
R and a priori
(for comparison)
R, ϕ_1, ϕ_2
a priori
ϕ_{bias} and no ϕ_{bias}
Minimum RMS Error Near Rendezvous
Madrid
σ_R = 15 m
σ_{ϕ_1} = σ_{ϕ_2} = .001 rad.

Figure 1.

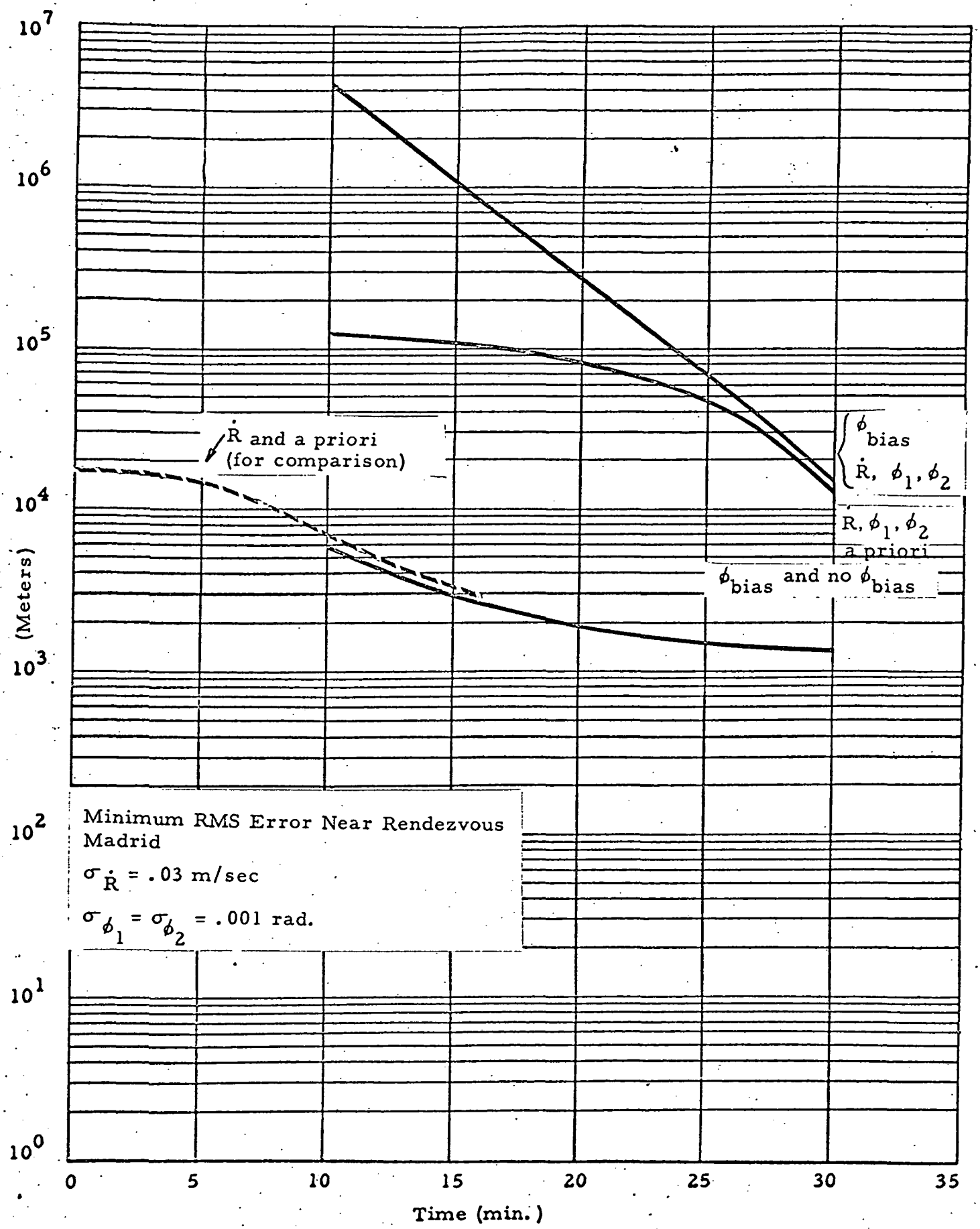
10^7
10^6
10^5
10^4
10^3
10^2
10^1
10^0
(Meters)
$\dot{R}$ and a priori
(for comparison)
ϕ_{bias}
$\dot{R}, \phi_1, \phi_2$
$\dot{R}, \phi_1, \phi_2$
a priori
ϕ_{bias} and no ϕ_{bias}
Minimum RMS Error Near Rendezvous
Madrid
$\sigma_{\dot{R}}$ = .03 m/sec
$\sigma_{\phi_1} = \sigma_{\phi_2}$ = .001 rad.
0
5
10
15
20
25
30
35
Time (min.)

Figure 2.

APOLLO NOTE NO. 137

L. Lustick
5 November 1963

ANALYTICAL TREATMENT OF RING AROUND SYSTEM

Purpose

The purpose of this note is to indicate how to determine the orbit parameter accuracy when a ring-around system is used.

Discussion

Consider the following geometry:

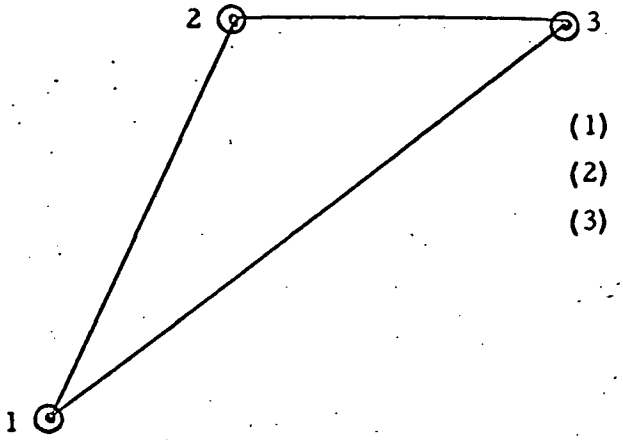

(1) station on Earth
(2) command module
(3) LEM

Assume that the following measurements are made

1. The measurable as a function of time over the path 1-2-3-1
2. The measurable over the path 1-3-1
3. Assume that the measurable 1-2-1 is known exactly

Error Model

The error in the measurable over the path 1-2-3-1 is given below

$$E_{1-2-3-1} = E_1 + E_{1-2} + E_2 + E_{2-3} + E_3 + E_{3-1} + \hat{E}_1$$

E_1 = transmit error

$E_{1-2}+E_{2-3}+E_{3-1}$ = path and medium errors

$E_2 + E_3$ = phase lock loop errors

$\hat{E}_1$ = receiver error

The error in the measurable over the path 1-3-1 is given below

$$e_{1-3-1} = e_1 + e_{1-3} + e_3 + e_{3-1} + \hat{e}_1$$

e_1	=	transmit error
$e_{1-3}+e_{3-1}$	=	path errors
e_3	=	phase lock loop errors
$\hat{e}_1$	=	receiver error

If the following is assumed:

1. $E_{1-2} + E_{2-3} + E_{3-1} = e_{1-3} + e_{3\,1}$

2. $E_1 = e_1$

then

$$\varepsilon_{2-3} = \overbrace{\left|E_2 + E_3 - e_3\right|}^{\text{phase lock errors}} + \overbrace{\left|\hat{E}_1 - \hat{e}_1\right|}^{\text{receiver errors}}$$

$$\overline{\varepsilon}_{2-3}^{2} = 3\sigma_p^2 + 2\sigma_R^2$$

where

σ_p^2	=	variance in error in each phase lock loop
σ_R^2	=	variance in the receiver error

If both the measurable from 2-3 and the measurable from 1-3-1 are to be used to determine the orbit parameters it is necessary to examine the correlation between the errors in the measurable.

$$\overline{\varepsilon_{2-3} \cdot e_{1-3-1}} = -\left[\overline{e_3^2} + \overline{\hat{e}_1^2}\right]$$

$$\overline{e_{1-3-1}^2} = \overline{e_1}^2 + \overline{\left(e_{1-3} + e_{3-1}\right)^2} + \overline{e_3^2} + \overline{\hat{e}_1^2}$$

$$\rho = \frac{\overline{\varepsilon_{2-3} \cdot \varepsilon_{1-3-1}}}{\sqrt{\overline{\varepsilon^2_{2-3}} \cdot \overline{e^2_{1-3-1}}}}$$

If the clock or receiver errors and the phase lock loop errors are considered to be the major source of error and that further the effect of each of these error sources is about the same then the following is approximately true.

$\overline{\varepsilon^2_{2-3}}$ = (2 to 3) x normal variance in measurable

$\overline{e^2_{1-3-1}}$ = normal variance in measurable

$\rho \cong \frac{1}{2}$

The method for obtaining the information matrix consistent with the two correlated variables is shown in Apollo Note No. 104. The elements of the information matrix C_{ij} are generated as shown below.

$$C_{ij} = \sum_{k=1}^{N} \left[\frac{1}{\sigma^2_{m_1}} \frac{\partial m_1(t_k)}{\partial a_i} \frac{\partial m_1(t_k)}{\partial a_j} - \frac{\rho}{\sigma_{m_1} \sigma_{m_2}} \frac{\partial m_2(t_k)}{\partial a_i} \frac{\partial m_1(t_k)}{\partial a_j} \right.$$

$$- \frac{\rho}{\sigma_{m_1} \sigma_{m_2}} \frac{\partial m_1(t_k)}{\partial a_i} \frac{\partial m_2(t_k)}{\partial a_j}$$

$$\left. + \frac{1}{\sigma^2_{m_2}} \frac{\partial m_2(t_k)}{\partial a_i} \frac{\partial m_2(t_k)}{\partial a_j} \right]$$

where

$m_1 + m_2$ are the two correlated measurables.

The cross product terms between the two measurables would require an alteration of the existing computer program.

An alternate method of employing the ring-around system is as follows.

1. obtain the measurable along the path 1-2-3-2-1
2. obtain independently the measurable along the path 1-3-1
3. assume the measurable is known along the path 1-2-1

This method is equivalent to having a station located at the command module (2) and another station on the Earth at (1) and can be treated with the existing program.

APOLLO NOTE NO. 138

H. Engel
6 November 1963

COMBINATION OF MSFN AND CSM OBSERVATIONS

Introduction

A number of computer runs have been made to examine the effect of combining data obtained from one MSFN station with data obtained from the CSM in predicting LEM rendezvous with the CSM. The LEM trajectory described in Apollo Note No. 136 is employed again. In each case the results are compared with those that can be obtained from two MSFN stations.

For the assumed accuracies the prediction accuracy obtainable with one MSFN station and the CSM with or without a priori data is about the same as that obtainable using two MSFN stations--except when the only CSM data used is range. In this last case, the combination of MSFN and CSM data without a priori data is an order of magnitude worse than data from two MSFN stations.

Details

The MSFN radar accuracy is taken as 15 m in range and 0.03 m/sec. in range-rate for one minute observations.

The CSM radar accuracy is taken as 750 m (1/2% of range) for one minute observations.

The CSM angular data is assumed to have a standard deviation of 0.001 radians, obtained optically, with one observation per minute.

The a priori data has a position accuracy of 10^3 m in each component, and a velocity accuracy of $\sqrt{10}$ m/sec. in each component.

The cases considered are:

	Madrid	CSM
1.	R	R
2.	$\dot{R}$	R
3.	R, $\dot{R}$	R
4.	R	ϕ_1, ϕ_2
5.	$\dot{R}$	ϕ_1, ϕ_2
6.	R, $\dot{R}$	ϕ_1, ϕ_2
7.	R	R, ϕ_1, ϕ_2
8.	$\dot{R}$	R, ϕ_1, ϕ_2
9.	R, $\dot{R}$	R, ϕ_1, ϕ_2

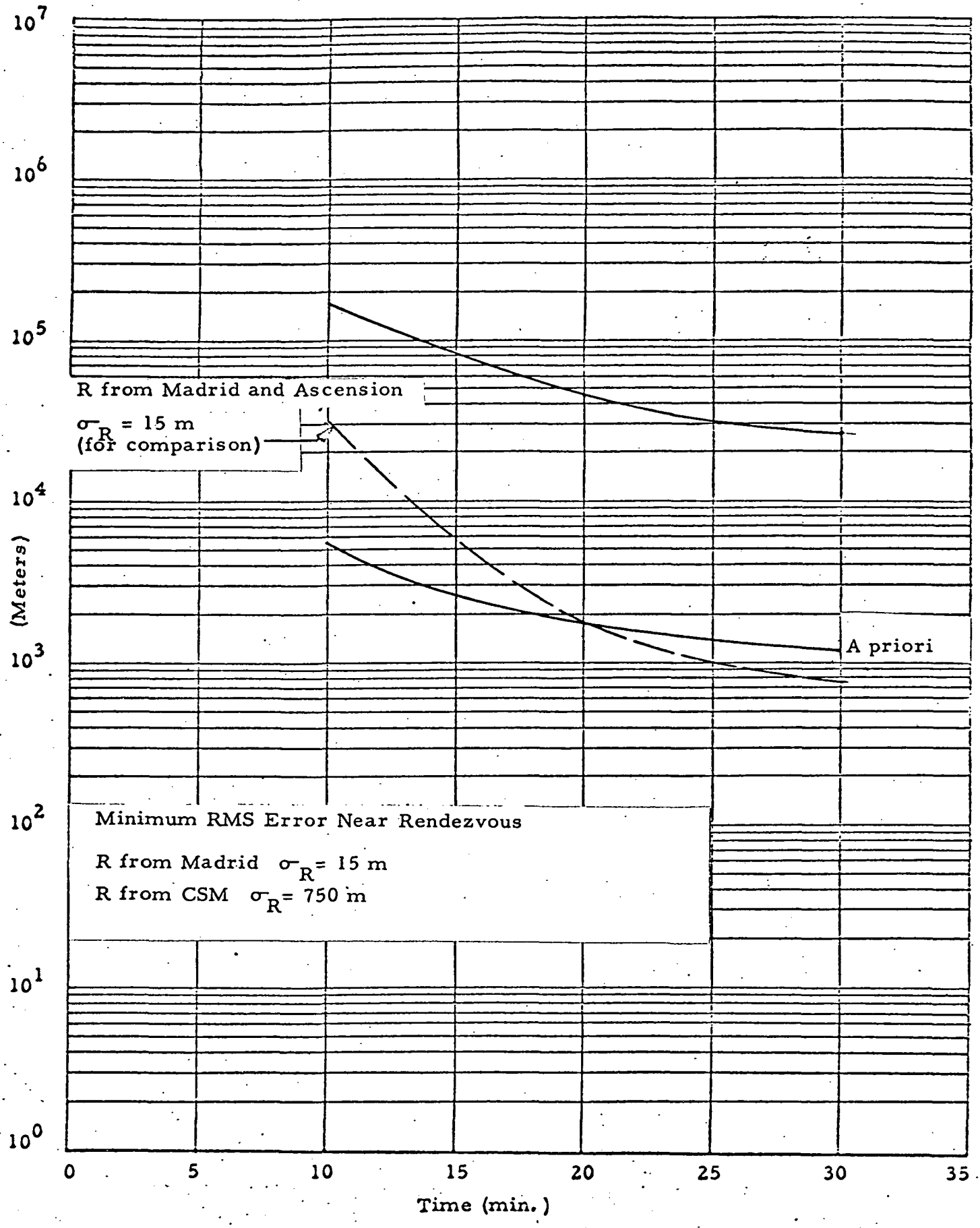
10^7
10^6
10^5
10^4
10^3
10^2
10^1
10^0
(Meters)
R from Madrid and Ascension
σ_R = 15 m
(for comparison)
A priori
Minimum RMS Error Near Rendezvous
R from Madrid σ_R = 15 m
R from CSM σ_R = 750 m
0
5
10
15
20
25
30
35
Time (min.)

Figure 1.

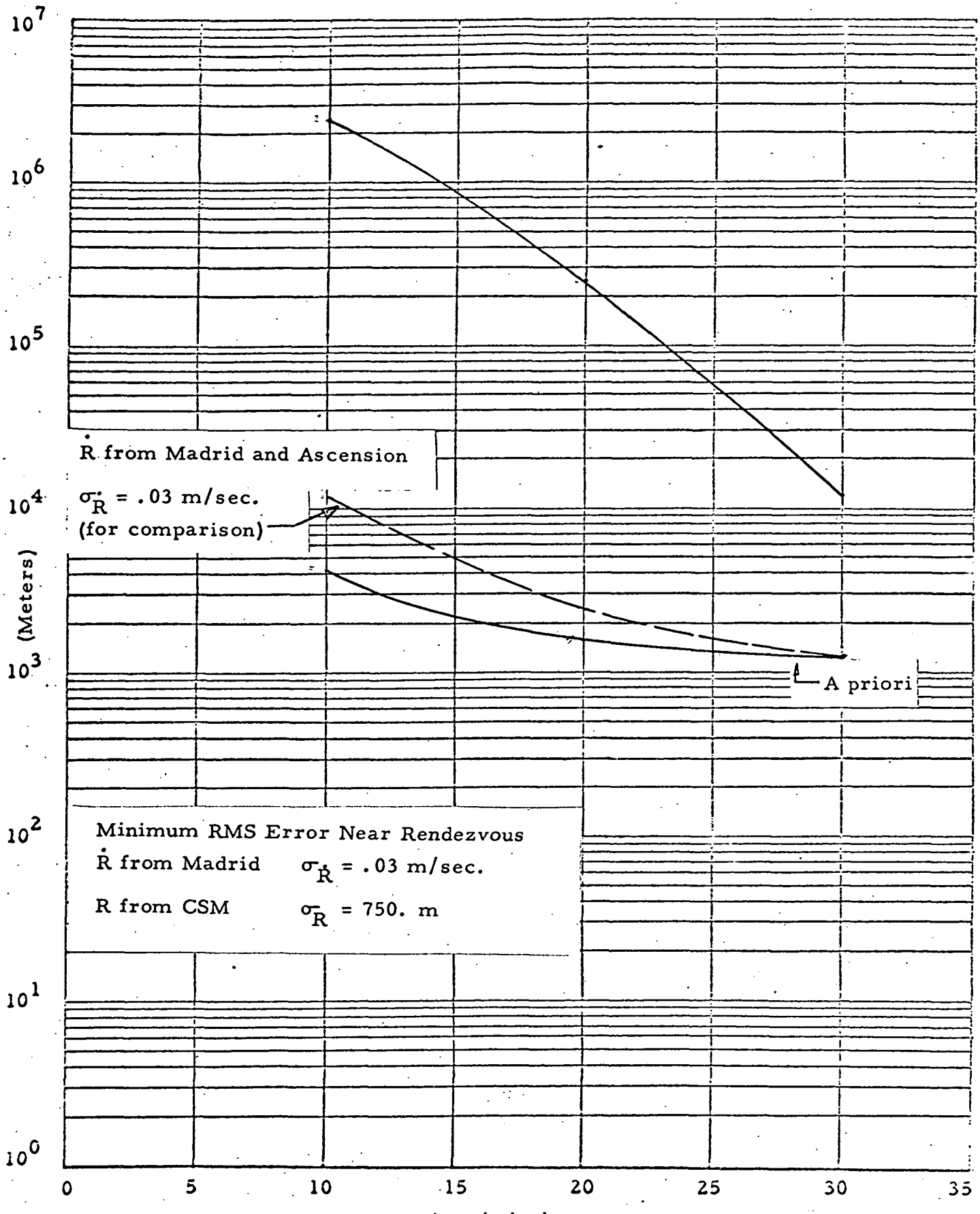
10^7
10^6
10^5
10^4
10^3
10^2
10^1
10^0
(Meters)
$\dot{R}$ from Madrid and Ascension
$\sigma_{\dot{R}}$ = .03 m/sec.
(for comparison)
A priori
Minimum RMS Error Near Rendezvous
$\dot{R}$ from Madrid $\sigma_{\dot{R}}$ = .03 m/sec.
R from CSM σ_R = 750. m
0
5
10
15
20
25
30
35
Time (min.)

Figure 2.

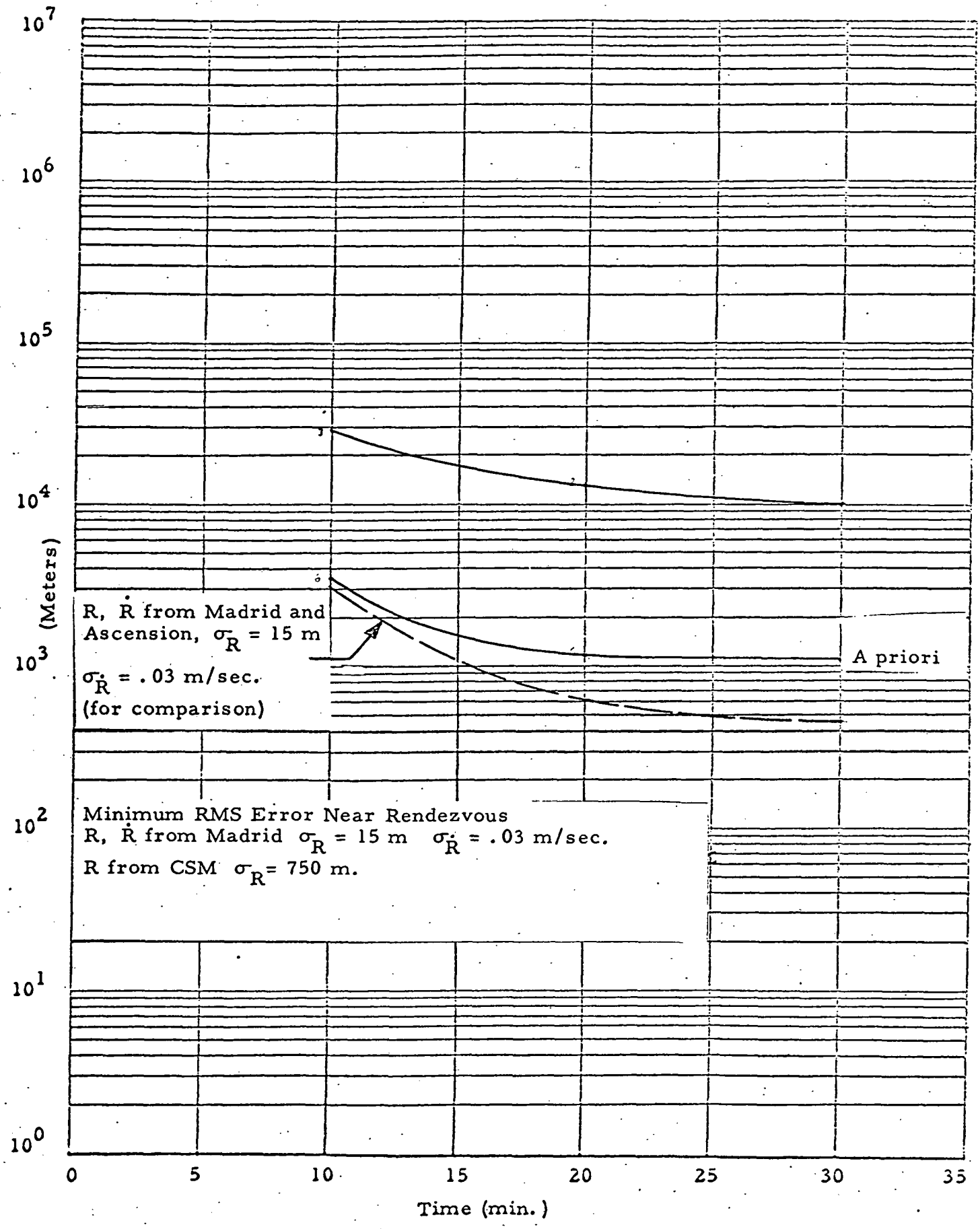
10^7
10^6
10^5
10^4
10^3
10^2
10^1
10^0
(Meters)
R, $\dot{R}$ from Madrid and Ascension, σ_R = 15 m
$\sigma_{\dot{R}}$ = .03 m/sec.
(for comparison)
A priori
Minimum RMS Error Near Rendezvous
R, $\dot{R}$ from Madrid σ_R = 15 m $\sigma_{\dot{R}}$ = .03 m/sec.
R from CSM σ_R = 750 m.
0
5
10
15
20
25
30
35
Time (min.)

Figure 3.

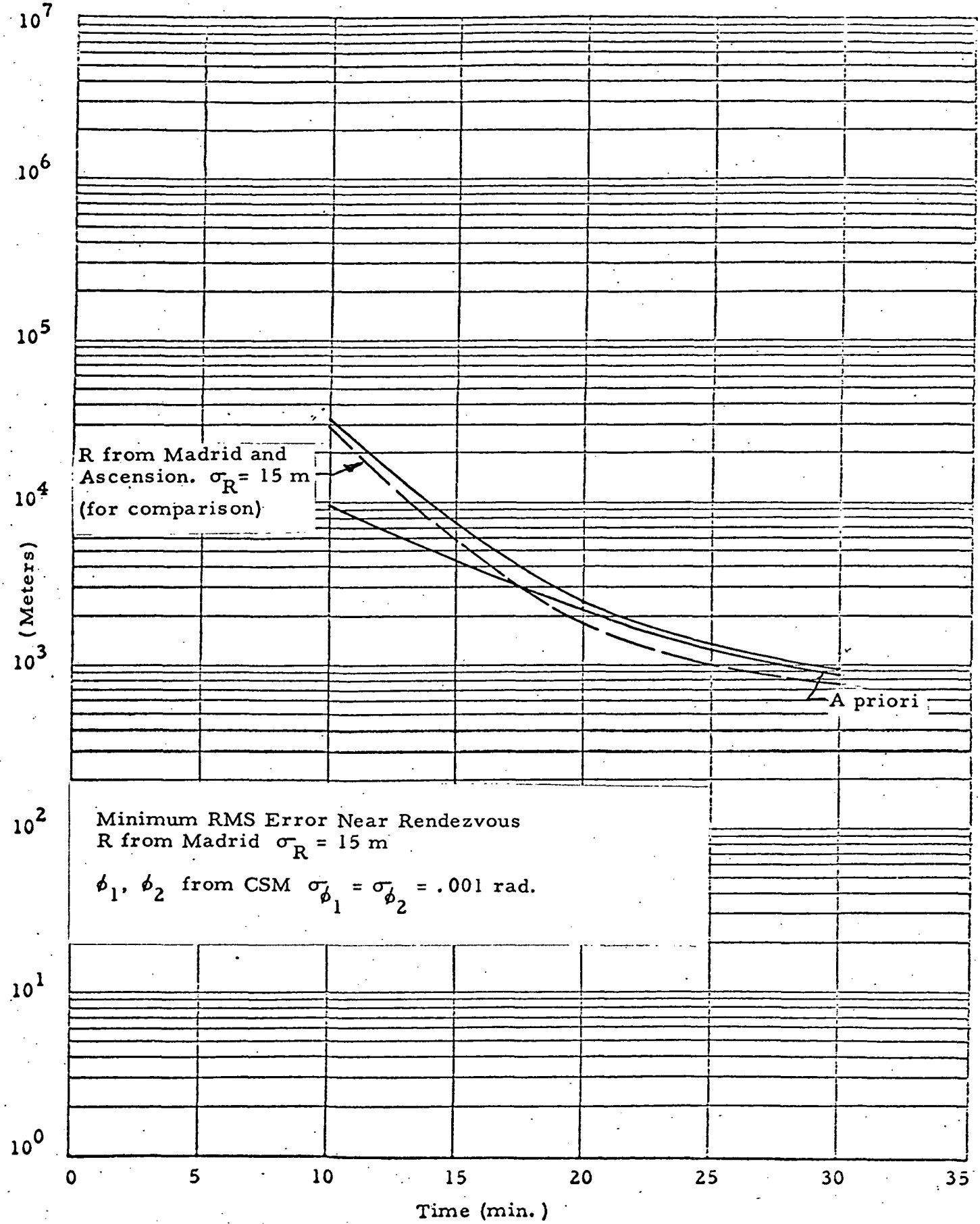
10^7
10^6
10^5
10^4
10^3
10^2
10^1
10^0
(Meters)
R from Madrid and Ascension. σ_R = 15 m (for comparison)
A priori
Minimum RMS Error Near Rendezvous
R from Madrid σ_R = 15 m
ϕ_1, ϕ_2 from CSM $\sigma_{\phi_1} = \sigma_{\phi_2}$ = .001 rad.
0
5
10
15
20
25
30
35
Time (min.)

Figure 4.

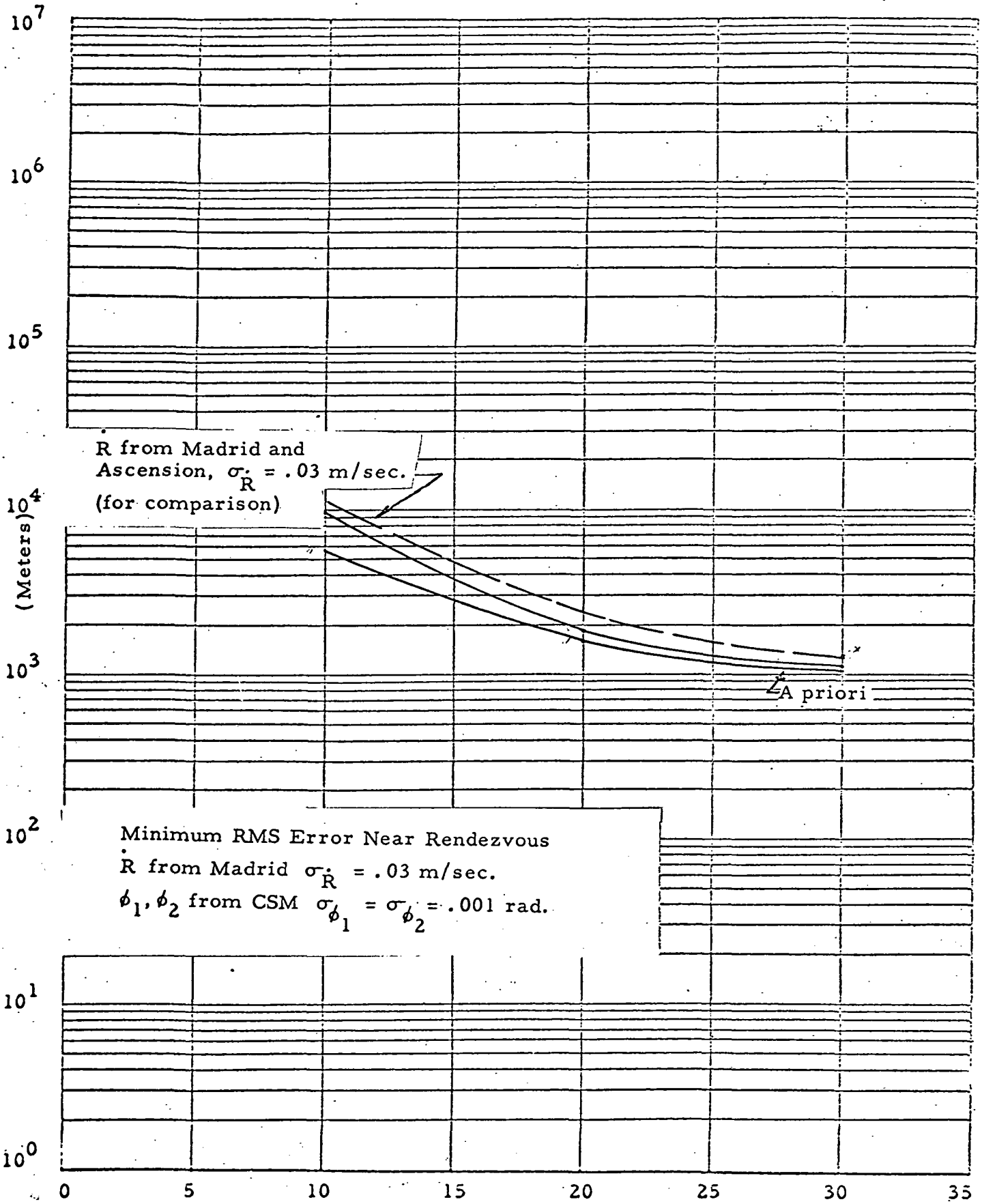
10^7
10^6
10^5
10^4
10^3
10^2
10^1
10^0
(Meters)
R from Madrid and Ascension, $\sigma_{\dot{R}}$ = .03 m/sec.
(for comparison)
A priori
Minimum RMS Error Near Rendezvous
$\dot{R}$ from Madrid $\sigma_{\dot{R}}$ = .03 m/sec.
ϕ_1, ϕ_2 from CSM $\sigma_{\phi_1} = \sigma_{\phi_2}$ = .001 rad.
0
5
10
15
20
25
30
35
Time (min.)

Figure 5.

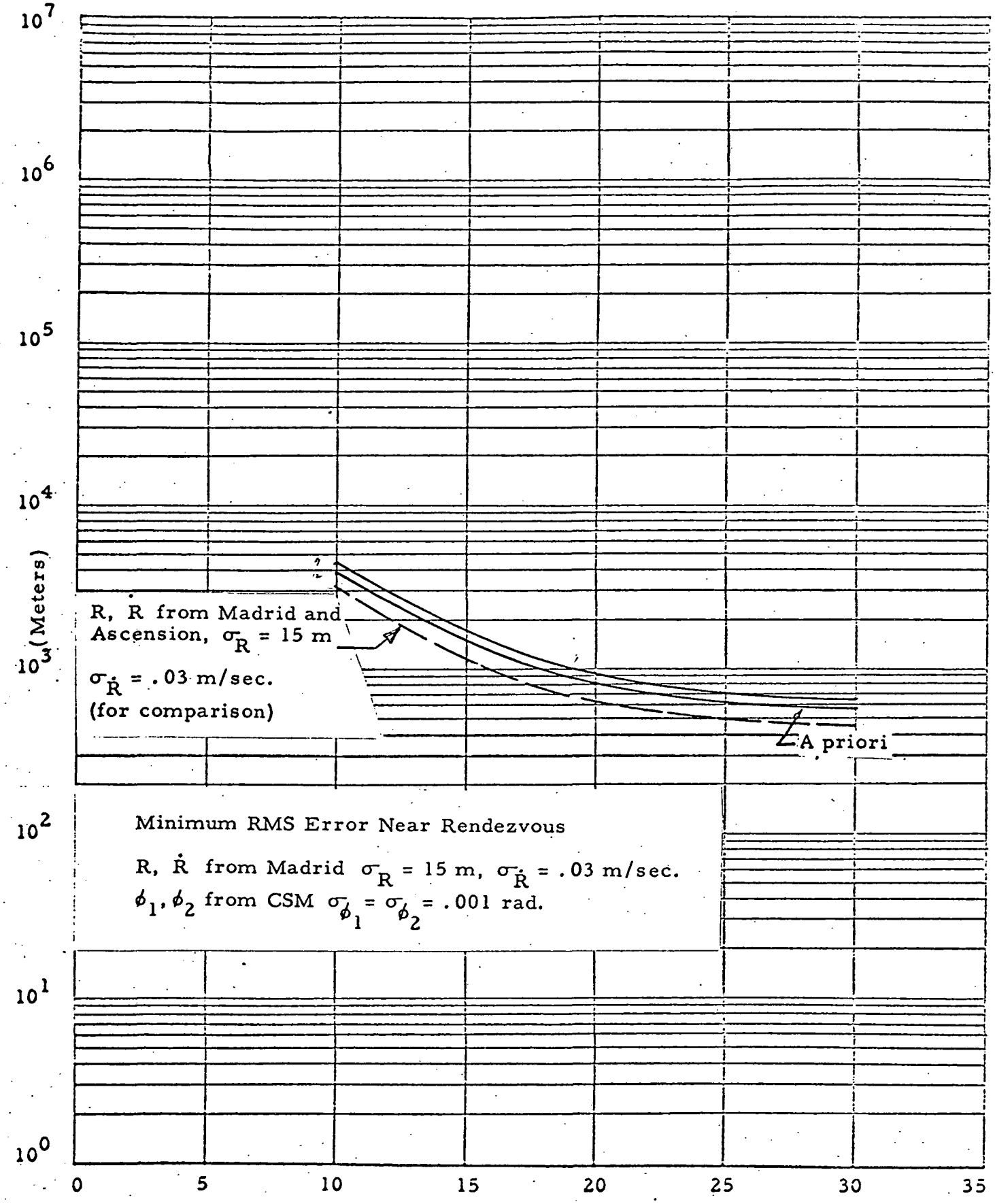
10^7
10^6
10^5
10^4
10^3
10^2
10^1
10^0
(Meters)
R, $\dot{R}$ from Madrid and Ascension, σ_R = 15 m
$\sigma_{\dot{R}}$ = .03 m/sec.
(for comparison)
A priori
Minimum RMS Error Near Rendezvous
R, $\dot{R}$ from Madrid σ_R = 15 m, $\sigma_{\dot{R}}$ = .03 m/sec.
ϕ_1, ϕ_2 from CSM $\sigma_{\phi_1} = \sigma_{\phi_2}$ = .001 rad.
0
5
10
15
20
25
30
35
Time (min.)

Figure 6.

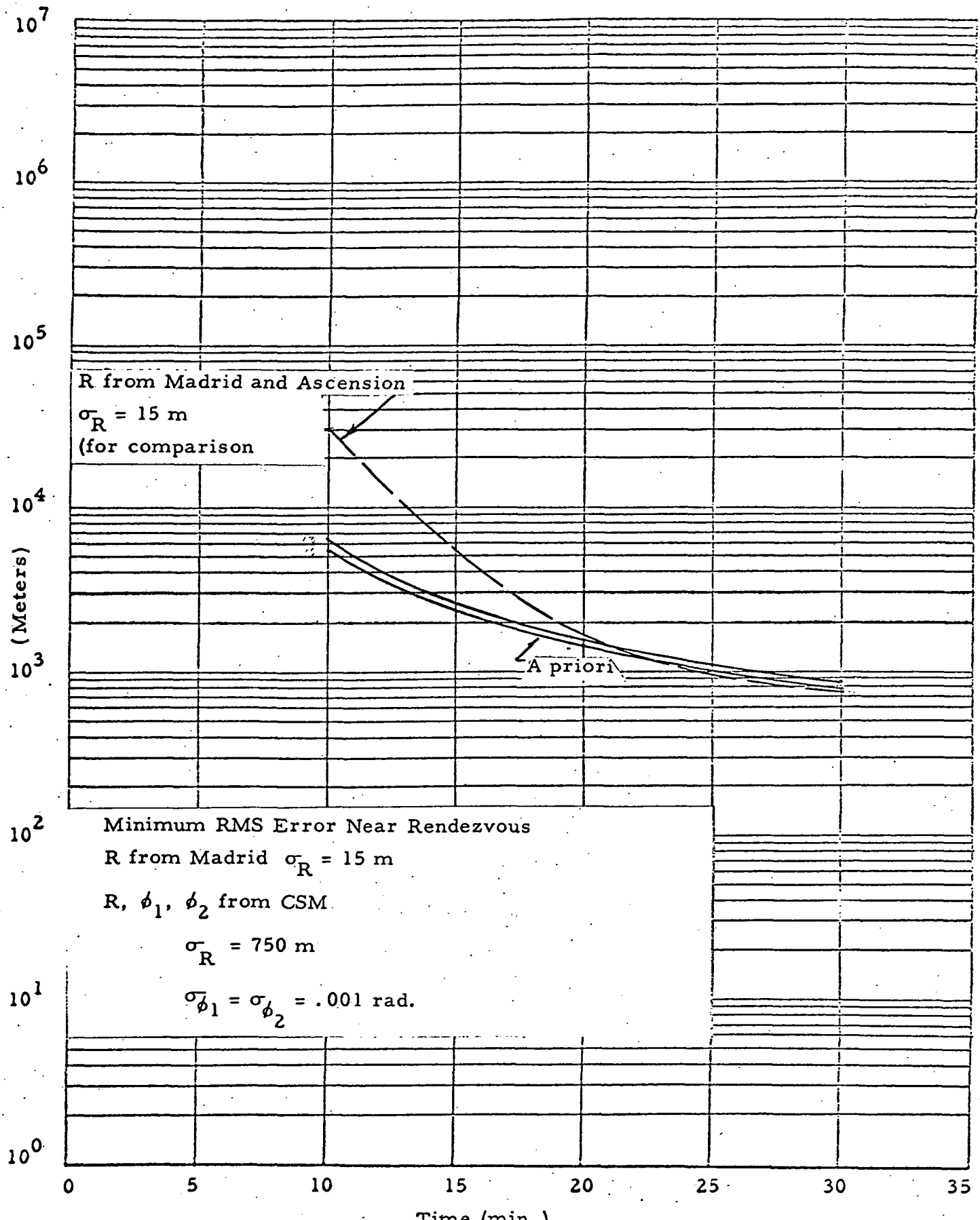
10^7
10^6
10^5
10^4
10^3
10^2
10^1
10^0
(Meters)
R from Madrid and Ascension
σ_R = 15 m
(for comparison
A priori
Minimum RMS Error Near Rendezvous
R from Madrid σ_R = 15 m
R, ϕ_1, ϕ_2 from CSM
σ_R = 750 m
$\sigma_{\phi_1} = \sigma_{\phi_2}$ = .001 rad.
0
5
10
15
20
25
30
35
Time (min.)

Figure 7.

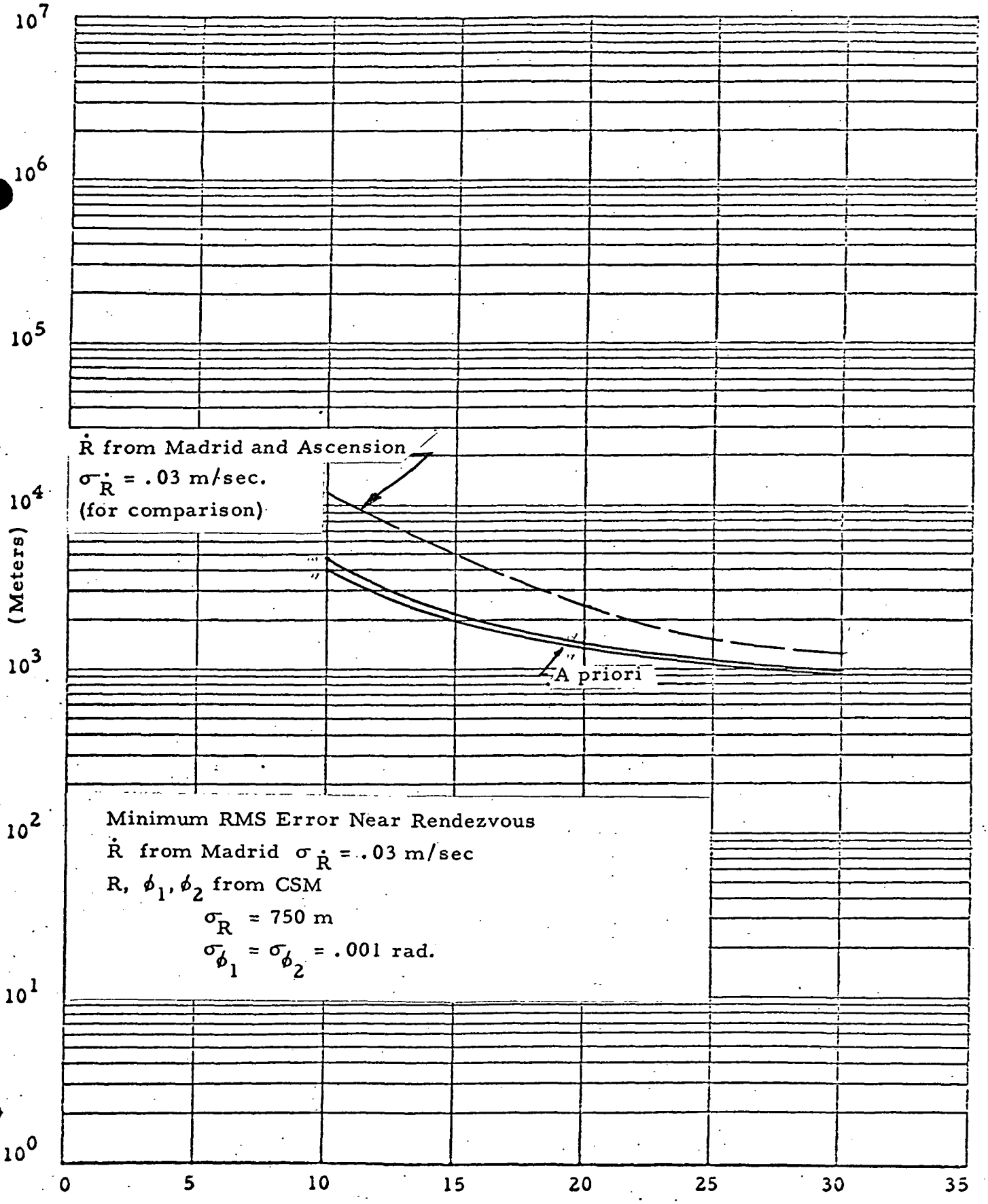
10^7
10^6
10^5
10^4
10^3
10^2
10^1
10^0
(Meters)
$\dot{R}$ from Madrid and Ascension
$\sigma_{\dot{R}}$ = .03 m/sec.
(for comparison)
A priori
Minimum RMS Error Near Rendezvous
$\dot{R}$ from Madrid $\sigma_{\dot{R}}$ = .03 m/sec
R, ϕ_1, ϕ_2 from CSM
σ_R = 750 m
$\sigma_{\phi_1} = \sigma_{\phi_2}$ = .001 rad.
0
5
10
15
20
25
30
35
Time (min.)

Figure 8.

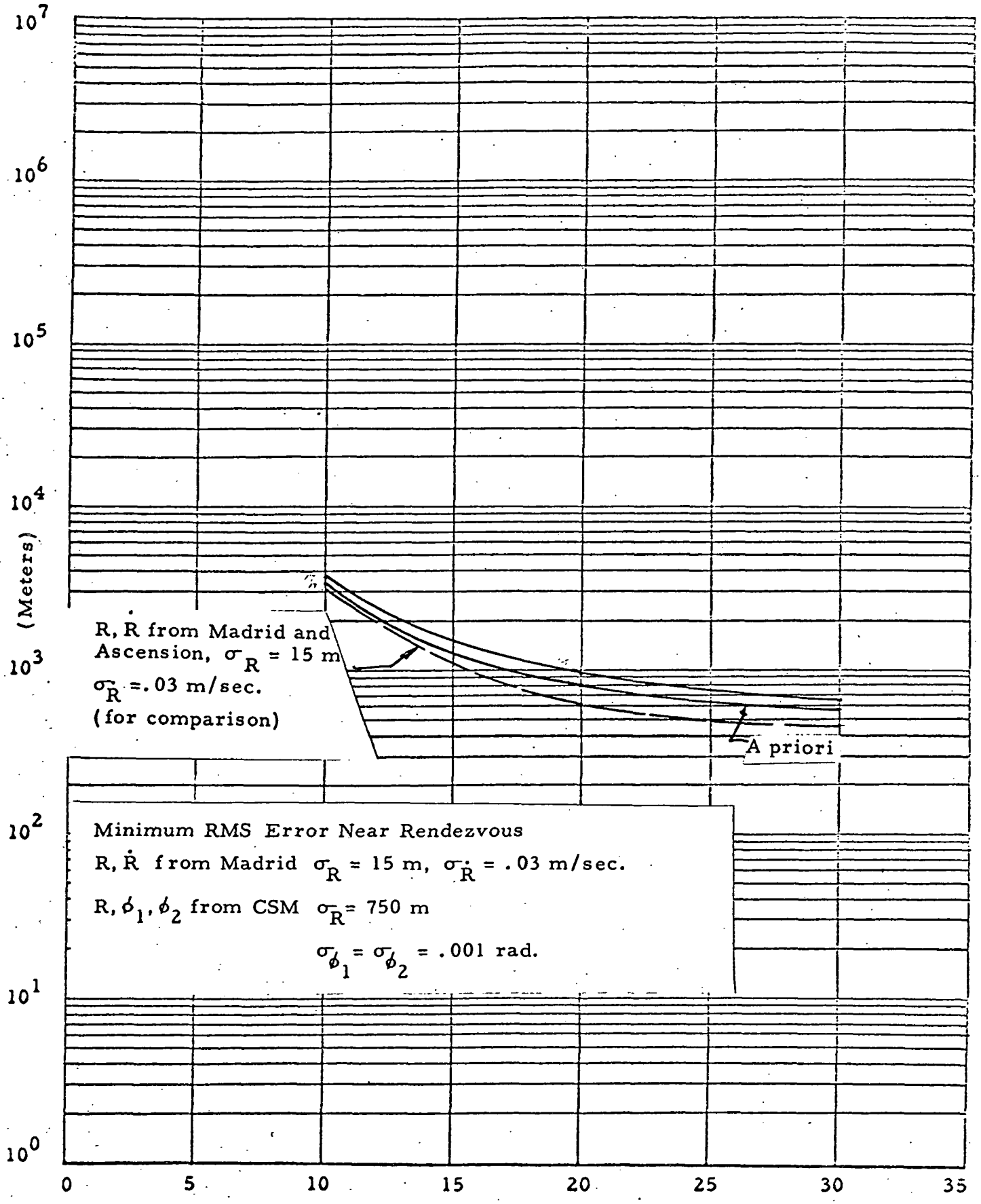
10^7
10^6
10^5
10^4
10^3
10^2
10^1
10^0
(Meters)
R, Ṙ from Madrid and Ascension, σ_R = 15 m
$\sigma_{\dot{R}}$ = .03 m/sec.
(for comparison)
A priori
Minimum RMS Error Near Rendezvous
R, Ṙ from Madrid σ_R = 15 m, $\sigma_{\dot{R}}$ = .03 m/sec.
R, ϕ_1, ϕ_2 from CSM σ_R = 750 m
$\sigma_{\phi_1} = \sigma_{\phi_2}$ = .001 rad.
0
5
10
15
20
25
30
35
Time (min.)

Figure 9.

APOLLO NOTE NO. 139

H. Engel
8 November 1963

MSFN STATION LOCATIONS AND LUNAR RENDEZVOUS DETERMINATION

The effect of MSFN station location on the accuracy with which lunar rendezvous for an LEM orbit in the Earth-Moon plane of rotation can be predicted has been examined. In this investigation we have considered the case of range-rate observations from two stations separated by a great circle distance of 40°, with different relative azimuths and different locations relative to the Earth-Moon line.

The results indicate that stations in a North-South line can predict lunar rendezvous 2 to 3 times more accurately than stations in an East-West line, and that for stations in a SW - NE line the predictions are almost as good as for a North - South line. Thus, the critical factor appears to be North - South separation of the stations.

The sublunar point at the start of observations was at 0° latitude, 0° longitude. In Figures 1, 2 and 3 respectively, the point halfway between the observing stations was at 0° latitude, and at 0°, 20°W and 40°W longitude. Comparison of these figures indicates that the longitude of the stations relative to that of the Earth-Moon line is of relatively small importance.

Accuracy of prediction will tend to vary inversely as station separation.

The MSFN radar accuracy is taken as 0.03 m/sec. in range-rate for 1 minute observations.

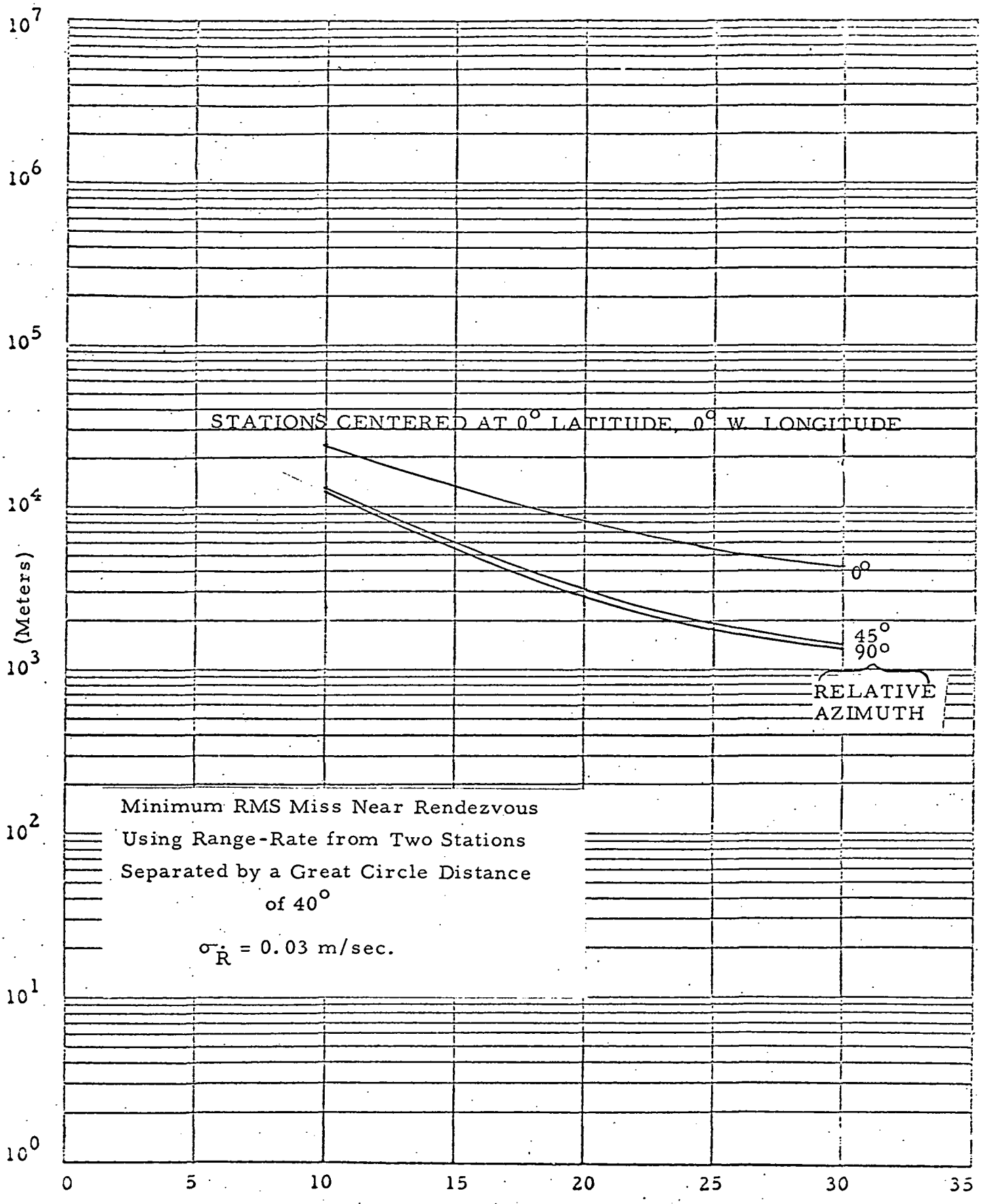
10^7
10^6
10^5
10^4
10^3
10^2
10^1
10^0
(Meters)
STATIONS CENTERED AT 0° LATITUDE, 0° W. LONGITUDE
0°
45°
90°
RELATIVE AZIMUTH
Minimum RMS Miss Near Rendezvous
Using Range-Rate from Two Stations
Separated by a Great Circle Distance
of 40°
$\sigma_{\dot{R}}$ = 0.03 m/sec.
0
5
10
15
20
25
30
35
Time (min.)

Figure 1.

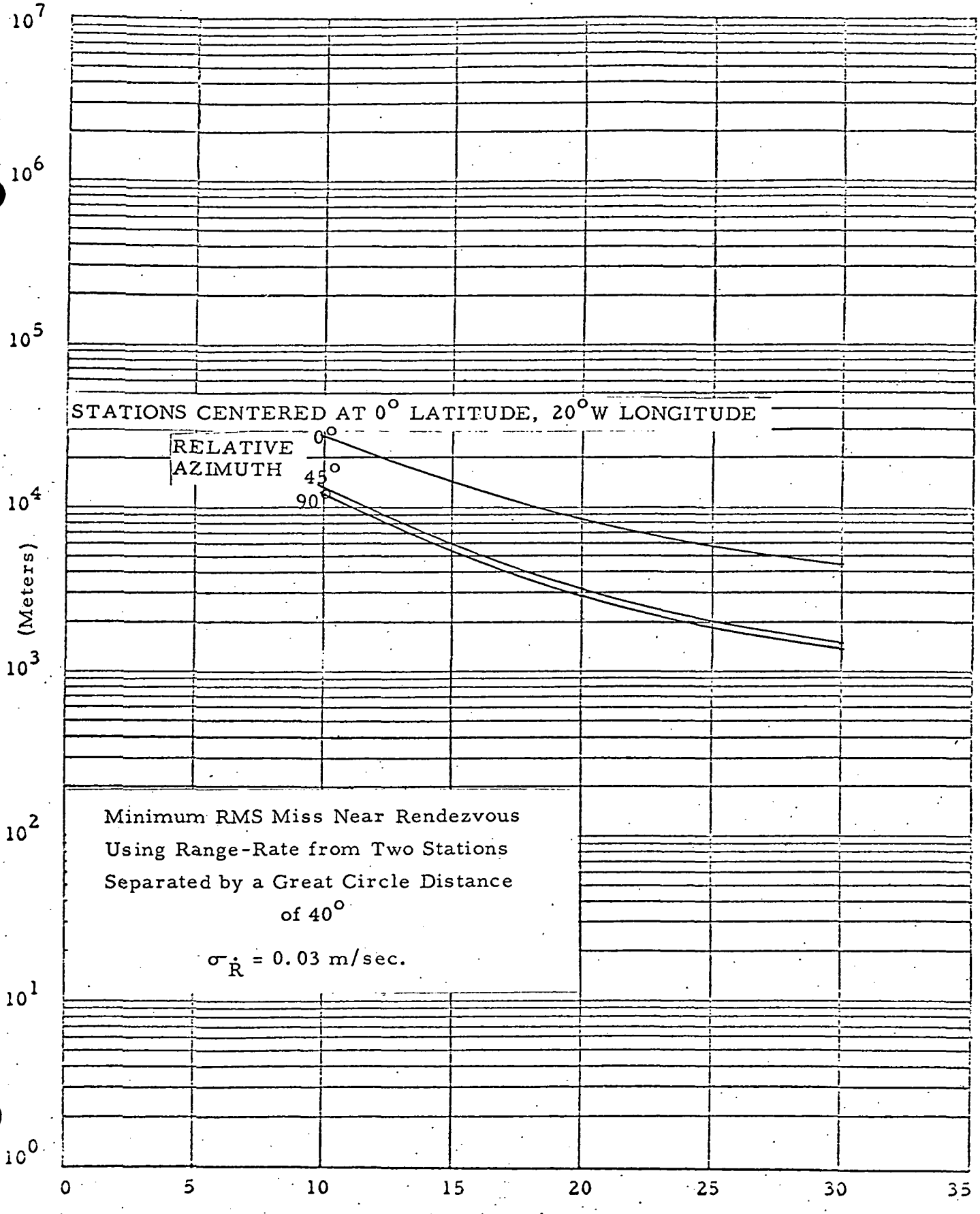
10^7
10^6
10^5
10^4
10^3
10^2
10^1
10^0
(Meters)
STATIONS CENTERED AT 0° LATITUDE, 20°W LONGITUDE
RELATIVE AZIMUTH
0°
45°
90°
Minimum RMS Miss Near Rendezvous
Using Range-Rate from Two Stations
Separated by a Great Circle Distance
of 40°
$\sigma_{\dot{R}}$ = 0.03 m/sec.
0
5
10
15
20
25
30
35
Time (min.)

Figure 2.

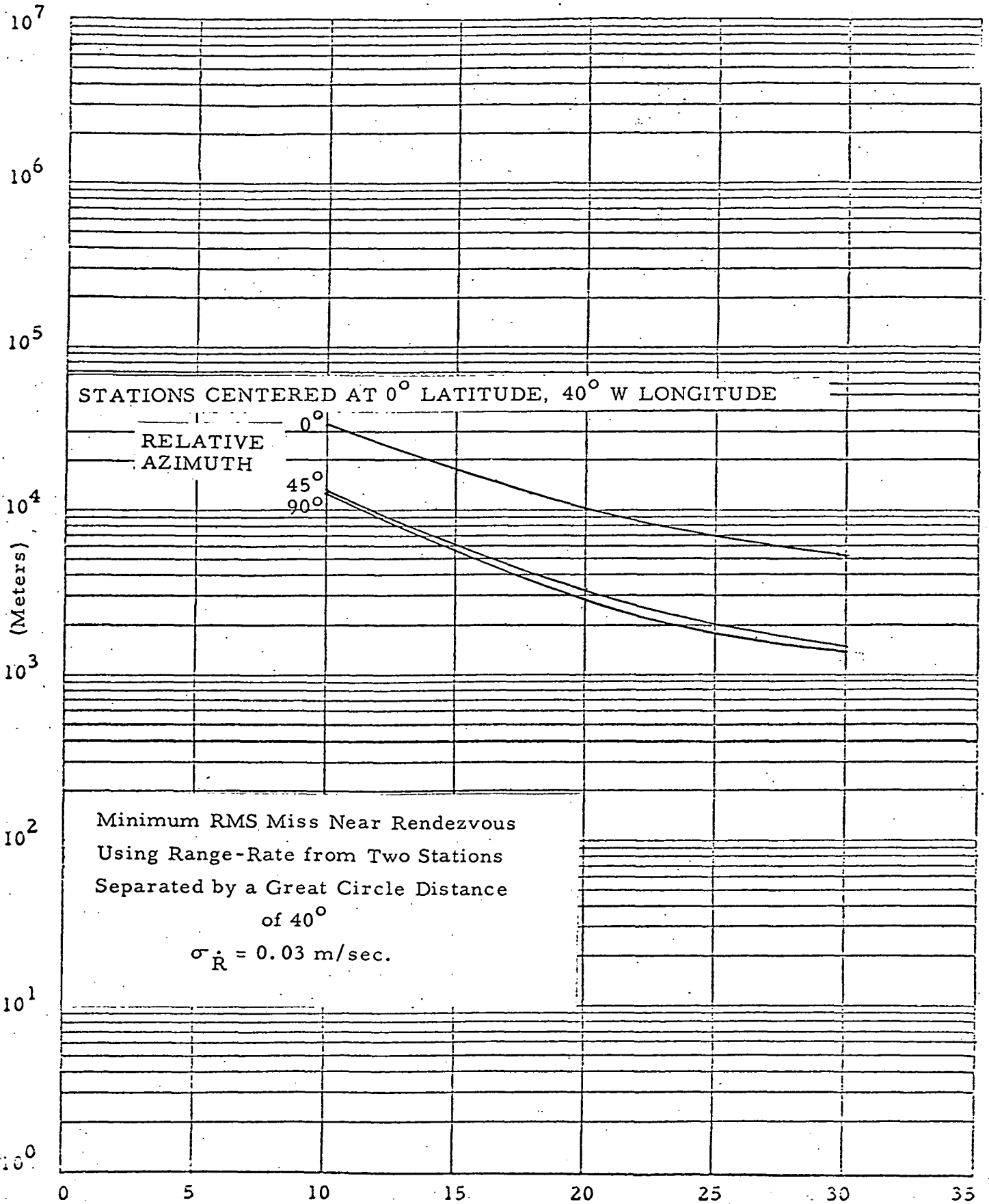
STATIONS CENTERED AT 0° LATITUDE, 40° W LONGITUDE
RELATIVE AZIMUTH
0°
45°
90°
Minimum RMS Miss Near Rendezvous
Using Range-Rate from Two Stations
Separated by a Great Circle Distance
of 40°
$\sigma_{\dot{R}}$ = 0.03 m/sec.
(Meters)
10^7
10^6
10^5
10^4
10^3
10^2
10^1
10^0
0
5
10
15
20
25
30
35
Time (min.)

Figure 3.

APOLLO NOTE NO. 140

H. Epstein
11 November 1963

SOME COMMENTS ON FREQUENCY AND TIME STANDARDS

This note deals primarily with a summary of information presented at a Frequency Comparison Techniques Seminar held at the Boulder Laboratories of the National Bureau of Standards (NBS). It is convenient to consider the material presented in terms of time standards, frequency standards, and time synchronization. Actually, a time standard is effectively a frequency standard, and a frequency standard at least a measure of time interval. The material being presented at this time should be considered as providing the background for later notes treating the accuracy limitations imposed by frequency standards on range and range-rate measurements. It should be recognized that atomic frequency is the most stable quantity that has ever been measured. For example, two cesium atomic standards have been compared at NBS over a period of three years indicating frequency offset of about 1 part in 10^{11} with a fluctuation of about 2 parts in 10^{12}. The best astronomical time standards possess an accuracy of only about one part in 10^{8}, and the velocity of light in a vacuum itself is presently only known to about several parts in 10^{7}.

1. Time Standards

There are presently seven standard time scales in use at this time; atomic, ephemeris, true sidereal, mean sidereal, UT0, UT1, and UT2. To circumvent difficulties associated with the multiplicity of time scales, a convention was adopted in May 1962 by the International Consultative Committee for Radio (CCIR). These are:

a. That the standard frequency and time pulses at each transmitting station be generated from the same oscillator;

b. That the frequency be maintained constant each year with reference to atomic standards of frequency, but be offset to keep the time pulses in close agreement with

UT2. The offset to be used each year will be that adopted by the Bureau De l'heure after consultation with the observatories concerned. This offset is expressed in the time scale in which the frequency of cesium has a value equal to 9, 192, 631, 770 cycles per second.

c. That the time signals should consist of impulses repeated at intervals of one second and maintained within approximately 100 milliseconds of universal time (UT2). Changes in the phase of the pulses should be exactly 50 milliseconds and should be made simultaneously by the stations concerned.

The UT or Universal Time Standards are based on the Earth's rotation and require about one month to be determined to a useable accuracy. UT0 is an astronomically observed universal time or mean solar time uncorrected for polar variation and annual fluctuation in the Earth's speed of rotation; UT1 is UT0 corrected for polar variation; and, UT2 is UT1 corrected for annual variation. Unfortunately, none of the UT standard seconds is constant. The ephemeris time (ET) is related to the orbital motion of the Earth about the Sun. In October 1956, the International Committee on Weights and Measures effectively adopted the second of ET as a fundamental unit of time by resolving that "the second is the fraction one divided by 31, 556, 925. 9747 of the tropical year commencing January 1900." This definition was one of many attempts to define a unit of time which: 1, remains constant with epic; 2, is physically realizable to high precision; and 3, which is permanently available for observation. However, a period of several years is required to determine ephemeris time to a useful degree of accuracy. Ephemeris time has to a large extent replaced universal time as a fundamental definition of a second.

The better accuracy, constancy, and shorter time measurement intervals (several minutes) involved in atomic frequency standards

make it highly desirable that an atomic frequency standard be adopted as a time source. With this in mind, the A1 atomic standard has been defined for a cesium atomic standard. The cesium atomic standard has been assumed as operating at a frequency (with zero uniform magnetic field) as 9,192,631,770 cycles per second. This number was chosen to be consistent with the present accuracy of ephemeris time available. It is important to bear in mind that absolute frequency can only be measured to a given accuracy related to the frequency or time standard employed. For the most accurate frequency standards, it is only possible to compare one against the other. In effect, this made the selection of the precise value of the cesium frequency somewhat arbitrary. An atomic time standard is expected to be formally adopted by 1966.

2. Atomic Frequency Standards

Three basic techniques have been employed for atomic frequency standards. The present technique employed for the primary time standard involves atomic beam techniques utilizing cesium. In addition, a thallium beam is in use at NBS. A second technique involves optical gas cells (normally rubidium). A third technique involves wall coatings in place of the buffer gas for gas standards such as rubidium. Presently hydrogen appears as the most promising element for this technique. The present ammonia maser is also of this latter type.

It is important to recognize that crystals at a convenient frequency (such as 5 megacycles) are associated with atomic standards. For example, the crystal frequency is multiplied to the atomic standard frequency and a frequency or phase-lock loop is employed to lock the crystal frequency to the standard frequency. The combination of a high quality crystal to give excellent short-term stability in an atomic standard to give the required long-term stability is an excellent approach to obtaining standards with both good long-term and short-term stability. The present United States Frequency Standard actually

consists of three oscillators. A rubidium oscillator with its associated crystal is employed as the working standard and a cesium atomic beam standard, the actual United States frequency standard (the USFS) is employed for the long-term stability. The working standard is calibrated daily against the USFS and reports are circulated weekly pertaining to the accuracy of the working standard. The transfer functions employed are such that for times in the order of a tenth of a second or less the crystal short-term characteristics determines the frequency accuracy. Stability for periods of times up to about one day, are determined by the rubidium standard, (which runs continuously to adjust for the drift in the crystal oscillator.). The rubidium standard itself is daily calibrated in terms of the USFS with the correction being distributed weekly as was mentioned earlier.

The crystals employed for this application typically have about a 90 to 96 db signal-to-noise ratio in a four kilocycle bandwidth at about five megacycle center frequency. The best oscillator presently used with the cesium beam clock has a 96 db signal-to-noise ratio. Two techniques are employed for measurement purposes on these oscillators. One technique may be considered as an elapsed phase method and employs cycle counters. Normally the counters measure a fixed number of positive zero crossings of the beat frequency between the standard frequency and the oscillator to be measured. For measurement convenience, the standard frequency is typically offset from the frequency to be measured. The second method typically employs tunable filters or the equivalent, and is essentially a direct measure of the fourier components.

The ammonia beam maser is employed to calibrate the frequency stability for oscillators in the frequency range of about a few cycles to several hundred cycles. The spectral density of the noise associated with ammonia beam maser at 5 megacycles is about 150 db down in a one cycle per second bandwidth from the power in the oscillator desired frequency.

There are a few more comments that should be made about the atomic beam standard presently in use. For cesium, the transition between the upper level for which F = 4, $m_F = 0$ and the lower level for which F = 3, $m_F = 0$ is the transition that has been adopted as a standard frequency. For this transition, the frequency absorbed and emitted in a weak magnetic field is the frequency for zero magnetic field plus the frequency proportional to the square of the magnetic field. The uncertainty in this weak magnetic field is one of the major contributors to the accuracy of the cesium standards. This factor has led to the design of a thallium beam atomic standard. Thallium is about a factor of 50 less sensitive to the uniform magnetic field than cesium. The spectrum of the noise associated with the cesium atomic beam has a flicker-like character for low frequencies. For flicker noise the spectral density is inversely proportional to the frequency. Measurements made at NBS indicate that flicker noise exists at least to as low a frequency as one cycle per half year. The high frequency limit to the flicker contribution is about a tenth to one cycle per second. At somewhat higher frequencies, the noise is substantially white and for yet higher frequencies, the noise appears to increase with frequency. The advantage for the atomic beam standards such as cesium are that the precise frequency is readily specifiable and not effected to a large extent by external parameters. Stability over long periods of time is obtained and high signal-to-noise ratios are available. The primary disadvantage to these atomic beam standards deals with the size and cumbersome nature of this standard for operational conditions. The rubidium gas maser, while not possessing some of the long-term stability of the cesium maser (at least in the present times), is a very much more practical source for most purposes and particularly for radar purposes should satisfy most requirements. It has the advantage of being quite compact and rather inexpensive and is typically designed for constant usage which the present cesium atomic standard is not designed to perform. The hydrogen maser, while not yet available commercially, appears to

represent a source for quite stable operations, perhaps one to two order of magnitudes better in performance than present rubidium standards. Narrow spectrums are obtained for both the hydrogen and rubidium standards as compared to the spectrum of the cesium standard. Preliminary experimental results have been quite encouraging for this type standard.

The system of atomic time, A. 1, is based on the operation of cesium resonators at 9 laboratories, five in the United States, one in Canada, one in England, one in France and one in Switzerland. These laboratories monitor the frequency of NBA on 18 kilocycles per second, and report each month the value of the frequency for each day with respect to its cesium resonator. A weight is accorded to each resonator depending upon the deviation of the monthly average with respect to the mean of all nine stations. Systematic correction with respect to the weight mean is obtained for each resonator for each month. These corrections are applied to obtain adopted deviations in frequency of NBA, GBR, WWV, etc., for each day on the system A. 1. The system A. 1 standard is stable month to month to about in part 10^{11}.

3. Time and Frequency Synchronization

The most accurate method of transferring time in the frequency is by radio transmissions. The foremost familiar stations employed are WWV at Beltsville, Maryland; WWVH at Maui, Hawaii; WWVB at Fort Collins, Colorado, and WWVL at Fort Collins, Colorado. WWV and WWVH are at HF and as a consequence rely on skywave propagation for most of their coverage region. An example of the deterioration in accuracy is given by the two and one-half megacycle frequency for WWV. For ground-wave operation, about one part in 10^{11} can be maintained on frequency (with proper corrections applied) while typical skywave accuracy is about a part in 10^{7}. These skywave limitations led to the use of VLF and LF broadcasts such as WWVB and WWVL. For these frequencies the frequency can be calibrated to about a part 10^{11} over a 24 hour period. The most promising technique for time

synchronization at the present time rests with the LORAN C System Type System. A network of LORAN C stations could be made world-wide and make possible time synchronization between various master and slave stations to about a tenth of a microsecond. To obtain the very long-range groundwave coverage, the frequency of an LF frequency of about 100 kc is employed for the transmitter. A pulsed signal is used in this application. The pulsed signal makes it possible to discriminate against the skywave return by essentially operating on the leading portion of the waveform an eight-pulse group is employed by the transmitter. Pulses in the pulse group are separated by about one millisecond and the pulse trains are repeated about twenty times a second. With just the master in operation propagation affects would only allow accuracies in the order of about a microsecond due to the uncertainty in the propagation paths, particularly over land. Higher accuracy is obtained when the slave stations retransmit the signal from the master and calibration is made for propagation affects. The slaves employ a nine pulse code rather than an eight pulse code for the master to simplify recognition of the various signals. The primary limitation to transmission bandwidth in this frequency range is associated with the transmitting antennas that can be practically realized. Bandwidths in the order of about 10 kc are about all that can be practically attained in this portion of the frequency spectrum. For a network of radars such as employed in the Apollo program, the LORAN C technique appears to afford the greatest possibility for time synchronization between the various stations with the greatest accuracy at this time. Careful calibration technique should allow time synchronization to the order of about the tenth microsecond, but probably this represents the limitation to the over-all technique.

The only other technique which can even hope to attain better accuracy would involve precise stable oscillators originally set to the same frequency and possessing essentially negligible long-term drift. These standards would then need to be transported to the respective locations and recalibrated at times corresponding to the accuracy

requirements that can be practically afforded. In summary, it can be stated that with the advent of the atomic frequency standards the possibilities for very precise frequency operation and good time synchronization is well within the realm of reason.

APOLLO NOTE NO. 141

G. F. Floyd
14 November 1963

RANGE VERSUS DOPPLER MEASUREMENTS

Each spacecraft has only one transponder so only one MSFN station can be transmitting at a time. However, all MSFN stations that can see the Moon 5^{o} above horizon can receive the returned signal. From Apollo Note No. 116 this means that at least three and usually four stations can receive.

Range Mode

If we operate in the ranging mode (pseudo-random range code), then the receiving stations must use a clock to decide the time at which the transmitting station transmitted the long coded pulse. The bias error in measured range associated with the range measurement is then just $(\frac{c}{2}\Delta t)$. Thus if the clocks are synchronized to 1/10 of a millisecond, the bias would be $1.5 \times 10^{8} \times 10^{-4} = 15,000$ meters and synchronization to 1 microsecond implies a bias of 150 meters. Also since the Moon is 4×10^{8} meters from the Earth, an uncertainty in the speed of light of a part in 10^{6} gives a bias of 400 meters. Consequently, when we consider the operation of the MSFN with multiple stations measuring range, to be realistic we should assume a bias which is large enough that it is best to compute it.

Doppler Mode

In the doppler mode, the received signal is mixed with the signal from the signal from the local frequency reference and cycles of the beat frequency (which is proportional to $\dot{R}$), are simply counted. Thus the measured quantity is really cycles of the doppler and each cycle of the beat frequency corresponds to a range change of $\lambda/2$. Thus, with a perfect system if we started the counter at time zero, the measured quantity at time (t) would be $R(t) - R(0)$. Such

measurements are usually reported in terms of range-rate by taking differences of the doppler cycle count and dividing by the elapsed time between readings. The fact remains, however, that in the doppler mode, the system is measuring the change in range which has occurred since lock-on was achieved. Thus in the doppler mode, we can accurately think of the measurement as being a range measurement with a large unknown bias (where the "bias" is the initial value of ranges).

In addition, in the doppler mode, we can also have an average error rate, due solely to the average error rate of our time standard. If the clock has an error rate of k sec/sec or k parts, then the measured range has an error rate $\Delta\dot{R}$ of $\frac{c}{2}$ k, so that over a time (t) the doppler range (change) measurement will be in error by $\frac{c}{2}$ kt.

Modern clocks (temperature controlled rubidium standards), have long term drift rates of 2×10^{-12} so that over 1/2 hr. the range error introduced by the clock is

$$2 \times 10^{-12} \times 1.5 \times 10^{8} \times 1.8 \times 10^{3} = 1/2 \text{ meter.}$$

This drift rate is of the same order as the Mariner II measured and 2 kmc calculated (Apollo Note No. 118), propagation effects due to uncertainties in the integrated electron density in space and in the troposphere. These yield drift errors of $3 \times 10^{-12} = 3/4$ m with correlation times of 20 minutes or so.

The other major error in the doppler mode is not really a measurement error but arises because the transponder is not located at the center of gravity. Therefore, spacecraft attitude oscillations cause the measured doppler range to vary. Since the transponder is about 2 m from the center of gravity (1/2 spacecraft diameter), spacecraft wobble will cause range changes between $\pm$ 2 m with a 1σ of say 3/4 m.

There are no other significant errors in the doppler mode since transponder jitter only amounts to fractions of a cycle or fractions of $\lambda/2 = .075$ m.

Therefore, over measurement intervals of 1/2 hour, the performance of the MSFN in its doppler mode may be computed by assuming that the measurable is Range with a large bias, a σ of 1 meter, and a correlation time of say 1 minute (although the propagation errors will change more slowly and the attitude errors more rapidly).

It is expected that the long term stability of clocks will be improved by at least another order of magnitude in the next few years and then we could use these numbers for the doppler mode over times of 5 hours or longer.

With both the range and doppler mode being equivalent to "range with a bias," it is obvious that the choice between them depends only on the σ. On the doppler mode, over 1/2 hour or less, we have $\sigma \simeq 1$ meter, while in the range mode $\sigma \simeq 15$ meters so the doppler mode will yield misses just 15 times smaller and is preferred for short observation times such as during rendezvous. On the other hand, for observations over days, the clock drift error would cause the doppler error to grow beyond that of the ranging mode, and so range mode operation would be best.

APOLLO NOTE NO. 142

C. H. Dale
18 November 1963

FURTHER ESTIMATES OF EARTH-MOON INJECTION ERRORS

This note presents a continuation of the work started in Apollo Note No. 122. The injection trajectory studied is the same and the stations used are Carnarvon and Canberra as before. However, this note considers variations in tracking time and radar characteristics.

In Apollo Note No. 122 two UFS radars (in Canberra and Carnarvon) each measured range and range-rate. No bias error in range is predicated. This is probably not realistic since, in the doppler mode range and range-rate are not independent, and with simultaneous stations only one can transmit and thus measure range directly. With the UFS in the doppler mode, each receiving station can surely measure doppler range. This is equivalent to measuring range with an unknown but constant bias added to the random, zero-mean noise. The actual data sample rate is probably closer to one (1) second than one (1) minute. The assumption used here is: $\sigma R =$ 15 meters for one second samples. The results shown in Figure 1 for the UFS scale directly with σR.

The poor results for the two UFS stations shown in Figure 1 can be improved in a number of ways: first, σR may well be an order of magnitude better than the assumed 15 m. ; second, a priori knowledge of the range bias may help; and third, antenna angle information ($\sigma\phi_1 = \sigma\phi_2 = 8 \times 10^{-4}$ radians) might be expected to improve the out-of plane component of velocity sizably.

The result of using an FPS-16 type radar from one station is significantly better than the above UFS example. The assumed characteristics of the FPS-16 are: $\sigma R = 6$ meters, angle accuracy ($\sigma\phi_1 = \sigma\phi_2$) = 2×10^{-4} radians, for one second uncorrelated data samples. No biases are assumed.

Also shown is the result of combining the data of the two UFS stations with the single FPS-16.

A conclusion, regarding the FPS-16, is that a single radar

appears to be capable of resolving the required GO/NO GO decision in well less than the allotted ten-minute tracking time.

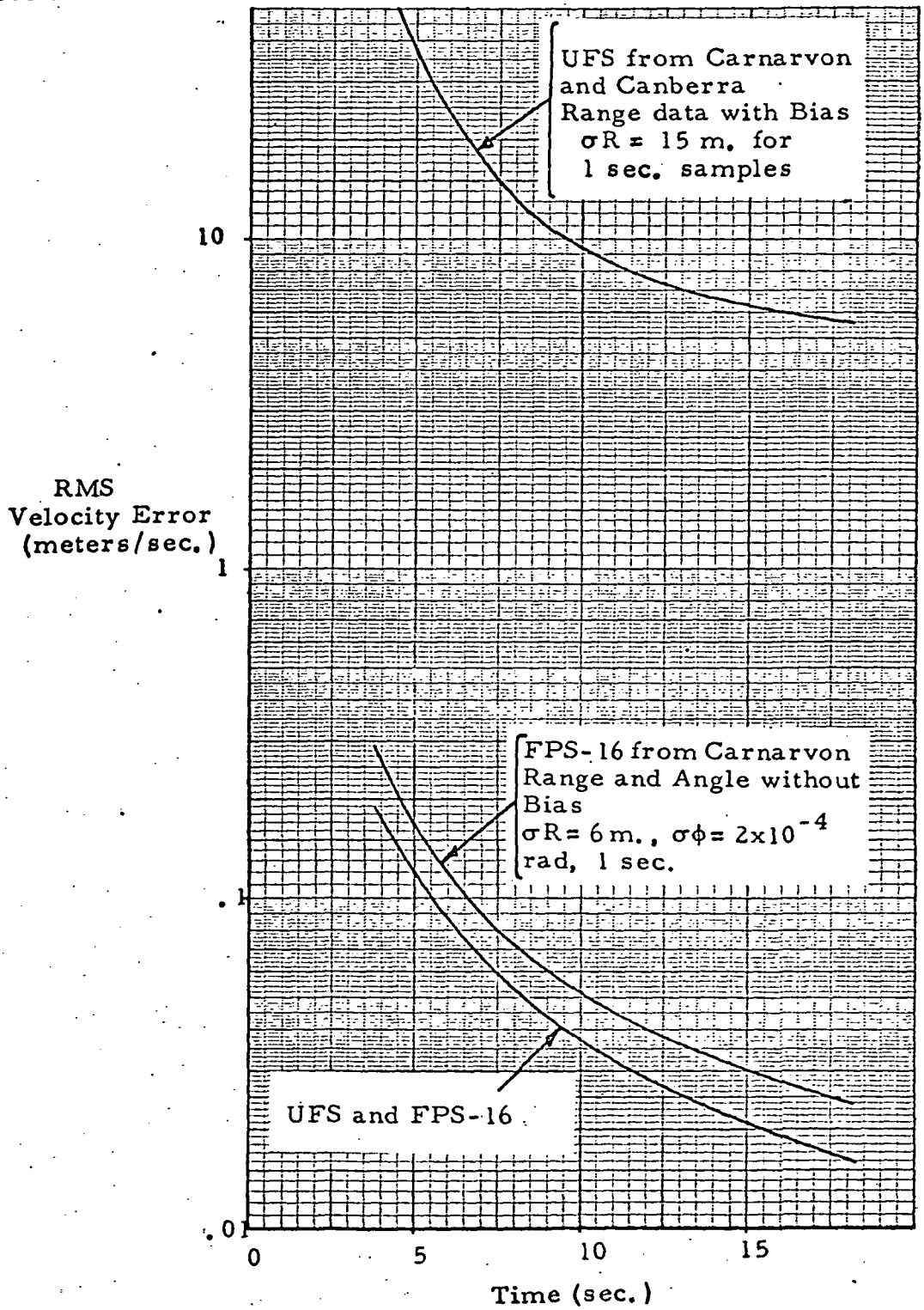
UFS from Carnarvon and Canberra Range data with Bias σR = 15 m. for 1 sec. samples
FPS-16 from Carnarvon Range and Angle without Bias σR = 6 m., σφ = 2x10^-4 rad, 1 sec.
UFS and FPS-16
RMS Velocity Error (meters/sec.)
10
1
.1
.01
0
5
10
15
Time (sec.)

Figure 1

A comparison of UFS and FPS-16 Tracking for Trans-Lunar Injection

APOLLO NOTE NO. 143

H. Engel
19 November 1963

COMMUNICATION AND COMPUTATION LOAD

Introduction

Apollo Note No. 93 has already outlined the computations that must be performed for best determination of the orbit parameters of a vehicle in orbit about the Moon. This note examines further some of the problems of communication and computation in obtaining timely results.

Communications

Let us first dispose of the communications problem. We assume that only range-rate measurements are used. If range-rate transmission is to be accurate to 10^{-3} m/sec. and the maximum range-rate magnitude is 12,000 m/sec, then 25 bits suffice to specify range-rate. In non-boosting flight the acceleration is less than 10 m/sec^2., so if the range-rate measurements are to be accurate to the order of 10^{-3} m/sec., the time of the range-rate measurement does not have to be specified to better than 10^{-4} seconds. If, to avoid ambiguity, the time code does not repeat for five seconds, 16 bits are adequate to indicate time to the desired accuracy.

Together, specification of range-rate and time of measurement require 41 bits. If the range-rate and time are completely specified once per second, the necessary bit rate is 41 bits per second. For comparison, metallic telegraph has a bit rate of the order of 30 bits/sec., and high-speed lines have capacities of 1200 or 2400 bits/sec.

The amount of data that must be transmitted may be reduced, however, since it is highly redundant. If range-rate is transmitted every second, the difference between two successive range-rates cannot exceed 10 m/sec., and can be specified accurate to 10^{-3} m/sec.

with only 14 bits. If the times of measurement are specified beforehand, then it is only necessary to identify each measurement, and this can probably be done accurately with only 6 bits. The required data rate is then just 20 bits/sec. This rate will have to be increased by a slight amount to permit less frequent but periodic transmission of the full 41 bits of range-rate and time to avoid propagation of any chance errors.

In any case the data rate requirements are not high, even with one measurement per second, and communications does not appear to limit the data processing rate.

Computation

There are at least two computation problems, with different requirements, to be considered. In the first, a comparatively long time (like a minute or more) is available for computation and complex computations are required. In the second, very little time (a second or two) is available for computation, but fortunately the computations are simpler.

The first kind of problem has already been described in Apollo Note No. 93, in which it was found that the necessary computations can be performed in just a few seconds if a complete set of data is received once a minute.

It is of some interest to discover the maximum rate at which data can be accepted for processing in this first kind of problem. The time, τ, required per iteration can be expressed as

$$\tau = a + b^2/T^2$$

in which a and b are constants and T is the time between successive sets of data. At the highest allowable data rate, the iteration time is equal to the time between successive sets of data. At any higher data rate, the computations lag further and further behind. From Apollo Note No. 93 it appears that reasonable values for a and b are 0 and 14.7 seconds, respectively, if the computations are

performed in the manner indicated in that note but using range-rate from two stations. Substituting in the equation given above indicates that the minimum interval at which sets of data can be accepted and processed in this manner is 14.7 seconds.

In this first kind of problem the total time that may be allowed for observations may vary from five to thirty minutes or more so 20 to more than 120 sets of observations must be processed in each iteration, and this can be done in the prescribed 14.7 seconds. In general, the variance associated with the range-rate measurements varies inversely with the measurement duration, so that increasing the number of measurements by decreasing the duration of each does not improve the accuracy with which the orbit parameters can be determined, so long as the number of measurements is not small. In this case, then, it does not pay to try to decrease the measurement interval.

In the second kind of problem it is necessary to obtain an estimate of the vehicle position and velocity in a short time--of the order of seconds or a very few minutes. Since the vehicle does not move very far in this time, it is possible to simplify the equations of motion, ignoring all gravitational effects but the radially symmetric portion of the Moon's field for lunar orbits. Still further, a linear technique such as the Kalman-Schmitt method can be used to determine the position and velocity to sufficient accuracy. The far smaller amount of computation required in these linear techniques makes it possible to accept a complete set of data every second for processing. In this case, it is desirable to accept data at the higher rate in order to obtain a reasonable number of data points in a very short time.

Appendix

A linear method of determination of orbit parameters, given a reference or a priori set of orbit parameters is given here. The advantages of this method are that the results are not obtained iteratively and that only one matrix inversion is required each time the orbit parameters are to be evaluated, no matter how many

intermediate data sets are used.

We use the following definitions:

x_n State column vector at time t_n. 0 on reference trajectory.

ϕ_n $x_n = \phi_n x_o$. We assume that ϕ_n is not function of x_o (linear assumption)

y_n Measurement column vector at t_n. 0 on the reference trajectory.

M_n $y_n = M_n x_n$

u_n Random noise in measurement of y_n.
$E(u_n) = 0$

Q_n $Q_n = E(u_n u_n^T)$. $E(u_n u_m^T) = \delta_{mn} Q_n$

Q_n is assumed known a priori

y_n^* Measured value of y_n. $y_n^* = y_n + u_n$

x_{on}^* Best linear estimate of x_o based on all y_i^* $(i = 0, \ldots, n)$.
$E(x_{on}^*) = x_o$

Then, $\phi_i x_{on}^*$ is the best linear estimate of x_i, and $M_i \phi_i x_{on}^*$ is the best estimate of y_i. In order to obtain the best least squares fit to the data we must minimize $\mathcal{L}_n$,

$$\mathcal{L}_n = -\frac{1}{2} \sum_{i=0}^{n} (y_i^* - M_i \phi_i x_{on}^*)^T Q_i^{-1} (y_i^* - M_i \phi_i x_{on}^*)$$

In order to do this we set the first partial derivatives of $\mathcal{L}_n$ with respect to each of the components of x_o equal to 0.

$$0 = \sum_{i=0}^{n} (M_i \phi_i)^T Q_i^{-1} (y_i^* - M_i \phi_i x_{on}^*)$$

$$+ \sum_{i=0}^{n} (y_i^* - M_i \phi_i x_{on}^*)^T Q_i^{-1} (M_i \phi_i)$$

or

$$0 = \sum_{i=0}^{n} (M_i \phi_i)^T Q_i^{-1} (y_i^* - M_i \phi_i x_{on}^*)$$

Letting

$$V_n = \sum_{i=0}^{n} (M_i \phi_i)^T Q_i^{-1} (M_i \phi_i)$$

and

$$W_n = \sum_{i=0}^{n} (M_i \phi_i)^T Q_i^{-1} y_i^*$$

We find by substitution in the equation above that

$$x_{on}^* = V_n^{-1} W_n.$$

Let

$$Z_n = \sum_{i=0}^{n} (M_i \phi_i)^T Q_i^{-1} y_i$$

Then, since $E(x_{on}^*) = x_o$, the covariance matrix of $x_{on}^* - x_o$ is P_n^*,

$$P_n^* = E\left[(x_{on}^* - x_o)\ (x_{on}^* - x_o)^T \right]$$

$$= E\left[\left\{ V_n^{-1} (W_n - Z_n) \right\} \left\{ V_n^{-1} (W_n - Z_n) \right\}^T \right]$$

$$= V_n^{-1}\ E\left[\left\{ \sum_{i=0}^{n} (M_i \phi_i)^T Q_i^{-1} u_i \right\} \left\{ \sum_{i=0}^{n} (M_i \phi_i)^T Q_i^{-1} u_i \right\}^T \right] V_n^{-1}$$

$$= V_n^{-1}\ E\left[\left\{ \sum_{i=0}^{n} (M_i \phi_i)^T Q_i^{-1} u_i \right\} \left\{ \sum_{i=0}^{n} u_i^T Q_i^{-1} (M_i \phi_i) \right\} \right] V_n^{-1}$$

However, $E(u_n u_m) = \delta_{mn} Q_n$, so

$$P_n^* = V_n^{-1}\ E\left[\sum_{i=0}^{n} (M_i \phi_i)^T Q_i^{-1} Q_i\ Q_i^{-1} (M_i \phi_i) \right] V_n^{-1}$$

$$= V_n^{-1}\ E\left[\sum_{i=0}^{n} (M_i \phi_i)^T Q_i^{-1} (M_i \phi_i) \right] V_n^{-1}$$

$$= V_n^{-1}\ V_n\ V_n^{-1}$$

$$= V_n^{-1}$$

In summary,

$$V_n = \sum_{i=0}^{n} (M_i \phi_i)^T Q_i^{-1} (M_i \phi_i)$$

$$P_n^* = V_n^{-1}$$

$$W_n = \sum_{i=0}^{n} (M_i \phi_i)^T Q_i^{-1} y_i^*$$

$$x_{on}^* = P_n^* W_n$$

The quantities M_i, ϕ_i, Q_i^{-1} are all known beforehand so the quantities P_n^* and $(M_i \phi_i)^T Q_i^{-1}$ can be computed beforehand leaving only some simple matrix multiplications.

APOLLO NOTE NO. 144

C. H. Dale
20 November 1963

EARTH ORBIT INJECTION AND TRACKING ERRORS

On September 27, 1963 a letter was sent to us from Dr. F. O. Vonbun which defined four problems suitable for our analysis. This Apollo Note partially solves the first three problems. These three problems are listed below for reference.

1. Calculate the position and velocity errors and the corresponding errors in the orbital elements for a one station solution for parking orbit number one, see GSFC Report X-520-62-211, page 9. Also calculate the 3 σ ellipsoid of error and its eigenvectors in inertial space. $\alpha = 90^{\circ}$ - case, all other information is on the graph on page 9.
   a. The station should be Bermuda.
   b. The station should be Carnarvon.

2. Calculate the same for the two and three stations, namely:
   a. Bermuda and Carnarvon.
   b. Bermuda, Carnarvon and Guaymas.

Use the following errors for the FPS-16 radars and the Unified Frequency System (UFS) respectively:

FPS-16: (RCA data!)
$\delta r = 6$ m
$\delta \alpha = \alpha e = 2.10^{-4}$ rad.
$\delta \dot{r} = 6$ m/s

Assume one measurement every second.

Unified S-Band System:
$\delta r = 15$ m
$\delta \alpha = \delta e = 8.10^{-4}$ rad.
$\delta \dot{r} = 0.1$ m/s

Calculate these errors, first assuming that the location of the stations are known exactly, then assume a station error of $\pm$ 64 meters in the north, $\pm$ 64 meters in the east and $\pm$ 10 meters

for the error in the height of the station. The sampling rate is one measurement per second, therefore, it is assumed that the data are uncorrelated. ($\rho \leq 0.1$ to 0.2; AMR results)

3. Calculate the position and velocity errors for the $\alpha = 90^{\circ}$ orbit as shown in Figure 1 of GSFC Report X-500-63-190 after the spacecraft leaves the 5° horizon of ship number one.

a. Use FPS-16 radar data only.

b. Use FPS-16 and UFS data.

For a. and b. above use station errors such as:

Cape	None
Bermuda	$\pm$ 64 m north and $\pm$ 64 m east $\pm$ 10 m height
Ship Number One	(1) $\pm$ 200 m north and $\pm$ 200 m east and $\pm$ 20 m height
	(2) $\pm$ 1000 m north and $\pm$ 1000 m east and $\pm$ 20 m height

A number of detail computer program deficiencies have held up a quick answer to the above problems, and as yet we have not included the effect of station location errors (see Apollo Note No. 108). The covariance matrix of position and velocity errors may be diagonalized thus giving positional and velocity error ellipsoids (see Apollo Notes No. 126 and 136). This also has not been programmed; thus the results presented in this note are $\sigma_{\dot{x}}$, $\sigma_{\dot{y}}$, $\sigma_{\dot{z}}$, and RMS V at the end of tracking as defined in Apollo Note No. 82. The RMS V is simply the square root of the sum of the fourth, fifth, and sixth diagonal elements of the covariance matrix of the orbital parameter estimators defined at the termination of tracking for the last station.

The following chart is a tabulation of the computer results showing velocity errors and the RMS positional error at the last point of tracking.

Stations	Radar	Bias Errors	$\sigma\dot{x}$	$\sigma\dot{y}$	$\sigma\dot{z}$	RMS V	RMS Position Error
			meters/second				meters
Bermuda	UFS	YES	39.9	10.5	161.	167.	26×10^3
Alone		NO	3.16	.134	1.75	3.65	164
	FPS-16	YES	13.1	8.9	47.0	49.6	11×10^3
(.86 min.)		NO	1.10	.445	.740	1.40	50
	BOTH	YES	11.1	3.16	43.1	44.6	7.1×10^3
		NO	1.02	.071	.538	1.16	44
Bermuda and	UFS	YES	.059	.039	.063	.095	60
Ship No. 1		NO	.048	.015	.032	.060	20
	FPS-16	YES	.156	.086	.125	.218	81
		NO	.040	.010	.026	.049	11
Carnarvon	UFS	YES	.100	.110	1.21	1.22	1720
Alone		NO	.086	.020	.361	.371	33
	FPS-16	YES	.184	.167	.546	.600	240
(5.0 min.)		NO	.051	.013	.140	.149	13
	BOTH	YES	.082	.087	.380	.397	110
		NO	.044	.010	.122	.130	11
Bermuda and	UFS	YES	.067	.022	.870	.873	95
Carnarvon		NO	.026	.006	.267	.269	16
	FPS-16	YES	.130	.020	.259	.290	83
		NO	.010	.003	.088	.089	8.4
Bermuda,	UFS	NO	.002	.002	.015	.015	3.6
Ship No.1	FPS-16	NO	.002	.002	.010	.011	2.7
and Carnarvon							

Computer Results

"Bias Errors" are defined as unknown constant errors in the measurables (range and angle but not range-rate) which must be estimated along with the orbit parameters. When the number of data samples is small the inclusion of the effect of bias errors degrades the results drastically. Thus with the Bermuda station alone, which can track the reference trajectory for only 0.86 minutes after booster cut-off, a forty-to-one degradation in the measurement of velocity occurs if unknown bias errors are assumed. As the measuring time increases, or the number of stations increase, this degradation is soon reduced to less than three-to-one.

The very short observation time appears to limit the utility of the "Bermuda alone" measurement of the Earth orbit insertion. Even without bias-error effects, the FPS-16 appears to be of only borderline utility. However, the true ability of the FPS-16 is probably closer to the "unbiased" result than it is to the 49.6 m/s result obtained with biases. This can be shown by looking at how well the three biases (range and two angles) were estimated by smoothing the 0.86 minutes of FPS-16 data. From the print-out of the covariance matrix:

$$\sigma \text{ Range Bias} = 2200 \text{ meters}$$
$$\sigma \text{ Angle Bias}_1 = 13.2 \text{ mils}$$
$$\sigma \text{ Angle Bias}_2 = 6.4 \text{ mils}$$

These numbers are quite a bit larger than what would be an a priori guess of the biases for the FPS-16. For instance, there is no reason to assume an angular bias error any larger than the random noise (0.8 mils). A proper evaluation of the Bermuda-alone case would thus include these a priori guesses at the biases and would probably reduce the FPS-16 velocity error to about ten meters per second. This, however, would still be too large (especially if the effects of station location errors were included) and thus the absolute necessity of Ship No. 1 (assuming radar-only orbit determination) is shown.

With Bermuda and Ship No. 1, it appears that a tenth of a meter per second is possible. The effect of station location errors must be determined before much more can be said.

By the time the vehicle first passes Carnarvon, the combined data (Bermuda, Ship No. 1 and Carnarvon) will yield the velocity to 0.015 meters/second. Again the effect of station location errors should be made before this number is taken too seriously.

ADDENDUM TO

APOLLO NOTE NO. 144

H. Dale
16 December 1963

CORRECTIONS DUE TO ERROR IN CARNARVON RISE TIME

The rise and set times at Carnarvon are wrong in Apollo Note 144, and this addendum presents the corrected computer results using the correct rise and set times. The following is an apologetic explanation of what happened.

Given the initial orbit conditions at insertion, the present computer program will calculate the rise and set times for any station. In the case of interest, the rise time at Carnarvon is 43.02 minutes, and the set time is 48.02 minutes, both measured from booster burnout which occurs at 200 km altitude with a latitude of 27.0° N and longitude of 60.5° W. The orbit is circular.

However, when Apollo Note No. 144 was written, rise and set times were not computed within the program and were required as inputs. The rise time was incorrectly estimated as 39.4 minutes through the use of Figure 4c of "Trajectory Studies for Use in Determining Tracking Requirements for Project Apollo," dated August 30, 1963, prepared by NASA Manual Spacecraft Center/Mission Planning Department. The result of using this "too early" time caused the Carnarvon to track a distant target which did not move much in angle. Using the convected time thus gives much better results since the angular motion of the pass is much larger.

Following is a chart showing the corrected results.

Corrected Computer Results

Stations	Radar	Bias Errors	$\sigma \dot{x}$	$\sigma \dot{y}$	$\sigma \dot{z}$	RMS V	RMS Position Error
			meters/second				meters
Carnarvon	UFS	YES	.055	.020	.147	.159	49.6
Alone		NO	.054	.010	.142	.152	23.2
	FPS-16	YES	.105	.024	.052	.119	19.3
(5.0 min.)		NO	.045	.007	.038	.059	9.3
	BOTH	YES	.047	.010	.039	.061	13.6
		NO	.034	.005	.036	.050	7.7
Bermuda and	UFS	YES	.018	.008	.135	.136	28.2
Carnarvon		NO	.014	.005	.085	.087	18.4
	FPS-16	YES	.034	.021	.048	.063	12.7
		NO	.008	.004	.029	.030	5.4
Bermuda,	UFS	NO	.001	.002	.014	.015	3.6
Ship No. 1	FPS-16	NO	.001	.001	.010	.010	2.0
and Carnarvon							

APOLLO NOTE NO. 145

H. Engel
4 December 1963

OPTIMUM ONE-BOOST CORRECTION TO LEM ASCENT TRAJECTORY

The optimum one-boost correction to the LEM ascent trajectory is defined as the single impulsive boost during the LEM ascent transfer orbit that will minimize the distance between the LEM and CSM at the nominal time of rendezvous. An optimum exists because of two conflicting factors:

1. The longer the LEM is observed before boost the better the necessary boost can be determined, and

2. The later the LEM boosts, the larger the required boost and the larger the error in the performance of the commanded boost.

Let x(t) be a 6-dimensional column state vector denoting the difference between the position and velocity on the nominal ascent trajectory and the actual position and velocity at time t. x(t) is zero on the nominal ascent trajectory. t_o corresponds to burnout, t_1 is the time just before the impulsive boost correction, t_2 is the time just after the impulsive boost correction ($t_2 - t_1 = 0$), and t_3 is the nominal time of rendezvous. x_o x_1, x_2 and x_3 are the state vectors on the actual trajectories corresponding to the times t_o through t_3. x_F is the state vector at t_3 if there were no corrective boost.

We also let $Q_{a,b}$ be the 6 x 6 Jacobian matrix that translates a state vector x_u at time t_a into one x_v at time t_b.

$$Q_{a,b} = \left[\frac{\partial x_{ui}(t_b)}{\partial x_{vj}(t_a)}\right]$$

where x_u, x_v are on the same trajectory.

Then for the actual vehicle motion,

$$x_1 = Q_{o,1}\, x_o$$

and with a change in state Δx due to the impulsive correction boost,

$$x_2 = x_1 + \Delta x$$

and the resultant state vector at the time of rendezvous is

$$x_3 = Q_{1,F}\, x_2.$$

By substitution, we find

$$x_3 = Q_{1,F}\, x_1 + Q_{1,F}\, \Delta x$$

$$= x_F + Q_{1,F}\, \Delta x$$

Now each x_i and Δx are six dimensional column state vectors, the first three elements representing position and the last three representing velocity. Let us then write

$$\begin{bmatrix} x_i \end{bmatrix} = \begin{bmatrix} P_i \\ V_i \end{bmatrix}$$

in which P_i and V_i are 3-dimensional column vectors representing the position and velocity components, respectively, of x_i.

We let $\hat{x}_F$ be the estimated value of the state vector at t_3 in the absence of boost, based on a priori data and on observations between t_o and t_1. The estimated change in the state vector at time t_1 required to cause the miss to be zero at time t_3 is called $\Delta\hat{x}$. Then we have

$$\hat{x}_3 = \hat{x}_F + Q_{1,F}\, \Delta\hat{x}$$

in which $\hat{x}_3$ is the state vector that would result at t_3 from $\hat{x}_F$ and $\Delta\hat{x}$. Since the desired value of $\hat{P}_3$ is zero, this leads to

$$\begin{bmatrix} 0 \\ \hat{V}_3 \end{bmatrix} = \begin{bmatrix} \hat{P}_F \\ \hat{V}_F \end{bmatrix} + \begin{bmatrix} Q_{1,F} \end{bmatrix} \begin{bmatrix} 0 \\ \Delta\hat{V} \end{bmatrix}$$

Now, writing

$$Q_{1,F} = \begin{bmatrix} \alpha & \beta \\ \gamma & \delta \end{bmatrix}$$

we find that

$$\beta \Delta\hat{V} = -\hat{P}_F$$

or

$$\Delta\hat{V} = -\beta^{-1}\hat{P}_F$$

The actual change in the state vector at time t_1 differs from $\Delta\hat{V}$ because the autopilot is not perfect. We denote the error in the execution of $\Delta\hat{V}$ by $\Delta\tilde{V}$, and assume that the standard deviation of $\Delta\tilde{V}$ is proportional to $\Delta\hat{V}$ and is equally likely to be in any direction. Then

$$\Delta x = \begin{bmatrix} 0 \\ \Delta\hat{V} + \Delta\tilde{V} \end{bmatrix}$$

and, by substitution, in

$$x_3 = x_F + Q_{1,F}\,\Delta x$$

we find

$$P_3 = P_F + \beta\,(\Delta\hat{V} + \Delta\tilde{V})$$

$$= P_F + \beta\,\Delta\hat{V} + \beta\,\Delta\tilde{V}$$

$$= P_F - \hat{P}_F + \beta\,\Delta\tilde{V}$$

Now $\hat{P}_F - P_F$ is the error in the estimate of P_F, and we shall denote it by P_{Fe}. Thus

$$P_3 = -P_{F_e} + \beta \Delta \tilde{V}$$

The expected values of P_3, P_{F_e} and $\Delta \tilde{V}$ are zero, and

$$\overline{P_3 P_3^T} = \overline{(-P_{F_e} + \beta \Delta \tilde{V})(-P_{F_e} + \beta \Delta \tilde{V})^T}$$

$$= \overline{P_{F_e} P_{F_e}^T} + \overline{\beta \Delta \tilde{V} \Delta \tilde{V}^T \beta^T}$$

since the directions of P_{F_e} and $\Delta \tilde{V}$ are uncorrelated.

Now,

$$\overline{\Delta \tilde{V} \Delta \tilde{V}} = k^2 \overline{\Delta \hat{V}^T \Delta \hat{V}} = \text{tr } \overline{\Delta \tilde{V} \Delta \tilde{V}^T}$$

and further $\overline{\Delta \tilde{V} \Delta \tilde{V}^T}$ is a diagonal matrix, so

$$\overline{P_3^T P_3} = \text{tr } \overline{P_3 P_3^T}$$

$$= \text{tr } \overline{P_{F_e} P_{F_e}^T} + \text{tr } \beta \overline{\Delta \tilde{V} \Delta \tilde{V}^T} \beta^T$$

$$= \text{tr } \overline{P_{F_e} P_{F_e}^T} + k^2 \overline{\Delta \hat{V}^T \Delta \hat{V}} \text{ tr } \beta\beta^T$$

In other words, the mean square miss at rendezvous is equal to the mean square error of the miss at rendezvous in the absence of a corrective boost plus a quantity directly proportional to the estimated required corrective boost.

Proceeding further, we have that

$$\Delta \hat{V} \Delta \hat{V}^T = (-\beta^{-1} \hat{P}_F)(-\beta^{-1} \hat{P}_F)^T$$

$$= \beta^{-1} \hat{P}_F \hat{P}_F^T \beta^{-T}$$

$$= \beta^{-1} (P_F + P_{F_e})(P_F + P_{F_e})^T \beta^{-T}$$

and

$$\overline{\Delta\hat{V}\,\Delta\hat{V}^T} = \beta^{-1}\left(\overline{P_F P_F^T} + \overline{P_{F_e} P_{F_e}^T}\right)\beta^{-T}$$

so the mean square miss is

$$\overline{P_3^T P_3} = \text{tr}\ \overline{P_{F_e} P_{F_e}^T} + k^2\ \text{tr}\,(\beta\beta^T)\,\text{tr}\left[\beta^{-1}\left(\overline{P_F P_F^T} + \overline{P_{F_e} P_{F_e}^T}\right)\beta^{-T}\right].$$

As the time t_1 increases, the first term in the above equation decreases, but the second may increase because of changes in β. Therefore to find the optimum time of boost, we evaluate $\overline{P_3^T P_3}$ for varying t_1.

APOLLO NOTE NO. 146

G. F. Floyd
21 November 1963

BISSETT-BERMAN PRESENTATION
at
GODDARD SPACE FLIGHT CENTER

November 21, 1963

1.	Orbit Errors Program	Now
2.	Orbit Errors Program	Soon
	Orbit Errors Program	Future
3.	Long Range, Short Time MSFN Operation	
4.	Best MSFN Operating Modes	
5.	MSFN Rendezvous Miss Uncertainty	
6.	Effect of Station Location	
7.	MSFN Stations	
8.	Ground Computations for Rendezvous	
9.	Earth Orbit Injection and Tracking Errors	
10.	Trans-Lunar Injection Tracking	
11.	Return to Earth Tracking Geometry	
12.	Return to Earth - No A priori Data	

ORBIT ERRORS PROGRAM Now

1. USE

Range, Range-Rate, Angle

Fixed Biases in Range and Angle

A priori Data on Position, Velocity or Biases

Any Combination of the above with Boosts Between Measurements

2. MEASURED FROM

Fixed Points on Rotating Earth

Fixed Points on Moon in Orbit about Earth

Vehicles in Circular Orbit about Moon or Earth

Any Combination of the above

3. DETERMINE

Position and Velocity of Vehicle at anytime in Circular or Elliptic Orbit about Earth or Moon

Covariance Matrix of Errors in Position and Velocity at any time

Accuracy of Prediction of Re-entry Conditions

ORBIT ERRORS PROGRAM — Soon

1. Hyperbolic Orbits
2. Station Location Errors
3. Visibility
4. Time-or Position-Varying Measurement Errors
5. Orientation and Principal Axes of Error Ellipsoids

ORBIT ERRORS PROGRAM — Future

1. Crossing LSOI
2. Correlated Data
3. Gravitational and Speed of Light Errors

LONG RANGE, SHORT TIME MSFN OPERATION

1) Multiple Station Range Data Implies Large Bias

Due to time synchronization (.01 ms = 1500 m),

and uncertainty in velocity of light ($10^{-6} \rightarrow$ 400 m).

Has large σ = 15 m.

2) "$\dot{R}$" Data Really $\left(\frac{\Delta R}{t_{meas}}\right)$

Clock drift only amounts to 0.5 m in 25 min.

So get R with Bias (R_o) from Doppler with

σ = 1 m = Propagation Uncertainties plus

Spacecraft wobble.

3) Multiple Station 1 m Range with Bias

Via Doppler Cycle Counting.

BEST MSFN OPERATING MODES

Observation Time	RANGE	
	SHORT	LONG
Short	Vector Range (R + 2 Angles)	Doppler Ranging (R + Bias)
Long	Vector Range	Random Range Code (Time Share Stations)

MSFN RENDEZVOUS MISS UNCERTAINTY

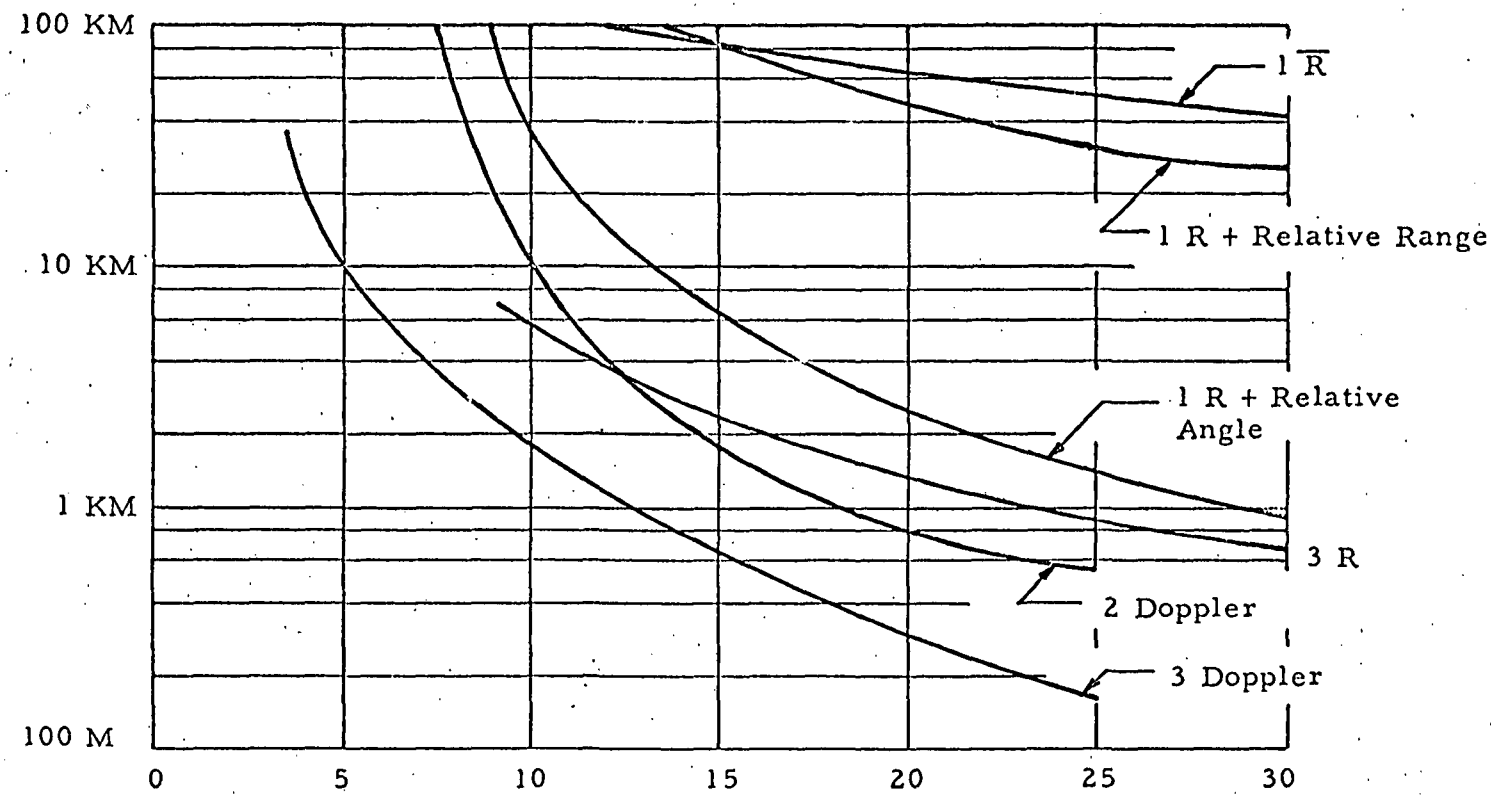

No A Priori Used

1 σ Values

Doppler:	1 m at 1 min.
Range:	15 m at 1 min. No Bias
Angles:	1 mil. (Rel); 0.8 mil (UFS)
Relative Range:	750 m. (1/2%)

EFFECT OF STATION LOCATION

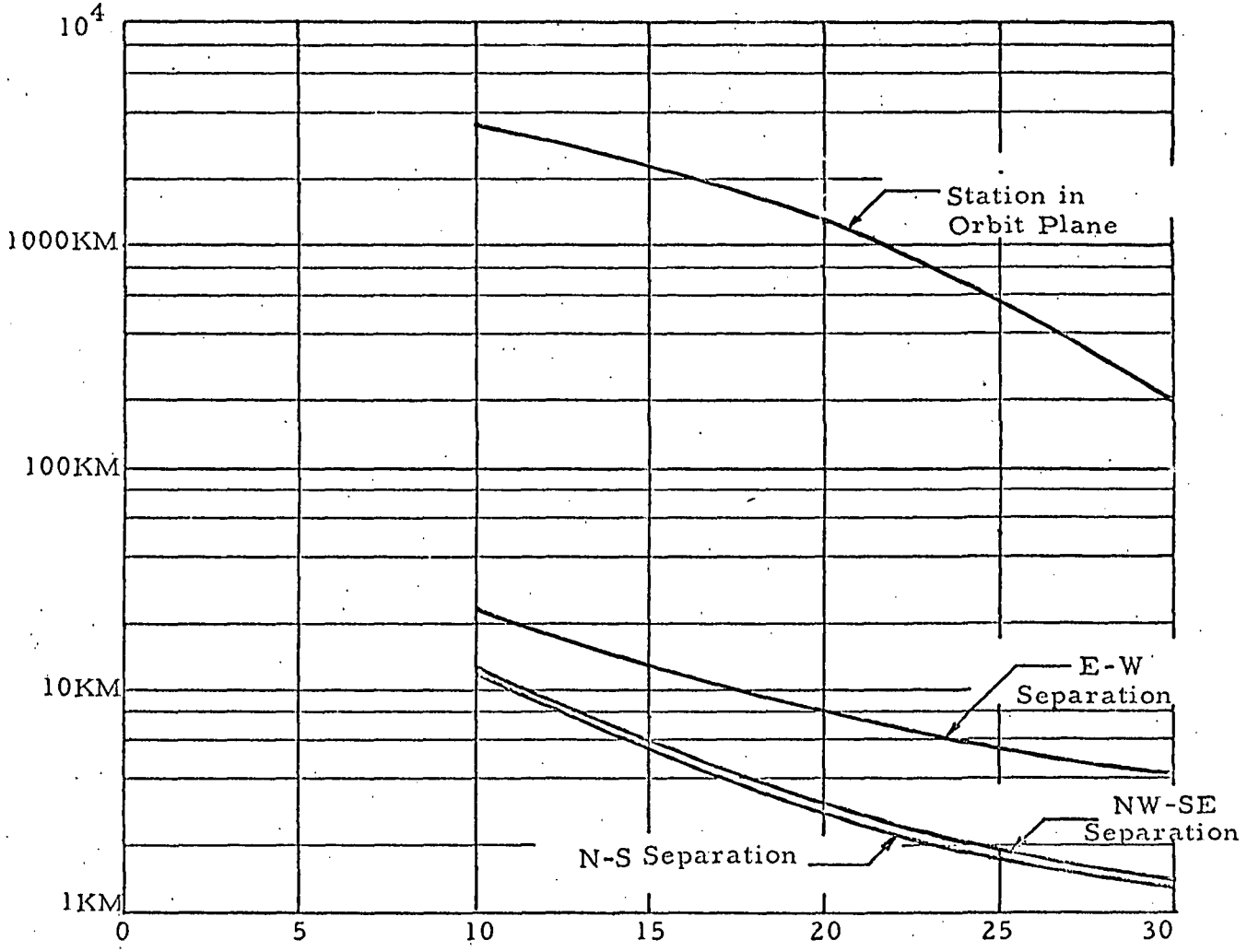

Minimum RMS Miss Near Rendezvous Using Range-Rate from Two Stations Separated by a Great Circle Distance of 40°

$\sigma_{\dot{R}} = 0.03$ m/sec.

MSFN STATIONS

Must Be Out Of Orbit Plane

Want Minimum of 3 MSFN Stations That Can See Moon

Goldstone, Canaveral, Hawaii, Guam,

Carnarvon, Canberra, Ascension,

Johannesburg, Madrid

GROUND COMPUTATIONS FOR RENDEZVOUS

GIVEN:

30 Values of Range, Range-Rate and Angle from each of 3 ground stations.

Six estimated orbit parameters.

COMPUTE:

Ephemeris of vehicle using Encke method.

Expected values of measurements.

Likelihood of measurements.

Corrections to orbit parameters.

TIMING:

One complete iteration of the above using all data requires 7 seconds on 7094.

EARTH ORBIT INJECTION AND TRACKING ERRORS

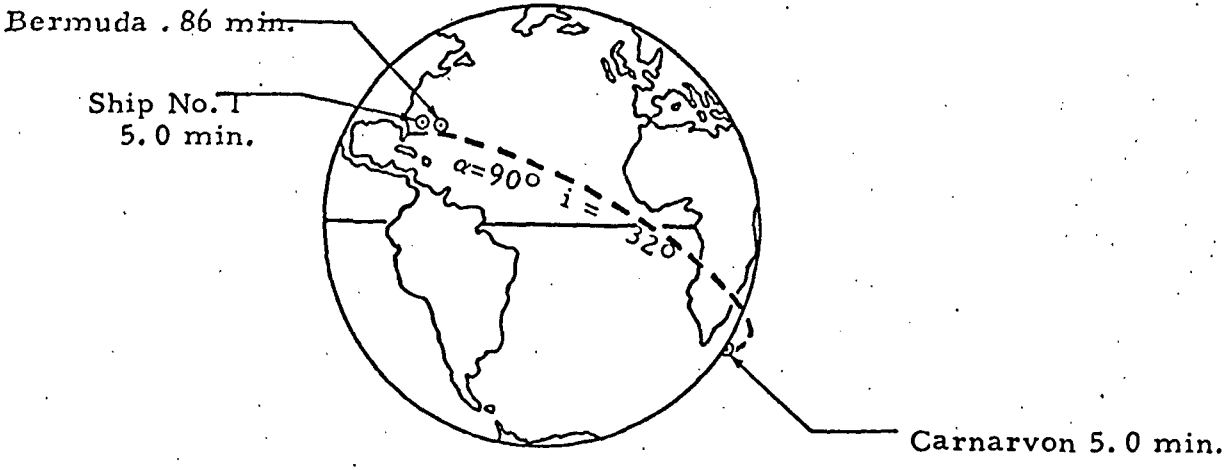

	RMS VELOCITY ERROR (M/S)		
	Bermuda Only	Bermuda + Ship No. 1	Bermuda + Ship No. 1 + Carnarvon
UFS: σ_R = 15 m; $\sigma_{\dot{R}}$ = 0.1 m/s; $\sigma_{\phi_1} = \sigma_{\phi_2} = 8 \times 10^{-4}$ r	3.65 (167.0)	.060 (.095)	.015
FPS-16 Only: σ_R = 6 m; $\sigma_{\dot{R}}$ = 6 m/s; $\sigma_{\phi_1} = \sigma_{\phi_2} = 2 \times 10^{-4}$ r	1.40 (49.6)	.049 (.218)	.011
UFS + FPS - 16	1.16 (44.6)		

(Numbers in parenthesis indicate unknown Range and Angle Biases were included in computations)

TRANS-LUNAR INJECTION TRACKING

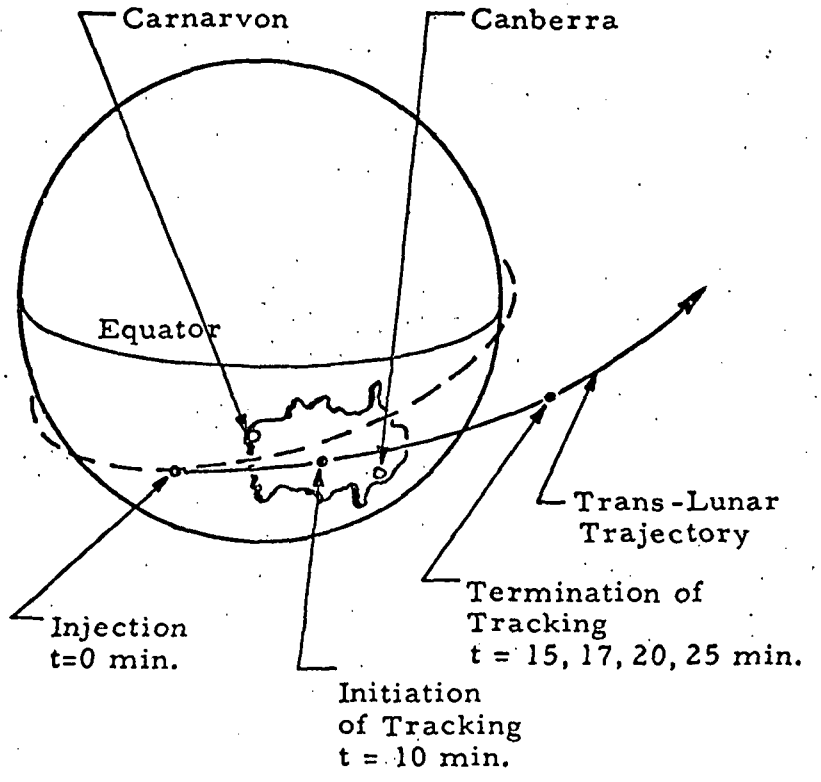

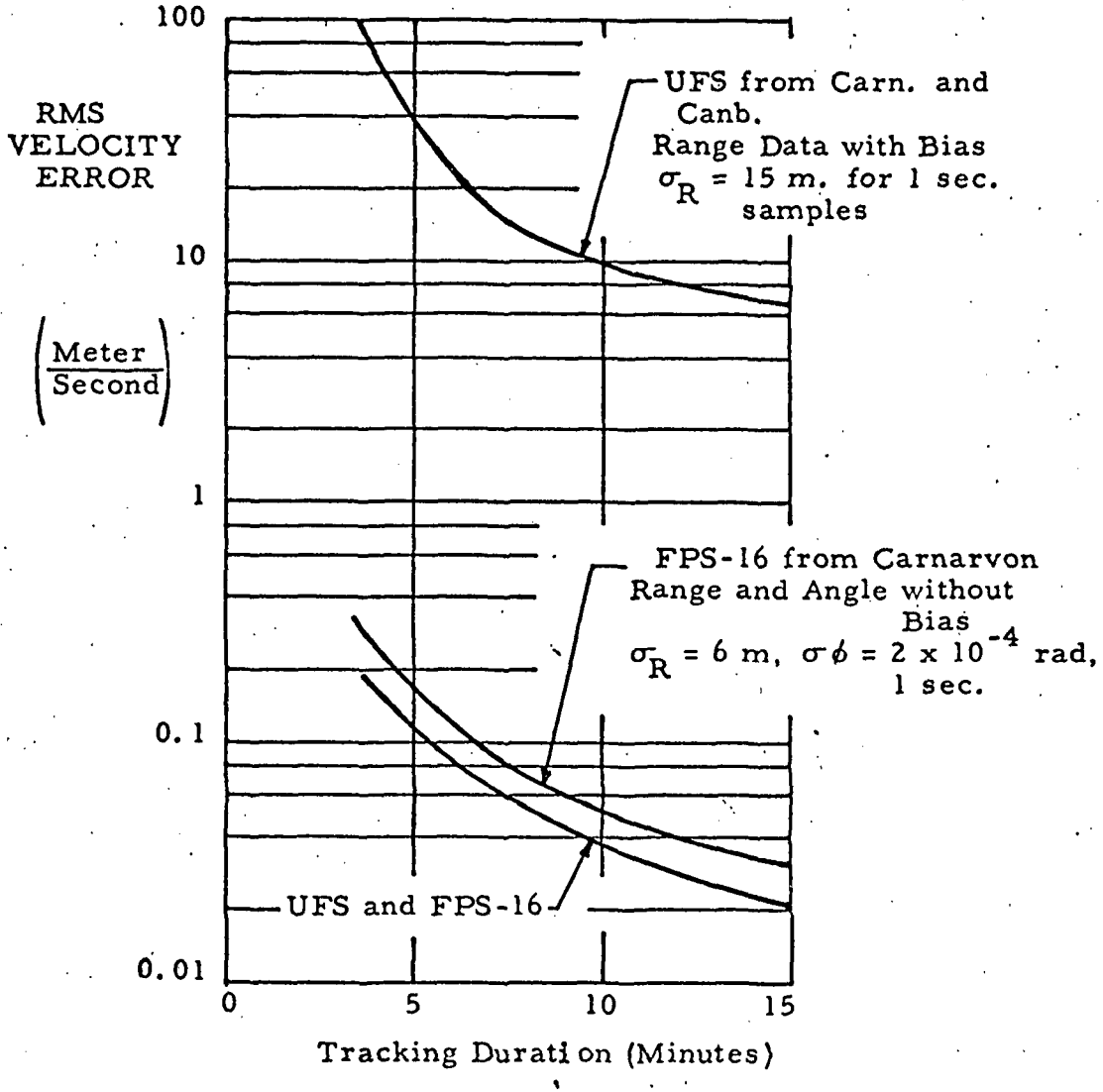

RETURN TO EARTH TRACKING GEOMETRY

Station	Lat.	Long.
1	-20°	+50°
2	+20°	-50°
3	-20°	-50°

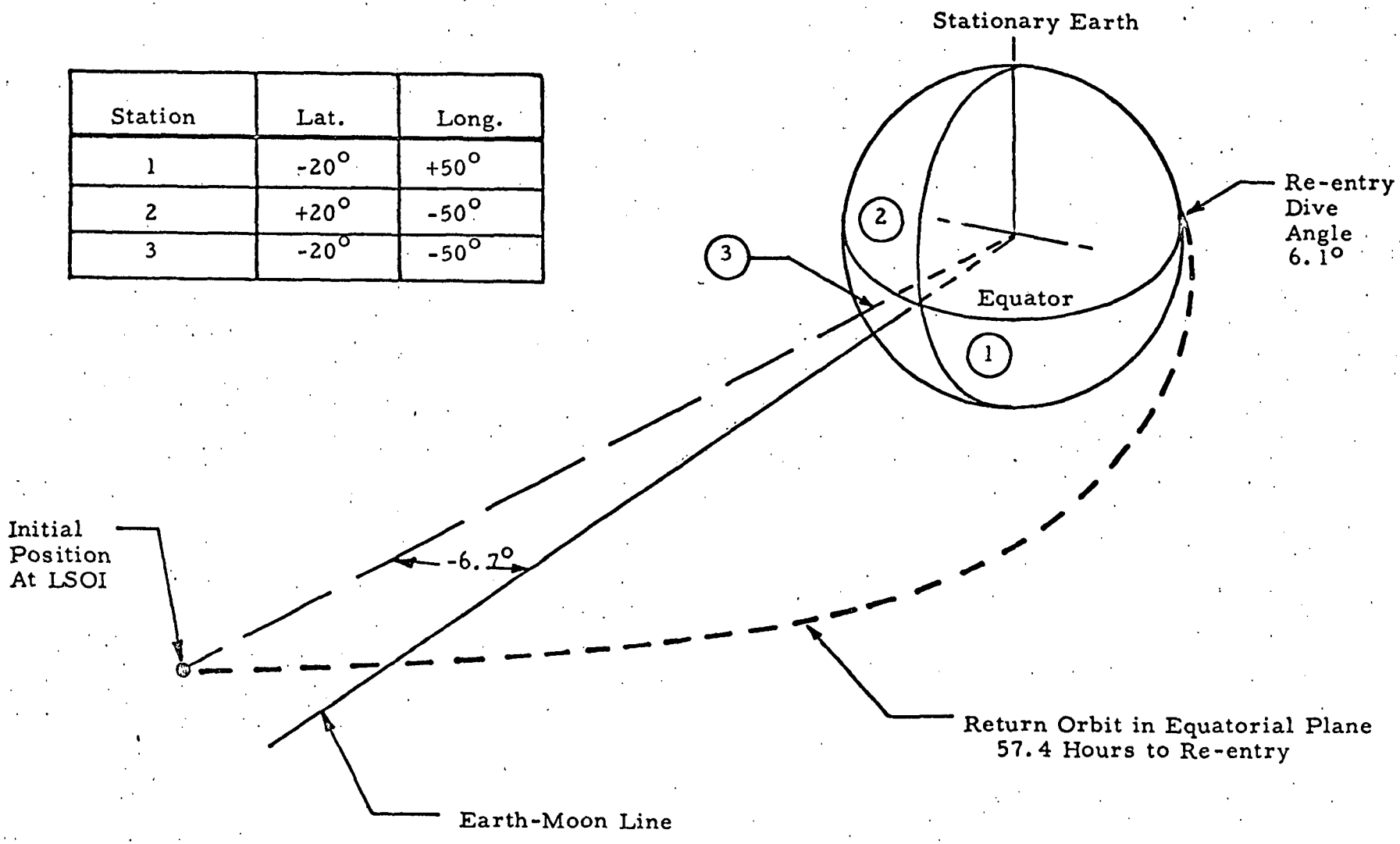

RETURN TO EARTH ——— NO A PRIORI DATA							
STATIONS	Hours To Re-Entry	Range Without Bias		Range With Bias		Range Rate	
		Dive Angle σ	RMS Miss	Dive Angle σ	RMS Miss	Dive Angle σ	RMS Miss
① ② ③	45	.0081°	1.70 KM	.455°	141 KM	5.020°	1570 KM
	33	.0017°	0.35 KM	.053°	17 KM	1.130°	374 KM
	21	.0005°	0.11 KM	.010°	4 KM	0.299°	115 KM
	9	.0002°	0.04 KM	.002°	1 KM	0.045°	27 KM
① ②	45	17.14°	8630 KM	194.0°	102000 KM	2350°	1.2×10^6 KM
	33	3.26°	1640 KM	21.8°	11000 KM	324°	1.6×10^5 KM
	21	1.14°	575 KM	3.6°	1740 KM	68°	3.3×10^4 KM
	9	0.06°	32 KM	0.36°	156 KM	6.3°	2.7×10^3 KM

Range σ = 15 meters Range Rate σ = 3 cm/sec.

APOLLO NOTE NO. 147

H. Engel
20 November 1963

MSFN STATION LOCATIONS AND LUNAR RENDEZVOUS DETERMINATION, II

The graphs in Apollo Note No. 139 did not show the variation in accuracy of orbit determination with station pair orientation that was expected.

Consideration of the kinematics of the problem lead to the belief that the worst station pair orientation would occur when the two stations and the lunar orbit were all in the plane of Earth-Moon rotation, since in this case only the motion of the stations due to the rotation of the Earth and motion of the Moon in its orbit would give any information about orbit parameters a_3 and a_6.

Computations have been performed for this case, the inclination being 18.31°. From the accompanying figure, it can be seen that the error in the prediction of minimum RMS miss near rendezvous is increased by two orders of magnitude in this case.

In general, the errors vary like the secant of the angle between the orbit plane and the line joining the two stations.

Data Set 60.

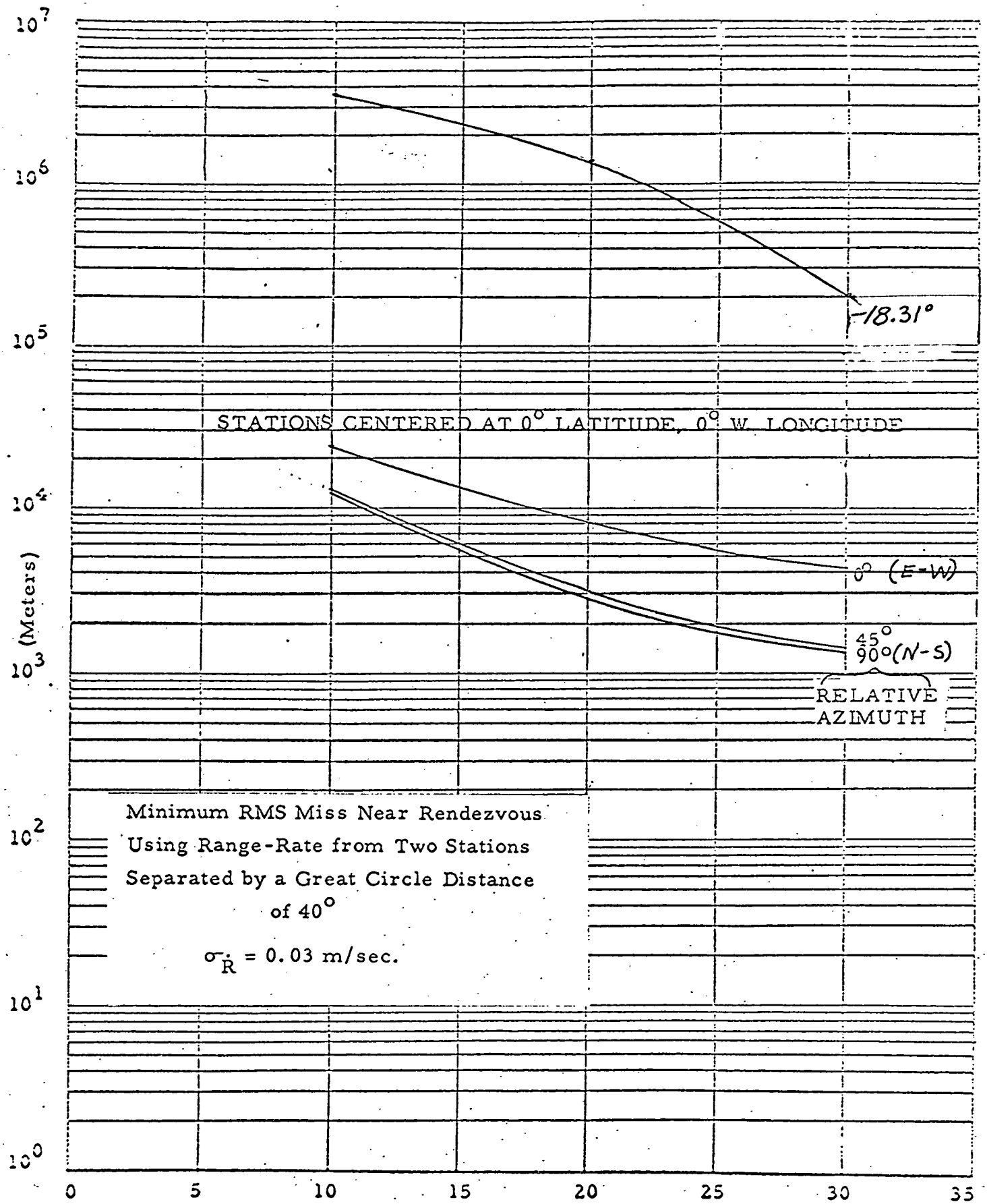
10^7
10^6
10^5
10^4
10^3
10^2
10^1
10^0
(Meters)
STATIONS CENTERED AT 0° LATITUDE, 0° W. LONGITUDE
-18.31°
0° (E-W)
45°
90° (N-S)
RELATIVE AZIMUTH
Minimum RMS Miss Near Rendezvous
Using Range-Rate from Two Stations
Separated by a Great Circle Distance
of 40°
$\sigma_{\dot{R}}$ = 0.03 m/sec.
0
5
10
15
20
25
30
35
Time (min.)

Figure 1.

APOLLO NOTE NO. 148

H. Engel
20 November 1963

RANGE-RATE PREDICTION OF RENDEZVOUS

With only one transponder aboard the lunar vehicle, the best way to determine lunar orbits using multiple ground stations appears to be through use of the three-way Doppler mode.

The Doppler measures change in range, not range-rate. This can be viewed as measurement of range to the same accuracy, but with a fixed, unknown range bias. The results presented here are for range measurements with bias having a standard deviation of 0.6 m in range for one minute measurements.

The "standard" ascent trajectory used is the same as that described in Apollo Note No. 136, and the a priori data used are the same as in that note.

The accompanying figure shows the errors in the prediction of the minimum RMS miss near rendezvous for range with bias measurements from 1, 2 and 3 stations with a priori data. For comparison the like errors are shown for range with bias measurements from 1 station without a priori data, and for range without bias from 3 stations without a priori data.

Data Set 44.

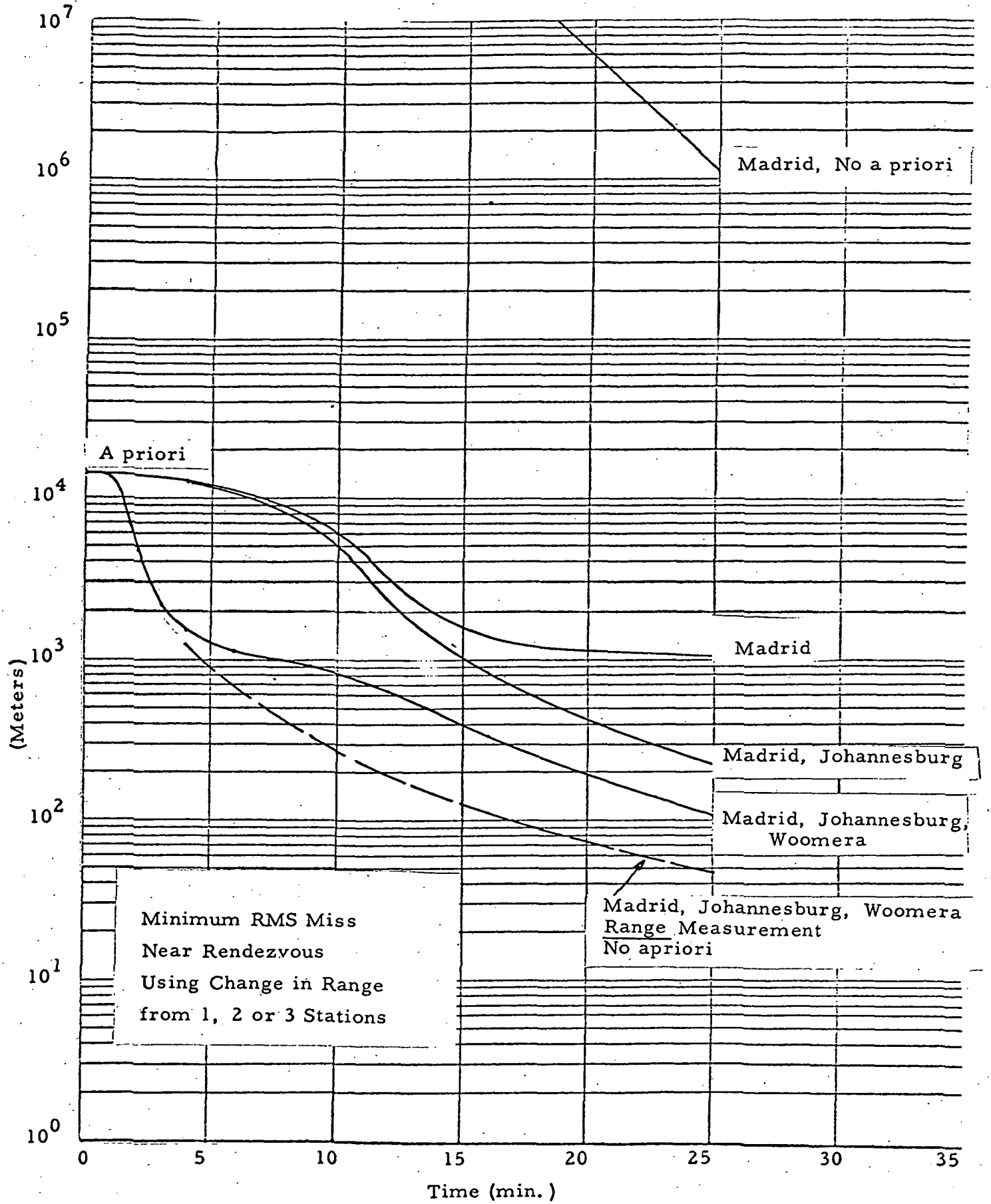
10^7
10^6
10^5
10^4
10^3
10^2
10^1
10^0
(Meters)
Madrid, No a priori
A priori
Madrid
Madrid, Johannesburg
Madrid, Johannesburg, Woomera
Madrid, Johannesburg, Woomera
Range Measurement
No apriori
Minimum RMS Miss
Near Rendezvous
Using Change in Range
from 1, 2 or 3 Stations
0
5
10
15
20
25
30
35
Time (min.)

Figure 1.

APOLLO NOTE NO. 149

H. Engel/
L. Lustick
20 November 1963

MODIFICATIONS OF ORBIT DETERMINATION PROGRAM FOR VELOCITY OF LIGHT AND GRAVITATIONAL ATTRACTION UNCERTAINTY

Purpose

The purpose of this note is to describe the necessary alterations in the orbit determination program, to account for uncertainties in the speed of light and in the planetary gravitational constant.

Uncertainty in Velocity of Light

An uncertainty in the velocity of light results in a proportional error in the measurement of range s, or range-rate $\dot{s}$. The ratio of the actual speed of light to the nominal speed of light can be treated as one more parameter to be found in the orbit determination, contributing an extra row and column to the information matrix. If the ratio of the actual speed of light to the nominal speed of light is denoted by a_c, then the partial derivatives of the computed values of the observed range and range-rate with respect to a_c are s and $\dot{s}$, respectively.

The resulting elements of the information matrix are C_{jc} and C_{cj},

$$C_{jc} = C_{cj}$$

$$= \sum_i s \frac{\partial s}{\partial a_j} \quad \text{for range}$$

$$= \sum_i \dot{s} \frac{\partial \dot{s}}{\partial a_j} \quad \text{for range-rate.}$$

Uncertainty in Gravitational Constant

The acceleration caused by an attracting mass with gravitational constant μ at a distance R is μ/R^2. If there is an uncertainty in μ, then μ can be treated as a further orbit parameter leading to the additional elements in the information matrix,

$$C_{\mu j} = C_{j\mu}$$

$$= \sum_i \frac{\partial s}{\partial \mu} \frac{\partial s}{\partial a_j} \quad \text{for range}$$

$$= \sum_i \frac{\partial \dot{s}}{\partial \mu} \frac{\partial \dot{s}}{\partial a_j} \quad \text{for range-rate}$$

$$= \sum_i \frac{\partial \phi}{\partial \mu} \frac{\partial \phi}{\partial a_j} \quad \text{for angles.}$$

In this instance evaluation of the partials of s, $\dot{s}$ and ϕ with respect to μ is involved.....

Let $\delta_{\mu j} = 1 \quad \text{if } j = \mu$

$= 0 \quad \text{if } j \neq \mu$

The changes in the equations of Apollo Note No. 82 that will allow the calculation of

$\frac{\partial s}{\partial \mu}$, $\frac{\partial \dot{s}}{\partial \mu}$ and $\frac{\partial \phi}{\partial \mu}$ are as follows:

$$\boxed{\frac{\partial E}{\partial a_j} = \delta_{1j} \frac{\mu}{a_1^2} + \delta_{4j} a_4 + \delta_{5j} a_5} - \frac{1}{a_1} \delta_{\mu j}$$

$$\frac{\partial e^2}{\partial a_j} = 2\left(\frac{H}{\mu}\right)^2\left[\frac{\partial E}{\partial a_j} + \frac{2E}{H}\frac{\partial H}{\partial a_j}\right] + \delta_{uj}\, 2\,\frac{(1-e^2)}{\mu}$$

$$\frac{\partial (e\cos\theta_o)}{\partial a_j} = \frac{a_5}{\mu}\left[2\frac{\partial H}{\partial a_j} - \delta_{1j}\, a_5\right] - \delta_{uj}\frac{(1+e\cos\theta_o)}{\mu}$$

$$\frac{\partial (e\sin\theta_o)}{\partial a_j} = \frac{a_5}{\mu}\left(a_1\frac{\partial \dot{r}_o}{\partial a_j}\right) + \frac{a_4}{\mu}\frac{\partial H}{\partial a_j} - \frac{e\sin\theta_o\,\delta_{\mu j}}{\mu}$$

$$\frac{\partial n}{\partial a_j} = \frac{3n}{2E}\frac{\partial E}{\partial a_j} - \frac{n}{\mu}\delta_{\mu j}$$

$$e\frac{\partial \theta}{\partial a_j} = \frac{(1-e^2)^{1/2}}{(1-e\cos\xi)^2}\left\{e(M-M_o)\left(\frac{3}{2E}\frac{\partial E}{\partial a_j} - \frac{\delta\mu_j}{\mu}\right) + \left(\frac{\partial M_o}{\partial a_j}\right) + \frac{\sin\xi}{2}\left(\frac{1-e\cos\xi}{1-e^2} + 1\right)\frac{\partial e^2}{\partial a_j}\right\}$$

$$\frac{\partial(\theta-\theta_o)}{\partial a_j} = (1-e^2)^{1/2}\left\{\frac{(M-M_o)\left(\frac{3}{2E}\frac{\partial E}{\partial a_j}-\frac{\delta\mu_j}{\mu}\right)+\sin\xi\left(\frac{1-e\cos\xi}{1-e^2}+1\right)\frac{\partial e}{\partial a_j}}{(1-e\cos\xi)^2}\right.$$

$$-\frac{\sin\xi_o\left(\frac{1-e\cos\xi_o}{1-e^2}+1\right)\frac{\partial e}{\partial a_j}}{(1-e\cos\xi_o)^2}$$

$$\left.+\frac{(\cos\xi-\cos\xi_o)\left(2-e\left[\cos\xi+\cos\xi_o\right]\right)}{(1-e\cos\xi)^2(1-e\cos\xi_o)^2}\left(e\frac{\partial M_o}{\partial a_j}\right)\right\}$$

$$\frac{\partial r}{\partial a_j} = 2\frac{r}{H}\frac{\partial H}{\partial a_j} - \frac{r}{1+e\cos\theta}\left[\cos\theta\frac{\partial e}{\partial a_j} - \sin\theta\left(e\frac{\partial\theta}{\partial a_j}\right)\right] - \frac{r}{\mu}\delta_{\mu j}$$

$$\frac{\partial \dot{r}}{\partial a_j} = \frac{\mu}{H}\left[\sin\theta\frac{\partial e}{\partial a_j} + \cos\theta\left(e\frac{\partial\theta}{\partial a_j}\right)\right] - \frac{\dot{r}}{H}\frac{\partial H}{\partial a_j} + \frac{\dot{r}}{\mu}\delta_{\mu j}$$

APOLLO NOTE NO. 150

H. Engel
3 December 1963

COMPARISON OF KALMAN-SCHMITT AND LINEAR LEAST SQUARES

Summary

It is shown that the orbit parameters and the covariance matrices of these parameters as determined by the Kalman-Schmitt method and by a linear least squares method are the same. Consequently, the Kalman-Schmitt method is equivalent to a linear least squares method,* or is equivalent to the first iteration of an optimum non-linear maximum likelihood method.

Some of material presented here appears in various earlier Apollo Notes.

Kalman-Schmitt Method

In order to avoid any confusion concerning the particular version of the Kalman-Schmitt method to which the above conclusion applies, the description and derivation of the Kalman-Schmitt method are presented here.

t_n Time of n-th set of observations.

x_n State (column)vector at t_n. The state vector has 6 elements if only 6 orbit parameters must be determined, or a larger number if additional parameters such as range bias, and location of an observing ground station must be determined. The elements of the state vector are the values of the parameters on the actual trajectory less the values on a fixed reference trajectory. Hence, the state vector is 0 on the reference trajectory.

The elements of x_n may be quantities that do not vary with time, such as semi-major axis and eccentricity, or may be time-varying quantities such

* What is called a linear least squares method in this note is more commonly known in the literature as a minimum variance method based on a reference trajectory.

as the position and velocity at t_n. In the on-board Apollo application of the Kalman-Schmitt method, position and velocity are chosen as the parameters for ease of computation.

y_n Measurement (column) vector at t_n. Each element corresponds to one measurable, whether or not that quantity is used at t_n. The elements of the measurement vector are the values of the measurables on the actual trajectory less the values on the reference trajectory. Thus they are 0 on the reference trajectory.

y_n^* Measured value of y_n.

u_n Zero mean random noise vector added to y_n that results in y_n^*. $y_n^* = y_n + u_n$. This noise has zero mean since all biases appear as part of the state vector.

Q_n Covariance of the noise u_n. $Q_n = E(u_n u_n^T)$. Q_n is assumed to be known a priori, and the noise at t_n is assumed to be uncorrelated with the noise at any different time t_m.

$\phi_{n+1,n}$ Square matrix that transforms orbit parameters on a trajectory near the reference trajectory at t_n into orbit parameters on the same trajectory at t_{n+1}. $\phi_{n+1,n}$ may be computed ahead of time. $x_{n+1} = \phi_{n+1,n} x_n$

M_n Rectangular matrix relating y_n and x_n. $y_n = M_n x_n$. M_n is a function of the orbit parameters, including time, on the reference trajectory and may be computed ahead of time.

The Kalman-Schmitt method assumes that the actual trajectory is sufficiently close to the reference trajectory that linear relationships hold; e.g., that y_n and x_n on the actual trajectory can be related by M_n which is evaluated on the reference trajectory, and that x_{n+1} may be obtained from x_n by application of $\phi_{n+1,n}$ which also is evaluated on the reference trajectory.

x_n^* Best estimate of x_n based on all y_i^* for $i < n$.
$E(x_n^* - x_n) = 0$.

$\bar{x}_{n+1}$ An estimate of x_{n+1} based on all y_i^* for $i < n$.
$E(\bar{x}_{n+1}) = x_{n+1}$

$\bar{y}_n$ An estimate of y_n^* based on x_n^*. $\bar{y}_n = M_n x_n^*$
$E(\bar{y}_n) = M_n E(x_n^*) = M_n x_n = y_n$

$\delta \bar{x}_n$ Error in $\bar{x}_n$. $\delta \bar{x}_n = \bar{x}_n - x_n$

$\delta \bar{y}_n$ Error in $\bar{y}_n$. $\delta \bar{y}_n = \bar{y}_n - y_n^* = M_n x_n^* - y_n^*$. $E(\delta \bar{y}_n) = 0$

$\delta \bar{x}_n^*$ Best estimate of $\delta \bar{x}_n$. $\delta \bar{x}_n^* = \bar{x}_n - x_n^*$
By means of Theorem 1, proved in the appendix,

$$\delta \bar{x}_{n+1}^* = \left[E(\delta \bar{x}_{n+1} \; \delta \bar{y}_n^T) \right] \left[E(\delta \bar{y}_n \; \delta \bar{y}_n^T) \right]^{-1} \delta \bar{y}_n$$

P_n^* Covariance matrix of errors in state vector at t_n.
$P_n^* = E\left[(x_n^* - x_n)(x_n^* - x_n)^T \right]$

After all these definitions, only a little computing remains:

$$E(\delta \bar{y}_n \, \delta \bar{y}_n^T) = E\left[(\bar{y}_n - y_n^*)(\bar{y}_n - y_n^*)^T\right]$$

$$= E\left[(\bar{y}_n - y_n - u_n)(\bar{y}_n - y_n - u_n)^T\right]$$

$$= E\left[\left\{M_n (x_n^* - x_n) - u_n\right\}\left\{(x_n^* - x_n)^T M_n^T - u_n^T\right\}\right]$$

$$= M_n E\left[(x_n^* - x_n)(x_n^* - x_n)^T\right] M_n^T + 0 + 0 + E(u_n u_n^T)$$

$$= M_n P_n^* M_n^T + Q_n$$

$$E(\delta \bar{x}_{n+1} \delta \bar{y}_n^T) = E\left[(\bar{x}_{n+1} - x_{n+1})(\bar{y}_n - y_n^*)^T\right]$$

$$= E\left[(\bar{x}_{n+1} - x_{n+1})(\bar{y}_n - y_n - u_n)^T\right]$$

$$= E\left[\phi_{n+1,n}(x_n^* - x_n)\left\{(x_n^* - x_n)^T M_n^T - u_n^T\right\}\right]$$

$$= \phi_{n+1,n} E\left[(x_n^* - x_n)(x_n^* - x_n)^T\right] M_n^T + 0$$

$$= \phi_{n+1,n} P_n^* M_n^T$$

From Theorem 1, given in the appendix,

$$\delta \bar{x}_{n+1}^* = \left[E(\delta \bar{x}_{n+1} \delta \bar{y}_n^T)\right]\left[E(\delta \bar{y}_n \delta \bar{y}_n^T\right]^{-1} \delta \bar{y}_n$$

and by substitution

$$\bar{x}_{n+1} - x_{n+1}^* = \left[\phi_{n+1,n} P_n^* M_n^T\right]\left[M_n P_n^* M_n^T + Q_n\right]^{-1} (M_n x_n^* - y_n^*)$$

or

$$\boxed{x_{n+1}^* = \phi_{n+1,n} x_n^* - \phi_{n+1,n} P_n^* M_n^T (M_n P_n^* M_n^T + Q_n)^{-1} (M_n x_n^* - y_n^*)}$$

For convenience we define Δ^*_n as

$$\Delta^*_n = \phi_{n+1,n} P^*_n M_n^T (M_n P^*_n M_n^T + Q_n)^{-1}$$

and define $\phi^*_{n+1,n}$ as

$$\phi^*_{n+1,n} = \phi_{n+1,n} - \Delta^*_n M_n$$

Then, by substitution,

$$x^*_{n+1} = \phi^*_{n+1,n} x^*_n + \Delta^*_n y^*_n$$

Next,

$$x^*_{n+1} - x_{n+1} = \phi^*_{n+1,n} x^*_n + \Delta^*_n y^*_n - \phi_{n+1,n} x_n + (\phi^*_{n+1,n} x_n - \phi^*_{n+1,n} x_n)$$

$$= \phi^*_{n+1,n} (x^*_n - x_n) + \phi^*_{n+1,n} x_n - \phi_{n+1,n} x_n + \Delta^*_n y_n + \Delta^*_n u_n$$

$$= \phi^*_{n+1}(x^*_n - x_n) + (\phi^*_{n+1,n} - \phi_n - \Delta^*_n M_n) x_n + \Delta^*_n u_n$$

$$= \phi^*_{n+1,n} (x^*_n - x_n) + 0 + \Delta^*_n u_n$$

$$P^*_{n+1} = E\left[(x^*_{n+1} - x_{n+1}) (x^*_{n+1})^T \right]$$

$$= E\left[\left\{ \phi^*_{n+1,n} (x^*_n - x_n) + \Delta^*_n u_n \right\} \left\{ (x^*_n - x_n)^T \phi^{*T}_{n+1,n} + u_n^T \Delta^{*T}_n \right\} \right]$$

$$= \phi^*_{n+1,n} P^*_n \phi^{*T}_{n+1,n} + 0 + 0 + \Delta^*_n Q_n \Delta^{*T}_n$$

$$= \phi^*_{n+1,n} P^*_n \left[\phi^{*T}_{n+1,n} + (\phi^T_{n+1,n} - \phi^T_{n+1,n}) \right] + \Delta^*_n Q_n \Delta^{*T}_n$$

$$= \phi^*_{n+1,n} P^*_n \phi^T_{n+1,n} + \phi^*_{n+1,n} P^*_n (\phi^*_{n+1,n} - \phi_{n+1,n})^T + \Delta^*_n Q_n \Delta^{*T}_n$$

$$= \phi^*_{n+1,n} P^*_n \phi^T_{n+1,n} + \phi^*_{n+1,n} P^*_n (-\Delta^*_n M_n)^T + \Delta^*_n Q_n \Delta^{*T}_n$$

$$= \phi^*_{n+1,n} P^*_n \phi_{n+1,n} - (\phi^*_{n+1,n} P^*_n M_n^T - \Delta^*_n Q_n) \Delta^{*T}_n$$

$$= \phi^*_{n+1,n} P^*_n \phi_{n+1,n} - (\phi_{n+1,n} P^*_n M_n^T - \Delta^*_n M_n P^*_n M_n^T - \Delta^*_n Q_n) \Delta^{*T}_n$$

$$= \phi^*_{n+1,n} P^*_n \phi_{n+1,n} - \left(\phi_{n+1,n} P^*_n M_n^T - \Delta^*_n \left\{ M_n P^*_n M_n^T + Q_n \right\}\right) \Delta^{*T}_n$$

From the definition of Δ_n^* we can substitute and find

$$P_{n+1}^* = \phi_{n+1,n}^* P_n^* \phi_{n+1,n} - (\phi_{n+1,n} P_n^* M_n^T - \phi_{n+1,n} P_n^* M_n^T) \Delta_n^{*T}$$

$$= \phi_{n+1,n}^* P_n^* \phi_{n+1,n}$$

In summary, in the Kalman-Schmitt method we start with a priori values of x_o^* and P_o^*, and given values of $\phi_{n+1,n}$, M_n and Q_n. We then compute

$$\Delta_n^* = \phi_{n+1,n} P_n^* M_n^T (M_n P_n^* M_n^T + Q_n)^{-1}$$

$$\phi_{n+1,n}^* = \phi_{n+1,n} - \Delta_n^* M_n$$

$$P_{n+1}^* = \phi_{n+1,n}^* P_n^* \phi_{n+1,n}^T$$

$$x_{n+1}^* = \phi_{n+1,n}^* x_n^* + \Delta_n^* y_n^*$$

Linear Least Squares

In this alternative method for obtaining the best linear estimate of the orbit parameters, no computation is done until all the measurements are collected. As in the Kalman-Schmitt method, a reference trajectory or a priori estimated trajectory is employed.

The definitions used above in the Kalman-Schmitt method are also used here. In addition we define

$\phi_{n,m}$ $x_n = \phi_{n,m} x_m$. Note: $\phi_{n,0} = \phi_{n,n-1} \phi_{n-1,n-2} \cdots \phi_{1,0}$.

x_{oN}^* Best linear estimate of x_o based on all y_i^* for $i < N$. $E(x_{o,N}^*) = x_o$

In order to obtain the best linear estimate of $x_{o,N}$ we must maximize the likelihood of the estimate. In order to do so we must minimize the quantity $\mathcal{L}_N$,

$$\mathcal{L}_N = -\frac{1}{2} \sum_{i=0}^{N-1} (y_i^* - M_i x_i^*)^T Q_i^{-1} (y_i^* - M_i x_i^*)$$

$$= -\frac{1}{2} \sum_{i=0}^{N-1} (y_i^* - M_i \phi_i x_{o,N}^*)^T Q_i^{-1} (y_i^* - M_i \phi_i x_{o,N}^*)$$

This requires that we set the first partial derivatives of $\mathcal{L}_N$ with respect to each of the components of x_o equal to 0:

$$0 = \sum_{i=0}^{N-1} (M_i \phi_{i,o})^T Q_i^{-1} (y_i^* - M_i \phi_{i,o} x_{oN}^* + \sum_{i=0}^{N-1} (y_i^* - M_i \phi_{i,o} x_{oN}^*)^T Q_i^{-1} (M_i \phi_{i,o})$$

Now Q_i is a symmetric matrix, $Q = Q^T$, so the above matrix equation is satisfied if

$$0 = \sum_{i=0}^{N-1} (M_i \phi_{i,o})^T Q_i^{-1} (y_i^* - M_i \phi_{i,o} x_{on}^*)$$

We now define V_N, W_N and Z_n,

$$V_N = \sum_{i=0}^{N-1} (M_i \phi_{i,o})^T Q_i^{-1} (M_i \phi_{i,o})$$

$$W_N = \sum_{i=0}^{N-1} (M_i \phi_{i,o})^T Q_i^{-1} y_i^*$$

$$Z_N = \sum_{i=0}^{N-1} (M_i \phi_{i,o})^T Q_i^{-1} y_i$$

and find that V_N is a symmetric matrix.

By substitution, we find

$$0 = W_N - V_N \, x^*_{o,N}$$

or

$$\boxed{x^*_{o,N} = V_N^{-1} \, W_N}$$

The covariance matrix of $x^*_{o,N} - x_o$ we shall call $P^{**}_{N,o}$. Then

$$P^{**}_{N,o} = E\left[(x^*_{o,N} - x_o)\,(x^*_{o,N} - x_o)^T\right]$$

$$= E\left[\left\{V_N^{-1}(W_N - Z_N)\right\}\left\{(W_N - Z_N)^T V_N^{-T}\right\}\right]$$

$$= V_N^{-1} \, E\left[(W_N - Z_N)\,(W_N - Z_N)^T\right] V_N^{-T}$$

$$= V_N^{-1} \, E\left[\left\{\sum_{i=0}^{N-1} (M_i \phi_{i,o})^T \, Q_i^{-1} \, u_i\right\}\left\{\sum_{i=0}^{N-1} u_i^T \, Q_i^{-1} (M_i \phi_{i,o})\right\}\right] V_N^{-1}$$

utilizing the symmetry of Q_i and of V_N. The expected value of $u_i \, u_j^T$ is 0 for $i \neq j$ and is Q_i for $i = j$.

$$P^{**}_{N,o} = V_N^{-1}\left[\sum_{i=0}^{N-1} (M_i \phi_{i,o})^T \, Q_i^{-1} \, Q_i \, Q_i^{-1} (M_i \phi_{i,o})\right] V_N^{-1}$$

$$= V_N^{-1}\left[\sum_{i=0}^{N-1} (M_i \phi_{i,o})^T \, Q_i^{-1} \, (M_i \phi_{i,o})\right] V_N^{-1}$$

$$= V_N^{-1} \, V_N \, V_N^{-1}$$

$$= V_N^{-1}$$

or, in another form

$$P^{**}_{N,o} = \left[\sum_{i=0}^{N-1} (M_i \phi_{i,o})^T Q_i^{-1} (M_i \phi_{i,o}) \right]^{-1}$$

Comparison of Results

In order to show that the linear least squares fit and the Kalman-Schmitt method are identical, we first show that they lead to the same covariance matrices of the orbit parameters.

The first difficulty to be overcome is that the Kalman-Schmitt method obtains the state vector at t_n while the least squares fit obtains it at t_o. We avoid the difficulty by selecting a state vector that does not vary with time.

The Kalman-Schmitt method, as presented here is not restricted to any particular kind of state vector. Given any particular kind of state vector $x(t_n)$, say position and velocity at t_n, any other kind of state vector $X(t_n)$, say the classical orbit elements, can be obtained by means of a simple transformation

$$X = A x$$

in which A is a square matrix having as elements the elements of the Jacobian $\partial X/\partial x$. Therefore, we need only consider the classical orbit elements that are unvarying with time. For these elements, $\phi_{n+1,n}$ is the identity matrix, so

$$\Delta^*_n = P^*_n M_n^T (M_n P^*_n M_n^T + Q_n)^{-1}$$

and

$$\phi^*_{n+1,n} = I - \Delta^*_n M_n$$

By substitution, we find

$$\phi^*_{n+1,n} = I - P^*_n M_n^T (M_n P^*_n M_n^T + Q_n)^{-1} M_n$$

We also have

$$P^*_{n+1} = \phi^*_{n+1,n} P^*_n I$$

so by substitution

$$P^*_{n+1} = \left[I - P^*_n \; M_n^T \; (M_n \; P^*_n \; M_n^T + Q_n)^{-1} \; M_n \right] P^*_n$$

Now, let us assume that the covariance matrices as determined by the Kalman-Schmitt and linear least squares methods are the same at some time t_n, and show that they are then the same at t_{n+1}. We let

$$P_n = P^*_n = P^{**}_{n,o}$$

and show that $P^*_{n+1} = P^{**}_{n+1,0}$.

Let

$$U = (P^{**}_{n+1,0})^{-1} \; P^*_{n+1}$$

Now,

$$(P^{**}_{n+1,0})^{-1} = \sum_{i=0}^{n} (M_i \; \phi_{i,o})^T \; Q_i^{-1} \; (M_i \; \phi_{i,o}),$$

but for the classical orbit elements $\phi_{i,o}$ is the identity matrix, so

$$(P^{**}_{n+1,0})^{-1} = \sum_{i=0}^{n} M_i^T \; Q_i^{-1} \; M_i$$

$$= \sum_{i=0}^{n-1} M_i^T \; Q_i \; M_i + M_n^T \; Q_n^{-1} \; M_n$$

$$= (P^{**}_{n,o})^{-1} + M_n^T \; Q_n^{-1} \; M_n$$

Then,

$$U = (P_n^{-1} + M_n Q_n^{-1} M_n) \left[I - P_n M_n^T (M_n P_n M_n^T + Q_n)^{-1} M_n \right] P_n$$

$$= I + M_n^T Q_n^{-1} \left[M_n P_n - (Q_n + M_n P_n M_n^T) (M_n P_n M_n^T + Q_n)^{-1} M_n P_n \right]$$

$$= I + M_n^T Q_n^{-1} \left[M_n P_n - M_n P_n \right]$$

$$= I$$

or premultiplying both sides by $P^{**}_{n+1,0}$,

$$P^{**}_{n+1,0} = P^{*}_{n+1}$$

Also, $P^{**}_{c,o}$ and P^{*}_{o} are equal, both being the same as the a priori knowledge of the trajectory. Thus, by induction,

$$P_n = P^{**}_{n,o} = P^{*}_{n}$$

for all n greater than 0.

Next we show that the state vectors determined by the Kalman-Schmitt and the linear least squares methods are the same. Again, we use the difference between the classical orbit parameters on the trajectory and on the reference trajectory as our state vector. Then,

$$x^*_{n+1} = \phi_{n+1,n} x^*_n - \phi_{n+1,n} P^*_n M_n^T (M_n P^*_n M_n^T + Q_n)^{-1} (M_n x^*_n - y^*_n)$$

$$= x^*_n - P_n M_n^T (M_n P_n M_n^T + Q_n)^{-1} (M_n x^*_n - y^*_n)$$

We show that if

$$x^*_n = x^*_{o,n}$$

for some n, it is true for n + 1.

$$x^*_{o,n} = x^*_n = P_n W_n$$

so

$$x^*_{n+1} = P_n W_n - P_n M_n^T (M_n P_n M_n^T + Q)^{-1} (M_n P_n W_n - y^*_n)$$

$$= \left[I - P_n M_n^T (M_n P_n M_n^T + Q_n)^{-1} M_n \right] P_n W_n$$

$$+ P_n M_n^T (M_n P_n M_n^T + Q_n)^{-1} y^*_n$$

Now

$$P_{n+1} = \left[I - P_n M_n^T (M_n P_n M_n^T + Q_n)^{-1} M_n \right] P_n$$

$$x^*_{n+1} = P_{n+1} W_n + P_n M_n^T (M_n P_n M_n^T + Q_n)^{-1} y^*_n$$

$$= P_{n+1} W_n + P_{n+1} M_n^T Q_n^{-1} y^*_n - P_{n+1} M_n^T Q_n^{-1} y^*_n$$

$$+ P_n M_n^T (M_n P_n M_n^T + Q_n)^{-1} y^*_n$$

$$= P_{n+1} W_{n+1} + P_{n+1} \left[-M_n^T Q_n^{-1} (M_n P_n M_n^T + Q_n) + P_{n+1}^{-1} P_n M_n^T \right]$$

$$(M_n P_n M_n^T + Q_n)^{-1} y^*_n$$

$$= P_{n+1} W_{n+1} + P_{n+1} \left[-M_n^T Q_n^{-1} M_n P_n M_n^T - M_n^T + (P_n^{-1} + M_n^T Q_n^{-1} M_n) P_n M_n^T \right]$$

$$(M_n P_n M_n^T + Q_n)^{-1} y^*_n$$

$$= P_{n+1} W_{n+1} + P_{n+1} \left[0 \right] (M_n P_n M_n^T + Q_n)^{-1} y^*_n$$

$$= P_{n+1} W_{n+1}$$

$$= x^*_{o, n+1}$$

Since the a priori vectors are the same, then, all state vectors determined by the Kalman-Schmitt and linear least squares methods are the same.

Thus it has been shown that the Kalman-Schmitt and linear least squares methods are identical.

Appendix

Theorem: Let α and β be two column vector random variables, not necessarily of the same dimension, with means zero and covariance matrices

$$\Lambda_\alpha = E\left[\alpha\ \alpha^T\right]$$

$$\Lambda_\beta = E\left[\beta\ \beta^T\right]$$

$$\Lambda_{\beta\alpha} = E\left[\beta\ \alpha^T\right]$$

Then the "best" linear estimate $\tilde{\beta}$ of β, given α, is

$$\tilde{\beta} = \Lambda_{\beta\alpha}\Lambda_\alpha^{-1}\alpha$$

where "best" means that the covariance matrix of the error in $\tilde{\beta}$ is such that variance in the estimate of any quantity, $\psi = a^T\beta$ is minimized. This can be shown as follows:

$$\sigma_\psi^2 = E\left[(\psi - \tilde{\psi})(\psi - \tilde{\psi})^T\right]$$

$$= E\left[a^T(\beta - \tilde{\beta})(\beta - \tilde{\beta})^T a\right]$$

$$= a^T E\left[(\beta - \tilde{\beta})(\beta - \tilde{\beta})^T\right] a$$

$$= a^T R\, a$$

in which

$$R = E\left[(\beta - \tilde{\beta})(\beta - \tilde{\beta})^T\right]$$

To minimize σ_ψ^2, only R can be varied. Now since $\tilde{\beta}$ is a linear estimate of β, given α, write

$$\tilde{\beta} = A\alpha$$

$$R = E\left[(\beta - A\alpha)(\beta - A\alpha)^T\right]$$

$$= E\left[\beta\beta^T\right] - E\left[\beta(A\alpha)^T\right] - E\left[(A\alpha)\beta^T\right] + E\left[(A\alpha)(A\alpha)^T\right]$$

$$= \Lambda_\beta - E\left[\beta\alpha^T A^T\right] - E\left[A\alpha\beta^T\right] + E\left[A\alpha\alpha^T A^T\right]$$

$$= \Lambda_\beta - \Lambda_{\beta\alpha} A^T - A\Lambda_{\alpha\beta} + A\Lambda_\alpha A^T$$

Now vary A (and A_T) to obtain a stationary value.

$$\delta R = -\Lambda_{\beta\alpha}\,\delta A^T + A\Lambda_\alpha\,\delta A^T - \delta A\Lambda_{\alpha\beta} + \delta A\Lambda_\alpha A^T = 0$$

$$= (A\Lambda_\alpha - \Lambda_{\beta\alpha})\,\delta A^T + \delta A(\Lambda_\alpha A^T - \Lambda_{\alpha\beta}) = 0$$

Hence, for a stationary solution

$$A = A_s = \Lambda_{\beta\alpha}\Lambda_\alpha^{-1} \quad \text{and} \quad A^T = A_s^T = \Lambda_\alpha^{-1}\Lambda_{\alpha\beta}$$

and

$$R = R_s = \Lambda_\beta - \Lambda_{\beta\alpha}\Lambda_\alpha^{-1}\Lambda_{\alpha\beta} - \Lambda_{\beta\alpha}\Lambda_\alpha^{-1}\Lambda_{\alpha\beta} + \Lambda_{\beta\alpha}\Lambda_\alpha^{-1}\Lambda_\alpha\Lambda_\alpha^{-1}\Lambda_{\alpha\beta}$$

$$= \Lambda_\beta - \Lambda_{\beta\alpha}\Lambda_\alpha^{-1}\Lambda_{\alpha\beta}$$

It is "easily" shown that this stationary solution results in a <u>minimum</u> σ_ψ^2.